

Renibacterium salmoninarum* and *Aeromonas salmonicida
Pathogenesis and Virulence in Lumpfish (*Cyclopterus lumpus*)

by

© Hajarrooba Gnanagobal, B.Sc. (Hons)

A thesis submitted to the School of Graduate Studies
in partial fulfilment of the requirements for the degree of
Doctor of Philosophy

Department of Ocean Sciences
Memorial University of Newfoundland
St. John's, Newfoundland and Labrador, Canada

Spring 2023

Abstract

Renibacterium salmoninarum, the etiological agent of Bacterial Kidney Disease (BKD), and *Aeromonas salmonicida*, which causes furunculosis, are economically important pathogens of marine fish. The marine teleost lumpfish (*Cyclopterus lumpus*) is an eco-friendly cleaner fish in Atlantic salmon (*Salmo salar*) farming. As the lumpfish demand in salmonid aquaculture continues to rise, understanding how lumpfish interact with well-known Gram-positive and Gram-negative fish pathogens is certainly required. Therefore, in my Ph.D. thesis, I studied the interactions between lumpfish host and Gram-positive *R. salmoninarum* or Gram-negative *A. salmonicida* with a particular focus on the fundamental aspects of bacterial pathogenicity and virulence.

First, I evaluated the lumpfish susceptibility and immune response to *R. salmoninarum* infection. Lumpfish showed typical BKD clinical signs and 35 % mortality when infected with a high dose of *R. salmoninarum* (1×10^9 cells dose⁻¹). High bacterial loads were observed in tissues (i.e., spleen, liver, and head kidney) at 28 days post-infection (dpi), and *R. salmoninarum* continued to persist in tissues until 98 dpi. Further, gene expression analysis using qPCR in the fish head kidney found that *R. salmoninarum* causes immune suppression at 28 dpi and lumpfish induce a cell-mediated immune response at 98 dpi.

Second, I profiled the lumpfish head kidney transcriptome response to *R. salmoninarum* at early (28 dpi) and chronic (98 dpi) infection using RNA sequencing. Compared to 98 dpi, lumpfish induced many molecular pathways and genes at 28 dpi. For instance, *R. salmoninarum*-induced genes at 28 dpi were linked to innate and adaptive

immunity, while *R. salmoninarum*-suppressed genes were involved in amino acid metabolism, cellular and developmental processes. In contrast, the transcriptome response of the lumpfish head kidney to this pathogen was minimal at 98 dpi, with *R. salmoninarum*-dependent dysregulation of genes primarily connected to cell-mediated adaptive immunity.

Third, I described the riboflavin supply pathways of *A. salmonicida*. Using *in silico* tools and RT-PCR, I found that *A. salmonicida* has a riboflavin biosynthesis pathway (RBP) and a riboflavin transporter. Moreover, I constructed the deletion mutants of riboflavin biosynthesis genes, their duplicated copies, and the transporter (*ribN*) of *A. salmonicida* and studied their role in virulence and potential as live-attenuated vaccine candidates using the lumpfish infection model. The results showed that riboflavin biosynthesis is crucial for *A. salmonicida* virulence.

Overall, the thesis provided fundamental insights into the pathogenicity and virulence of *R. salmoninarum* and *A. salmonicida* and lumpfish response. The findings presented here are valuable for developing immunoprophylactic measures for lumpfish against BKD and furunculosis.

Acknowledgements

It has been a truly life-changing experience for me to pursue this Ph.D., and I could not have done it without the support and guidance I received from so many individuals. First and foremost, I would like to thank my supervisor, Dr. Javier Santander, for his invaluable guidance, continuous encouragement, constant trust, and, sometimes, gentle prodding to make me move forward. Without your friendly mentoring, this Ph.D. would not have been achievable. I would also like to express my gratitude to my Ph.D. Committee, Dr. Matthew Rise and Dr. Víctor Antonio García-Angulo, for the in-depth conversations and insightful criticism that have substantially improved the thesis.

Many thanks to the staff of the Dr. Joe Brown Aquatic Research Building (JBARB; Danny Boyce) and the Cold Ocean Deep Sea Research Facility (CDRF; Stephen Hill and Gord Nash) for their help and collaboration during the animal experiments. Also, I am grateful to Dr. Jennifer Hall from Aquatic Research Cluster - CREAT Network, Ocean Sciences Centre, for helping with qPCR assays.

I am indeed obliged to all the Santander lab members for their continuous encouragement and help. Working with you as a team has been a fantastic experience. I am also indebted to the funding sources Graduate Scholarship from the School of Graduate Studies, Memorial University of Newfoundland, Canada First - Ocean Frontier Institute (sub-module J3), NSERC-Discovery grant (RGPIN-2018-05942), and Atlantic Fisheries Fund, Canada.

Last but not least, I owe hugely to my dear parents, Mr. R. Gnanagobal and Mrs. G. Suharniya, and to my little sister Ms. G. Bajaneetha, who has been by my side throughout

this Ph.D. and believes in me endlessly. Words cannot adequately explain how much I love, miss, and appreciate them. I dedicate this thesis to Amma, Appa, and Baji.

Table of Contents

Abstract.....	ii
Acknowledgement.....	iv
Table of contents.....	vi
List of Tables.....	xiii
List of Figures.....	xiv
List of abbreviations.....	xviii
List of Supplementary Files, Tables, and Figures.....	xxiv
Chapter 1. General Introduction.....	1
1.1. Bacterial pathogens of marine fish aquaculture.....	1
1.2. The Gram-positive pathogen <i>Renibacterium salmoninarum</i>	2
1.3. The Gram-negative pathogen: <i>Aeromonas salmonicida</i>	6
1.4. Bacterial riboflavin supply pathways.....	10
1.5. Lumpfish.....	13
1.6. Relevance and Hypotheses.....	16
1.6.1. <i>R. salmoninarum</i> and lumpfish.....	17
1.6.2. <i>A. salmonicida</i> riboflavin supply pathways and lumpfish.....	20
1.7. Thesis objectives.....	23
1.8. Publications from this thesis.....	24
1.9. References.....	27
Chapter 2. Host-pathogen interactions of marine Gram-positive bacteria.....	37
2.1. Abstract.....	38

2.2. Introduction.....	39
2.3. Pathogen-centric approaches.....	49
2.3.1. Adhesion / Host recognition.....	49
2.3.2. Invasion.....	55
2.3.3. Evasion.....	59
2.3.4. Proliferation and survival inside the host.....	65
2.4. Host-centric approaches - Fish host immune response.....	68
2.4.1. Toll-like receptors (Pathogen recognition).....	73
2.4.2. Nutritional immunity.....	75
2.4.3. Innate and adaptive (humoral and cell-mediated) immunity.....	77
2.4.4. Fish resistance/tolerance/susceptibility to marine Gram-positive bacteria.....	80
2.5. Conclusions.....	81
2.6. References.....	85
Chapter 3. Lumpfish susceptibility and immune response to <i>R. salmoninarum</i> infection.....	103
3.1. Abstract.....	104
3.2. Introduction.....	105
3.3. Materials and Methods.....	108
3.3.1. <i>Renibacterium salmoninarum</i> culture conditions and inoculum preparation.....	108
3.3.2. Lumpfish.....	112
3.3.3. <i>Renibacterium salmoninarum</i> infection in lumpfish.....	112
3.3.4. Determination of bacterial load in lumpfish tissues.....	113
3.3.5. Histopathological examination.....	115

3.3.6. RNA preparation.....	115
3.3.7. cDNA synthesis and qPCR parameters.....	116
3.3.8. Primer design and quality assurance testing.....	116
3.3.9. Endogenous control (normalizer) selection.....	118
3.3.10. Experimental qPCR analyses.....	123
3.3.11. Statistical analysis.....	124
3.4. Results.....	125
3.4.1. Lumpfish survival, <i>R. salmoninarum</i> infection kinetics and histopathology.	125
3.4.2. Lumpfish immune-related gene expression in response to <i>R. salmoninarum</i> infection.....	131
3.5. Discussion.....	140
3.6. Conclusions.....	150
3.7. References.....	151
3.8. Supplementary Materials.....	160
Chapter 4. Transcriptome profiling of lumpfish (<i>Cyclopterus lumpus</i>) head kidney to <i>Renibacterium salmoninarum</i> at early and chronic infection stages.....	168
4.1. Abstract.....	169
4.2. Introduction.....	170
4.3. Materials and Methods.....	173
4.3.1. <i>Renibacterium salmoninarum</i> culture.....	173
4.3.2. Lumpfish.....	174
4.3.3. Infection and sampling.....	175
4.3.4. Lumpfish head kidney transcriptome profiling by RNA-sequencing.....	177

4.3.4.1. RNA extraction.....	177
4.3.4.2. Library preparation and RNA-seq.....	177
4.3.4.3. RNA-Seq data analyses.....	178
4.3.4.4. GO (Gene Ontology) enrichment analyses and visualization of GO term networks.....	179
4.3.4.5. Correlation between RNA-seq and qPCR data.....	181
4.3.5. Fluorescence-based lysozyme activity assay.....	181
4.3.6. Indirect Enzyme-Linked Immunosorbent Assay (ELISA).....	183
4.3.7. Statistical Analysis.....	185
4.4. Results.....	185
4.4.1. Global transcriptome profile of lumpfish head kidney at early and chronic <i>R. salmoninarum</i> infection stages.....	185
4.4.2. Pathway enrichment analyses.....	189
4.4.3. DEGs associated with the enriched GO terms of interest at 28 and 98 dpi...	197
4.4.4. qPCR validation analysis.....	203
4.4.5. Lysozyme Activity in lumpfish serum.....	206
4.4.6. Specific serum antibody response.....	207
4.5. Discussion.....	210
4.6. Conclusions.....	227
4.7. References.....	228
4.8. Supplementary Materials.....	235
Chapter 5. Role of riboflavin biosynthesis gene duplication and transporter in <i>Aeromonas salmonicida</i> virulence in lumpfish.....	240

5.1. Abstract.....	241
5.2. Introduction.....	242
5.3. Materials and Methods.....	245
5.3.1. Bacterial strains, plasmids, media and reagents.....	245
5.3.2. <i>In-silico</i> characterization of riboflavin supply pathways and genes in <i>A. salmonicida</i>	247
5.3.3. Experimental characterization of riboflavin supply pathways in <i>A. salmonicida</i>	250
5.3.3.1. Bacterial growth in minimal media.....	250
5.3.3.2. Total RNA extraction, Reverse Transcription, and Polymerase Chain Reaction (RT-PCR).....	250
5.3.4. <i>A. salmonicida</i> gene functionality assays.....	251
5.3.4.1. Construction of complementation plasmids with <i>A. salmonicida</i> <i>ribB</i> , <i>ribBA</i> , <i>ribN</i>	251
5.3.4.2. Construction of <i>E. coli</i> Δ <i>ribA</i> mutant and complementation plasmid...	252
5.3.4.3. Functional complementation analysis in <i>E. coli</i> heterologous model...	252
5.3.5. <i>A. salmonicida</i> transcriptomics and qPCR analyses.....	253
5.3.5.1. Bacterial growth in minimal media with and without riboflavin, RNA extraction, and cDNA synthesis.....	253
5.3.5.2. Library preparation and RNA sequencing.....	253
5.3.5.3. RNA-seq data analyses.....	254
5.3.5.4. Gradient PCR.....	255
5.3.5.5. RT-qPCR.....	255

5.3.6. <i>A. salmonicida</i> mutants' construction and characterization.....	257
5.3.7. Evaluation of <i>A. salmonicida</i> virulence in lumpfish (<i>C. lumpus</i>).....	258
5.3.7.1. Bacterial inocula preparation.....	258
5.3.7.2. Fish holding.....	259
5.3.7.3. Infection and Challenge.....	259
5.3.7.4. Colonization of <i>A. salmonicida</i> wild-type and mutants in lumpfish tissues.....	260
5.3.8. Statistical analyses.....	260
5.4. Results.....	261
5.4.1. <i>A. salmonicida</i> encodes a full RBP with additional <i>ribB</i> and <i>ribE</i> copies and a RibN riboflavin transporter.....	261
5.4.2. Riboflavin influences the expression of a small set of genes, including <i>ribB</i>	275
5.4.3. Riboflavin biosynthesis genes <i>ribA</i> , <i>ribB</i> , and <i>ribE1</i> are required for <i>A. salmonicida</i> virulence in lumpfish.....	281
5.5. Discussion.....	290
5.6. Conclusions.....	298
5.7 References.....	299
5.8. Supplementary Materials.....	307
Chapter 6. General Conclusions.....	322
6.1. Summary of results.....	322
6.2. Future directions.....	328
6.3. Overall thesis conclusion.....	333

6.4. References.....334

List of Tables

Chapter 2

Table 2.1. Host-pathogen interactions of significant marine Gram-positive bacteria.....46

Table 2.2. Examples of recent studies on the host (fish) response to marine Gram-positive bacterial pathogens.....70

Chapter 3

Table 3.1. qPCR primers used in this study.....119

Chapter 4

Table 4.1. Selected DEGs associated with enriched pathways of interest from ClueGO analyses at 28 and 98 dpi.....200

Chapter 5

Table 5.1. List of strains and plasmids used in this study.....248

Table 5.2. Riboflavin supply genes in *A. salmonicida*.....265

Table 5.3. Nineteen Differentially Expressed Genes (DEG) from transcriptomics.....279

List of Figures

Chapter 1

Figure 1.1. *R. salmoninarum* and lumpfish.....19

Figure 1.2. *A. salmonicida* riboflavin supply pathways and lumpfish.....22

Chapter 2

Figure 2.1. Schematic representation of A. How virulence is modulated in a dynamic host-pathogen interaction and B. How the disease process occurs as a result of complex host-pathogen-environment interactions.....42

Figure 2.2. Host-centric and pathogen-centric views of dynamic host-pathogen interactions between marine Gram-positive bacteria and a marine fish host.....43

Figure 2.3. Schematic representation of host-pathogen interactions between marine fish and opportunistic *Streptococcus* spp.....52

Figure 2.4. Host-pathogen interactions during the intracellular entry, replication, and survival of *R. salmoninarum*.....54

Figure 2.5. Host-pathogen interactions during intracellular evasion strategies of *M. marinum*.....63

Chapter 3

Figure 3.1. *R. salmoninarum* infection in lumpfish.....110

Figure 3.2. Bacterial Kidney Disease clinical signs, survival rates, and tissue colonization of *R. salmoninarum* infected lumpfish.....126

Figure 3.3. Histopathology changes in lumpfish tissues during <i>R. salmoninarum</i> infection.....	129
Figure 3.4. Expression of transcripts related to pattern recognition (A-E) and cytokines (F-M) in lumpfish head kidney in response to <i>R. salmoninarum</i> infection at 28 and 98 days post-infection (dpi).....	132
Figure 3.5. Expression of transcripts related to the regulation of the innate (A-E) and inflammatory (F-I) immune response in lumpfish head kidney in response to <i>R. salmoninarum</i> infection at 28 and 98 dpi.....	135
Figure 3.6. Expression of transcripts related to humoral (A-F) and cellular mediated (G-K) immunity in lumpfish head kidney in response to <i>R. salmoninarum</i> infection at 28 and 98 dpi.....	138
 Chapter 4	
Figure 4.1. Overview of the experimental infection, cumulative mortality and RNA-seq-based transcriptomics.....	176
Figure 4.2. Global transcriptomic profiling of the lumpfish head kidney response to <i>Renibacterium salmoninarum</i> at early (28 dpi) and chronic (98 dpi) infection stages by RNA-seq.....	187
Figure 4.3. Global view of ClueGO-based gene ontology enrichment networks in lumpfish head kidney at 28 and 98 dpi.....	191
Figure 4.4. ClueGO-based enriched gene ontology terms of all upregulated and downregulated genes in lumpfish head kidney at 28 dpi.....	195

Figure 4.5. Gene expression correlation (high) between qPCR and RNA-seq data for 18 genes of interest.....	204
Figure 4.6. Lysozyme activity and antibody titers in lumpfish serum upon <i>R. salmoninarum</i> infection.....	208
Figure 4.7. Lumpfish head kidney transcriptome response to <i>R. salmoninarum</i> at early (28 dpi) and chronic (98 dpi) infection stages.....	224
Chapter 5	
Figure 5.1. <i>In-silico</i> and experimental characterization of riboflavin supply pathways in <i>A. salmonicida</i>	263
Figure 5.2. Sequence alignment, three-dimensional (3D) protein structures, and functionality of <i>ribB</i> , <i>ribA</i> , and <i>ribBA</i> (or <i>ribBX</i>) genes.....	268
Figure 5.3. Sequence and structural alignments of <i>A. salmonicida</i> riboflavin synthases RibE1 and RibE2.....	271
Figure 5.4. Functionality of <i>A. salmonicida</i> RibN family transporter is confirmed by complementing <i>E. coli ribB</i> mutant with the plasmid expressing the <i>A. salmonicida ribN</i>	274
Figure 5.5. Effect of extracellular riboflavin on <i>A. salmonicida</i> J223 global transcriptomic response and expression of riboflavin supply pathway genes.....	277
Figure 5.6. Growth of <i>A. salmonicida</i> J223 wild-type and mutant strains in M9 minimal media supplemented with (2 μ M) and without riboflavin (RF).....	283
Figure 5.7. Virulence and immune protection of <i>A. salmonicida</i> mutants in lumpfish...	286

Figure 5.8. Lumpfish spleen, liver, head kidney, brain, and blood tissue colonization by *A. salmonicida* J223 wild-type versus mutant strains $\Delta ribA$, $\Delta ribB$, $\Delta ribE1$, $\Delta ribA-\Delta ribE1$, $\Delta ribBA$, $\Delta ribE2$, and $\Delta ribN$ at 3, 7, and 10 dpi.....288

List of Abbreviations

4-MU	4-Methylumbelliferone
ABC transporter	ATP-binding cassette transporter
ANOVA	Analysis of variance
AQ3	Aquatic level 3
BCL3	B-cell lymphoma 3
BKD	Bacterial kidney disease
BP	Biological processes
C3b	Complement B
CARD	Caspase-associated recruitment domain
CC	Cellular components
CCL13	C-C motif chemokine-like 13
CCR7	C-C chemokine receptor 7-like
CD	Cluster of differentiation
CD4	Cluster of differentiation 4
Cd4a, Cd4b	T-cell surface glycoprotein CD4a/b
CD74	Cluster of differentiation 74
CD8	Cluster of differentiation 8
Cd8a	T-cell surface glycoprotein CD8a
CDRF	Cold-Ocean Deep-Sea Research Facility
CFU	Colony-forming units
Ch25a	cholesterol 25-hydroxylase-like protein a
CHSE	Chinook Salmon Embryo
CISH	Cytokine-inducible SH2 (Src homology 2) domain protein
CLCGWB	CLC Genomics Workbench
CLEC12b	C-type lectin domain family 12-member b
CLEC4E	C-type lectin domain family 4 member E
CLRs	C-type lectin receptors
CMI	Cell-mediated immunity

CNS	Central Nervous System
COX2	Cyclooxygenase 2
Ct	Cycle threshold
CTL	Cytotoxic T-lymphocytes
CXCL19	C-X-C motif chemokine 19
CXCR1	C-X-C chemokine receptor type 1-like
Cxcr4	C-X-C chemokine receptor type 4-like
DEG	Differentially expressed genes
dpi	Days post-infection
DtxR	Diphtheria toxin repressor
ELISA	Enzyme-Linked Immunosorbent Assay
EPC	Epithelioma Papillosum Cells
ER	Endoplasmic reticulum protein
ERK	Extracellular signal-regulated kinase
ESPrict	Easy Sequencing in PostScript
ESX	Early secreted antigenic target exporters
FAD	Flavin adenine dinucleotide
FAO	Food and Agriculture Organization
FC	Fold-change
FDR	False discovery rate
FMN	Flavin mononucleotide
Fur	Ferric uptake regulator family
GATA-3	Proteins recognize G-A-T-A nucleotide/types
GLM	General linear model
GO	Gene Ontology
GOI	Gene of Interests
GZm	Granzyme
HAMP	Hepcidin antimicrobial peptide
<i>hasA</i> and <i>hasB</i>	Hyaluronic acid synthesis encoding genes
Hly	Hemolysins

HmuTUV (HmuO)	Heme uptake and utilization
hpi	Hours post-infection
IdeR	Iron-dependent repressor
IFN- or <i>ifng</i>	Interferon gamma
Ig	Immunoglobulin
IL (<i>il1b, il8a, il8b, il6, il10</i>)	Interleukins
IL-10Rb	Interleukin-10 receptor subunit beta-like
iNOS	Inducible nitric oxide synthase
JAK-STAT	Janus Kinase and Signal Transducer and Activator of Transcription
KEGG	Kyoto Encyclopedia of Genes and Genomes
LB	Luria Bertani
Lcn2	Lipocalin
LD50	Median lethal dose
Log	Logarithm
LPS	Lipopolysaccharide
M9	Minimal media
MAPK	Mitogen-activated protein kinase
Mb	Megabase
MF	Molecular functions
mg	Milligram
MHCI	Major-histocompatibility class I
MHCII	Major-histocompatibility class II
mL	Milliliter
MSA	Major soluble antigen
MUN	Memorial University of Newfoundland
MX1-3	Interferon-induced GTP-binding protein 1–3
MyD88	Myeloid differentiation primary response 88
NADPH	Nicotinamide adenine dinucleotide phosphate hydrogen
NCBI	National Center for Biotechnology Information
NFkB	Nuclear factor kappa B

NKEF	Natural killer cell enhancing factor
NLRs	NOD-like receptors
OD	Optical density
P	Phosphorylation
PCA	Principal component analysis
PCR	Polymerase chain reaction
PE	Pro-Glu protein
PFN	Perforin
PGN	Peptidoglycans
PGRP	Peptidoglycan recognition proteins
PknG	Protein Kinase G
Pmol	Picomole
PPE	Pro-Pro-Glu protein
PRR	Pattern recognition receptors
PVS	Phenyl Vinyl Sulfone
q-PCR	Quantitative PCR
Q _H	Structural homology
RBP	Riboflavin biosynthetic pathway
RedOx	Reduction/oxidation
RIN	RNA integrity number
RMSD	Root mean square deviation
RNA-Seq	RNA sequencing
ROI	Reactive Oxygen Intermediates
ROS	Reactive oxygen species
RPS	Relative percentage survival
RQ	Relative quantity
RSEM	RNA-Seq by expectation maximization
<i>Rsh</i>	Cytolysin-encoding gene
RT-PCR	Reverse transcription polymerase chain reaction
RT-qPCR	Real-time quantitative polymerase chain reaction

Saa5	Serum amyloid A 5
Sag	Streptolysin S-associated protein
SD	Standard deviation
SE	Standard error
SimA	<i>Streptococcus iniae</i> M-like protein A
SLS	Streptolysin S
SOCS	Suppressors of cytokine signalling
SRA	Sequence read archive
SrtD	Sortase D
STAMP	Structural Alignment of Multiple Proteins
STAT	Signal transducer and activator of transcription
T-bet	T-box transcription factor
T3SS	Type three secretion system
TAP	Protein associated with antigen processing
TCR	T-cell receptor
TGF-/ <i>tgfb</i>	Transforming growth factor beta
Th1	T helper cell type 1
Th2	T helper cell type 2
TLR	Toll-like receptors
TMM	Trimmed mean of M-values
TNFA	Tumor necrosis factor alpha
Tnfrsf11b	Tumor necrosis factor receptor superfamily member 11b
Tnfrsf6b	Tumor necrosis factor receptor superfamily member 6b
TPM	Transcript per million reads
TSA	Trypticase soy agar
TSB	Trypticase soy broth
UV	Ultraviolet
VMD	Visual Molecular Dynamics
μg	Microgram
μL	Microlitre

μM

Micromolar

List of Supplementary Files, Tables, and Figures

Chapter 3

Supplementary File S3.1. A. Trinity IDs and respective sequences of Gene of Interests used in this study; B. Blastn against NCBI refseq results; C. Blastx against NCBI swissprot results (excel).

Supplementary Table S3.1. Relative quantity (RQ) values of Genes of Interest (GOI) from qPCR analyses (excel).

Supplementary Table S3.2. Cycle threshold (Ct) values of Gene of Interests (GOI) obtained from qPCR analyses (excel).

Supplementary Figure S3.1. *Renibacterium salmoninarum* colonization in high-dose infected lumpfish ($n = 6$) spleen, liver, and head kidney at A. 14, B. 28, C. 42, D. 56, E. 84, and F. 98 dpi.....161

Supplementary Figure S3.2. Expression of transcripts related to pattern recognition (A-E) and cytokines (F-M) in lumpfish head kidney in response to *R. salmoninarum* infection at 28 and 98 dpi162

Supplementary Figure S3.3. Expression of transcripts related to the regulation of the innate (A-E) and inflammatory (F-I) immune response in lumpfish head kidney in response to *R. salmoninarum* infection at 28 and 98 dpi.....164

Supplementary Figure S3.4. Expression of transcripts related to humoral (A-F) and cellular mediated (G-K) immunity in lumpfish head kidney in response to *R. salmoninarum* infection at 28 and 98 dpi.....166

Chapter 4

Supplementary File S4.1. Total and differentially expressed genes in lumpfish head kidney at 28 and 98 dpi (excel).

Supplementary Table S4.1. Bioanalyzer data for the RNA samples ($n = 12$) used in the transcriptomic profiling of the lumpfish head kidney infected with *R. salmoninarum* at 28 and 98 dpi.....235

Supplementary Table S4.2. Mapping Statistics of the RNA-seq data.....236

Supplementary Table S4.3. Enriched GO terms in lumpfish head kidney from ClueGO analysis performed on the list of total DEGs ($n=1971$) at 28 dpi (excel).

Supplementary Table S4.3. Enriched GO terms in lumpfish head kidney from ClueGO analysis performed on the list of total DEGs ($n=1971$) at 28 dpi (excel)

Supplementary Table S4.4. Enriched GO terms in lumpfish head kidney from ClueGO analysis performed on the list of total DEGs ($n=139$) at 98 dpi (excel)

Supplementary Table S4.5. Enriched GO terms in lumpfish head kidney from ClueGO analysis performed on the list of total upregulated genes ($n=434$) at 28 dpi (excel).

Supplementary Table S4.6. Enriched GO terms in lumpfish head kidney from ClueGO analysis performed on the list of total downregulated genes at 28 dpi (excel).

Supplementary Figure S4.1. RNA-seq data quality.....237

Supplementary Figure S4.2. Gene expression correlation (mid to low) between qPCR and RNA-seq data for 12 genes of interest. RNA-seq data are presented as \log_2 TPM (X axis).....238

Chapter 5

Supplementary File S5.1. Total genes expressed in <i>A. salmonicida</i> in response to extracellular riboflavin (excel)	
Supplementary Table S5.1. Primers for Reverse Transcription PCR (RT-PCR) used to amplify gene junctions of <i>rib</i> gene operons.....	308
Supplementary Table S5.2. qPCR primers and primer efficiency.....	309
Supplementary Table S5.3. Primers for mutants and plasmids construction.....	310
Supplementary Table S5.4. Mapping Statistics of Transcriptomics.....	311
Supplementary Table S5.5. Biochemical profiles of wild-type and mutants of <i>A. salmonicida</i> using the API 20E.....	312
Supplementary Table S5.6. Biochemical profiles of wild-type and mutants of <i>A. salmonicida</i> using the API 20NE.....	313
Supplementary Table S5.7. Enzymatic profiles of wild-type and mutants of <i>A. salmonicida</i> using the API-ZYM.....	314
Supplementary Figure S5.1. Experimental designs for <i>A. salmonicida</i> transcriptomics and qPCR analyses.....	315
Supplementary Figure S5.2. Gradient PCR, Primer efficiency and Endogenous control genes selection for qPCR analysis.....	316
Supplementary Figure S5.3. Evaluation of <i>A. salmonicida</i> J223 wild type and mutant strains virulence in lumpfish (<i>C. lumpus</i>).....	318
Supplementary Figure S5.4. <i>A. salmonicida</i> RNA-seq and gene expression correlation.....	319

Supplementary Figure S5.5. Deletion maps and PCR verifications of Single (A-F) and double (G) deletion mutants of *A. salmonicida* constructed and used in this study.....321

Chapter 1: General Introduction

1.1. Bacterial pathogens of marine fish aquaculture

Aquaculture, the process of farming aquatic organisms (i.e., fish, shellfish, and aquatic plants), is one of the fastest growing food production sectors with an annual average growth rate of 3.3% during the period 2015-2020 and has an undeniable role in food security, helping to supply the global demand for seafood nutrition [1]. The live-weight volume of global aquaculture production has increased by more than three times, from 34 Mt in 1997 to 112 Mt in 2017, and is still growing, though at a slower rate [2]. Per-capita aquatic animal food consumption was 20.2 kg in 2020, and approximately half of the fish consumed globally is currently produced by aquaculture (i.e., 56% in 2020), and its share is anticipated to rise by a further 15% by 2030 [1].

Given its rapid expansion and intensified production, the aquaculture industry has become increasingly vulnerable to infectious diseases (i.e., viral, bacterial, fungal, and parasitic fish diseases). Bacterial fish pathogens are a chronic risk to aquaculture and cause economic losses in both wild and cultured fish [2,3]. Over 13 bacterial genera have been reported as potential disease-causing agents in the aquaculture industry worldwide [4]. Bacterial fish pathogens, either Gram-positive or Gram-negative, can cause systemic infections by infecting several fish organs, or they may cause ulcerations in the skin, gills, fins, and mouth, which lead to external infections [5]. The majority of the marine fish pathogens are Gram-negative bacteria, such as *Aeromonas salmonicida*, *Vibrio anguillarum*, *Moritella viscosa*, *Piscirickettsia salmonis*, and *Yersinia ruckeri* [4,6]. On the other hand, Gram-positive bacteria, including a few acid-fast, are less frequent than Gram-

negative pathogens but still can cause substantial losses in marine fish culture [6]. The most prevalent marine Gram-positive pathogens are *Renibacterium salmoninarum*, *Mycobacterium marinum*, *Lactococcus garviae*, and *Streptococcus* spp.

Fish disease development is a complex process that depends on the pathogen's ability to cause the disease, bacterial virulence, fish host immunity, and environmental conditions. The key to understanding the disease, its treatment and prevention is investigating host-pathogen interactions [7]. Despite the current knowledge on bacterial virulence, several fundamental aspects of Gram-positive and Gram-negative bacterial pathogens of marine fish need to be determined to develop sustainable and effective control measurements towards eradication plans. In the thesis, the Gram-positive *R. salmoninarum* and the Gram-negative *A. salmonicida* were selected to study some aspects of pathogenicity and/or virulence by considering their prevalence and economic importance in the marine finfish aquaculture industry.

1.2. The Gram-positive pathogen *Renibacterium salmoninarum*

R. salmoninarum is a small (i.e., 0.8-2 μm), rod-shaped, facultative intracellular, non-motile, non-acid-fast Gram-positive fish pathogen that causes Bacterial kidney disease (BKD) in wild and cultured salmonid fish [8,9]. BKD is a slowly progressing systemic infection that causes mortalities in juvenile salmonids and cultured brood stocks [10]. BKD affects sustainable salmonid production where economic losses of 80% and 40% have been reported in Pacific salmon (*Oncorhynchus* spp.) and Atlantic salmon (*Salmo salar*), respectively [11]. Due to the chronic nature of infections and the frequent presence of co-infections, the impact of *R. salmoninarum* on fish populations is difficult to assess [11].

Natural outbreaks of BKD have affected salmonid family members [10], and the susceptibility of salmonids to BKD varies [12]. For instance, Pacific salmon, pink salmon (*Oncorhynchus gorbuscha*), sockeye salmon (*Oncorhynchus nerka*), and chinook salmon (*Oncorhynchus tshawytscha*) are more susceptible compared to Atlantic salmon and rainbow trout (*Oncorhynchus mykiss*) [9,13]. *R. salmoninarum* infection has also been reported in non-salmonid fish and bivalve mollusks [12]. Several non-salmonids, such as sablefish (*Anoplopoma fimbria*) [14] and Pacific herring (*Clupea harengus pallasii*) [15], have been experimentally infected and demonstrated mortality, raising the possibility that the non-salmonids could serve as a vector for *R. salmoninarum* [13]. Although *R. salmoninarum* primarily infects salmonids, the range of non-salmonid host species vulnerable to its infection or functioning as a carrier is considerably greater and more diversified than is typically believed [16].

R. salmoninarum is more persistent within fish populations as it may transmit horizontally (i.e., fish to fish) and vertically (i.e., parent to progeny) [15]. Ingestion of infected fish carcasses (i.e., fish viscera) or feces in marine and freshwater might result in horizontal transmission [10,17]. Given that the *R. salmoninarum*'s survival outside the host is generally brief (4-21 days at 10-18 °C), horizontal transmission via inhabited water is restricted [10,18,19]. On the other hand, vertical transmission involves the eggs, where *R. salmoninarum* is present in the coelomic fluid and enters the egg yolk during fertilization [10,20]. *R. salmoninarum* transmission has also been documented from farm to farm, within farm cages, and via infected wild or escaped fish, which may serve as a reservoir [19]. Interestingly, the sea louse (*Lepeophtheirus salmonis*), an ectoparasitic copepod

crustacean and the most pathogenic parasite in salmon farming [21], has also been speculated to be a vector for *R. salmoninarum*; however, this has not been verified [22,23].

Generally, fish with BKD showed clinical signs, such as lethargy, skin darkening, abdominal distension by ascites, petechial hemorrhages on the body, pseudomembrane formation on the internal tissues, and enlargement of the spleen and head kidney [10]. BKD is histologically characterized by bacteremia associated with systemic, chronic granulomatous inflammation and pigment dispersal in tissues as a result of melanomacrophage lysis [24,25].

R. salmoninarum is a facultative intracellular pathogen that can withstand host defenses by intracellularly surviving and replicating within the fish macrophages [10]. *R. salmoninarum*'s capacity for immunosuppression, both *in vitro* and *in vivo*, has been amply elucidated [13].

Major soluble antigen (MSA) p57, a significant outer membrane, and secretory protein, is a predominant virulence factor of *R. salmoninarum* that mediates immune suppression [9]. The biological functions of p57 have been well demonstrated, including binding and agglutinating fish leucocytes and suppressing respiratory burst, salmonid antibody production, and bactericidal activity of phagocytes [9,10]. Hydrophobic and hemagglutinating characteristics of p57 aid *R. salmoninarum* in adhering to host cells [26–28]. Specific and non-specific binding of p57 to host cell receptors and its interaction with host proteins facilitate the intracellular invasion of *R. salmoninarum* [25,29]. There is no homolog of the *msa* gene, which encodes for the p57 protein, in any other bacterial species [30]. The *msa* genes are present in two copies (i.e., *msa1* and *msa2*) in the majority of *R. salmoninarum* strains, and both are essential for virulence and the development of disease

[31,32]. In addition, multiple *msa* gene copies (i.e., ranging from 2-5) were reported in various *R. salmoninarum* isolates [33,34]. Overall, the virulence of *R. salmoninarum* is linked to the p57 abundance at the bacterial surface and the number of functional *msa* gene copies [33,35].

Another major virulence protein associated with immune suppression is p22, a 22 kDa surface protein [36]. p22 suppressed antibody production by Atlantic salmon B cells *in vitro* and agglutinated Atlantic salmon leucocytes more strongly than p57 [36]. Intriguingly, similar to p57, p22 exhibits *msa* copy number variation ranging from 1 to 5 copies, indicating a functional relationship between these two *R. salmoninarum* virulence proteins [34]. Future research is needed to determine the precise function of p22 in virulence, the immune suppressor domains of p57 and p22, and the interaction of p22 and p57 during immune suppressive infection of *R. salmoninarum*.

R. salmoninarum pathogenesis is still not completely understood. On the other hand, fish immune response to *R. salmoninarum* is an active area of research. Host-pathogen interactions between salmonid fish and *R. salmoninarum* have been examined in several studies by measuring gene expression changes or analyzing the global transcriptomic and proteomic profiles during infection *in vitro* and *in vivo* [37–41]. These studies, however, are limited to salmonids only. Establishing experimental infection models and analyzing the host immune response of non-salmonid fish species would be valuable in understanding the *R. salmoninarum* pathogenesis in non-salmonids, especially in light of the growing list of susceptible hosts to *R. salmoninarum* infection. Further research will also require to comprehend the pathogen-specific immune evasion mechanisms, the host-specific killing mechanisms, humoral/cell-mediated adaptive

immunity-related pathways, and biomarkers of protective immunity / favorable immune responses / vaccine efficacy.

Major BKD control strategies include the administration of chemotherapeutants, vaccines, dietary modifications, and improved hygiene, husbandry, and biosecurity procedures [9]. Vaccine design for *R. salmoninarum* has centered on heat/formalin-inactivated whole cell or lysed bacterins as well as live vaccines containing attenuated *R. salmoninarum* strains with reduced or normal cell-associated MSA [12].

Renogen[®], a lyophilized preparation that contains live cells of the non-pathogenic environmental bacterium *Arthrobacter davidanieli*, is the only BKD vaccine that has received a commercial license [12]. The phylogenetic relationship between *R. salmoninarum* and *A. davidanieli* is relatively close, which is probably the reason why Renogen[®] offers cross-species protection [30]. An *Arthrobacter* surface carbohydrate that resembles the exopolysaccharide of *R. salmoninarum* is thought to be responsible for the live vaccine's stimulatory effects [42]. Renogen[®] conferred significant protection for Atlantic salmon [42], in contrast, it showed no or limited efficacy in juvenile chinook salmon [43,44]. Developing an effective vaccine design against BKD for a broader range of salmonid and non-salmonid fish is crucial. To do so, finding immune protective epitopes using a reverse vaccinology approach or altering the immune suppressor domains of virulence factors p57 and p22 would be beneficial.

1.3. The Gram-negative pathogen: *Aeromonas salmonicida*

Aeromonas salmonicida subsp. *salmonicida* is a Gram-negative, facultative intracellular pathogen that causes furunculosis in a wide range of fresh and marine water

fish species [45,46]. This bacterium is a non-motile, anaerobic, and rod-shaped psychrotroph [46]. *A. salmonicida* is associated with systemic infections in salmonids, including brown trout (*Salmo trutta*), Atlantic salmon, rainbow trout, and coho salmon (*Oncorhynchus kisutch*) [47]. In addition to salmonids, *A. salmonicida* infection is reported in non-salmonids, such as Atlantic cod (*Gadus morhua*), carp (*Cyprinus carpio*), turbot (*Scophthalmus maximus*), sablefish, cunners (*Tautoglabrus adspersus*) and lumpfish (*Cyclopterus lumpus*) [5,47,48].

Furunculosis is primarily transmitted horizontally, such as when susceptible fish come into contact with diseased or carrier fish, contaminated water, or equipment [6,49]. Entry points include the skin, gut, and gills [49,50]. Salmonids experience acute, sub-acute, and chronic *A. salmonicida* infections and present furuncles or “boil-like” lesions [51,52]. The skin and musculature of fish with acute and chronic forms of furunculosis exhibit furuncles [5]. External hemorrhagic lesions around the fin base and oral cavity, skin darkening, loss of appetite, lethargy, and irregular swimming are clinical indications of chronic or peracute disease, whereas infected fish rapidly die without any clinical signs in the acute disease [5]. In the early stage of furunculosis, *A. salmonicida* microcolonies can be found in the spleen, kidney, heart, muscles, and gills [53]. Histopathological observations of the acute disease include petechia and hemorrhages externally and in internal organs, enlarged spleen and kidney, pale liver, intestinal congestion, and necrosis [5,51]. Chronic disease causes widespread necrosis [52].

The A-layer, extracellular products, type three secretion system (T3SS), and iron acquisition mechanisms are among the virulence factors that contribute to the *A. salmonicida* pathogenicity to fish [46,54]. The A-layer, an outer membrane protein (OMP)

that is associated with lipopolysaccharides (LPS), allows *A. salmonicida* to adhere to host proteins and aid colonization [54]. Black rockfish (*Sebastes schlegeli*) infected with *A. salmonicida* outbreak strains that have A-layer and hemolytic potential showed clinical signs of furunculosis and mortality compared to the strains that lacked A-layer or were not hemolytic [55]. Thus, the presence of the A-layer is linked to *A. salmonicida* virulence. Extracellular products such as proteases, lipases, and hemolysins are the virulence factors that support *A. salmonicida* proliferation and disease development by weakening the host defense mechanisms and obtaining host nutrients [46,54]. T3SS also referred to as ‘injectisome’, has been found to have a major impact on virulence so far among the several *A. salmonicida* virulence factors [56]. Intracellular survival of *A. salmonicida* has been linked to a number of T3SS effector proteins that have been identified [56,57]. For instance, one of the effector proteins, AopO, which is overexpressed by *A. salmonicida* during the infection process, affected its virulence during an immersion challenge in Atlantic salmon [58,59]. The effector proteins AopP, AopN, and AopS may contribute to immune suppressive infection of *A. salmonicida* [52]. Iron is an essential nutrient for pathogenic bacteria and is often associated with their virulence and survival within the host [54]. *A. salmonicida* can acquire iron using siderophores (i.e., amonabactin, acinetobactin, and anguibactin-like siderophores), which are low-molecular-weight iron chelators that aid in liberating iron from host iron-binding proteins (e.g., transferrin, ferritin, hepcidin, and lipocalin) and allowing it to enter into bacterial cells through iron-regulated outer membrane receptor proteins [60–62]. In contrast, *A. salmonicida* can also use siderophore-independent iron acquisition mechanisms, including iron removal from hemoglobin by haem-binding proteins [60,63]. For instance, *A. salmonicida* expressed both a ferric

siderophore and a haem outer membrane receptor under *in vitro* iron-limited conditions [64]. Bacterial acquisition of other essential nutrients, such as vitamins, and their role in *A. salmonicida* growth and pathogenesis inside the fish host are still poorly understood and warrant future research.

Strategies to prevent furunculosis include vaccines, antimicrobial agents, and selective breeding for disease resistance. Three vaccines are currently licensed to prevent furunculosis in salmonids, including Forte Micro® (*Aeromonas salmonicida*-*Vibrio anguillarum-ordalii-salmonicida* bacterin), Forte VII® (Infectious Salmon Anaemia killed virus vaccine, *A. salmonicida*, *Vibrio anguillarum-ordalii-salmonicida* bacterin), and Alpha Ject Micro 4® (*A. salmonicida*-*Listonella (Vibrio) anguillarum-Vibrio salmonicida* bacterin) [47]. However, studies on vaccine efficacy under field conditions and vaccine designs against *A. salmonicida* infection for new aquaculture species are insufficient. Florfenicol (Aquaflor®), sulfadimethoxine/ormetoprim (Romet® 30), and oxytetracycline hydrochloride (Terramycin-Aqua) are the only antibiotics now licensed in Canada to treat furunculosis in fish and must be delivered through feed [47]. However, there is rising concern over the emergence of bacteria that are resistant to antibiotics. The use of probiotics and phage therapy may be the most promising alternative remedies now being researched [52].

Overall, while *A. salmonicida* as a globally distributed and most significant bacteria affecting aquaculture, fundamental research is still desperately needed to better understand this pathogen, its nutrient supply pathways, virulence, and physiology, and how they interact with the immune system of salmonids and non-salmonids.

1.4. Bacterial riboflavin supply pathways

Vitamins are essential components of fish diet formulations and the most expensive ingredient in finfish aquafeeds. Vitamins have been shown to enhance fish immune responses to infection by influencing the migration and proliferation of immune cells, such as phagocytic cells, and improve fish resistance to bacterial diseases [65–67]. On the other hand, vitamins are also vital for bacterial pathogens, influencing their physiology and virulence [68–72]. Vertebrates sequester essential micronutrients, like amino acids and vitamins, from invading pathogens as a means of nutritional immunity [73,74]. For instance, vertebrates limit the availability of essential vitamins (e.g., vitamin A, B-vitamins, vitamin D, and vitamin K) in their tissues by employing high-affinity vitamin-binding proteins (e.g., Retinol-binding protein, B vitamin-binding proteins, vitamin D-binding protein) and deprive pathogens of key growth components (i.e., vitamins) [68–72,75–79]. Thus, bacterial pathogens have to either biosynthesize vitamins or scavenge them through uptake systems.

B vitamins (e.g., Riboflavin B₂) are among the most commonly required biochemical cofactors in living systems, with very limited availability in marine environments [80,81]. Riboflavin is the precursor of canonical cofactors, flavin mononucleotide (FMN) and flavin adenine dinucleotide (FAD), which are collectively known as flavins and crucial for intracellular flavoprotein-mediated redox reactions [82,83]. Flavoenzymes participate in diverse biological processes, including the metabolism of carbohydrates, proteins, fats, and vitamins (i.e., folate and pyridoxine), oxidative stress response, and photosensitization [84–86]. The utilization of extracellular

riboflavin by bacteria has been related to various processes, such as iron reduction, extracellular respiration, symbiotic interactions, and quorum sensing [87–90].

While vertebrates obtain riboflavin through their diets or from symbiotic microorganisms, most bacteria biosynthesize riboflavin *de novo* through the riboflavin biosynthetic pathway (RBP) or uptake riboflavin from their extracellular milieu through high-affinity transporters [91–97]. In the context of cell energy, riboflavin biosynthesis is more costly than uptake [88,98]. When riboflavin is environmentally available, bacteria switch from vitamin biosynthesis to uptake [99].

Bacterial riboflavin supply pathways are diverse and adapt to the species-specific metabolic needs of this essential vitamin. Different bacterial species have different transcriptional orchestration of RBP genes, some species grouping the pathway genes into a single operon and others placing their RBP genes in various transcriptional units throughout the chromosome [99]. To produce riboflavin, RBP involves five enzymes, including GTP cyclohydrolase II (RibA), a bifunctional pyrimidine deaminase/reductase (RibD), 3,4-dihydroxy-2-butanone-4-phosphate (3,4-DHBP) synthase (RibB), 6,7-dimethyl-8-ribityllumazine (lumazine) synthase (RibH) and riboflavin synthase (RibE) [83,86,100]. There have been nine distinct families of bacterial riboflavin transport systems identified: the energy-coupling factor-RibU, RibM, RibN, RfuABCD, ImpX, RibXYZ, RfnT, RibZ, and RibV [99]. Mostly, a single species of bacteria may conserve both biosynthesis and uptake functions [99]. Conserved FMN riboswitches appear to control the regulatory network of riboflavin biosynthesis and transport in response to intracellular flavin levels [93,94,101–104]. Interestingly, bacteria may encode a variable number of paralogs (i.e., homologous genes or gene copies that arise from a gene duplication event

within the same genome) of RBP enzymes. These gene duplications may provide greater flexibility to bacteria in managing their riboflavin supply [99]. The extra copies of RBP genes may possess specific functions and provide adaptive benefits to the bacteria [99]. Recently, the roles of these redundant subsets of riboflavin-producing genes have begun to be understood [99]. For instance, *Brucella abortus*, which causes brucellosis in mammals, has two copies of the lumazine synthase-encoding gene, *ribH* (i.e., *ribH1* is in the main RBP operon, while *ribH2* is a monocistronic unit located outside of the main operon) [68]. These two gene copies of *ribH* share 21% identity and are active lumazine synthases [105]. When growing in liquid media, the double mutant $\Delta ribH1-\Delta ribH2$ became a riboflavin auxotroph, and single $\Delta ribH1$ or $\Delta ribH2$ mutants grew similarly to the wild-type levels, indicating that RibH1 and RibH2 could be functionally substitutable [68]. However, in a macrophagic cell line and in mice, $\Delta ribH2$ showed significant attenuation (i.e., evident reduction in the CFU counts) while $\Delta ribH1$ and wild-type strains behaved similarly [68]. Overall, the additional copy of the *ribH* gene (i.e., *ribH2*) in *B. abortus* was mainly associated with its intracellular survival and replication in murine macrophages, and spleen colonization in mice, suggesting the modularized RBP with RibH2 to provide this vitamin under specific circumstance (i.e., host colonization) [68,99].

Biosynthesis and transport systems of riboflavin have been identified and characterized in human and terrestrial animal bacterial pathogens [106–108]. However, riboflavin supply pathways of marine pathogens of fish, like *A. salmonicida*, have not been reported.

1.5. Lumpfish

Salmonids contribute 4.6% of the world's seafood supply [1]. Canada contributes 5.06% of the world's salmon production and is the fourth-largest producer of farmed salmon [1,109]. Salmon production represents over 70% of Canada's overall production volume and over 80% of the overall farm-gate value [109]. Atlantic salmon, which is also Canada's top aquaculture export, is the salmonid that is most frequently farmed commercially. Global Atlantic salmon production reached 2.89 million metric tons in 2021 [1].

The major fish health issue compromising the sustainability of the salmon aquaculture industry is sea lice (*Lepeophtheirus salmonis* and *Caligus elongatus*) infestation. *L. salmonis*, an obligate caligid ectoparasite of salmonid fish (especially Atlantic salmon), feed on the fish skin, mucus, and blood in marine environments [110,111]. Sea lice infestations produce physical and biochemical damages, primarily skin lesions, and may result in the risk of secondary infections, osmoregulatory imbalance, stress, and immune suppression [112]. Sea lice infection and transmission potential to a wide range of available hosts, together with the serious damage (i.e., skin injuries) it may inflict on in both wild and farmed fish, make this as the greatest disease challenge in the global Atlantic salmon industry [113]. The effect of sea lice and their treatments accounts for 15% of Atlantic salmon mortalities in Norway and Scotland during 2013-2019 [114]. Globally, the estimated cost of combatting sea lice is 6-9 % of the farm revenues [115]. In Canada, the cost of sea lice control ranged from 16-17 million USD during 2015-2019 [114]. The use of brushes or water jets (i.e., hydrolicers), warm water bath treatments (i.e., thermolicers),

physical barriers (i.e., lice skirts and snorkel cages), light regimes (to influence salmon swimming behavior), and laser technologies are some of the sea lice control methods used in salmon farming [112]. Only a small number of antiparasitic chemotherapeutants (i.e., organophosphates, pyrethroids, and hydrogen peroxide) are currently licensed for sea lice treatment [48,113]. However, parasite resistance to chemotherapeutants makes their efficacy questionable [116,117]. In addition, there is no effective vaccine against sea lice [48]. Recently, non-medical methods, particularly the use of cleaner fish (e.g., Ballan wrasse and lumpfish in North Atlantic countries), have been relied upon primarily to reduce the sea lice infestation in salmon farming [48,112]. Globally around 60 million cleaner fish are used each year for delousing Atlantic salmon [118]. Cleaner fish as a bio-control agent is proved successful and enticing since it is more economical and eco-friendlier compared to chemotherapeutics [111,119] and can be less stressful for farmed fish [120].

The Atlantic lumpfish, a cold water marine teleost native to the North Atlantic, has been utilized as an eco-friendly cleaner fish for sea lice control in Atlantic salmon sea cages. It picks off sea lice of passing fish and consumes them. Lumpfish stocking ratios together with salmon range from 2-5% [112]. Lumpfish is preferred over wrasses because of their ability to feed at low temperatures (i.e., 4 °C) [121] and can be ready for deployment in salmon farms in 4 months post-fertilization [122]. Therefore, demand for lumpfish as cleaner fish has been increasing exponentially in recent years [48]. For instance, in 2019, Norway, the world's largest producer of Atlantic salmon, farmed and marketed 39.1 million juvenile lumpfish. In 2018, Norway deployed 49 million cleaner fish for sea-lice control, and 31 million were lumpfish, most of which were farmed (approximately 93%) [123].

Lumpfish is a relatively new aquaculture species in Canada, and its farming is still emerging. Despite the vast amounts of cleaner fish used, there are still significant knowledge gaps about lumpfish health and welfare that must be filled in order to ensure the sustainability of lumpfish production. Cleaner fish mortality in sea cages in Norwegian aquaculture ranged from 18-48 % over 2013-2019 and reported daily mortality is about 150,000 fish within a year of production cycle [123]. The most significant cause of mortality in lumpfish and one of the key health and welfare issues in its aquaculture are bacterial infections [112]. When lumpfish and salmon coexist in high biomass environments in sea pens, the risk of bacterial infections as well as the risk of infected lumpfish transmitting disease to salmon or vice versa, increases [112,124]. Lumpfish is susceptible to several bacterial pathogens. Typical and atypical *A. salmonicida*, *V. anguillarum*, *V. ordalii*, *Pasteurella* sp., *Pseudomonas anguilliseptica*, *Tenacibaculum* spp., *M. viscosa*, and *P. salmonis* are the fish pathogenic bacteria affecting lumpfish and causing diseases and mortalities [123]. As the number of lumpfish used in salmonid aquaculture continues to rise, it is anticipated that the number of bacterial infections will undoubtedly increase [48], and research so far does not provide a sufficient overview on lumpfish susceptibility to various bacterial pathogens. Research on the likelihood that lumpfish get infected with the main bacterial pathogens of Atlantic salmon farming is imperative to mitigate the disease pressure on lumpfish and Atlantic salmon, thus, both species may be treated simultaneously. Since lumpfish may serve as a reservoir or carrier of potential bacterial pathogens [48,112], the risk they may pose for Atlantic salmon must be thoroughly evaluated in future studies. In addition, basic knowledge of lumpfish biology, immune functions, and how they or their immune system interact with the Gram-positive,

and Gram-negative bacterial pathogens, which are crucial for the development of immune prophylactic measures, are still poorly understood.

To increase survival, decrease antimicrobial usage, and prevent the development of bacterial infections in lumpfish, vaccination is crucial [112]. Commercial vaccines supplied by Pharmaq, Elanco, and Vaxxinova Norway help lumpfish to combat *A. salmonicida* and *Vibrio* sp. infection [123]. In a lumpfish vaccination study by Rønneseth et al. (2017), monovalent and trivalent vaccines containing virulent atypical *A. salmonicida* isolates provided 73 and 60 relative percent survival, respectively [125]. Given that millions of lumpfish are utilized as living pest-removers in aquaculture, the number of available vaccines for lumpfish that induce protective immunity against well-known bacterial pathogens and diverse vaccine trials conducted so far are surprisingly low. In addition, new vaccine designs and vaccination strategies for lumpfish are lagging behind the current situation for main-aquacultured species. For instance, there have been no reports of using live-attenuated vaccines for lumpfish. Overall, research with a strong emphasis on lumpfish host-pathogen interactions, and immune prophylactic measures, including vaccine development and optimization, will not only provide fundamental insights to improve lumpfish health but also lower the risk of transferring infectious bacterial pathogens to Atlantic salmon.

1.6. Relevance and Hypotheses

Deep insight into host-pathogen interactions during pathogenic infection is the key to better understanding the disease and to develop immune prophylactic measures. There are no systematic reviews compiling host-pathogen interactions of fish pathogens,

including marine Gram-positive bacterial pathogens. Therefore, I provided an overview of the host-pathogen interactions between marine finfish and Gram-positive bacteria and summarized the intricate details of pathogen-centric and host-centric points of view in Chapter 2.

Since lumpfish is a relatively new aquaculture species, studying its host-pathogen interactions with Gram-positive *R. salmoninarum* and Gram-negative *A. salmonicida* with a particular focus on fundamental aspects of bacterial pathogenicity and virulence would be valuable. Therefore, I examined the infection kinetics of *R. salmoninarum* in a non-salmonid fish (i.e., lumpfish) and determined how lumpfish respond to *R. salmoninarum* in Chapters 3 and 4. In Chapter 5, I focused on studying the functional role of riboflavin (Vitamin B₂) supply pathways in *A. salmonicida* virulence in lumpfish. The following are chapter-specific relevance and hypotheses:

1.6.1. *R. salmoninarum* and lumpfish

Lumpfish are not only delousing the salmon skin by consuming the parasite but also ingest other potential pathogens transmitted by sea lice and salmon. There is a risk of disease transfer between lumpfish and Atlantic salmon when they cohabit in marine cages due to infected fish acting as disease-transmitting agents and/or the potential for sea lice to act as a disease vector. High biomass environments and open seawater flow in and out of sea cages would increase the opportunity for disease transmission. On the other hand, despite *R. salmoninarum*'s preference for salmonid hosts, a much wider variety of non-salmonid host species are susceptible to its infection or acting as carriers than is typically thought [16], and this pathogen can transmit itself horizontally between different fish species [126,127]. Therefore, my hypothesis for Chapter 3 was that because *R.*

salmoninarum has a wide host range and is capable of horizontal transmission, lumpfish may be a susceptible host to this pathogen and may potentially be at risk for BKD (Figure. 1.1).

Investigating host-pathogen interactions between non-salmonids (i.e., lumpfish) and *R. salmoninarum* is crucial to understand not only the pathogenesis or virulence of *R. salmoninarum* in non-salmonids at molecular levels but also to unravel non-salmonid fish defense to a Gram-positive pathogen. RNA-sequencing-based fish transcriptomics approaches can provide crucial insights into how the host and pathogen interact throughout an infection, revealing the host defense pathways triggered by the pathogen and how the pathogen circumvents host-mediated immune responses. Considering the findings (i.e., qPCR) from Chapter 3, my hypothesis for Chapter 4 was that *R. salmoninarum* causes immune suppression at early infection, whereas lumpfish induce cell-mediated immune response at chronic infection. At the end of Chapter 4, I anticipated presenting a comprehensive picture of the lumpfish host's molecular pathways involved in *R. salmoninarum* infection (Figure. 1.1).

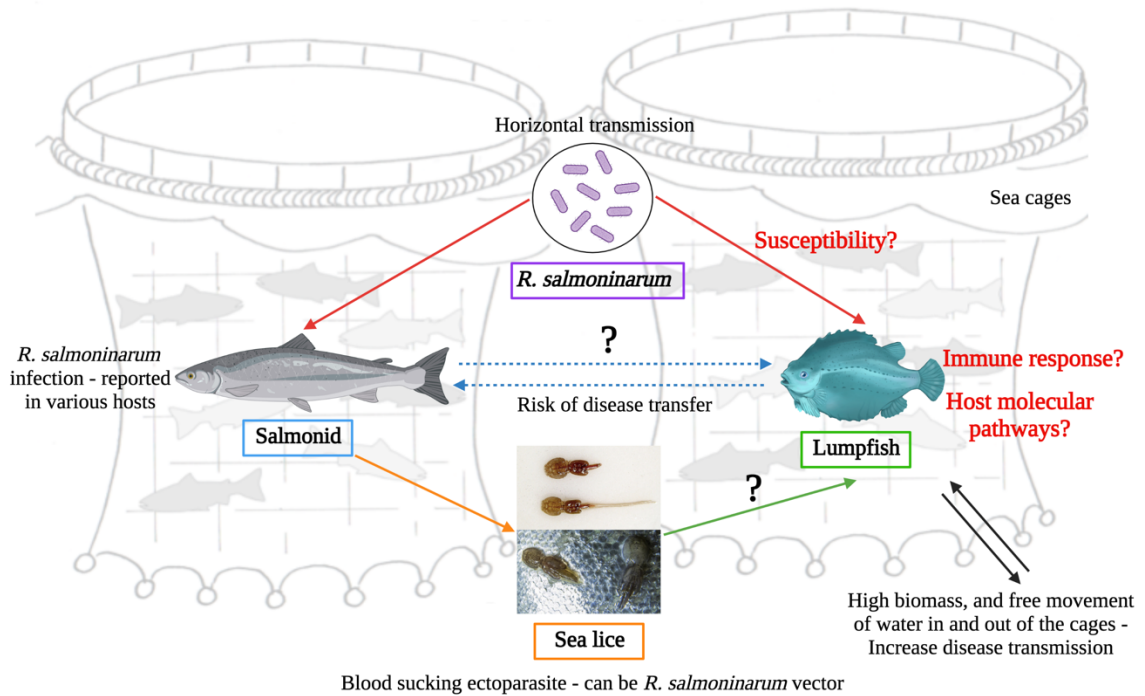


Figure 1.1. *R. salmoninarum* and lumpfish. Due to *R. salmoninarum*'s ability for horizontal transmission [15,126,127], its wide host range [10,16,23,128], the possibility of sea lice as disease vectors while lumpfish are delousing salmon [129], and sea cage conditions that favor such disease transmission (i.e., high biomass inside the cages and unrestricted water flow in and out of the cages) [130], lumpfish may have potential BKD risk. Lumpfish susceptibility and immune response to *R. salmoninarum* have yet to be reported. This figure was created in BioRender (<https://biorender.com/>).

1.6.2. *A. salmonicida* riboflavin supply pathways and lumpfish

A. salmonicida, a pathogen that causes furunculosis in lumpfish, is a good model to study marine psychrotropic pathogenesis [46,57,131–133]. Riboflavin supply pathways of *A. salmonicida* had not been explored prior to the current research.

To provide context for host-pathogen-riboflavin interactions during nutritional immunity, host (lumpfish) and pathogen (*A. salmonicida*) points of view were presented in Figure 1.2. A successful pathogen needs essential micronutrients, like riboflavin, to proliferate inside the host during infection. At pathogen invasion, fish could restrict the availability of riboflavin from its systemic circulation and tissues; as a result, bacteria either biosynthesize riboflavin using its own cellular machinery or uptake it through high-affinity importer systems (Figure 1.2). Riboflavin biosynthesis is essential for the virulence of pathogenic bacteria, and extra RBP gene copies impact pathogenesis, as observed in *B. abortus* [68]. Overall, a better understanding of *A. salmonicida* physiology and virulence mechanisms related to its riboflavin acquisition would be valuable in designing effective prophylaxis. Given the importance of riboflavin in bacteria, my hypothesis for Chapter 5 was that riboflavin provision systems with the assortment of RBP genes, their additional copies, and riboflavin importer might impact *A. salmonicida* physiology and virulence.

Defined biochemical mutations on riboflavin provision pathways in a pathogenic bacterium can be attenuating, limiting bacterial growth and virulence *in vivo* [134]. Mammal pathogens, *Rhodococcus equi*, and *Actinobacillus pleuropneumoniae* lost their virulence when their riboflavin biosynthesis operon/genes were disrupted, making them suitable candidates for live-attenuated vaccines [135,136]. There have not been any reports of employing live-attenuated vaccines for lumpfish. Therefore, I further hypothesized in

Chapter 5 that *A. salmonicida* mutants with defined deletions of riboflavin supply genes may attenuate inside the lumpfish host and may be employed as live-attenuated vaccines in lumpfish aquaculture.

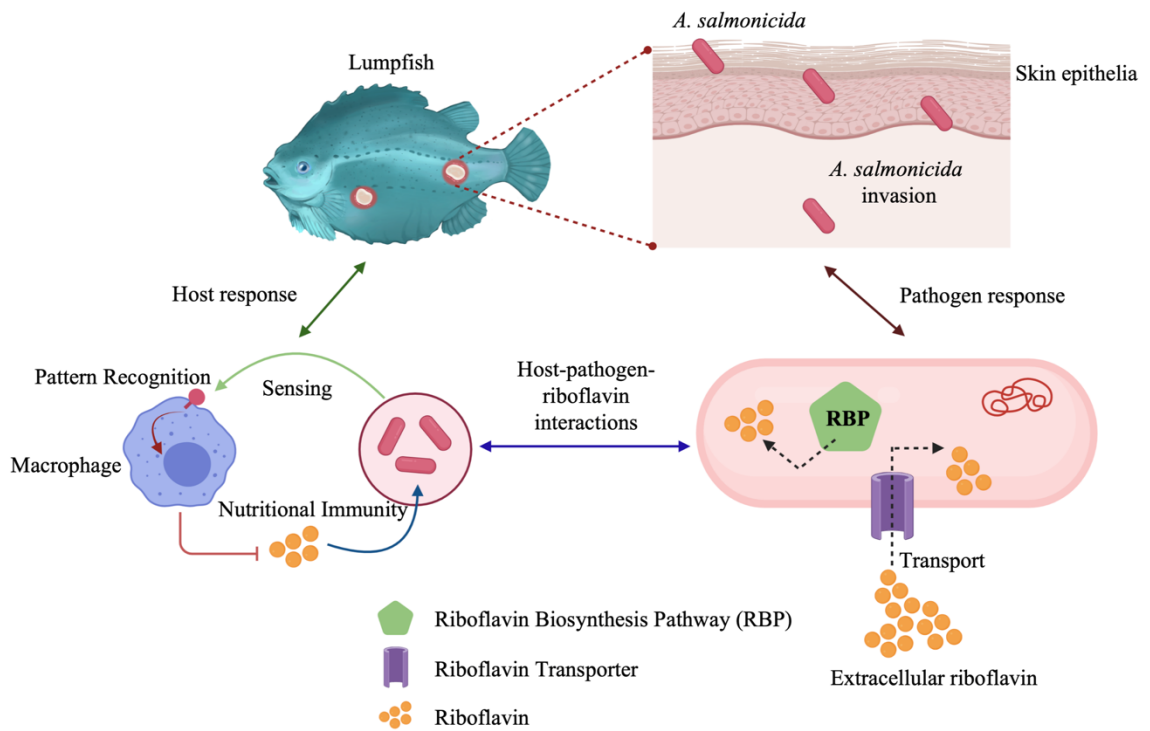


Figure 1.2. *A. salmonicida* riboflavin supply pathways and lumpfish. During host (lumpfish) - pathogen (*A. salmonicida*) - vitamin (riboflavin) interactions, the host initiates nutritional immunity to restrict the essential vitamin supply, while the pathogen either *de novo* biosynthesizes or uptakes the vitamin. Riboflavin supply pathways of *A. salmonicida* have yet to be described. This figure was created in BioRender (<https://biorender.com/>).

1.7. Thesis objectives

Based on the relevance and hypotheses described in section 1.6, the overall general objective of the thesis is to study some fundamental aspects of the pathogenesis and virulence of *R. salmoninarum* and *A. salmonicida* in lumpfish. My thesis chapters' objectives were as follows:

1. To provide a holistic host-invader view of host-pathogen interactions of marine Gram-positive bacteria (Chapter 2);
2. To evaluate the susceptibility and immune response of lumpfish to *R. salmoninarum* infection (Chapter 3);
3. To profile the transcriptome response of lumpfish head kidney to *R. salmoninarum* at early and chronic infection stages (Chapter 4); and
4. To study the role of riboflavin provision systems in *A. salmonicida* physiology and virulence in lumpfish (Chapter 5).

The specific objectives of the thesis chapter 2 were: i) how economically important marine Gram-positive bacterial pathogens adhere to, invade, evade, proliferate, and cause damage in the fish host (invader-centric view); and ii) how the host immune system responds in an attempt to control the invader (host-centric view).

In thesis chapter 3, the specific objectives were to: i) develop *R. salmoninarum* infection model for lumpfish; ii) study lumpfish susceptibility to *R. salmoninarum*; and iii) evaluate the immune response of lumpfish to *R. salmoninarum* infection.

The specific objectives of the thesis chapter 4 were to: i) profile the lumpfish head kidney transcriptome response to *R. salmoninarum* at the 28 and 98 days post infection; ii)

identify and compare the immune pathways differentially regulated in response to early and chronic *R. salmoninarum* infection; and iii) examine lysozyme activity and antibody titers in lumpfish serum upon *R. salmoninarum* infection.

In thesis chapter 5, the specific objectives were to: i) *in-silico* and experimentally characterize the riboflavin supply pathways in *A. salmonicida*; ii) evaluate the functionality of *A. salmonicida* riboflavin supply genes in the *Escherichia coli* heterologous model; iii) determine the effect of extracellular riboflavin on *A. salmonicida* gene expression; and iv) assess whether riboflavin biosynthesis, its duplicated genes, and riboflavin uptake are required for *A. salmonicida* virulence in lumpfish.

1.8. Publications from this thesis

All of the findings from this thesis have either been published or have been submitted to journals for publication as follows:

1. The literature review from Chapter 2 has been published in *Biology* as: Gnanagobal, H. and Santander. J. (2022). Host-Pathogen Interactions of Marine Gram-Positive Bacteria. *Biology*, 11, 1316. DOI: 10.3390/biology11091316. Author contributions: conceptualization: HG and JS; writing-original draft preparation and figure generation: HG; writing-review and editing: HG and JS; supervision: JS; funding acquisition: JS. All authors contributed to the article and approved the submitted version.
2. The research described in Chapter 3 has been published in *Frontiers in Immunology* as: Gnanagobal, H., Cao, T., Hossain, A., Dang, M., Hall, J., Kumar, S., Cuong, D.

V., Boyce, D., and Santander. J. (2021). Lumpfish (*Cyclopterus lumpus*) is Susceptible to *Renibacterium salmoninarum* Infection and Induces Cell-Mediated Immunity in the Chronic Stage. *Frontiers in immunology* 22(12): 733266. doi: 10.3389/fimmu.2021.733266. Author contributions: conceptualization: HG and JS; methodology: HG, TC, AH, MD, JH, SK, DVC, DB, and JS; investigation: HG, TC, MD, AH, JH, SK, DVC, DB, and JS; resources: JS and DB; writing original-draft: HG, JH, and JS; writing-review & editing: HG, TC, AH, MD, JH, SK, DC, DB, and JS; visualization: HG and JS; supervision: JS; funding acquisition: JS and DB. All authors contributed to the article and approved the submitted version.

3. The research described in Chapter 4 has been submitted to *Developmental and Comparative Immunology* as: Gnanagobal, H., Chakraborty, S., Ignacio, V., Chukwu-Osazuwa, J., Cao, T., Hossain, A., Kumar, S., Bindea, G., Hill, S., Boyce, D., Hall, J., and Santander, J. (2023). Transcriptome profiling of lumpfish (*Cyclopterus lumpus*) head kidney to *Renibacterium salmoninarum* at early and chronic infection stages. Author contributions: conceptualization: HG and JS; methodology: HG, SC, IV, JC, TC, AH, SK, GB, SH, DB, JH, and JS; investigation: HG, SC, IV, JC, TC, AH, SK, GB, SH, DB, JH, and JS; resources: JS and DB; writing original-draft: HG and JS; writing-review & editing: HG, SC, IV, JC, TC, AH, SK, GB, SH, DB, JH, and JS; visualization: HG and JS; Supervision: JS; Funding acquisition: JS, and DB. All authors contributed to the article and approved the submitted version.

4. The research described in Chapter 5 has been published in *Virulence* as: Gnanagobal, H., Cao, T., Hossain, A., Vasquez, I., Chakraborty, S., Chukwu-Osazuwa, J., Boyce, D., Jesus Espinoza, M., García-Angulo, V. A. and Santander. J. (2023). Role of Riboflavin Biosynthesis Gene Duplication and Transporter in *Aeromonas salmonicida* Virulence in Marine Teleost Fish. *Virulence* 14(1):2187025. doi.org/10.1080/21505594.2023.2187025. Author contributions: conceptualization: HG, VAG, and JS; methodology: HG, TC, AH, IV, SC, JC, MJE, DB, VAG, and JS; investigation: HG, TC, AH, IV, SC, JC, MJE, DB, VAG, and JS; resources: JS, VAG, DB; writing original-draft: HG, VAG, JS; writing-review & editing: HG, TC, AH, IV, SC, JC, MJE, DB, VAG, and JS; visualization: HG, VAG, and JS; Supervision: JS; Funding acquisition: JS, VAG, and DB. All authors contributed to the article and approved the submitted version.

1.9. References

1. FAO. *The State of World Fisheries and Aquaculture 2022. Towards Blue Transformation.*; Rome, 2022, doi:10.4060/cc0461en.
2. Naylor, R. L.; Hardy, R. W.; Buschmann, A. H.; Bush, S. R.; Cao, L.; Klinger, D. H.; Little, D. C.; Lubchenco, J.; Shumway, S. E.; Troell, M. A 20-Year Retrospective Review of Global Aquaculture. *Nature* **2021**, *591* (7851), 551–563.
3. Lafferty, K. D.; Harvell, C. D.; Conrad, J. M.; Friedman, C. S.; Kent, M. L.; Kuris, A. M.; Powell, E. N.; Rondeau, D.; Saksida, S. M. Infectious Diseases Affect Marine Fisheries and Aquaculture Economics. **2015**.
4. Pridgeon, J. W.; Klesius, P. H. Major Bacterial Diseases in Aquaculture and Their Vaccine Development. *CABI Rev.* **2012**, No. 2012, 1–16.
5. Austin, B.; Austin, D. A. *Bacterial Fish Pathogens: Disease of Farmed and Wild Fish, Sixth Edition*; Springer International Publishing, 2016, doi:10.1007/978-3-319-32674-0.
6. Roberts, R. J. The Bacteriology of Teleosts. In *Fish pathology*; Roberts, R. J., Ed.; Wiley-Blackwell: West Sussex, UK, 2012; pp 339–382, doi:10.1111/j.1751-0813.2002.tb14791.x.
7. Southwood, D.; Ranganathan, S. *Host-Pathogen Interactions*; Elsevier Ltd., 2018; Vol. 1–3, doi:10.1016/B978-0-12-809633-8.20088-5.
8. Fryer, J. L.; Sanders, J. E. Bacterial Kidney Disease of Salmonid Fish. *Annu. Rev. Microbiol.* **1981**, *35*, 273–298, doi:10.1146/annurev.mi.35.100181.001421.
9. Wiens, G. D. Bacterial Kidney Disease (*Renibacterium salmoninarum*). In *Fish Diseases and Disorders*; Woo, P. T. K., Bruno, D. W., Eds.; CABI: Wallingford, UK, 2011; pp 338–374.
10. Pascho, R. J.; Elliott, D. G.; Chase, D. M. Comparison of Traditional and Molecular Methods for Detection of *Renibacterium salmoninarum*; 2002; pp 157–209, doi:10.1007/978-94-017-2315-2_7.
11. Evenden, A. J.; Grayson, T. H.; Gilpin, M. L.; Munn, C. B. *Renibacterium salmoninarum* and Bacterial Kidney Disease - the Unfinished Jigsaw. *Annu. Rev. Fish Dis.* **1993**, *3* (C), 87–104, doi:10.1016/0959-8030(93)90030-F.
12. Elliott, D. G.; Wiens, G. D.; Hammell, K. L.; Rhodes, L. D. Vaccination against Bacterial Kidney Disease. *Fish Vaccin.* **2014**, *9780470674*, 255–272, doi:10.1002/9781118806913.ch22.
13. Elliott, D. G. *Renibacterium salmoninarum*. In *In Fish Viruses and Bacteria: Pathobiology and Protection*; Woo, P.T.K and Ciaprino, R. , Ed.; CABI, U.K, 2017; pp 286–297.
14. Bell, G. R.; Hoffmann, R. W.; Brown, L. L. Pathology of Experimental Infections of the Sablefish, *Anoplopoma fimbria* (Pallas), with *Renibacterium salmoninarum*, the Agent of Bacterial Kidney Disease in Salmonids. *J. Fish Dis.* **1990**, *13* (5), 355–367.
15. Evelyn, T. P. Bacterial Kidney Disease – BKD. In *Bacterial Disease of Fish*; V., Roberts, R. J. and Bromage, N. R., Ed.; Blackwell Scientific: London, 1993; pp 177–195.

16. Delghandi, M. R.; El-Matbouli, M.; Menanteau-Ledouble, S. *Renibacterium salmoninarum*-The Causative Agent of Bacterial Kidney Disease in Salmonid Fish. *Pathog. (Basel, Switzerland)* **2020**, *9* (10), 845, doi:10.3390/pathogens9100845.
17. Elliott, D. G.; McKibben, C. L.; Conway, C. M.; Purcell, M. K.; Chase, D. M.; Applegate, L. J. Testing of Candidate Non-Lethal Sampling Methods for Detection of *Renibacterium salmoninarum* in Juvenile Chinook Salmon *Oncorhynchus tshawytscha*. *Dis. Aquat. Organ.* **2015**, *114* (1), 21–43, doi:10.3354/dao02846.
18. Plumb, J. A. *Health Maintenance of Cultured Fishes: Principal Microbial Diseases*; CRC Press, 2018.
19. Murray, A. G.; Munro, L. A.; Wallace, I. S.; Allan, C. E. T.; Peeler, E. J.; Thrush, M. A. Epidemiology of *Renibacterium salmoninarum* in Scotland and the Potential for Compartmentalised Management of Salmon and Trout Farming Areas. *Aquaculture* **2012**, *324–325*, 1–13, doi:https://doi.org/10.1016/j.aquaculture.2011.09.034.
20. Suzuki, K.; Misaka, N.; Mizuno, S.; Sasaki, Y. PCR- Based Detection and Quantification of *Renibacterium salmoninarum* in Ovarian Fluid of Returning Chum Salmon *Oncorhynchus keta* and Masu Salmon *O. masou* in Hokkaido, Japan. *Fish Pathol.* **2017**, *52* (2), 100–103, doi:10.3147/jfsfp.52.100.
21. Costello, M. J. The Global Economic Cost of Sea Lice to the Salmonid Farming Industry. *J. Fish Dis.* **2009**, *32* (1), 115–118, doi:10.1111/j.1365-2761.2008.01011.x.
22. Boerlage, A. S.; Elghafghuf, A.; Stryhn, H.; Sanchez, J.; Hammell, K. L. Risk Factors Associated with Time to First Clinical Case of Bacterial Kidney Disease (BKD) in Farmed Atlantic Salmon (*Salmo salar* L.) in New Brunswick, Canada. *Prev. Vet. Med.* **2018**, *149*, 98–106, doi:10.1016/j.prevetmed.2017.11.014.
23. Eissa, A. E.; Elsayed, E. E.; McDonald, R.; Faisal, M. First Record of *Renibacterium salmoninarum* in the Sea Lamprey (*Petromyzon marinus*). *J. Wildl. Dis.* **2006**, *42* (3), 556–560, doi:10.7589/0090-3558-42.3.556.
24. Bruno, D. W. Histopathology of Bacterial Kidney Disease in Laboratory Infected Rainbow Trout, *Salmo gairdneri* Richardson, and Atlantic Salmon, *Salmo salar* L., with Reference to Naturally Infected Fish. *J. Fish Dis.* **1986**, *9* (6), 523–537, doi:10.1111/j.1365-2761.1986.tb01049.x.
25. Flaño, E.; López-Fierro, P.; Razquin, B.; Kaattari, S. L.; Villena, A. Histopathology of the Renal and Splenic Haemopoietic Tissues of Coho Salmon *Oncorhynchus kisutch* Experimentally Infected with *Renibacterium salmoninarum*. *Dis. Aquat. Organ.* **1996**, *24* (2), 107–115, doi:10.3354/dao024107.
26. Wiens, G. D.; Kaattari, S. L. Monoclonal Antibody Characterization of a Leukoagglutinin Produced by *Renibacterium salmoninarum*. *Infect. Immun.* **1991**, *59* (2), 631–637.
27. Daly, J. G.; Stevenson, R. M. W. Characterization of the *Renibacterium salmoninarum* Haemagglutinin. *J. Gen. Microbiol.* **1990**, *136* (5), 949–953, doi:10.1099/00221287-136-5-949.
28. Dubreuil, J. D.; Jacques, M.; Graham, L.; Lallier, R. Purification, and Biochemical and Structural Characterization of a Fimbrial Haemagglutinin of *Renibacterium salmoninarum*. *J. Gen. Microbiol.* **1990**, *136* (12), 2443–2448,

- doi:10.1099/00221287-136-12-2443.
29. Rose, A. S.; Levine, R. P. Complement-Mediated Opsonisation and Phagocytosis of *Renibacterium salmoninarum*. *Fish Shellfish Immunol.* **1992**, *2* (3), 223–240, doi:10.1016/S1050-4648(05)80061-0.
 30. Wiens, G. D.; Rockey, D. D.; Wu, Z.; Chang, J.; Levy, R.; Crane, S.; Chen, D. S.; Capri, G. R.; Burnett, J. R.; Sudheesh, P. S.; Schipma, M. J.; Burd, H.; Bhattacharyya, A.; Rhodes, L. D.; Kaul, R.; Strom, M. S. Genome Sequence of the Fish Pathogen *Renibacterium salmoninarum* Suggests Reductive Evolution Away from an Environmental *Arthrobacter* Ancestor. *J. Bacteriol.* **2008**, *190* (21), 6970–6982, doi:10.1128/JB.00721-08.
 31. O’Farrell, C. L.; Strom, M. S. Differential Expression of the Virulence-Associated Protein p57 and Characterization of Its Duplicated Gene *msa* in Virulent and Attenuated Strains of *Renibacterium salmoninarum*. *Dis. Aquat. Organ.* **1999**, *38* (2), 115–123, doi:10.3354/dao038115.
 32. Coady, A. M.; Murray, A. L.; Elliott, D. G.; Rhodes, L. D. Both *msa* Genes in *Renibacterium salmoninarum* Are Needed for Full Virulence in Bacterial Kidney Disease. *Appl. Environ. Microbiol.* **2006**, *72* (4), 2672–2678, doi:10.1128/AEM.72.4.2672-2678.2006.
 33. Rhodes, L. D.; Coady, A. M.; Deinhard, R. K. Identification of a Third *msa* Gene in *Renibacterium salmoninarum* and the Associated Virulence Phenotype. *Appl. Environ. Microbiol.* **2004**, *70* (11), 6488–6494, doi:10.1128/AEM.70.11.6488-6494.2004.
 34. Brynildsrud, O.; Gulla, S.; Feil, E. J.; Nørstebø, S. F.; Rhodes, L. D. Identifying Copy Number Variation of the Dominant Virulence Factors *msa* and p22 within Genomes of the Fish Pathogen *Renibacterium salmoninarum*. *Microb. genomics* **2016**, *2* (4), e000055, doi:10.1099/mgen.0.000055.
 35. Senson, P. R.; Stevenson, R. M. Production of the 57 kDa Major Surface Antigen by a Non-Agglutinating Strain of the Fish Pathogen *Renibacterium salmoninarum*. *Dis. Aquat. Organ.* **1999**, *38* (1), 23–31, doi:10.3354/dao038023.
 36. Fredriksen, Å.; Endresen, C.; Wergeland, H. I. Immunosuppressive Effect of a Low Molecular Weight Surface Protein from *Renibacterium salmoninarum* on Lymphocytes from Atlantic Salmon (*Salmo salar* L.). *Fish Shellfish Immunol.* **1997**, *7* (4), 273–282, doi:10.1006/fsim.1997.0082.
 37. Grayson, T. H.; Cooper, L. F.; Wrathmell, A. B.; Evenden Andrew J, J. R.; Gilpin, M. L. Host Responses to *Renibacterium salmoninarum* and Specific Components of the Pathogen Reveal the Mechanisms of Immune Suppression and Activation. *Immunology* **2002**, *106* (2), 273–283.
 38. Rhodes, L. D.; Wallis, S.; Demlow, S. E. Genes Associated with an Effective Host Response by Chinook Salmon to *Renibacterium salmoninarum*. *Dev. Comp. Immunol.* **2009**, *33* (2), 176–186, doi:10.1016/j.dci.2008.08.006.
 39. Metzger, D. C.; Elliott, D. G.; Wargo, A.; Park, L. K.; Purcell, M. K. Pathological and Immunological Responses Associated with Differential Survival of Chinook Salmon Following *Renibacterium salmoninarum* Challenge. *Dis. Aquat. Organ.* **2010**, *90* (1), 31–41, doi:10.3354/dao02214.
 40. Eslamloo, K.; Caballero-Solares, A.; Inkpen, S. M.; Emam, M.; Kumar, S.; Bouniot,

- C.; Avendaño-Herrera, R.; Jakob, E.; Rise, M. L. Transcriptomic Profiling of the Adaptive and Innate Immune Responses of Atlantic Salmon to *Renibacterium salmoninarum* Infection. *Front. Immunol.* **2020**, *11* (October), doi:10.3389/fimmu.2020.567838.
41. Eslamloo, K.; Kumar, S.; Caballero-Solares, A.; Gnanagobal, H.; Santander, J.; Rise, M. L. Profiling the Transcriptome Response of Atlantic Salmon Head Kidney to Formalin-killed *Renibacterium salmoninarum*. *Fish Shellfish Immunol.* **2020**, *98* (September 2019), 937–949, doi:10.1016/j.fsi.2019.11.057.
 42. Griffiths, S. G.; Melville, K. J.; Salenius, K. Reduction of *Renibacterium salmoninarum* Culture Activity in Atlantic Salmon Following Vaccination with Avirulent Strains. *Fish Shellfish Immunol.* **1998**, *8* (8), 607–619, doi:10.1006/fsim.1998.0169.
 43. Rhodes, L. D.; Rathbone, C. K.; Corbett, S. C.; Harrell, L. W.; Strom, M. S. Efficacy of Cellular Vaccines and Genetic Adjuvants against Bacterial Kidney Disease in Chinook Salmon (*Oncorhynchus tshawytscha*). *Fish Shellfish Immunol.* **2004**, *16* (4), 461–474, doi:10.1016/j.fsi.2003.08.004.
 44. Alcorn, S.; Murray, A. L.; Pascho, R. J.; Varney, J. A Cohabitation Challenge to Compare the Efficacies of Vaccines for Bacterial Kidney Disease (BKD) in Chinook Salmon *Oncorhynchus tshawytscha*. *Dis. Aquat. Organ.* **2005**, *63* (2–3), 151–160, doi:10.3354/dao063151.
 45. Janda, J. M.; Abbott, S. L. The Genus *Aeromonas*: Taxonomy, Pathogenicity, and Infection. *Clin. Microbiol. Rev.* **2010**, *23* (1), 35–73, doi:10.1128/CMR.00039-09.
 46. Dallaire-Dufresne, S.; Tanaka, K. H.; Trudel, M. V.; Lafaille, A.; Charette, S. J. Virulence, Genomic Features, and Plasticity of *Aeromonas salmonicida* subsp. *salmonicida*, the Causative Agent of Fish Furunculosis. *Vet. Microbiol.* **2014**, *169* (1–2), 1–7, doi:10.1016/j.vetmic.2013.06.025.
 47. Boily, F.; Malcolm, G.; Johnson, S. C. Characterization of *Aeromonas salmonicida* and Furunculosis to Inform Pathogen Transfer Risk Assessments in British Columbia; Canadian Science Advisory Secretariat, 2019.
 48. Powell, A.; Treasurer, J. W.; Pooley, C. L.; Keay, A. J.; Lloyd, R.; Imsland, A. K.; Garcia de Leaniz, C. Use of Lumpfish for Sea-lice Control in Salmon Farming: Challenges and Opportunities. *Rev. Aquac.* **2018**, *10* (3), 683–702.
 49. McCarthy, D. H.; Roberts, R. J. Furunculosis of Fish—the Present State of Our Knowledge. **1980**.
 50. Jutfelt, F.; Sundh, H.; Glette, J.; Mellander, L.; Thrandur Björnsson, B.; Sundell, K. The Involvement of *Aeromonas salmonicida* Virulence Factors in Bacterial Translocation across the Rainbow Trout, *Oncorhynchus mykiss* (Walbaum), Intestine. *J. Fish Dis.* **2008**, *31* (2), 141–151.
 51. Cipriano, R. C.; Austin, B. 12 Furunculosis and Other Aeromonad Diseases. *Fish Dis. Disord. Vol. 3 Viral, Bact. Fungal Infect.* **2011**, 424.
 52. Menanteau-Ledouble, S.; Kumar, G.; Saleh, M.; El-Matbouli, M. *Aeromonas salmonicida*: Updates on an Old Acquaintance. *Dis. Aquat. Organ.* **2016**, *120* (1), 49–68, doi:10.3354/dao03006.
 53. Oidtmann, B.; LaPatra, S. E.; Verner-Jeffreys, D.; Pond, M.; Peeler, E. J.; Noguera, P. A.; Bruno, D. W.; St-Hilaire, S.; Schubiger, C. B.; Snekvik, K. Differential

- Characterization of Emerging Skin Diseases of Rainbow Trout—a Standardized Approach to Capturing Disease Characteristics and Development of Case Definitions. *J. Fish Dis.* **2013**, *36* (11), 921–937.
54. Beaz-Hidalgo, R.; Figueras, M. J. *Aeromonas* spp. Whole Genomes and Virulence Factors Implicated in Fish Disease. *J. Fish Dis.* **2013**, *36* (4), 371–388, doi:10.1111/jfd.12025.
 55. Han, H.; Kim, D.; Kim, W.; Kim, C.; Jung, S.; Oh, M.; Kim, D. Atypical *Aeromonas salmonicida* Infection in the Black Rockfish, *Sebastes schlegeli* Hilgendorf, in Korea. *J. Fish Dis.* **2011**, *34* (1), 47–55.
 56. Vanden Bergh, P.; Frey, J. *Aeromonas salmonicida* subsp. *salmonicida* in the Light of Its Type-three Secretion System. *Microb. Biotechnol.* **2014**, *7* (5), 381–400.
 57. Fast, M. D.; Tse, B.; Boyd, J. M.; Johnson, S. C. Mutations in the *Aeromonas salmonicida* subsp. *salmonicida* Type III Secretion System Affect Atlantic Salmon Leucocyte Activation and Downstream Immune Responses. *Fish Shellfish Immunol.* **2009**, *27* (6), 721–728, doi:10.1016/j.fsi.2009.09.009.
 58. Menanteau-Ledouble, S.; El-Matbouli, M. Antigens of *Aeromonas salmonicida* subsp. *salmonicida* Specifically Induced *in vivo* in *Oncorhynchus mykiss*. *J. Fish Dis.* **2016**, *39* (8), 1015.
 59. Dacanay, A.; Knickle, L.; Solanky, K. S.; Boyd, J. M.; Walter, J. A.; Brown, L. L.; Johnson, S. C.; Reith, M. Contribution of the Type III Secretion System (TTSS) to Virulence of *Aeromonas salmonicida* subsp. *salmonicida*. *Microbiology* **2006**, *152* (6), 1847–1856.
 60. Najimi, M.; Lemos, M. L.; Osorio, C. R. Identification of Heme Uptake Genes in the Fish Pathogen *Aeromonas salmonicida* subsp. *salmonicida*. *Arch. Microbiol.* **2008**, *190* (4), 439–449.
 61. Reith, M. E.; Singh, R. K.; Curtis, B.; Boyd, J. M.; Bouevitch, A.; Kimball, J.; Munholland, J.; Murphy, C.; Sarty, D.; Williams, J.; Nash, J. H.; Johnson, S. C.; Brown, L. L. The Genome of *Aeromonas salmonicida* subsp. *salmonicida* A449: Insights into the Evolution of a Fish Pathogen. *BMC Genomics* **2008**, *9* (1), 427, doi:10.1186/1471-2164-9-427.
 62. Balado, M.; Souto, A.; Vences, A.; Careaga, V. P.; Valderrama, K.; Segade, Y.; Rodríguez, J.; Osorio, C. R.; Jiménez, C.; Lemos, M. L. Two Catechol Siderophores, Acinetobactin and Amonabactin, Are Simultaneously Produced by *Aeromonas salmonicida* subsp. *salmonicida* Sharing Part of the Biosynthetic Pathway. *ACS Chem. Biol.* **2015**, *10* (12), 2850–2860, doi:10.1021/acscchembio.5b00624.
 63. Janda, J. M. *Aeromonas* and *Plesiomonas*. In *Molecular medical microbiology*; Elsevier, 2002; pp 1237–1270.
 64. Ebanks, R. O.; Goguen, M.; McKinnon, S.; Pinto, D. M.; Ross, N. W. Identification of the Major Outer Membrane Proteins of *Aeromonas salmonicida*. *Dis. Aquat. Organ.* **2005**, *68* (1), 29–38.
 65. Gatlin, D. M. *Dietary Supplements for the Health and Quality of Cultured Fish*; Cabi, 2007.
 66. Blazer, V. S. Nutrition and Disease Resistance in Fish. *Annu. Rev. Fish Dis.* **1992**, *2*, 309–323, doi:https://doi.org/10.1016/0959-8030(92)90068-9.
 67. Sealey, W. M.; Gatlin, D. M. Overview of Nutritional Strategies Affecting Health of

- Marine Fish. *J. Appl. Aquac.* **1999**, *9* (2), 11–26, doi:10.1300/J028v09n02_02.
68. Bonomi, H. R.; Marchesini, M. I.; Klinke, S.; Ugalde, J. E.; Zylberman, V.; Ugalde, R. A.; Comerci, D. J.; Goldbaum, F. A. An Atypical Riboflavin Pathway is Essential for *Brucella abortus* Virulence. *PLoS One* **2010**, *5* (2), e9435, doi:10.1371/journal.pone.0009435.
 69. Dick, T.; Manjunatha, U.; Kappes, B.; Gengenbacher, M. Vitamin B₆ Biosynthesis is Essential for Survival and Virulence of *Mycobacterium tuberculosis*. *Mol. Microbiol.* **2010**, *78* (4), 980–988, doi:10.1111/j.1365-2958.2010.07381.x.
 70. Grubman, A.; Phillips, A.; Thibonnier, M.; Kaparakis-Liaskos, M.; Johnson, C.; Thiberge, J. M.; Radcliff, F. J.; Ecobichon, C.; Labigne, A.; de Reuse, H.; Mendz, G. L.; Ferrero, R. L. Vitamin B₆ Is Required for Full Motility and Virulence in *Helicobacter pylori*. *MBio* **2010**, *1* (3), doi:10.1128/mBio.00112-10.
 71. Kijewski, A.; Witsø, I. L.; Iversen, H.; Rønning, H. T.; L'Abée-Lund, T.; Wasteson, Y.; Lindbäck, T.; Aspholm, M. Vitamin K Analogs Influence the Growth and Virulence Potential of Enterohemorrhagic *Escherichia coli*. *Appl. Environ. Microbiol.* **2020**, *86* (24), 1–16, doi:10.1128/AEM.0583-20.
 72. Uebanso, T.; Shimohata, T.; Mawatari, K.; Takahashi, A. Functional Roles of B-vitamins in the Gut and Gut Microbiome. *Mol. Nutr. Food Res.* **2020**, *64* (18), 2000426.
 73. Skaar, E. P. The Battle for Iron between Bacterial Pathogens and Their Vertebrate Hosts. *PLoS Pathog.* **2010**, *6* (8), 1–2, doi:10.1371/journal.ppat.1000949.
 74. Kehl-Fie, T. E.; Skaar, E. P. Nutritional Immunity beyond Iron: A Role for Manganese and Zinc. *Curr. Opin. Chem. Biol.* **2010**, *14* (2), 218–224, doi:10.1016/j.cbpa.2009.11.008.
 75. Bellovino, D.; Morimoto, T.; Mengheri, E.; Perozzi, G.; Garaguso, I.; Nobili, F.; Gaetani, S. Unique Biochemical Nature of Carp Retinol-Binding Protein: N-Linked Glycosylation and Uncleavable NH₂-Terminal Signal Peptide. *J. Biol. Chem.* **2001**, *276* (17), 13949–13956.
 76. Sammar, M.; Babin, P. J.; Durliat, M.; Meiri, I.; Zchori, I.; Elizur, A.; Lubzens, E. Retinol Binding Protein in Rainbow Trout: Molecular Properties and MRNA Expression in Tissues. *Gen. Comp. Endocrinol.* **2001**, *123* (1), 51–61.
 77. Baruah, C.; Devi, P.; Sharma, D. K. A Comparative Study on Retinol Binding Protein in Two Freshwater Fishes, *Danio rerio* and *Cyprinus carpio*. **2016**.
 78. Benoit, C. R.; Stanton, A. E.; Tartanian, A. C.; Motzer, A. R.; McGaughey, D. M.; Bond, S. R.; Brody, L. C. Functional and Phylogenetic Characterization of Noncanonical Vitamin B₁₂-Binding Proteins in Zebrafish Suggests Involvement in Cobalamin Transport. *J. Biol. Chem.* **2018**, *293* (45), 17606–17621, doi:10.1074/jbc.RA118.005323.
 79. Allewaert, K.; Van Baelen, H.; Bouillon, R. Vitamin D-Binding Protein in Pisces. *Steroids* **1988**, *52* (4), 357–358.
 80. Sañudo-Wilhelmy, S. A.; Cutter, L. S.; Durazo, R.; Smail, E. A.; Gómez-Consarnau, L.; Webb, E. A.; Prokopenko, M. G.; Berelson, W. M.; Karl, D. M. Multiple B-vitamin Depletion in Large Areas of the Coastal Ocean. *PNAS* **2012**, *109* (35), 14041–14045, doi:10.1073/pnas.1208755109.
 81. Mopper, K.; Zika, R. G. Natural Photosensitizers in Sea Water: Riboflavin and its

- Breakdown Products; 1987; pp 174–190, doi:10.1021/bk-1987-0327.ch013.
82. De Colibus, L.; Mattevi, A. New Frontiers in Structural Flavoenzymology. *Curr. Opin. Struct. Biol.* **2006**, *16* (6), 722–728, doi:https://doi.org/10.1016/j.sbi.2006.10.003.
 83. Abbas, C. A.; Sibirny, A. A. Genetic Control of Biosynthesis and Transport of Riboflavin and Flavin Nucleotides and Construction of Robust Biotechnological Producers. *Microbiol. Mol. Biol. Rev.* **2011**, *75* (2), 321–360, doi:10.1128/MMBR.00030-10.
 84. Ashoori, M.; Saedisomeolia, A. Riboflavin (Vitamin B₂) and Oxidative Stress: A Review. *Br. J. Nutr.* **2014**, *111* (11), 1985–1991, doi:10.1017/S0007114514000178.
 85. Beztsinna, N.; Solé, M.; Taib, N.; Bestel, I. Bioengineered Riboflavin in Nanotechnology. *Biomaterials* **2016**, *80*, 121–133, doi:10.1016/j.biomaterials.2015.11.050.
 86. Haase, I.; Gräwert, T.; Illarionov, B.; Bacher, A.; Fischer, M. Recent Advances in Riboflavin Biosynthesis. *Methods Mol. Biol.* **2014**, *1146*, 15–40, doi:10.1007/978-1-4939-0452-5_2.
 87. Crossley, R. A.; Gaskin, D. J. H.; Holmes, K.; Mulholland, F.; Wells, J. M.; Kelly, D. J.; van Vliet, A. H. M.; Walton, N. J. Riboflavin Biosynthesis is Associated with Assimilatory Ferric Reduction and Iron Acquisition by *Campylobacter jejuni*. *Appl. Environ. Microbiol.* **2007**, *73* (24), 7819–7825, doi:10.1128/AEM.01919-07.
 88. Marsili, E.; Baron, D. B.; Shikhare, I. D.; Coursolle, D.; Gralnick, J. A.; Bond, D. R. *Shewanella* Secretes Flavins That Mediate Extracellular Electron Transfer. *Proc. Natl. Acad. Sci. U. S. A.* **2008**, *105* (10), 3968–3973, doi:10.1073/pnas.0710525105.
 89. Yurgel, S. N.; Rice, J.; Domreis, E.; Lynch, J.; Sa, N.; Qamar, Z.; Rajamani, S.; Gao, M.; Roje, S.; Bauer, W. D. *Sinorhizobium meliloti* Flavin Secretion and Bacteria-Host Interaction: Role of the Bifunctional RibBA Protein. *Mol. Plant. Microbe. Interact.* **2014**, *27* (5), 437–445, doi:10.1094/MPMI-11-13-0338-R.
 90. Rajamani, S.; Bauer, W. D.; Robinson, J. B.; Farrow, J. M. 3rd; Pesci, E. C.; Teplitski, M.; Gao, M.; Sayre, R. T.; Phillips, D. A. The Vitamin Riboflavin and Its Derivative Lumichrome Activate the LasR Bacterial Quorum-Sensing Receptor. *Mol. Plant. Microbe. Interact.* **2008**, *21* (9), 1184–1192, doi:10.1094/MPMI-21-9-1184.
 91. Rodionova, I. A.; Li, X.; Plymale, A. E.; Motamedchaboki, K.; Konopka, A. E.; Romine, M. F.; Fredrickson, J. K.; Osterman, A. L.; Rodionov, D. A. Genomic Distribution of B-Vitamin Auxotrophy and Uptake Transporters in Environmental Bacteria from the Chloroflexi Phylum. *Environ. Microbiol. Rep.* **2015**, *7* (2), 204–210, doi:10.1111/1758-2229.12227.
 92. Sun, E. I.; Leyn, S. A.; Kazanov, M. D.; Saier, M. H.; Novichkov, P. S.; Rodionov, D. A. Comparative Genomics of Metabolic Capacities of Regulons Controlled by Cis-Regulatory RNA Motifs in Bacteria. *BMC Genomics* **2013**, *14* (1), 597, doi:10.1186/1471-2164-14-597.
 93. Angulo, V. A. G.; Bonomi, H. R.; Posadas, D. M.; Serer, M. I.; Torres, A. G.; Zorreguieta, Á.; Goldbaum, F. A. Identification and Characterization of RibN, a Novel Family of Riboflavin Transporters from *Rhizobium leguminosarum* and Other Proteobacteria. **2013**, *195*, 4611–4619, doi:10.1128/JB.00644-13.

94. Gutiérrez-Preciado, A.; Gabriel Torres, A.; Merino, E.; Ruy Bonomi, H.; Alberto Goldbaum, F.; Antonio García-Angulo, V.; Moreno-Hagelsieb, G. Extensive Identification of Bacterial Riboflavin Transporters and Their Distribution across Bacterial Species. **2015**, doi:10.1371/journal.pone.0126124.
95. Jaehme, M.; Slotboom, D. J. Diversity of Membrane Transport Proteins for Vitamins in Bacteria and Archaea. *Biochim. Biophys. Acta* **2015**, *1850* (3), 565–576, doi:10.1016/j.bbagen.2014.05.006.
96. Vogl, C.; Grill, S.; Schilling, O.; Stülke, J.; Mack, M.; Stolz, J. Characterization of Riboflavin (Vitamin B₂) Transport Proteins from *Bacillus subtilis* and *Corynebacterium glutamicum*. *J. Bacteriol.* **2007**, *189* (20), 7367–7375, doi:10.1128/JB.00590-07.
97. Burgess, C. M.; Slotboom, D. J.; Geertsma, E. R.; Duurkens, R. H.; Poolman, B.; Van Sinderen, D. The Riboflavin Transporter RibU in *Lactococcus lactis*: Molecular Characterization of Gene Expression and the Transport Mechanism. *J. Bacteriol.* **2006**, *188* (8), 2752–2760, doi:10.1128/JB.188.8.2752-2760.2006.
98. Bacher, A.; Eberhardt, S.; Fischer, M.; Kis, K.; Richter, G. Biosynthesis of Vitamin B₂ (Riboflavin). *Annu. Rev. Nutr.* **2000**, *20* (1), 153–167, doi:10.1146/annurev.nutr.20.1.153.
99. García-Angulo, V. A. Overlapping Riboflavin Supply Pathways in Bacteria. *Crit. Rev. Microbiol.* **2017**, *43* (2), 196–209, doi:10.1080/1040841X.2016.1192578.
100. Fischer, M.; Bacher, A. Biosynthesis of Flavocoenzymes. *Nat. Prod. Rep.* **2005**, *22* (3), 324–350, doi:10.1039/b210142b.
101. Winkler, W. C.; Cohen-Chalamish, S.; Breaker, R. R. An mRNA Structure That Controls Gene Expression by Binding FMN. *Proc. Natl. Acad. Sci. U. S. A.* **2002**, *99* (25), 15908–15913, doi:10.1073/pnas.212628899.
102. Vicens, Q.; Mondragón, E.; Batey, R. T. Molecular Sensing by the Aptamer Domain of the FMN Riboswitch: A General Model for Ligand Binding by Conformational Selection. *Nucleic Acids Res.* **2011**, *39* (19), 8586–8598, doi:10.1093/nar/gkr565.
103. Pedrolli, D.; Langer, S.; Hobl, B.; Schwarz, J.; Hashimoto, M.; Mack, M. The RibB FMN Riboswitch from *Escherichia coli* Operates at the Transcriptional and Translational Level and Regulates Riboflavin Biosynthesis. *FEBS J.* **2015**, *282* (16), 3230–3242, doi:10.1111/febs.13226.
104. Vitreschak, A. G.; Rodionov, D. A.; Mironov, A. A.; Gelfand, M. S. Riboswitches: The Oldest Mechanism for the Regulation of Gene Expression? *Trends Genet.* **2004**, *20* (1), 44–50, doi:10.1016/j.tig.2003.11.008.
105. Zylberman, V.; Klinke, S.; Haase, I.; Bacher, A.; Fischer, M.; Goldbaum, F. A. Evolution of Vitamin B₂ Biosynthesis: 6, 7-Dimethyl-8-Ribityllumazine Synthases of *Brucella*. *J. Bacteriol.* **2006**, *188* (17), 6135–6142.
106. Wilson, A. C.; Pardee, A. B. Regulation of Flavin Synthesis by *Escherichia coli*. *J. Gen. Microbiol.* **1962**, *28* (2), 283–303, doi:10.1099/00221287-28-2-283.
107. Fuller, T. E.; Mulks, M. H. Riboflavin Biosynthesis Genes. **1995**, *177* (24), 7265–7270.
108. Perkins, J. B., and J. G. P. Biosynthesis of Riboflavin, Biotin, Folic Acid, and Cobalamin. *Am. Soc. Microbiol.* **1993**, 391–394.
109. Fisheries and Oceans Canada. Species Farmed in Canada: Farmed Salmon

- <https://www.dfo-mpo.gc.ca/aquaculture/sector-secteur/species-especes/salmon-saumon-eng.htm> (accessed 2023 -01 -13).
110. Kabata, Z. Parasitic Copepoda of British Fishes. *Ray Soc. London* **1979**, *152*, 1–468.
 111. Pike, A. W.; Wadsworth, S. L. Sealice on Salmonids: Their Biology and Control. *Adv. Parasitol.* **1999**, *44*, 233–337.
 112. Brooker, A. J.; Papadopoulou, A.; Gutierrez, C.; Rey, S.; Davie, A.; Migaud, H. Sustainable Production and Use of Cleaner Fish for the Biological Control of Sea Lice: Recent Advances and Current Challenges. *Vet. Rec.* **2018**, *183* (12), 383.
 113. Sommerset, I.; Bang Jensen, B.; Bornø, B.; Haukaas, A.; Brun, E. *The Health Situation in Norwegian Aquaculture 2020.*; 2021.
 114. Just Economics. Dead Loss: The high cost of poor farming practices and mortalities on salmon farms.
 115. Abolofia, J.; Asche, F.; Wilen, J. E. The Cost of Lice: Quantifying the Impacts of Parasitic Sea Lice on Farmed Salmon. *Mar. Resour. Econ.* **2017**, *32* (3), 329–349.
 116. Lees, F.; Baillie, M.; Gettinby, G.; Revie, C. W. Factors Associated with Changing Efficacy of Emamectin Benzoate against Infestations of *Lepeophtheirus salmonis* on Scottish Salmon Farms. *J. Fish Dis.* **2008**, *31* (12), 947–951.
 117. Jones, P. G.; Hammell, K. L.; Gettinby, G.; Revie, C. W. Detection of Emamectin Benzoate Tolerance Emergence in Different Life Stages of Sea Lice, *Lepeophtheirus salmonis*, on Farmed Atlantic Salmon, *Salmo salar* L. *J. Fish Dis.* **2013**, *36* (3), 209–220.
 118. Misters, A.; Purchase, D. *Use of ‘Cleaner Fish’ in UK Aquaculture: Current Use, Concerns, and Recommendations*; 2021.
 119. Liu, Y.; vanhauwaer Bjelland, H. Estimating Costs of Sea Lice Control Strategy in Norway. *Prev. Vet. Med.* **2014**, *117* (3–4), 469–477.
 120. Treasurer, J. W. A Review of Potential Pathogens of Sea Lice and the Application of Cleaner Fish in Biological Control. *Pest Manag. Sci. Former. Pestic. Sci.* **2002**, *58* (6), 546–558.
 121. Nytrø, A. V.; Vikingstad, E.; Foss, A.; Hangstad, T. A.; Reynolds, P.; Eliassen, G.; Elvegård, T. A.; Falk-Petersen, I.-B.; Imsland, A. K. The Effect of Temperature and Fish Size on Growth of Juvenile Lumpfish (*Cyclopterus lumpus* L.). *Aquaculture* **2014**, *434*, 296–302.
 122. Helland, S.; Dahle, S. W.; Hough, C.; Borthen, J. Production of Ballan Wrasse (*Labrus bergylta*). Science and Practice. Norway: The Norwegian Seafood Research Fund (FHF) 2014.
 123. Erkinharju, T.; Dalmo, R. A.; Hansen, M.; Seternes, T. Cleaner Fish in Aquaculture: Review on Diseases and Vaccination. *Rev. Aquac.* **2021**, *13* (1), 189–237.
 124. VKM, R. E.; Basic, D.; Gulla, S.; Hjeltne, B.; Mortensen, S. Risk Assessment of Fish Health Associated with the Use of Cleaner Fish in Aquaculture. Opinion of the Panel on Animal Health and Welfare of the Norwegian Scientific Committee for Food and Environment. *VKM), VFOMM (ed.)*. Oslo, Norway. [Cited 16 Jun 2020] Available from URL <https://vkm.no/risikovurderinger/allevurderinger/resefiskogrisikoforoverforingavsmittetiloppdrettslaks> **2017**, *4*, d44969415d.
 125. Rønneseth, A.; Haugland, G. T.; Colquhoun, D. J.; Brudal, E.; Wergeland, H. I. Protection and Antibody Reactivity Following Vaccination of Lumpfish

- (*Cyclopterus lumpus* L.) against Atypical *Aeromonas salmonicida*. *Fish Shellfish Immunol.* **2017**, *64*, 383–391, doi:<https://doi.org/10.1016/j.fsi.2017.03.040>.
126. Bell, G. R.; Higgs, D. A.; Traxler, G. S. The Effect of Dietary Ascorbate, Zinc, and Manganese on the Development of Experimentally Induced Bacterial Kidney Disease in Sockeye Salmon (*Oncorhynchus nerka*). *Aquaculture* **1984**, *36* (4), 293–311.
 127. Murray, C.; Evelyn, T.; Beacham, T.; Bamer, L.; Ketcheson, J.; Prospero-Porta, L. Experimental Induction of Bacterial Kidney Disease in Chinook Salmon by Immersion and Cohabitation Challenges. *Dis. Aquat. Organ.* **1992**, *12*, 91–96, doi:[10.3354/dao012091](https://doi.org/10.3354/dao012091).
 128. Byford, G. J.; Faisal, M.; Tempelman, R. J.; Scribner, K. T. Prevalence and Distribution of *Renibacterium salmoninarum* in Non-Salmonid Fishes from Laurentian Great Lakes and Inland Habitats. *J. Great Lakes Res.* **2020**, *46* (6), 1709–1715, doi:<https://doi.org/10.1016/j.jglr.2020.09.014>.
 129. Scientific Committee on Animal Health and Animal Welfare. *Bacterial Kidney Disease - BKD*; 1999.
 130. Conlon, H.; Imsland, A. K. D. Lumpfish Habitat Development for Use in Salmon Farming. **2019**, No. May.
 131. Valderrama, K.; Saravia, M.; Santander, J. Phenotype of *Aeromonas salmonicida* subsp. *salmonicida* Cyclic Adenosine 3',5'-Monophosphate Receptor Protein (Crp) Mutants and Its Virulence in Rainbow Trout (*Oncorhynchus mykiss*). *J. Fish Dis.* **2017**, *40* (12), 1849–1856, doi:[10.1111/jfd.12658](https://doi.org/10.1111/jfd.12658).
 132. Vasquez, I.; Cao, T.; Hossain, A.; Valderrama, K.; Gnanagobal, H.; Dang, M.; Leeuwis, R. H. J.; Ness, M.; Campbell, B.; Gendron, R.; Kao, K.; Westcott, J.; Gamperl, A. K.; Santander, J. *Aeromonas salmonicida* Infection Kinetics and Protective Immune Response to Vaccination in Sablefish (*Anoplopoma fimbria*). *Fish Shellfish Immunol.* **2020**, *104* (May), 557–566, doi:[10.1016/j.fsi.2020.06.005](https://doi.org/10.1016/j.fsi.2020.06.005).
 133. Gauthier, J.; Marquis, H.; Paquet, V. E.; Charette, S. J.; Levesque, R. C.; Derome, N. Genomic Perspectives on *Aeromonas salmonicida* subsp. *salmonicida* Strain 890054 as a Model System for Pathogenicity Studies and Mitigation of Fish Infections. *Front. Mar. Sci.* **2021**, *8* (November), 1–8, doi:[10.3389/fmars.2021.744052](https://doi.org/10.3389/fmars.2021.744052).
 134. Fuller, T. E.; Thacker, B. J.; Mulks, M. H. A Riboflavin Auxotroph of *Actinobacillus pleuropneumoniae* is Attenuated in Swine. *Infect. Immun.* **1996**, *64* (11), 4659–4664.
 135. Lopez, A. M.; Townsend, H. G. G.; Allen, A. L.; Hondalus, M. K. Safety and Immunogenicity of a Live-Attenuated Auxotrophic Candidate Vaccine against the Intracellular Pathogen *Rhodococcus equi*. *Vaccine* **2008**, *26* (7), 998–1009, doi:[10.1016/j.vaccine.2007.10.069](https://doi.org/10.1016/j.vaccine.2007.10.069).
 136. Fuller, T. E.; Thacker, B. J.; Duran, C. O.; Mulks, M. H. A Genetically-Defined Riboflavin Auxotroph of *Actinobacillus pleuropneumoniae* as a Live Attenuated Vaccine. *Vaccine* **2000**, *18* (25), 2867–2877, doi:[10.1016/S0264-410X\(00\)00076-1](https://doi.org/10.1016/S0264-410X(00)00076-1).

Chapter 2. Host-pathogen Interactions of Marine Gram-positive Bacteria

The research described in Chapter 2 was published in *Biology* as: Gnanagobal, H. and Santander. J. (2022). Host-Pathogen Interactions of Marine Gram-Positive Bacteria. *Biology*, 11, 1316. DOI: 10.3390/biology11091316.

2.1. Abstract

Marine Gram-positive bacterial pathogens, including *Renibacterium salmoninarum*, *Mycobacterium marinum*, *Nocardia seriolae*, *Lactococcus garvieae*, and *Streptococcus* spp. cause economic losses in marine fish aquaculture worldwide. Comprehensive information on these pathogens and their dynamic interactions with their respective fish-host systems are critical to developing effective prophylactic measures and treatments. While much is known about bacterial virulence and fish immune response, it is necessary to synthesize the knowledge in terms of host-pathogen interactions as a centerpiece to establish a crucial connection between the intricate details of marine Gram-positive pathogens and their fish hosts. Therefore, this review provides a holistic view and discusses the different stages of the host-pathogen interactions of marine Gram-positive pathogens. Gram-positive pathogens can invade fish tissues, evade the fish defenses, proliferate in the host system, and modulate the fish immune response. Marine Gram-positive pathogens have a unique set of virulence factors that facilitate adhesion (e.g., adhesins, hemagglutination activity, sortase, and capsules), invasion (e.g., toxins, hemolysins/cytolysins, the Type VII secretion system, and immune-suppressive proteins), evasion (e.g., free radical quenching, actin-based motility, and the inhibition of phagolysosomal fusion), and proliferation and survival (e.g., haem utilization and siderophore-mediated iron acquisition systems) in the fish host. After infection, the fish host initiates specific innate and adaptive immune responses according to the extracellular or intracellular mechanism of infection. Although efforts have continued to be made in understanding the complex interplay at the host-pathogen interface, integrated omics-based

investigations targeting host-pathogen-marine environment interactions hold promise for future research.

Keywords: Gram-positive pathogen; virulence; fish immune response

2.2. Introduction

Marine Gram-positive bacteria include two major subdivisions, the phylum *Actinobacteria*, with high guanine and cytosine (G + C) contents (>50%) in their genomes, and the phylum *Firmicutes*, with low (G + C) contents (<50%) [1]. In most marine environments, Gram-positive bacterial abundance is lower compared to Gram-negative bacteria [2–4], and the presence of Gram-positive bacteria in marine sediments could be linked to nutrient availability [2].

Most marine Gram-positive bacteria have a land origin, and it is believed that they were introduced into marine environments from terrestrial soils [5,6]. For instance, *Arthrobacter* spp., which are soil bacteria, are the closest relatives of *Renibacterium salmoninarum*, a pathogen of marine and freshwater fish [7]. The *R. salmoninarum* genome (~3 Mb) had a significant reduction compared to the *Arthrobacter* spp. genome (~5 Mb), and other Gram-positive environmental bacteria, reflecting its parasitic lifestyle within the host [8].

Non-pathogenic marine Gram-positive bacteria could benefit the host and have practical utilizations as probiotics in aquaculture (e.g., *Lactococcus* spp.) [9,10]. For instance, *Lactococcus lactis* isolated from the gastrointestinal tract of a wild olive flounder (*Paralichthyes olivaceus*) conferred protection against *Streptococcus parauberis* through competitive exclusion [11].

Although Gram-negative bacteria are the most significant pathogens of wild and cultured fish (i.e., *Vibrio* spp., *Aeromonas* spp., and *Edwardsiella* spp.), Gram-positive pathogens, including acid-fast bacteria, can also cause severe economic losses to the marine finfish aquaculture industry, but they are less frequently reported [12,13].

Only a few marine Gram-positive bacteria are primary pathogens (e.g., *M. marinum* and *R. salmoninarum*) [14,15], and the majority are considered opportunistic, causing disease if they are present in high numbers or infect immunocompromised hosts [12,13]. Intracellular marine Gram-positive pathogens (*R. salmoninarum*, *Mycobacterium*, and *Nocardia* spp) can cause chronic persistent infections [16], and several extracellular Gram-positive cocci (e.g., *Lactococcus garviae* and *Streptococcus iniae*) can affect the central nervous systems of fish [17].

Fish diseases continue to be a significant economic threat in aquaculture worldwide and a concern for wild fish populations, especially under the current climate change scenario [18]. Understanding the host-pathogen interactions of marine Gram-positive bacteria will help improve current prophylaxis strategies and the development of novel strategies to prevent infectious diseases in aquaculture environments.

A pathogen is a microbe (e.g., virus, bacterium, protozoan, fungus) that can cause disease to the host, and this ability also depends on host immunity. Pathogenicity means the “potential of a microbe to cause damage in a host.” On the other hand, virulence is either the “degree of pathogenicity” or the “relative capacity of a microbe to cause damage in a host” [19]. After a successful infection, the host is damaged due to either direct microbial activity or an uncontrolled host immune response [19], which ultimately affects host homeostasis [20].

The host-pathogen interaction is a trade-off between host and pathogen that depends on the environmental conditions [21,22]. Methot and Alison (2014) suggest that virulence is an outcome of a specific host-pathogen interaction, not a fixed microbial or host property (Figure 2.1A) [22]. For instance, a virulent microbe can become avirulent or less pathogenic in an immune host, whereas an avirulent microbe can become virulent (i.e., pathogenic) in an immunocompromised host [23]. Infectious diseases occur when a susceptible host and a virulent microbe meet in an environmental context that facilitates such an occurrence (i.e., environmental stressors in the marine environment, high stocking densities in cultured conditions, and parasitic infestations) (Figure 2.1B) [24,25]. The trade-off between the host and pathogen could result in fitness-related costs to both the host (i.e., measurable damage) [13] and the pathogen (i.e., limited ability to spread within the host) (Figure 2.2) [22].

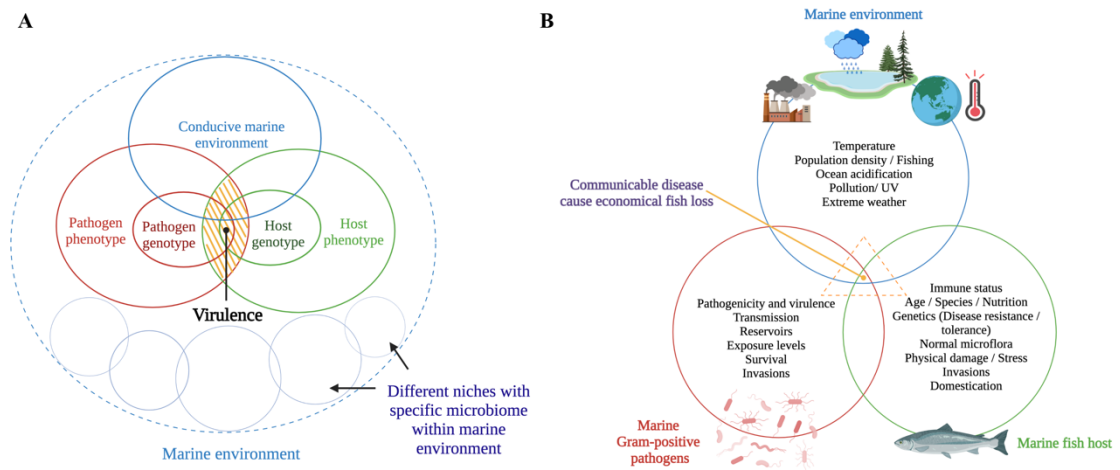


Figure 2.1. Schematic representation of **A.** How virulence is modulated in a dynamic host-pathogen interaction [22] (The yellow shaded area expresses the virulence as an outcome of a dynamic host-pathogen interaction in a conducive marine environment) and **B.** How the disease process occurs as a result of complex host-pathogen-environment interactions. This figure was generated using BioRender (<https://biorender.com/>).

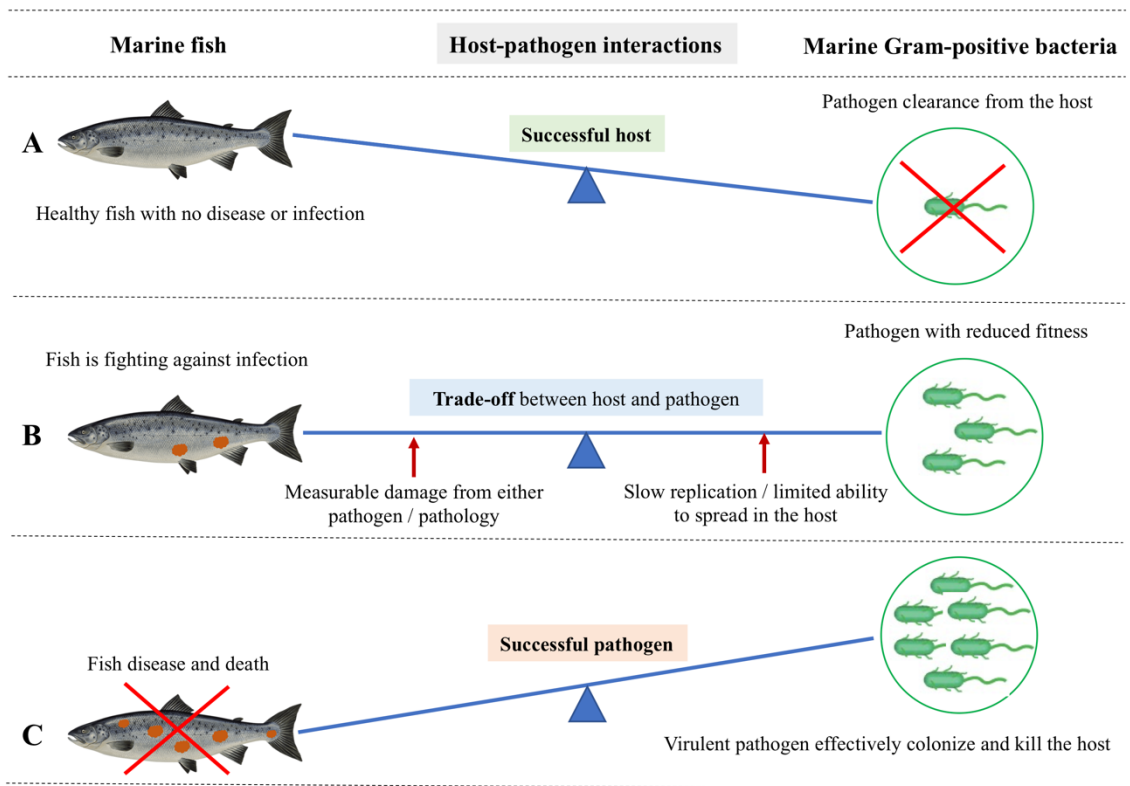


Figure 2.2. Host-centric and pathogen-centric views of dynamic host-pathogen interactions between marine Gram-positive bacteria and a marine fish host. **A.** Successful host: Fish show no disease or infection because of successful pathogen clearance by the host-induced pathogen-specific immune response. Therefore, fish stay healthy, with effective immunological and physiological homeostasis upon an infection event. **B.** The trade-off between host and pathogen: It is the actual tug-of-war scenario between the fish host and pathogen. Here, the fish is still alive but fighting against the infection with an initiated specific immune response. In this trade-off, the pathogen compromises its fitness, thereby slowly replicating without alerting the fish immune response and exploiting the fish host without killing it. On the other hand, the fish is measurably damaged as a result of either the pathogen's action or a host-specific pathology. There is a scenario where increased

acquisition and allocation of nutrients occur at the host/pathogen nutritional interface as opposed to a trade-off. Here, the host withdraws an essential nutrient supply to suppress pathogen proliferation while increasingly allocating the nutrients to fuel immune proliferation. The pathogen, on the other hand, gradually acquires host nutrients to fuel its own replication and survival. **C. Successful pathogen:** A virulent pathogen effectively colonizes using host resources and killing the host by successfully escaping the barriers of the fish host's innate and adaptive immunity, leaving and infecting a new host. Therefore, the fish shows severe disease and death.

Climate change is currently affecting several food-producing sectors, and marine aquaculture has already been impacted. Extremely high temperatures in summer and extremely low temperatures in winter lead to immune suppression of farmed fish, increasing the susceptibility to infectious diseases. The effects of climate change on the virulence and evolution of marine Gram-positive bacterial pathogens have not been addressed. Moreover, how the current environmental and ecological changes (e.g., the migration of invasive species) affect the host-pathogen interactions and how changes in this interplay affect therapeutic and prophylactic measurements have yet to be investigated. Considerable attention has been devoted to studying marine Gram-positive pathogenesis and fish immune responses. However, research using multidisciplinary analyses (i.e., integrated omics) to study the host-pathogen-environment interactions of marine Gram-positive bacteria is insufficient and requires future investigation.

This review provides a comprehensive synopsis of how economically important marine Gram-positive bacterial pathogens (Table 2.1) adhere, invade, evade, proliferate, and cause damage in the fish host (i.e., pathogen-centric approaches) and how the host responds and controls the invader (i.e., host-centric approaches).

Table 2.1. Host-pathogen interactions of significant marine Gram-positive bacteria

Pathogen	Disease (Water Temperature)	Host(s)-Marine Fish ¹	Damage to the Host ²	Main Virulence Factors	References
Aerobic acid-fast rods and cocci					
<i>Mycobacterium</i> spp. <i>M. chelonae</i> subsp. <i>piscarium</i> <i>M. fortuitum</i> <i>M. marinum</i> <i>M. neoaurum</i>	Mycobacteriosis/ fish tuberculosis (17-30 °C)	Most fish spp: turbot (<i>Scophthalmus maximus</i>), Atlantic salmon (<i>Salmo salar</i>), chinook salmon (<i>Oncorhynchus tshawytscha</i>), coho salmon (<i>Oncorhynchus kisutch</i>), sea bass (<i>Lateolabrax japonicus</i>)	a. Scale loss, dermal ulceration, pigmentary changes, abnormal behavior and emaciation, and ascites; b. Haemorrhagic ascites, nodular lesions in the spleen, liver, kidney; c. Granulomatous inflammation	SecA2 substrate-PknG, PE, PPE family proteins; T7SS, mycolactone, <i>iipA</i> gene - invasion and intracellular persistence protein	[26–28]
<i>Nocardia</i> spp. <i>N. asteroides</i> <i>N. salmonicida</i> <i>N. seriolae</i>	Nocardiosis (24-28 °C)	Most fish spp: grey mullet (<i>Mugil cephalus</i>), seabass, largemouth bass (<i>Micropterus salmoides</i>), yellowtail (<i>Seriola quinqueradita</i>)	a. Erratic swimming, anorexia; b. White-yellow nodules in spleen, kidney, and liver; c. Granulomatous lesions with necrosis	ATP binding cassette transporters, capsule, sortase A, ESX-1, fibronectin-binding protein, myosin cross-reactive antigen, serine protease, virulence genes for cell invasion and alteration of phagocytic function	[29,30]
Aerobic rods and cocci					
<i>Renibacterium salmoninarum</i>	Bacterial Kidney Disease (8-15 °C)	1. Salmonids: Atlantic salmon, brown trout (<i>Salmo trutta</i>), Rainbow trout (<i>Oncorhynchus mykiss</i>), chinook salmon, coho salmon; 2. non-salmonids: ayu (<i>Plecoglossus altivelis</i>), north Pacific hake (<i>Merluccius productus</i>), Pacific herring (<i>Clupea pallasii pallasii</i>), sablefish (<i>Anoplopoma fimbria</i>)	a. Skin darkening, lethargy, ascites, exophthalmia, skin blisters, hemorrhages around the vent, shallow skin ulcers, large cystic cavities in the skeletal muscle; b. Greyish-white nodular lesions in kidney, spleen, liver; enlarged spleen and kidney, pseudo-membrane in internal organs, turbid fluid in	Hemolytic, proteolytic, catalase, DNase, and iron reductase activities, exotoxin, virulence genes - hemolysin (<i>rsh</i>), a zinc-metalloprotease (<i>hly</i>), glucose kinase; capsule, fimbriae, immune suppressive proteins p57 and p22	[7,31]

			abdominal/pericardial cavities; c. Bacteremia with chronic granulomatous inflammation		
<i>Rhodococcus</i> sp.	Ocular oedema (12 °C)	Atlantic salmon, chinook salmon	a. Ocular melanosis; b. Ocular lesions, nodules in muscle and organs; c. Granulomas in kidney	Very low-level mortality with high dose (5×10^8 bacteria/fish)	[32]
The “lactic acid bacteria”.					
<i>Lactococcus garviae</i>	Lactococcosis (16-18 °C)	Most fish spp: yellowtail, grey mullet, Japanese or olive flounder (<i>Paralichthys olivaceus</i>), rainbow trout	a. Exophthalmia, lethargy, erosion of tail fin, redness of anal fin, petechiae inside operculum; b. Hemorrhages and petechias at the internal organs’ surface; c. Ocular lesions have fibrous tissue formation with infiltrated inflammatory cells	Hemolysins, Capsule Cell-associated toxin NADH oxidase, superoxide dismutase, adhesins, sortase, and phosphoglucosyltransferase encoding genes	[33–35]
<i>Streptococcus iniae</i>	Streptococcosis / Meningo- encephalitis (15-18 °C)	Most fish spp: yellowtail, olive flounder, sea bass, barramundi (<i>Lates calcarifer</i>), European seabass (<i>Dicentrarchus labrax</i>), gilthead seabream (<i>Sparus aurata</i>)	a. Exophthalmia, petechiae around the mouth, anus, fins, loss of orientation exophthalmia; b. Fluid in the peritoneal cavity; c. Intravascular lesions leading to pericarditis, focal necrosis in liver, spleen, and kidney	Capsular polysaccharide, phosphoglucosyltransferase, fibronectin-binding proteins, streptolysin, hemolysins, plasminogen binding protein, <i>simA</i> M- like protein	[36–39]
<i>Streptococcus parauberis</i>	Streptococcosis (>15 °C)	Turbot	a. Bilateral exophthalmia, emaciation; b. Hemorrhages in anal and pectoral fins, eyes, pale liver, congested kidney, and spleen; c. Haemorrhagic inflammation in the intestine	<i>simA</i> encoding M-like protein, <i>hasA</i> and <i>hasB</i> genes for capsule production and phagocytic resistance	[40,41]
<i>Streptococcus dysgalactiae</i>	Streptococcosis (>15 °C)	Amberjack (<i>Seriola dumerili</i>), yellowtail	a. Typical form of necrosis in the caudal peduncle; b. Septicemia	Cell hydrophobicity, M protein, streptolysin S, superantigen, streptococcal pyrogenic exotoxin G	[42–44]

<i>Streptococcus phocae</i>	Streptococcosis (5-15 °C)	Atlantic salmon	<p>a. Exophthalmia, haemorrhagic eyes with the accumulation of purulent fluid, skin abscesses; b. Hemorrhage in the abdominal fat, pericarditis, enlarged liver, spleen, and kidney; c. Pathological lesions in the spleen, liver, heart, and muscle, leucocytic perivascular infiltration in the spleen, and moderate vascular degeneration in the liver.</p>	Hemolysins, collagen adhesion protein, capsule, cell hydrophobicity	[45,46]
-----------------------------	------------------------------	-----------------	---	---	---------

¹Marine fish hosts for the respective marine Gram-positive bacteria were gathered by considering Austin and Austin (2016) [13].

²Damage from direct bacterial damage and host pathology: a) external signs; b) internal signs; c) histopathology [12,47].

2.3. Pathogen-centric approaches

2.3.1. Adhesion / Host recognition

Pathogen adherence to host surfaces (cells or substrates) is the first step that initiates the host-pathogen interaction, and it is a prerequisite for invasion [48]. One of the factors affecting bacterial adhesion to the host surface (e.g., fish mucus) is bacterial hydrophobicity [49]. High bacterial hydrophobicity is correlated with high adhesion, and therefore this phenotype has an important role in pathogenicity [43]. For instance, the higher surface hydrophobicity and hemagglutinating activity of *Streptococcus dysgalactiae* correlate with its strong adherence ability *in vitro* to carp epithelioma papillosum cells (EPCs). The relationship between hydrophobicity and virulence has also been reported in *R. salmoninarum*, where virulent strains with hydrophobic cell surfaces showed higher adherence and auto-agglutination [50].

Bacterial adhesins, made up of proteins and carbohydrates, enable interaction with the adhesive molecules on the host tissue surface. Protein adhesins include fimbrial (or pili) and afimbrial structures [48]. Bacterial adhesins have been identified based on the bacterial hemagglutination potential [51]. Even though *S. dysgalactiae* and *L. garviae* have fimbria-like structures on their surfaces, *S. dysgalactiae* isolates showed hemagglutination, while *L. garviae* did not, suggesting that the fimbria-like structures of *S. dysgalactiae* were functionally mediating its hemagglutination activity [33,42,43]. The role of surface-anchoring M family proteins as adhesins is well-known [52,53]. For example, *S. iniae simA* gene encodes an M-like protein that contributes to adhesion, subsequent invasion, and phagocytic killing resistance (Figure 2.3). *S. iniae simA* mutant provided 100% protection

in hybrid striped bass (*Morone chrysops* × *Morone saxatilis*), and it could be utilized as an effective live attenuated vaccine [39].

The major soluble antigen (*msa*) p57, which is both a major cell surface (70% of the surface protein) and a secretory protein, is the main virulence factor of *R. salmoninarum* [7]. p57 binds to eucaryotic cells and causes immune suppression [7,54]. Because of its hydrophobic and hemagglutinating characteristics, the p57 monomer resembles bacterial adherence structures (i.e., fimbrial adhesins) and could facilitate adhesion to host cells [55–57]. For example, p57 has been shown to be one of the protein components that make up the peritrichous fimbriae of *R. salmoninarum* [57]. The biological functions of p57, such as binding and agglutinating fish leucocytes, enable *R. salmoninarum* adhesion and invasion [55].

Intriguingly, a recent proteome study found a high abundance of p57, p22 (a second key immune suppressive protein), and proteins implicated in bacterial adhesion in membrane vesicles of *R. salmoninarum*, suggesting that the membrane vesicles could play a role in the pathogen attachment and subsequent Bacterial Kidney Disease (BKD) development [58–60].

Purified p57 loses its immunosuppressive activity when treated with a temperature-dependent endogenous *R. salmoninarum* serine protease [61]. This protease could post-translationally modulate the function of p57 by altering the amount of functionally active p57 at the bacterial surface [7]. Moreover, iron-limited conditions reduced p57 processing into mature and functional protein [62] and, in contrast, facilitated the overproduction of p57, according to a proteomic analysis [63]. Thus, the iron-restricted conditions of fish serum, as the mean of nutritional immunity during the early infection stages of *R.*

salmoninarum, might affect the p57 stability or expression before intracellular invasion [7]. Overall, the hydrophobic surface protein p57 binds with the fish host cell receptors during adhesion (Figure 2.4) and contributes to the pathogen's entry [55].

Fish mucosal surfaces, besides being a physical barrier to pathogens, have antibacterial molecules (e.g., immunoglobulins, antimicrobial peptides, etc.) to prevent infections. However, pathogens have developed mechanisms to overcome this immune defense [64]. For example, the virulence of *S. phocae* is attributed to its capsule, which allows the pathogen to adhere to the Atlantic salmon (*Salmo salar*) mucus and withstand the mucus and serum's bactericidal activity [65] (Figure 2.3).

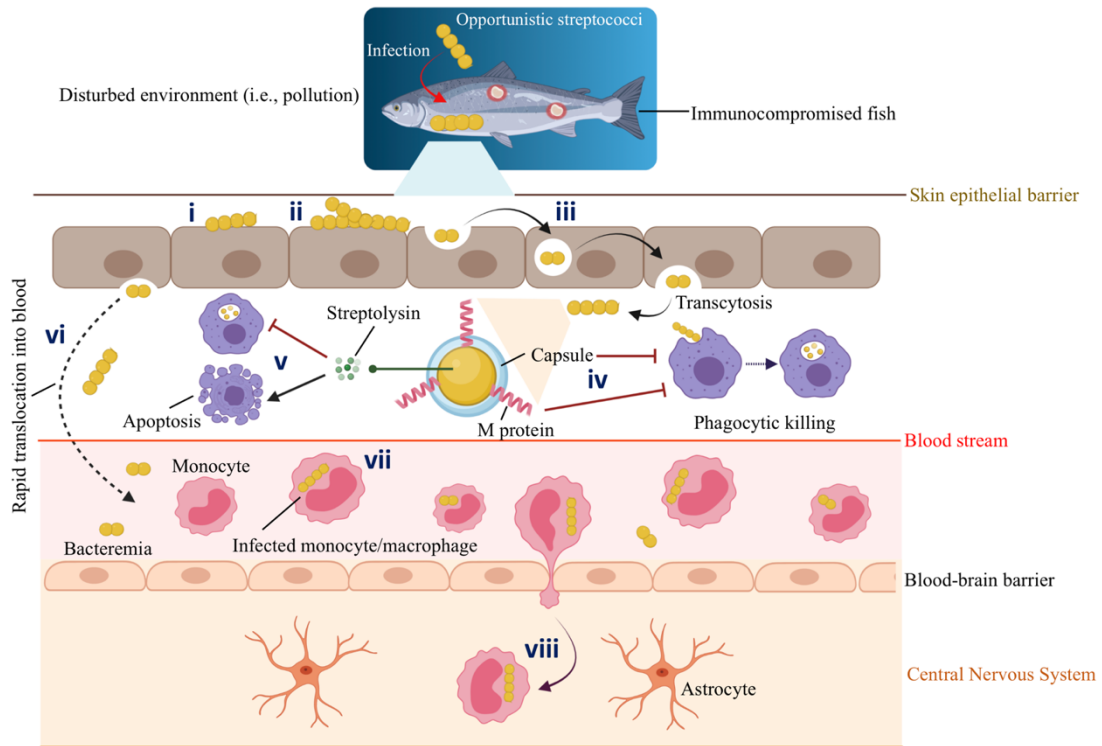


Figure 2.3. Schematic representation of host-pathogen interactions between marine fish and opportunistic *Streptococcus* spp. Gram-positive streptococci infects immunocompromised fish with a decreased immune response that lives in a conducive environment (e.g., polluted marine environment) that facilitates such an infection: **i.** Adhesion. **ii.** Colonization in the epithelial barrier (i.e., mucus). **iii.** Epithelial invasion by transcytosis. **iv.** Antiphagocytic factors such as capsule and M protein aid *S. iniae* to survive phagocytic killing. **v.** Streptolysins secreted by *S. iniae* inhibit phagocytic killing and, at the same time, induce the apoptosis of phagocytes. Thus, infected macrophages undergo apoptotic death and fail to prime a specific immune response. **vi.** Invasive streptococci persist intracellularly for a short time and rapidly translocate into the blood circulation system. **vii.** *S. iniae* hijacks the migrating monocytes or macrophages. For instance, Zlotkin

et al. (2003) observed the presence of 70% of the *S. iniae* in the infected monocytes in the blood of diseased fish [66]. **viii.** Infected monocytes/macrophages act as trojan horses that carry *S. iniae*, cross the blood-brain barrier, transmigrate, and deliver bacteria to the fish central nervous system (CNS). Thus, *S. iniae* can enter the CNS through its association with the migrating monocytes. This original illustration was generated using BioRender (<https://biorender.com/>).

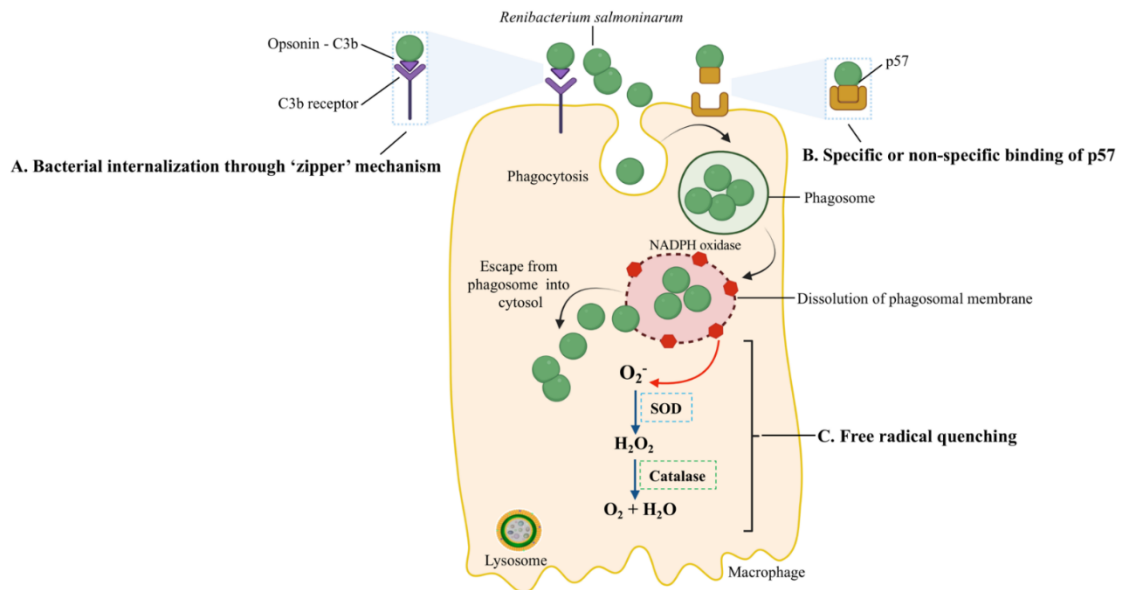


Figure 2.4. Host-pathogen interactions during the intracellular entry, replication, and survival of *R. salmoninarum*. *R. salmoninarum*'s entry into macrophages is facilitated in two ways: **A.** Bacterial internalization through a 'zipper' mechanism. Here, opsonin C3b binds to the bacterial surface, followed by ligation to C3b-receptor-bearing fish phagocytes, and the intracellular invasion of bacteria into host cells. **B.** Specific or non-specific binding of p57 to host cell. The hydrophobic surface protein, p57, which resembles adhesion protein, may allow bacterial adherence to host cell receptors through specific or non-specific binding. Phagocytized *R. salmoninarum* escapes from the phagosome into the cytosol by budding out of the phagosome or phagosomal membrane lysis. **C.** *R. salmoninarum* evades oxidative stress from reactive oxygen species by 'free radical quenching.' Here, NADPH oxidase generates ROS. Superoxide (O_2^-) is converted into H_2O_2 , and then O_2 and H_2O by superoxide dismutase (SOD) and catalase, respectively. This original illustration was generated using BioRender (<https://biorender.com/>).

Another virulence factor related to adhesion is sortase, which has a role in covalent anchoring cell surface proteins in Gram-positive bacteria and contributes to bacterial virulence and modulation of the host immune system. The importance of sortase in adhesion/invasion and virulence of *R. salmoninarum* was demonstrated by Sudheesh et al. (2007) [67]. Reduced virulence in *R. salmoninarum* was observed after treating the pathogen with phenyl vinyl sulfone (PVS), a sortase inhibitor. PVS-treated bacteria showed reduced binding to chinook salmon (*O. tshawytscha*) fibronectin, a ligand for many bacterial adhesins that is abundantly present in eukaryotic extracellular matrix and plasma [68]. Moreover, it showed inhibited cell adherence, invasion, replication, and cytopathic effects on chinook salmon embryo cells compared to the untreated bacteria. In addition, the inhibition of sortase activity has potential use in anti-virulence chemotherapy [69].

Overall, studies focusing on anti-adhesion therapies, the use of potential drugs that block adhesion (i.e., PVS), and the design of DNA vaccine encoding adhesins will contribute to preventing Gram-positive infections in marine farmed fish.

2.3.2. Invasion

Invasion is the ability of a pathogen to spread to different tissues or organs and/or enter host cells. Once the pathogen adheres and colonizes at the host mucosal surfaces, it obtains deeper access into the host, allowing it to sustain the infection cycle [48]. Gram-positives can extracellularly invade by breaking down the tissue boundaries and dispersing in the host while remaining outside of host cells or can intracellularly invade and persist within the host cells [48,70].

Streptococci are usually extracellular pathogens, but several strains are capable of invading eucaryotic cells [71]. Some *S. phocae* isolates attached to the chinook salmon embryo (CHSE) cell line (adhesion values: 18.7-145.3 %), but they were unable to intracellularly invade (invasion values: 0-0.42 %), suggesting a lack of structural components/pathways to facilitate the intracellular invasion [65]. In contrast, some *S. phocae* isolates reach the cytoplasm of CHSE cells at 2 and 20 h post-infection, implying that *S. phocae* is using its virulence mechanism to find a nutritionally compatible niche (i.e., cytosol) within the host to support its further proliferation and survival [72]. Also, Eyngor et al. (2007) demonstrated the critical role of the intracellular epithelial invasion of *S. iniae* for rapid translocation to internal tissues and further infection in rainbow trout (*O. mykiss*) [73] (Figure 2.3). Overall, pathogens employ virulence mechanisms to navigate through the extracellular matrix, breach the barriers between tissues, extend into adjacent tissues or cells, and obtain factors (i.e., nutrients) that sustain their growth.

Gram-positive marine pathogens also synthesize the toxins required for intracellular invasion. *R. salmoninarum* secreted an unknown exotoxin that is lethal to Atlantic salmon fingerlings (9-12 g) at an intraperitoneal (i.p.) dose of 160 µg [74]. Mycolactone F, a *Mycobacterium* spp. toxin that causes apoptosis and necrosis, has been purified from fish pathogens *M. marinum* and *M. pseudoshottsii* [75]. However, the role of this toxin has not been characterized in fish cells [27].

Extracellular toxins, such as hemolysins and cytotoxins, are essential for systemic infection during the extracellular invasion. These toxins lyse erythrocytes and release iron, heme, or hemoglobin for bacterial growth by forming pores on them or altering phospholipid structures in the membrane [48,76,77]. Hemolysins and genes related to

hemolytic activity have been reported in marine Gram-positive bacteria. For instance, *S. iniae* secretes a β -hemolytic streptolysin S (SLS) homolog, a pore-forming cytotoxin [78]. Loss of SLS production in *S. iniae* caused virulence attenuation in hybrid striped bass host. SLS contributes to *S. iniae* virulence by causing local tissue necrosis, helping the pathogen to resist phagocytic killing (Figure 2.3) [78]. The genome of *R. salmoninarum* contains 3 hemolysin encoding genes [8], which could be critical for its intracellular infection and progression. One of these *R. salmoninarum* hemolysins was recently described as helping *R. salmoninarum* cope with stressful conditions in the host during iron limitation [63]. Further, the expression of the hemolysin genes *hly1* and *hly2* in the α -hemolytic bacterium *L. garviae* is associated with its pathogenicity [35]. Another protein related to extracellular invasion is α -enolase. This cell wall-associated, and plasminogen-binding protein of *S. iniae* is partially responsible for tissue invasion. *S. iniae* crossed tissue barriers through plasminogen activation and might migrate faster in the fish extracellular matrix using the proteolytic activity of plasmin [79,80].

Bacterial secretion systems aid pathogenic bacteria in secreting virulence factors (i.e., effector proteins) from bacterial cytosol into host cells during the intracellular invasion, and they can target professional and non-professional phagocytic cells [48,81]. There are two main invasion mechanisms that facilitate bacterial internalization into host cells, called trigger and zipper. In the trigger mechanism, bacteria transfect effectors into the cytoplasm of the host cell via specific secretion systems, causing massive cytoskeletal rearrangements and the development of ruffles, allowing the bacterium to be internalized [82]. For instance, *Mycobacterium* spp. use the type VII secretion system (T7SS), which is encoded by the *esx* loci (*esx1-5*), for intracellular protein trafficking and macrophage

survival [83–85]. *M. marinum* *esx1* is essential for infection in the fish host [86]. *esxA* and *esxB* are essential effectors translocated by the ESX-1 system [86,87]. *esx5* has been identified as an active protein secretion system in *M. marinum*, translocating a variety of PE (Pro-Glu protein) and PPE (Pro-Pro-Glu protein) effector proteins [85,88]. Several of these proteins are found on the surface of mycobacterial cells, which explains their interactions with host cells [89–91]. *M. marinum* *esx5* mutants were utilized by Abdallah et al. (2008) to demonstrate the role of *M. marinum* ESX-5 in triggering host (i.e., human monocytes) cell death and modulating macrophage cytokine responses [92]. *M. marinum* *esx5* mutants were slightly attenuated in the zebrafish embryos but were hypervirulent in the adult zebrafish, which was characterized by higher *esx5* mutant bacterial loads and the early initiation of granuloma formation. This difference in virulence between the embryonic and the adult zebrafish does not appear to be mediated by the adaptive immune system since the *rag*-deficient zebrafish, which lack functional B and T lymphocytes, also exhibited the hypervirulent phenotype. Therefore, other factors that differ between embryonic and adult zebrafish may mediate *M. marinum* hypervirulence in adult zebrafish. For instance, it could be caused by more local and possibly intracellular effects that result from the interplay between the fish host and *M. marinum* rather than a general immune response or modified extracellular environment [93]. A new subclass of type IV secretion system (T4SS), Type-IV-C, was proposed in the Gram-positive genus *Streptococcus* in humans, which could mediate DNA transfer across the cell envelope and enhance bacterial pathogenicity [94]. Interestingly, proteins from T4SS have been identified as virulence factors in *R. salmoninarum* [63]. The presence of this novel secretion system in marine

Gram-positive Streptococci, however, has yet to be reported and opens avenues for future research.

In the zipper mechanism, the interaction of bacterial surface proteins with host proteins causes cytoskeleton and membrane rearrangements, resulting in the pathogen's internalization [82]. Because *R. salmoninarum* has an affinity for phagocytes, sinusoidal cells, and reticular and barrier cells, a putative mechanism (i.e., zipper) (A in Figure 2.4) of its intracellular invasion has been linked to the surface protein p57 [95]. This mechanism involves C3b, a complement pathway opsonin, binding to the bacterial surface, ligation to C3b-receptor-bearing salmonid phagocytes, and subsequently increased internalization [96] (Figure 2.4). In a histopathological examination, Bruno (1986) detected live *R. salmoninarum* cells in phagocytes of the kidneys and spleens of rainbow trout and Atlantic salmon 45 min after i.p. injection and high numbers of bacteria in macrophages after 6-10 days [97].

Overall, most known invasion mechanisms of marine Gram-positive bacteria proceed via protein-protein interactions. Studies focusing on reducing cellular invasiveness and weakening the interactions between pathogen surface proteins and fish host proteins in the extracellular matrix would be beneficial in giving insights into chemotherapeutic treatments in aquaculture.

2.3.3. Evasion

Bacterial immune evasion is a process by which pathogens avoid or inactivate the host immune response once they gain access to the intracellular host milieu. Waxy hydrophobic cell walls or mycolic acids in the mycobacterial capsule prevent digestion by

lysosomal enzymes during evasion [98]. For instance, capsules in *L. garviae* and *S. iniae* enable these pathogens to resist phagocytosis by the macrophages [38,99].

Various bacterial pathogens have adapted to survive and multiply within host cells (i.e., professional phagocytes and non-phagocytic cells) after the invasion. The interaction of *S. iniae* with fish phagocytes (Figure 2.3) is crucial in its evasion and contributes to its virulence [100]. Fish infected with *S. iniae* showed evident bacteremia and diseased fish hold up to 70% of the bacteria in the blood within its phagocytes [66]. After the invasion, *S. iniae* survived phagocytic killing and rapidly disseminated to systemic tissues through the blood. According to Zlotkin et al. (2003), *S. iniae* hijacked the peripheral monocytes/macrophages and used them as trojan horses to enter the central nervous system [66]. Moreover, this pathogen effectively circumvented the host's immune system by inducing apoptosis in fish macrophages [66].

Since professional phagocytic cells, such as macrophages or neutrophils, have mechanisms to eliminate ingested bacteria, the survival and replication inside them are remarkable. One of these killing mechanisms is the production of reactive oxygen species (ROS). The pathogen's ability to resist the host oxidative burst caused by the ROS (i.e., superoxide (O_2^-) and hydrogen peroxide (H_2O_2)), which are produced in phagocytic vacuoles [101,102], is related to free radical quenching (Figure 2.4). The microbicidal component of the phagosome, NADPH oxidase, generates ROS [103]; the superoxide dismutase (SOD) converts O_2^- to H_2O_2 , and the bacterial catalase converts H_2O_2 to $O_2 + H_2O$ to prevent damage. The higher O_2^- production by rainbow trout macrophages in response to heat-killed opsonized *R. salmoninarum*, in contrast to live bacteria, showed that the bacterium's catalase and SOD quench the macrophages' O_2^- production [104–106].

Furthermore, the *R. salmoninarum* genome contains genes for peroxidase, thioredoxin peroxidase, and the SOD enzymes that confer resistance to oxygen radicals [8].

After the intracellular invasion, pathogens can reside in three intracellular niches: the phagolysosome, phagosome, and host-cell cytosol. Another host mechanism to eliminate bacteria is lowering the pH of pathogen-containing vesicles. To bypass this anti-bacterial mechanism, bacterial pathogens can survive and multiply in the phagolysosome (pH = 5.0-5.5), or preclude the formation of the phagolysosome, or escape to the host cell cytoplasm [102,103]. After *R. salmoninarum* is phagocytized, this bacterium escapes to the host cytosol by disrupting or lysing the phagosome membrane (Figure 2.4) [107]. *R. salmoninarum* hemolytic proteins, p57 antigen, hemolysin (*hly*), and cytolysins (*rsh*) facilitated the budding out from the phagosome to the host-cell cytoplasm [62,107–110].

The intracellular survival and replication of *R. salmoninarum* are attributed to its cell wall resistance to lysozyme and slow growth rate [15]. While optimal growth rates are required to initiate infection in the host, *R. salmoninarum* switches to sub-optimal growth rates (e.g., slow growth) to maintain its intracellular survival [101]. For example, this switching has been observed within the macrophages infected *in vitro* with *R. salmoninarum*, where the pathogen showed a decreased growth rate during the chronic infection [107]. Here, a slower growth rate makes the *R. salmoninarum* dormant, thereby resisting the action of antibiotics targeting actively replicating bacteria. Overall, *R. salmoninarum* exhibits prolonged persistence (i.e., chronic intracellular survival) along with a decreased growth rate in the host-pathogen trade-off (Figure 2.2B) [21]. Otherwise, rapid intracellular growth kills the host cells, which is a disadvantage for the long-term survival of the pathogen in fish. Dormant *R. salmoninarum* can then make its own "wake-

up call" under favorable conditions (i.e., when fish are under stress) and start optimal replication through resuscitation-promoting factors [8,111,112].

Bacteria that survive intracellularly either multiply and spread to cells in the infected tissues or migrate to adjacent tissues from the primary site of colonization. *M. marinum* uses two methods to evade phagocytosis, it escapes from phagosomes (Figure 2.5A) and/or blocks phagolysosome fusion (Figure 2.5B). *M. marinum* can escape from the phagosome to the cytosol, where it can recruit host cell cytoskeletal factors to induce actin-based motility that leads to direct cell-to-cell spread [113].

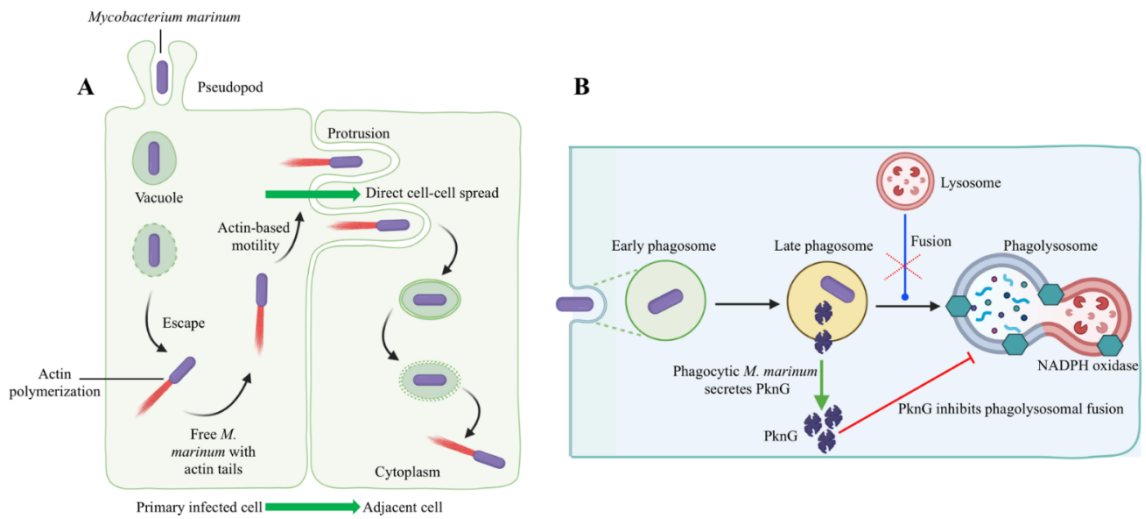


Figure 2.5. Host-pathogen interactions during intracellular evasion strategies of *M. marinum*. *M. marinum* has been shown to use two methods to evade phagocytic killing: **A.** Escape from phagosomes into the cytosol and cell-to-cell spread via actin-based motility [114]. The initial uptake of *M. marinum* into phagocytic vacuoles is followed by an escape from vacuoles into the cytoplasm. According to Stamm et al. 2003, *M. marinum* polymerized actin through the recruitment of host cell cytoskeletal factors in the cytoplasm [113]. Thus, free *M. marinum* with actin tails was observed in the host cell cytoplasm. The acquisition of actin-based motility allows *M. marinum* to spread cell to cell directly from primarily infected cells to adjacent cells without leaving the cytoplasm. **B.** *M. marinum* blocks phagolysosomal fusion (late phagosome fused with phagocytic lysosome), thus resisting the discharge of lysosomal contents into the phagosome. Here, protein kinase G (PknG) secretion through the SecA2 pathway is initiated by phagocytic *M. marinum*. Secreted PknG directly inhibits the fusion of late phagosome with the lysosome. This illustration was created using BioRender (<https://biorender.com/>).

The late phagosome fuses with phagocytic lysosome during phagosome maturation into a phagolysosome, which is induced by the vesicle-mediated delivery of antimicrobial effectors such as proteases, antimicrobial peptides, and lysozyme [115]. Evidence for the phagolysosomal fusion of *M. marinum* phagosomes was observed in striped bass (*Morone saxatilis*) peritoneal macrophages and rainbow trout primary macrophages [116,117]. The morphological presence of the intact mycobacteria within phagolysosomes indicated the pathogen's ability to withstand the hostile phagolysosomal environment [116,117]. In contrast, pathogenic *M. marinum* inhibited phagosome-lysosome fusion in fish monocytes and resided within unfused vacuoles of the carp leucocyte culture cells infected with *M. marinum*, which did not acidify [118]. Mycobacterial protein kinase G (PknG), secreted by SecA2 into the cytosol of infected host cells, is implicated in preventing phagosome-lysosome fusion and facilitating the intracellular survival of mycobacteria [119–122]. *M. marinum* intracellular survival and virulence have been linked to PknG and SecA2 pathway [123,124]. For example, mycobacteria were incapable of preventing phagosomal maturation when SecA2 mutated [123]. On the other hand, the restoration of phagosomal maturation block by overexpressing the PknG in SecA2 mutants suggests a role of PknG in mycobacterial pathogenicity [124].

Investigating the insights of bacterial mechanisms related to the survival of mycobacteria within phagolysosomes will be noteworthy. For instance, Parikka et al. (2012) demonstrated the latency mechanism of *M. marinum* in a zebrafish model [125]. Mycobacteria became dormant in response to the immune response to an infection and hypoxia and were reactivated by an *ex vivo* resuscitation-promoting factor addition [125]. Thus, research on host-pathogen-environment interactions is essential to predict or avoid

the risk of reversion of latent mycobacterial infection in wild or cultured fish populations from polluted marine environments or sea farms.

2.3.4. Proliferation and survival inside the host

After entry, pathogens commandeer and use the host cells not only for their own replication and survival but also for thriving in the host [126]. Pathogens, particularly opportunistic pathogens, proliferate more easily within the host than they do outside the host (e.g., environment) [127]. *R. salmoninarum* cannot survive for extended periods of time outside of its host, and the survival times for *R. salmoninarum* in environmental samples ranged from 4-21 days at 10-18 °C, which is relatively a short time and suggests that this pathogen replicates within the host rather than in the environment [8,112]. The pathogen requires a minimal set of metabolic pathways and a significantly smaller number of genes to multiply inside the host than in the environment, implying that it obtains a considerable amount of essential nutrients directly from the host and that several of its biosynthetic pathways are inactive when it is inside the host [101]. For instance, the presence of several pseudogenes in the *R. salmoninarum* genome may have contributed to the apparent decrease in many anabolic pathways. Simultaneously, the number of bacterial proteins involved in energy metabolism, transcription, and signal transduction in the genome of *R. salmoninarum* was lower than that of its environmental relative, *Arthrobacter* spp. [8]. The reduction of metabolic pathways and bacterial proteins suggests that *R. salmoninarum* depends on the host for its unique requirements. As a result, *R. salmoninarum* should have evolved to exploit the fish host's intrinsic machinery.

Nutritional immunity is a mechanism used by the host to restrict the availability of essential nutrients in their tissues and fluids, such as iron and vitamins, and prevent the proliferation of potential pathogenic invaders [76,128,129]. For instance, the battle over limited iron is critical for the host and the pathogen during infections [130]. Iron is a co-factor of many enzymes, and it is involved in bacterial physiological processes, including central metabolism, transcription, and DNA replication [131]. The ability to acquire iron from the host during infection is essential for bacterial virulence and survival [132,133]. This is also critical for marine pathogens outside their hosts since iron richness in marine environments is extremely low (picograms per liter) [17]. Pathogenic bacteria usually have various iron-acquisition mechanisms for ‘iron-piracy’ to circumvent the nutritional immunity within the host [129,134]. Indeed, iron-depleted conditions inside the host act as a signal for the expression of virulence genes [76,135].

Three iron-acquisition mechanisms have been reported in *R. salmoninarum*, including NADPH reductase, siderophore production, and heme utilization [136,137]. Under iron limitation, ferric iron is converted to a ferrous complex by iron reductase and readily bound to and transported by bacteria [138,139]. Siderophore trafficking in Gram-positive pathogens, which only have a single membrane, is a comparatively simple uptake mechanism compared to Gram-negative bacteria. This mechanism involves a siderophore-binding protein and an associated permease located on the cell membrane [130]. Following iron capture, siderophores bound to receptors on the bacterial surface are internalized, and iron is released in the cytoplasm for growth and colonization during infection. A significant role of iron-acquisition mechanisms (siderophores) in virulence is supported by Bethke et al. (2019) [140]. In this study, an *R. salmoninarum* strain (H-2) with a high siderophore

production capability was grown under the iron-limited condition and showed significant over-expression of the iron-acquisition-related genes compared to the bacteria grown under normal conditions. On the other hand, *R. salmoninarum* H-2 displayed higher virulence in terms of cytotoxicity, cytopathic effects and induced the expression of pro-inflammatory cytokines in the Atlantic salmon kidney cell line than a strain with lower siderophore production capacity [140]. A proteome analysis of *R. salmoninarum* H-2 grown under iron-limited conditions indicated that the iron homeostasis pathway and critical virulence factors related to iron deprivation were significantly enriched [63].

Genomic analyses of *R. salmoninarum* conducted by Wiens et al. (2008) and Bethke et al. (2016; 2018) revealed important facts about *R. salmoninarum* iron homeostasis [8,137,141]. *R. salmoninarum* has gene clusters that encode for a ferric siderophore import system [8]. The heme acquisition mechanism of *R. salmoninarum* could be similar to the other Gram-positive bacteria based on the genes that encode for heme uptake in *R. salmoninarum* (i.e., receptors, permeases, ATPase subunits, and heme oxygenases similar to the HmuTUV (HmuO) ABC transporter system) [137,142,143]. According to Wiens et al. (2008), the heme acquisition operons in the *R. salmoninarum* genome were acquired via horizontal gene transfer during species divergence [8]. As *R. salmoninarum* falls under high G + C content (56.3%) Gram-positive bacteria, the presence of additional iron-dependent repressors belonging to the DtxR/IdeR family and their binding sites upstream of important iron-acquisition-related genes were observed [8,141,144,145].

The *S. phocae* isolate of Atlantic salmon secretes siderophores and can acquire heme directly through binding receptors [146]. Interestingly, *S. phocae* expressed an unknown iron-regulated protein (95 kDa) under iron-limited conditions, which could be a

receptor for siderophore-iron complexes/heme groups or interact with host-iron-carrying components (e.g., transferrin) [146]. In addition, biofilm formation was observed in the iron-limited condition, indicating *S. phocae*'s ability to sense iron availability in the host. Therefore, the bacterium could develop strategies for bacterial adherence, which leads to successful colonization within the host.

More is known about Gram-negative than Gram-positive iron acquisition systems [147]. Therefore, it is expected that the iron-regulated proteins of marine Gram-positive bacteria require more research. Recent proteomic data obtained from *R. salmoninarum* grown under iron-limited conditions identified important virulence factors related to their iron acquisition mechanisms (e.g., heme uptake and siderophore synthesis), which could aid in designing therapeutic approaches targeting these essential bacterial proteins [63]. For instance, blocking siderophore-mediated iron uptake (e.g., siderophore receptor protein which is responsible for transporting siderophore-iron complexes into the bacterial cytosol) would be an option for combating infection of Gram-positive pathogens, such as *R. salmoninarum*.

2.4. Host-centric approaches - Fish host immune response

Marine Gram-positive bacterial pathogens use diverse mechanisms to infect and manipulate fish host cells and evade immune responses. In contrast, the fish host will mount an immune defense to control the infection and subsequently eliminate it from the system to maintain its homeostasis (Figure 2.2A). Fish immune responses to marine Gram-positive pathogens have been studied in several fish species (Table 2.2). Fish immune responses at different stages of infection with marine Gram-positive pathogens are discussed in this

section, including innate immunity and pathogen recognition, nutritional immunity, and adaptive immunity.

Table 2.2. Examples of recent studies on the host (fish) response to marine Gram-positive bacterial pathogens.

Host (Tissue/cell type)	Pathogen	Method	Host response*	Reference
Chinook salmon: Wisconsin and Green River stocks (Kidney)	<i>R. salmoninarum</i> ATCC 33209	qPCR	<p>↑ interferon response in both stocks (<i>ifng</i>, <i>mx1</i>)</p> <p>↑ <i>iNOS</i> expression and ↑ prevalence of membranous glomerulopathy in lower surviving stock than the higher surviving stock</p> <p>↑ iron binding protein response (<i>transferrin</i>) in higher surviving stock than lower surviving stock</p>	[148]
Atlantic salmon (Kidney cell line)	<i>R. salmoninarum</i> : H-2 and DSM20767 have high and low siderophore production abilities, respectively	qPCR	<p>↑ pro-inflammatory cytokines (<i>il1β</i>, <i>tnfa</i>), Gram-positive pattern recognition receptor (<i>TLR</i>), and interferon (<i>ifng</i>)</p> <p>Reduced expression of <i>tnfa</i> and <i>TLR1</i> at 24 hpi</p> <p>Strain (H-2) grown under iron-limited conditions induced a significantly higher immune response in host cells than DSM20767 and bacteria grown under normal conditions.</p>	[140]
Atlantic salmon (Head kidney)	Formalin killed <i>R. salmoninarum</i> ATCC 33209	Transcriptomics (44K microarray) and qPCR	<p>↑ pathogen recognition receptors (<i>tlr5</i>, <i>clec12b</i>)</p> <p>↑ immunoregulatory receptors (<i>tnfrsf6b</i>, <i>tnfrsf11b</i>)</p> <p>↑ antimicrobial effectors (<i>hamp</i>)</p> <p>↑ interferon-induced response (<i>ch25ha</i>)</p> <p>↑ chemokine (<i>ccl13</i>) and ↓ chemokine receptor (<i>cxcr1</i>)</p>	[149]
Lumpfish (<i>Cyclopterus lumpus</i>) (Head kidney)	<i>R. salmoninarum</i> ATCC 33209	qPCR	<p>Early stage (28 dpi): immune suppressive infection</p> <p>↑ pro-inflammatory cytokines (<i>il1b</i>, <i>il8a</i>, <i>il8b</i>), anti-inflammatory cytokine (<i>il10</i>), pattern recognition (<i>tlr5a</i>), iron regulation (<i>hamp</i>), and acute phase reactant (<i>saa5</i>) related genes</p> <p>↑ interferon induce response (<i>ifnγ</i>, <i>mxα</i>, <i>mxβ</i>, <i>mxγ</i>, <i>rsad2</i>, and <i>stat1</i>)</p> <p>↓ <i>tnfa</i> and cellular mediated adaptive immunity (<i>cd4a</i>, <i>cd4b</i>, <i>cd8a</i>, <i>cd74</i>) related genes</p> <p>Chronic stage (98 dpi): cell-mediated adaptive immunity</p> <p>↑ <i>ifng</i> and <i>cd74</i></p>	[150]

Japanese flounder vaccinated with <i>sagH</i> DNA vaccine (Spleen and blood)	<i>S. iniae</i> SF1 (Serotype I) and 29177 (Serotype II)	qPCR and ELISA	<p>↑ innate and adaptive immune response (<i>il1b, il1, il6, il8, il10, tnfa, ifng, mx, nkef, tgfb, MHCI and II, cd40 and cd8a</i>)</p> <p>↑ titer of specific serum antibodies</p>	[151]
Asian seabass vaccinated with a commercial vaccine, Norvax Strep Si (Spleen and head kidney)	<i>S. iniae</i>	Transcriptomics (8×60K microarray) and qPCR	<p>Effect of vaccination was early and transient in the spleen (1-7 dpv) compared to the head kidney, which showed a delayed response (21 dpv)</p> <p>In vaccinated spleens:</p> <p>↑ NFκB, chemokine, and toll-like receptor signalling</p> <p>↑ genes related to proteolysis, phagocytosis, and apoptosis</p> <p>Rapid T cell-mediated adaptive immune response</p>	[152]
Atlantic salmon and rainbow trout (Mucus, serum, and macrophages)	<i>S. phocae</i> subsp. <i>salmonis</i> isolates: 2 from Atlantic salmon (LM-08-Sp and LM-13-Sp) and 2 from seal (ATCC 51973T and P23)	Comparative innate immune response analysis	<p>↑ lysozyme activity, phagocytic and bactericidal activity, reactive oxygen species, and NO production in rainbow trout compared to the Atlantic salmon</p> <p>Rainbow trout was more resistant to <i>S. phocae</i> than Atlantic salmon in terms of non-specific humoral and cellular barriers</p>	[153]
European Seabass (Spleen, head kidney, and blood)	<i>M. marinum</i> : virulent (Eilat) and heat-killed avirulent mutant (<i>ipa::kan</i>) strains	qPCR, ELISA	<p>↑ specific Immunoglobulin (IgM) response (1 and 2 mpc)</p> <p>↑ <i>tnfa</i> in the spleen at 1 mpc and return to basal levels in the spleen and head kidney at 2 mpc</p> <p>High survival (75%), strong immune response, and moderate tissue damage in avirulent mutant strain</p>	[154]
Amur sturgeon (<i>Acipenser schrenckii</i>) (Liver)	<i>M. marinum</i> ASCy-1.0	<i>De novo</i> Transcriptome analysis (Illumina RNA seq) and qPCR	<p>Total differentially expressed contigs (DEC): 4043 (↑ 2479, ↓ 1564)</p> <p>78 DEC - innate immune response (<i>iNos2, saa</i>), phagocytosis, antigen processing and presentation (<i>mhc1</i>), chemotaxis (<i>ccl19</i>), leucocyte regulation (<i>il8</i>)</p> <p>Strong leptin expression - Th1 immunity</p> <p>Immune pathways: TNF signaling, Toll-like receptor signaling</p>	[155]
Amberjack vaccinated with formalin killed <i>N. seriola</i> cells + mixture of 6 recombinant	Formalin killed <i>N. seriola</i> 024013 strain	qPCR	<p>↑ Th1-specific transcriptional factors (<i>ifng</i> and <i>T-bet</i>)</p> <p>↓ Th2-related genes (<i>il10</i> and <i>GATA-3</i>)</p> <p>↓ primary and secondary humoral immune response</p>	[156]

amberjack IL-12 (rIL-12) as adjuvant (Head kidney and spleen leucocytes)		rIL-12 proved as a CMI inducible adjuvant - produce Th1 immunity cells having antigen memory		
Largemouth bass (Spleen)	<i>N. seriolae</i>	<i>de novo</i> transcriptome analysis (RNA seq using Illumina hiseq) and qPCR	↑ 1384 genes, ↓ 1542 genes ↑ pro-inflammatory cytokines and signal transduction-related genes (<i>il1b, il8, tnfa</i> , TNF receptors, CXC chemokines, <i>tgfb</i>) Anti-bacterial mechanism at early-stage infection (24 hpi) involved cytokine-cytokine receptor interactions Immune pathway: JAK-STAT signalling	[157]
Grey mullet (Head kidney and spleen)	<i>L. garviae</i>	<i>De novo</i> transcriptome analysis (RNA seq using Illumina hiseq) and qPCR	Spleen: ↑ 3598 genes, ↓ 3682 genes (Total: 7280) Head kidney: ↑ 4211 genes, ↓ 2981 genes (Total: 7192) ↑ Pro-inflammatory cytokines, Fc receptor and <i>Ig, il10, mhc-I, mhc-II, cd4</i> , and <i>cd8</i> ↓ <i>il8</i> and <i>tnfa</i> Immune pathways: complement and coagulation cascade, TLR signaling, antigen processing, and presentation	[158]

*This column includes host immune response/activity and or immune signalling pathways differentially expressed after infection.

↑ upregulation or increase based on the response or process

↓ downregulation or decrease based on the response or process

hpi: hours post-infection; dpi: days post-infection; dpv: days post-vaccination; mpc: months post-challenge.

2.4.1. Toll-like receptors (Pathogen recognition)

In fish, TLRs (Toll-like receptors), NLRs (NOD-like receptors), CLRs (C-type lectin receptors), and PGRP (peptidoglycan recognition proteins) are the 4 main types of Pattern Recognition Receptors (PRRs) [159]. Only TLRs are the subject of this section because they are well-described signalling PRRs in fish innate immunity, detecting Gram-positive pathogen-associated molecular patterns (PAMPs) [160].

TLRs are the innate immune receptors that recognize conserved pathogen molecules (e.g., lipopolysaccharide (LPS), flagellin, and components of the cell wall) [161] and thereby trigger rapid inflammation and prime adaptive immunity [162–164]. The involvement of diverse TLRs in marine fish immunity upon infection with the marine Gram-positive bacteria *L. garviae* [158], *N. seriola* [157], and *S. dysgalactiae* [165] were reported in transcriptome analyses. In mammals, TLR2 forms a heterodimer with TLR1, which recognizes lipoteichoic acid and peptidoglycan from Gram-positive bacteria [166]. The upregulation of *tlr2* was observed in grey mullet (*M. cephalus*) in response to *L. garviae* [158]. Concurrently, *tlr1* and *tlr2* were upregulated in zebrafish following *M. marinum* infection, which agreed with the known functions of mammalian TLR1 and TLR2 in sensing acid-fast / Gram-positive cell wall components [167]. Though the specific ligand for TLR1 is unknown in fish, *tlr1* showed a similar expression pattern as *ifng* (interferon gamma) (i.e., significant upregulation at 6 and 12 hpi) in the Atlantic salmon kidney cell line (ATCC #CRL-2747) in response to *R. salmoninarum* [140,161]. This observation is in line with Miettinen et al. (2001), who described the ability of IFN- γ to upregulate TLR1 and TLR2 [168].

Fish TLR5 recognizes bacterial flagellin [169]. However, in response to non-motile (i.e., non-flagellated) Gram-positive pathogens such as *S. iniae* and *R. salmoninarum*, *tlr5* was upregulated in turbot (*S. maximus*) and Atlantic salmon, respectively [149,170,171]. This controversial observation demands future research to study the role of TLR5 beyond the recognition of flagellin.

Mammalian TLR4 recognizes Gram-negative LPS [169]. Teleost fish do not have a complete functional TLR4 [172]. While the presence of TLR4 and some co-receptors was reported in some fish species, the lack of essential co-receptors in teleost (e.g., CD14) makes this TLR4 not functional for LPS detection in all fish species [166]. Interestingly, the *tlr4* encoding gene in soiny mullet (*Liza haematocheila*) was upregulated in spleens upon Gram-positive *S. dysgalactiae* infection, suggesting an alternative role of TLR4 in the fish immune response to Gram-positive bacteria [165].

Among six fish-specific (i.e., not present in mammals) TLRs (TLR14, 19, 20, 21, 22, and 23) [161], TLR14, TLR20, and TLR22 showed interactions with marine Gram-positive pathogens. For instance, *S. iniae* infection increased *tlr14* expression in the Japanese flounder kidney at 1 dpi [173]. Moreover, upregulated expression levels of *tlr20* and *tlr22* in zebrafish infected with *M. marinum* suggest a role of fish-specific TLR clusters in recognizing bacterial infections [167].

Although the functions of fish-specific TLRs have yet to be reported [161], TLRs interaction with Gram-positive fish pathogens suggests that diverse fish TLRs are involved in fish immunity against marine Gram-positive infections.

2.4.2. Nutritional immunity

The host-mediated withholding of essential nutrients to limit bacterial colonization or nutritional immunity is one of the first lines of defense against bacterial infection. The most significant form of nutritional immunity is iron sequestration in host proteins because iron is essential for bacterial proliferation and virulence [76]. Like in mammals, several host iron-sequestering proteins have been described in marine teleosts, including transferrin [174], ferritin [175], hemoglobin [176], haptoglobin [177], hemopexin [178], and lipocalin (Lcn2) [179]. The hypoferric inflammatory response in fish is mediated by the stimulation of the proinflammatory cytokine interleukin-6 (Il6) [180], which increases the synthesis and secretion of Hepcidin (encoded by *hamp*) [181]. Increased hepcidin levels have an inhibitory effect on the expression of *ferroportin* (*fpn1*), an iron exporter that plays an important role in iron homeostasis [181,182]. As a result of decreased *fpn1* expression, the iron release is blocked, and iron uptake is decreased [183–185]. Overall, the iron in tissues is reduced to such a low concentration that the pathogen cannot replicate and cause disease [76]. In other words, iron limitation reduces bacterial growth to a level that enables the fish immune system to eliminate the infection [186].

Hepcidin is an anti-microbial peptide with iron regulatory properties [182]. Two functionally distinct Hepcidin types have been described in teleost fish; type 1 hepcidin (*hamp1*) is the iron metabolism regulator, and type 2 hepcidin (*hamp2*) presents an antimicrobial role [187]. Significantly increased expression of Hepcidin was observed in hybrid striped bass liver and Atlantic salmon head kidney during the early stages of infection with *S. iniae* [188] and *R. salmoninarum* [149,171], respectively. During an

evaluation of the antimicrobial potential of European sea bass hepcidins, elevated expression levels of *hamp1* and *hamp2* in the liver were observed in response to *S. parauberis* and *L. garviae* infection [189]. Here, *hamp 1* showed no antibacterial activity, similar to what was reported for Japanese flounder hepcidins against *L. garviae* and *S. iniae* infection [189,190]. However, *hamp2* exhibited significantly stronger antibacterial activity, especially against Gram-positive bacteria, compared to Gram-negative bacteria. Future studies will be required to investigate the potential prophylactic use of fish-derived hepcidins to control Gram-positive bacterial infections and to better understand the insights into their antimicrobial properties.

Transferrin is one of the serum proteins capable of binding and transporting iron and creating an environment where low levels of iron restrict the growth of pathogens [191]. The biological functions of transferrin have been linked with resistance to infectious diseases [192–194]. Metzger and co-workers (2010) observed that the expression of the transferrin-encoding gene was upregulated up to 71 dpi in two chinook salmon stocks following *R. salmoninarum* i.p. infection [148]. Interestingly, transferrin expression significantly differed between populations, where the *R. salmoninarum*-resistant salmon population showed higher transferrin expression than the susceptible population. In addition, differential resistance among the three transferrin genotypes of coho salmon (*O. kisutch*) was observed after injection with *R. salmoninarum* [193]. On the other hand, Stafford and Belosevic (2002) demonstrated a unique role of transferrin as a mediator of fish macrophage activation in combination with the TLR system [195]. In this study, adding exogenous transferrin to goldfish macrophages activated by *Mycobacterium chelonae* significantly increased their nitric oxide (NO) production [195]. The role of transferrin in

controlling intracellular bacterial pathogens (i.e., *R. salmoninarum* and *M. chelonae*) has not been explored and could reveal disease resistance mechanisms in fish and improve broodstock selection based on transferrin allelic variation.

The second layer of iron nutritional immunity involves Lcn2, which binds to bacterial siderophores and sequester ferric-siderophore complexes away from bacterial siderophore receptors [76,196]. A recent study found the first evidence of functional teleost Lcn2 with antimicrobial properties in triploid crucian carp [179]. Here, Lcn2 enhanced the bactericidal activity, triggered immune defense, and increased fish resistance against Gram-negative *Aeromonas hydrophila* infection. Developing research to understand the immune effects of Lcn2 and Lcn2-mediated resistance against marine Gram-positive pathogens might be useful.

2.4.3. Innate and adaptive (humoral and cell-mediated) immunity

The first protective barrier against infection is the fish mucus, which has bactericidal properties. It is also the first interaction site between skin epithelial cells and the pathogen [64]. Lysozyme is one of the components that helps the fish mucus have an antibacterial effect. For instance, it has been documented that the lysozyme activity in the mucus of rainbow trout controlled the growth of *S. phocae* [153]. In addition, higher levels of skin mucus in marine fish and increases in cholesterol (i.e., lipid rafting) in the fish cell membrane aided in resisting pathogen invasion [197–199].

In response to *R. salmoninarum*, rainbow trout macrophages activated inflammatory responses (upregulation of *il1b*, *cox2*, *mhcII*, *iNOS*, *cxcr4*, *ccr7*) at 2 h post-infection [200]. TNF- α , apart from its role in regulating inflammation, is associated with

the pathogenesis of chronic infections in fish [180]. *R. salmoninarum* survived initial contact with macrophages by avoiding/interfering with the TNF- α dependent killing pathways of fish [200]. Also, the chronic stimulation of TNF- α , which is implicated by p57, could assist a chronic inflammatory pathology (granulomas). IFN- γ is a Th1 cytokine associated with adaptive immunity [180]. Interferon systems play a role in priming and regulating the adaptive immune response against intracellular mycobacteria [201]. Interferon and interferon-induced effectors (Mx1, Mx2, and Mx3) are associated with the inflammatory response in fish [202–204]. Thus, the expression of *ifn γ* and *mx1-3* upon *R. salmoninarum* infection in chinook salmon and rainbow trout may be linked to the priming of adaptive immunity [148,200,201]. In addition, the early upregulation of interferon-induced effectors in response to an *R. salmoninarum* strain with reduced p57 suggests these genes as possible immune indicators in vaccine design [205,206].

The teleost adaptive immune system is subdivided into humoral immunity, which involves antibodies to neutralize pathogens in body fluids, and cell-mediated immunity, which kills and eliminates pathogen-infected cells [207]. Extracellular pathogens evoke humoral immune responses, while intracellular pathogens evoke both humoral and cell-mediated immune responses. Although salmonids mount a humoral response against *R. salmoninarum*, there is no clear correlation between this antibody response and protective immunity [7,112]. Moreover, the humoral response is counterproductive, as it is linked to exacerbated BKD pathology (i.e., antigen-antibody complex deposition in glomeruli) [7,208,209]. Antigen-antibody immune complexes formed during infection might weaken the effective antibody response by adsorbing the circulating antibodies before they bind to p57 and block its activity related to immune suppression [7,210].

Few studies reported the cell-mediated immune response of *R. salmoninarum* [200,211–213]. A p57-induced chronic reduction in MHC II expression might consequently skew the T-cell responses toward an MHC I-dependent cell-mediated response [200]. Khalil et al. (2020b) presented a complete picture of Atlantic salmon innate and adaptive immune response to live *R. salmoninarum* by using a 44 K salmonid microarray platform in a transcriptome profiling study [171]. For instance, *R. salmoninarum* differentially regulated the Atlantic salmon adaptive immune responses, including B or T cell differentiation, function, and antigen presentation. Additionally, *R. salmoninarum* infection levels have an impact on the JAK-STAT signalling pathway during host-pathogen interactions [171].

Sakai et al. (1989) demonstrated the protective immune response against streptococcal infection in rainbow trout immunized with β -haemolytic *Streptococcus* spp. bacterin [214]. Here, the serum of fish immunized with i.p. injected streptococcal bacterin showed no enhanced bactericidal activity but had agglutinating antibodies. However, these specific antibodies were not associated with protective immunity. Interestingly, increase in the phagocytic activity of kidney leucocytes observed in the vaccinated fish could be aided in the rapid bacterial clearance from the spleen, liver, kidney, and blood 72 h post-challenge, suggesting that cellular immunity plays a major role in rainbow trout defense against *Streptococcus* spp.

The cell-mediated immunity involving CD8⁺ T cells is effective in killing and eliminating intracellular Gram-positive pathogens (*R. salmoninarum* and *Mycobacterium* spp.) in fish [207,215], and protective cell-mediated immunity could be achieved by inducing these cells [207]. For instance, CD8⁺ T cells are activated into cytotoxic T

lymphocytes upon binding to MHC-I molecules that express processed antigens from intracellular pathogens. T lymphocytes secrete cytotoxic granules. The perforins and granzymes contents of these granules induce apoptosis of infected cells. Concurrently, cytokine signatures, such as TNF- α and IFN- γ that skew CD4+ cells towards Th1 differentiation, would help in priming of CD8+ cells as "immune-adjuvants" for producing protective immunity.

2.4.4. Fish resistance/tolerance/susceptibility to marine Gram-positive bacteria

Resistance is the ability to limit the pathogen in terms of its replication or spread. On the other hand, tolerant fish would show less pathology when comparing high- and low-tolerant fish populations with equivalent pathogen burden [216]. Metzger et al. (2010) demonstrated the 'resistance' and 'tolerance' in two chinook salmon stocks (higher-surviving WI stock and lower-surviving green river stock) following an *R. salmoninarum* challenge [148]. The WI stock showed a lower bacterial load than the green river stock at 28 dpi, which implied the resistance of higher-survival stock. Conversely, the green river stock exhibited higher mortality levels than the WI stock by 44 dpi, when both stocks had similar levels of bacterial load, which explained the tolerance of higher-survival stock. Thus, the authors pointed out that the enhanced tolerance of chinook salmon against *R. salmoninarum* could benefit the fitness of both the host and pathogen in the dynamic interaction. Sako (1992) observed an acquired immune resistance in yellowtail (*Seriola quinqueradita*) when the fish recovered from an experimental infection with *S. iniae* were reinfected [217]. Here, the bacterial loads in the spleen, kidney, and blood showed rapid decreases, whereas no bacterial proliferation was observed in the brain.

As water temperature affects both the rate of bacterial multiplication and the fish immune response, the rapid shifts in marine water temperature could alter host-pathogen interactions and reduce host resistance [218]. For instance, fish become susceptible to streptococcal infections during summers with high temperatures [219]. Lower water temperatures (8 °C) contributed to the disease progression and transmission potential in chinook salmon infected with *R. salmoninarum* [218]. Also, inhibited cell-mediated immunity and a higher risk of death during the late stage of infection were observed in Atlantic salmon pre-molt survivors upon *R. salmoninarum* infection in low water temperatures (11 °C) [220].

2.5. Conclusions

Taken together, this article provides an overview of host-centric and pathogen-centric approaches at the host-pathogen interface between economically important marine fish and Gram-positive pathogens. Marine Gram-positive pathogens developed a unique set of machinery/strategies to interact with their exclusive fish host cells and modulate the complex molecular and cellular networks of these cells to allow bacterial proliferation and spread while counteracting fish defenses. Pathogenicity of marine Gram-positive pathogens strongly depends on the host it is trying to interact. For instance, *R. salmoninarum* has primarily adapted to infect and persist in salmonids [7].

Knowledge of how the host and pathogen interact is crucial for a true understanding of disease and a key to developing control or prevention strategies. Studies in marine Gram-positive pathogens that have been conducted so far focused mostly on bacterial virulence and fish immune responses. A few studies considered how environmental stressors (i.e.,

temperature or hypoxia) affect host-pathogen interactions and alter disease progression [125,218]. Dynamic host-pathogen interactions between marine Gram-positive pathogens and fish hosts are complex. Exploring how host-pathogen-environment interactions mediate disease outcomes in marine fish populations with the help of integrative omics research will add another layer of complexity. Purcell et al. (2015) suggested that under a warming climate, *R. salmoninarum* may pose a lesser risk to chinook salmon since low temperatures (8 °C) favor its infection compared to higher temperatures (12 °C and 15 °C) [218]. It will be useful to conduct research to determine which Gram-positive bacterial pathogens may pose a threat to cultured fish due to climate change.

As prophylaxis design engages in either disabling bacterial virulence or boosting the host system, vaccines and immunostimulants are effective and sustainable in aquaculture [127,221,222]. Most licensed fish vaccines against streptococcal and lactococcal infections are traditional inactivated microorganisms [223]. A live vaccine contains non-pathogenic *Arthrobacter davidanieli*, which is closely phylogenetically related to *R. salmoninarum*, is commercially licensed for BKD control, and elicits cross-immunity [224]. However, the protective immunity of this vaccine is experimentally and intellectually questionable for protecting a wide range of salmonids [206]. The protective effect of DNA and sub-unit vaccines in fish has been demonstrated against *S. iniae* infection [151,225–227]. A rational fish vaccine design using alternative technologies beyond just bacterins, including recombinant live-attenuated or RNA vaccines, is essential [223]. These technologies have yet to be reported to prevent marine Gram-positive infections in fish. In contrast, there are several experimental reports of such vaccine designs against Gram-negative fish pathogens. For instance, the LcrV protein (V antigen) is an essential virulent

factor of *Yersinia pestis*, a Gram-negative pathogen and the causative agent of bubonic plague [228]. Variants of V antigen lacking the immune suppressor region induced protective immunity in mice [229–231]. p57 and p22 have been reported as immune suppressive proteins contributing to *R. salmoninarum* virulence. Thus, identifying or designing the variants of p57 and p22 with reduced immunomodulatory properties and using them as immune protective antigens will be an attractive vaccine design for BKD control in mariculture. Although the area of functional genomics of fish pathogenic bacteria has been slowly progressing, most of the economically important marine Gram-positive bacterial genomes were sequenced [232]. These available genomes open exciting opportunities in the search for universal vaccine candidates across the fish pathogens and shed light on using reverse vaccinology approaches. For example, a recent study used a reverse vaccinology pipeline to identify a set of antigens that could be used to develop a polyvalent vaccine against Gram-negative bacterial infections that impact Atlantic salmon and lumpfish aquaculture [233]. Vaccines against marine Gram-positive bacterial infections could be developed using similar techniques. In addition to vaccines, immunostimulants could be used as fish non-specific immune defense enhancers to improve fish resistance to disease. Improved phagocytic activity was observed in rainbow trout treated with the fermented chicken egg product, EF2013 during streptococcal and renibacterial infections [234,235]. Research on the use of immunostimulants to alter host-pathogen interactions and improve fish immunocompetency against marine Gram-positive bacteria will be beneficial.

As aquaculture continues to grow globally, applying bioinformatics to expand our knowledge on host-pathogen-environment interactions of marine Gram-positive bacteria will be valuable in solving emerging fish health issues.

2.6. References

1. Garrity, G. M.; Winters, M.; Searles, D. B. Taxonomic Outline of the Procaryotic Genera. In *Bergey's manual of systematic bacteriology*; Garrity, G. M., Boone, D. R., Castenholz, R. W., Eds.; Springer-Verlag: New York, 2001; pp 155–166.
2. Jensen, P. R.; Fenical, W. The Relative Abundance and Seawater Requirements of Gram-Positive Bacteria in Near-shore Tropical Marine Samples. *Microb. Ecol.* **1995**, *29* (3), 249–257, doi:10.1007/BF00164888.
3. Tamames, J.; Abellán, J. J.; Pignatelli, M.; Camacho, A.; Moya, A. Environmental Distribution of Prokaryotic Taxa. *BMC Microbiol.* **2010**, *10*, doi:10.1186/1471-2180-10-85.
4. Bolhuis, H.; Cretoiu, M. S. What Is so Special About Marine Microorganisms? Introduction to the Marine Microbiome—From Diversity to Biotechnological Potential. In *The Marine Microbiome*; Stal, L. J., Silvia, M., Eds.; 2016, doi:10.1007/978-3-319-33000-6.
5. Zobell, C. E.; Upham, H. C. A List of Marine Bacteria Including Descriptions of Sixty New Species. **1944**, *5*, 239–292.
6. Goodfellow, M.; Haynes, J. A. Actinomycetes in Marine Sediments. In *Biological, Biochemical and Biomedical Aspects of Actinomycetes*; Ortiz-Ortiz, L., Ed.; Academic Press: New York, 1984; pp 453–472.
7. Wiens, G. D. Bacterial Kidney Disease (*Renibacterium salmoninarum*). In *Fish Diseases and Disorders*; Woo, P. T. K., Bruno, D. W., Eds.; CABI: Wallingford, UK, 2011; pp 338–374.
8. Wiens, G. D.; Rockey, D. D.; Wu, Z.; Chang, J.; Levy, R.; Crane, S.; Chen, D. S.; Capri, G. R.; Burnett, J. R.; Sudheesh, P. S.; Schipma, M. J.; Burd, H.; Bhattacharyya, A.; Rhodes, L. D.; Kaul, R.; Strom, M. S. Genome Sequence of the Fish Pathogen *Renibacterium salmoninarum* Suggests Reductive Evolution Away from an Environmental *Arthrobacter* Ancestor. *J. Bacteriol.* **2008**, *190* (21), 6970–6982, doi:10.1128/JB.00721-08.
9. Caipang, C. M. A.; Suharman, I.; Avillanosa, A. L.; Bargoyo, V. T. Host-Derived Probiotics for Finfish Aquaculture. *IOP Conf. Ser. Earth Environ. Sci.* **2020**, *430* (1), doi:10.1088/1755-1315/430/1/012026.
10. Teasdale, M. E.; Donovan, K. A.; Forscher-Dancause, S. R.; Rowley, D. C. Gram-Positive Marine Bacteria as a Potential Resource for the Discovery of Quorum Sensing Inhibitors. *Mar. Biotechnol.* **2011**, *13* (4), 722–732, doi:10.1007/s10126-010-9334-7.
11. Nguyen, T. L.; Park, C. Il; Kim, D. H. Improved Growth Rate and Disease Resistance in Olive Flounder, *Paralichthys olivaceus*, by Probiotic *Lactococcus lactis* WFLU12 Isolated from Wild Marine Fish. *Aquaculture* **2017**, *471*, 113–120, doi:10.1016/j.aquaculture.2017.01.008.
12. Roberts, R. J. The Bacteriology of Teleosts. In *Fish pathology*; Roberts, R. J., Ed.; Wiley-Blackwell: West Sussex, UK, 2012; pp 339–382, doi:10.1111/j.1751-0813.2002.tb14791.x.
13. Austin, B.; Austin, D. A. *Bacterial Fish Pathogens: Disease of Farmed and Wild*

- Fish, Sixth Edition*; Springer International Publishing, 2016, doi:10.1007/978-3-319-32674-0.
14. Aronson, J. D. Spontaneous Tuberculosis in Salt Water Fish. *J. Infect. Dis.* **1926**, *39*, 312–320.
 15. Fryer, J. L.; Sanders, J. E. Bacterial Kidney Disease of Salmonid Fish. *Annu. Rev. Microbiol.* **1981**, *35*, 273–298, doi:10.1146/annurev.mi.35.100181.001421.
 16. Munn, C. B. Pathogens in the Sea: An Overview. In *Ocean and Health: PATHogens in Marine Environment*; Belkin, S., Colwel, R. R., Eds.; Springer Science, 2005.
 17. Munn, C. B. Microbial Diseases of Marine Organisms. In *Marine Microbiology Ecology and Applications*; Taylor and Francis CRC ebook account, 2011; pp 244–245, doi:10.1201/9780429061042-11.
 18. Burge, C. A.; Mark Eakin, C.; Friedman, C. S.; Froelich, B.; Hershberger, P. K.; Hofmann, E. E.; Petes, L. E.; Prager, K. C.; Weil, E.; Willis, B. L.; Ford, S. E.; Harvell, C. D. Climate Change Influences on Marine Infectious Diseases: Implications for Management and Society. *Ann. Rev. Mar. Sci.* **2014**, *6*, 249–277, doi:10.1146/annurev-marine-010213-135029.
 19. Casadevall, A.; Pirofski, L. A. Host-Pathogen Interactions: Redefining the Basic Concepts of Virulence and Pathogenicity. *Infect. Immun.* **1999**, *67* (8), 3703–3713, doi:10.1128/iai.67.8.3703-3713.1999.
 20. Casadevall, A.; Pirofski, L. A. What Is a Host? Incorporating the Microbiota into the Damage-Response Framework. *Infect. Immun.* **2015**, *83* (1), 2–7, doi:10.1128/IAI.02627-14.
 21. Alizon, S.; Hurford, A.; Mideo, N.; Van Baalen, M. Virulence Evolution and the Trade-off Hypothesis: History, Current State of Affairs and the Future. *J. Evol. Biol.* **2009**, *22* (2), 245–259, doi:10.1111/j.1420-9101.2008.01658.x.
 22. Méthot, P. O.; Alizon, S. What is a Pathogen? Toward a Process View of Host-Parasite Interactions. *Virulence* **2014**, *5* (8), 775–785, doi:10.4161/21505594.2014.960726.
 23. Casadevall, A.; Pirofski, L. Host-pathogen Interactions: The Attributes of Virulence. *J. Infect. Dis.* **2001**, *184* (3), 337–344.
 24. Snieszko, S. F. Nutritional Fish Diseases. In *Fish Nutrition*; Elsevier, 1972; pp 403–437, doi:10.1016/b978-0-12-319650-7.50014-6.
 25. Lafferty, K. D.; Harvell, C. D.; Conrad, J. M.; Friedman, C. S.; Kent, M. L.; Kuris, A. M.; Powell, E. N.; Rondeau, D.; Saksida, S. M. Infectious Diseases Affect Marine Fisheries and Aquaculture Economics. **2015**.
 26. Gao, L.-Y.; Pak, M.; Kish, R.; Kajihara, K.; Brown, E. J. A Mycobacterial Operon Essential for Virulence *in vivo* and Invasion and Intracellular Persistence in Macrophages. *Infect. Immun.* **2006**, *74* (3), 1757–1767, doi:10.1128/IAI.74.3.1757-1767.2006.
 27. Gauthier, D. T.; Rhodes, M. W. Mycobacteriosis in Fishes: A Review. *Vet. J.* **2009**, *180* (1), 33–47, doi:10.1016/j.tvjl.2008.05.012.
 28. Hashish, E.; Merwad, A.; Elgaml, S.; Amer, A.; Kamal, H.; Elsadek, A.; Marei, A.; Sitohy, M. *Mycobacterium marinum* Infection in Fish and Man: Epidemiology, Pathophysiology and Management; a Review. *Vet. Q.* **2018**, *38* (1), 35–46, doi:10.1080/01652176.2018.1447171.

29. Maekawa, S.; Yoshida, T.; Wang, P. C.; Chen, S. C. Current Knowledge of Nocardiosis in Teleost Fish. *J. Fish Dis.* **2018**, *41* (3), 413–419, doi:10.1111/jfd.12782.
30. Yasuike, M.; Nishiki, I.; Iwasaki, Y.; Nakamura, Y.; Fujiwara, A.; Shimahara, Y.; Kamaishi, T.; Yoshida, T.; Nagai, S.; Kobayashi, T.; Katoh, M. Analysis of the Complete Genome Sequence of *Nocardia seriolae* UTF1, the Causative Agent of Fish Nocardiosis: The First Reference Genome Sequence of the Fish Pathogenic *Nocardia* Species. *PLoS One* **2017**, *12* (3), 1–23, doi:10.1371/journal.pone.0173198.
31. Elliott, D. G. *Renibacterium salmoninarum*. In *In Fish Viruses and Bacteria: Pathobiology and Protection*; Woo, P.T.K and Ciaprino, R. , Ed.; CABI, U.K, 2017; pp 286–297.
32. Speare, D. J.; Brocklebank, J.; Macnair, N.; Bernard, K. A. Experimental Transmission of a Salmonid *Rhodococcus* Sp. Isolate to Juvenile Atlantic Salmon, *Salmo salar* L. *J. Fish Dis.* **1995**, *18* (6), 587–597, doi:10.1111/j.1365-2761.1995.tb00363.x.
33. Ooyama, T.; Hirokawa, Y.; Minami, T.; Yasuda, H.; Nakai, T.; Endo, M.; Ruangpan, L.; Yoshida, T. Cell-Surface Properties of *Lactococcus garvieae* Strains and Their Immunogenicity in the Yellowtail *Seriola quinqueradiata*. *Dis. Aquat. Organ.* **2002**, *51* (3), 169–177, doi:10.3354/dao051169.
34. Vendrell, D.; Balcázar, J. L.; Ruiz-Zarzuola, I.; de Blas, I.; Gironés, O.; Múzquiz, J. L. *Lactococcus garvieae* in Fish: A Review. *Comp. Immunol. Microbiol. Infect. Dis.* **2006**, *29* (4), 177–198, doi:10.1016/j.cimid.2006.06.003.
35. Teker, T.; Albayrak, G.; Akayli, T.; Urku, C. Detection of Haemolysin Genes as Genetic Determinants of Virulence in *Lactococcus garvieae*. *Turkish J. Fish. Aquat. Sci.* **2019**, *19* (7), 625–634, doi:10.4194/1303-2712-v19_7_09.
36. Bromage, E. S.; Owens, L. Infection of Barramundi *Lates calcarifer* with *Streptococcus iniae*: Effects of Different Routes of Exposure. *Dis. Aquat. Organ.* **2002**, *52* (3), 199–205, doi:10.3354/dao052199.
37. Buchanan, J. T.; Stannard, J. A.; Lauth, X.; Ostland, V. E.; Powell, H. C.; Westerman, M. E.; Nizet, V. *Streptococcus iniae* Phosphoglucomutase Is a Virulence Factor and a Target for Vaccine Development. *Infect. Immun.* **2005**, *73* (10), 6935–6944, doi:10.1128/IAI.73.10.6935-6944.2005.
38. Locke, J. B.; Colvin, K. M.; Datta, A. K.; Patel, S. K.; Naidu, N. N.; Neely, M. N.; Nizet, V.; Buchanan, J. T. *Streptococcus iniae* Capsule Impairs Phagocytic Clearance and Contributes to Virulence in Fish. *J. Bacteriol.* **2007**, *189* (4), 1279–1287, doi:10.1128/JB.01175-06.
39. Locke, J. B.; Aziz, R. K.; Vicknair, M. R.; Nizet, V.; Buchanan, J. T. *Streptococcus iniae* M-like Protein Contributes to Virulence in Fish and Is a Target for Live Attenuated Vaccine Development. *PLoS One* **2008**, *3* (7), 1–13, doi:10.1371/journal.pone.0002824.
40. Doménech, A.; Fernández-Garayzábal, J. F.; Pascual, C.; Garcia, J. A.; Cutuli, M. T.; Moreno, M. A.; Collins, M. D.; Dominguez, L. Streptococcosis in Cultured Turbot, *Scophthalmus maximus* (L.), Associated with *Streptococcus parauberis*. *J. Fish Dis.* **1996**, *19* (1), 33–38, doi:10.1111/J.1365-2761.1996.TB00117.X.
41. Nho, S. W.; Hikima, J.; Cha, I. S.; Park, S. Bin; Jang, H. Bin; del Castillo, C. S.;

- Kondo, H.; Hirono, I.; Aoki, T.; Jung, T. S. Complete Genome Sequence and Immunoproteomic Analyses of the Bacterial Fish Pathogen *Streptococcus parauberis*. *J. Bacteriol.* **2011**, *193* (13), 3356–3366, doi:10.1128/JB.00182-11.
42. Nomoto, R.; Munasinghe, L. I.; Jin, D.-H.; Shimahara, Y.; Yasuda, H.; Nakamura, A.; Misawa, N.; Itami, T.; Yoshida, T. Lancefield Group C *Streptococcus dysgalactiae* Infection Responsible for Fish Mortalities in Japan. *J. Fish Dis.* **2004**, *27* (12), 679–686, doi:10.1111/j.1365-2761.2004.00591.x.
 43. Abdelsalam, M.; Chen, S. C.; Yoshida, T. Surface Properties of *Streptococcus dysgalactiae* Strains Isolated from Marine Fish. *Bull. Eur. Assoc. Fish Pathol.* **2009**, *29* (1), 16–24.
 44. Abdelsalam, M.; Chen, S. C.; Yoshida, T. Dissemination of Streptococcal Pyrogenic Exotoxin G (Spegg) with an IS-like Element in Fish Isolates of *Streptococcus dysgalactiae*. *FEMS Microbiol. Lett.* **2010**, *309* (1), 105–113, doi:10.1111/j.1574-6968.2010.02024.x.
 45. Romalde, J. L.; Ravelo, C.; Valdés, I.; Magariños, B.; de la Fuente, E.; Martín, C. S.; Avendaño-Herrera, R.; Toranzo, A. E. *Streptococcus phocae*, an Emerging Pathogen for Salmonid Culture. *Vet. Microbiol.* **2008**, *130* (1–2), 198–207, doi:10.1016/j.vetmic.2007.12.021.
 46. Yañez, A. J.; Godoy, M. G.; Gallardo, A.; Avendaño-Herrera, R. Identification of *Streptococcus phocae* Strains Associated with Mortality of Atlantic Salmon (*Salmo salar*) Farmed at Low Temperature in Chile. *Bull. Eur. Assoc. Fish Pathol.* **2013**, *33* (2), 59–66.
 47. Roberts, R. J. *Bacteria from Fish and Other Aquatic Animals: A Practical Identification Manual*; 2005; Vol. 28, doi:10.1111/j.1365-2761.2005.00644.x.
 48. Wilson, J. W.; Schurr, M. J.; LeBlanc, C. L.; Ramamurthy, R.; Buchanan, K. L.; Nickerson, C. A. Mechanisms of Bacterial Pathogenicity. *Postgrad. Med. J.* **2002**, *78* (918), 216–224, doi:10.1136/pmj.78.918.216.
 49. Esperanza Cortés, M.; Consuegra Bonilla, J.; Dario Sinisterra, R. Biofilm Formation, Control and Novel Strategies for Eradication. *Sci. against Microb. Pathog. Commun. Curr. Res. Technol. Adv.* **2011**, *2* (January 2011), 896–905.
 50. Bruno, D. The Relationship between Auto-Agglutination, Cell Surface Hydrophobicity and Virulence of the Fish Pathogen *Renibacterium salmoninarum*. *FEMS Microbiol. Lett.* **1988**, *51* (2–3), 135–139, doi:10.1016/0378-1097(88)90387-4.
 51. Izumi, É.; Domingues Pires, P.; Bittencourt De Marques, E.; Suzart, S. Hemagglutinating and Hemolytic Activities of *Enterococcus faecalis* Strains Isolated from Different Human Clinical Sources. *Res. Microbiol.* **2005**, *156* (4), 583–587, doi:10.1016/j.resmic.2005.01.004.
 52. Ellen, R. P.; Gibbons, R. J. M Protein-Associated Adherence of *Streptococcus pyogenes* to Epithelial Surfaces: Prerequisite for Virulence. *Infect. Immun.* **1972**, *5* (5), 826–830, doi:10.1128/iai.5.5.826-830.1972.
 53. Caparon, M. G.; Stephens, D. S.; Olsén, A.; Scott, J. R. Role of M Protein in Adherence of Group A Streptococci. *Infect. Immun.* **1991**, *59* (5), 1811–1817, doi:10.1128/iai.59.5.1811-1817.1991.
 54. Wiens, G. D.; Chien, M. S.; Winton, J. R.; Kaattari, S. L. Antigenic and Functional

- Characterization of P57 Produced by *Renibacterium salmoninarum*. *Dis. Aquat. Organ.* **1999**, 37 (1), 43–52, doi:10.3354/dao037043.
55. Wiens, G. D.; Kaattari, S. L. Monoclonal Antibody Characterization of a Leukoagglutinin Produced by *Renibacterium salmoninarum*; 1991.
 56. Daly, J. G.; Stevenson, R. M. W. Characterization of the *Renibacterium salmoninarum* Haemagglutinin. *J. Gen. Microbiol.* **1990**, 136 (5), 949–953, doi:10.1099/00221287-136-5-949.
 57. Dubreuil, J. D.; Jacques, M.; Graham, L.; Lallier, R. Purification, and Biochemical and Structural Characterization of a Fimbrial Haemagglutinin of *Renibacterium salmoninarum*. *J. Gen. Microbiol.* **1990**, 136 (12), 2443–2448, doi:10.1099/00221287-136-12-2443.
 58. Fredriksen, Å.; Endresen, C.; Wergeland, H. I. Immunosuppressive Effect of a Low Molecular Weight Surface Protein from *Renibacterium salmoninarum* on Lymphocytes from Atlantic Salmon (*Salmo salar* L.). *Fish Shellfish Immunol.* **1997**, 7 (4), 273–282, doi:10.1006/fsim.1997.0082.
 59. Brynildsrud, O.; Gulla, S.; Feil, E. J.; Nørstebø, S. F.; Rhodes, L. D. Identifying Copy Number Variation of the Dominant Virulence Factors msa and p22 within Genomes of the Fish Pathogen *Renibacterium salmoninarum*. *Microb. genomics* **2016**, 2 (4), e000055, doi:10.1099/mgen.0.000055.
 60. Kroniger, T.; Flender, D.; Schlüter, R.; Köllner, B.; Trautwein-Schult, A.; Becher, D. Proteome Analysis of the Gram-positive Fish Pathogen *Renibacterium salmoninarum* Reveals Putative Role of Membrane Vesicles in Virulence. *Sci. Rep.* **2022**, 12 (1), 1–11.
 61. Rockey, D. D.; Turaga, P. S. D.; Wiens, G. D.; Cook, B. A.; Kaattari, S. L. Serine Proteinase of *Renibacterium salmoninarum* Digests a Major Autologous Extracellular and Cell-Surface Protein. *Can. J. Microbiol.* **1991**, 37 (10), 758–763, doi:10.1139/m91-130.
 62. Grayson, T. H.; Evenden, A. J.; Gilpin, M. L.; Munn, C. B. Production of the Major Soluble Antigen of *Renibacterium salmoninarum* in *Escherichia coli* K12. *Dis. Aquat. Organ.* **1995**, 22 (3), 227–231, doi:10.3354/dao022227.
 63. Avendaño-Herrera, R.; Saldivia, P.; Bethke, J.; Vargas, C.; Hernández, M. Proteomic Analysis Reveals *Renibacterium salmoninarum* Grown under Iron-limited Conditions Induces Iron Uptake Mechanisms and Overproduction of the 57-kDa Protein. *J. Fish Dis.* **2022**, 45 (2), 289–300.
 64. Benhamed, S.; Guardiola, F. A.; Mars, M.; Esteban, M. Á. Pathogen Bacteria Adhesion to Skin Mucus of Fishes. *Vet. Microbiol.* **2014**, 171 (1–2), 1–12, doi:10.1016/j.vetmic.2014.03.008.
 65. González-Contreras, A.; Magariños, B.; Godoy, M.; Irgang, R.; Toranzo, A. E.; Avendaño-Herrera, R. Surface Properties of *Streptococcus phocae* Strains Isolated from Diseased Atlantic Salmon, *Salmo salar* L. *J. Fish Dis.* **2011**, 34 (3), 203–215, doi:10.1111/j.1365-2761.2010.01228.x.
 66. Zlotkin, A.; Chilmonczyk, S.; Eyngor, M.; Hurvitz, A.; Ghittino, C.; Eldar, A. Trojan Horse Effect: Phagocyte-Mediated *Streptococcus iniae* Infection of Fish. *Infect. Immun.* **2003**, 71 (5), 2318–2325, doi:10.1128/IAI.71.5.2318-2325.2003.
 67. Sudheesh, P. S.; Crane, S.; Cain, K. D.; Strom, M. S. Sortase Inhibitor Phenyl Vinyl

- Sulfone Inhibits *Renibacterium salmoninarum* Adherence and Invasion of Host Cells. *Dis. Aquat. Organ.* **2007**, 78 (2), 115–127, doi:10.3354/dao01859.
68. Joh, D.; Wann, E. R.; Kreikemeyer, B.; Speziale, P.; Höök, M. Role of Fibronectin-Binding MSCRAMMs in Bacterial Adherence and Entry into Mammalian Cells. *Matrix Biol.* **1999**, 18 (3), 211–223, doi:10.1016/S0945-053X(99)00025-6.
 69. Marraffini, L. A.; DeDent, A. C.; Schneewind, O. Sortases and the Art of Anchoring Proteins to the Envelopes of Gram-positive Bacteria. *Microbiol. Mol. Biol. Rev.* **2006**, 70 (1), 192–221, doi:10.1128/mmbr.70.1.192-221.2006.
 70. OECD. *Bacteria: Pathogenicity Factors*; 2016; Vol. 5, doi:10.1787/9789264253018-4-en.
 71. Nitsche-Schmitz, D. P.; Rohde, M.; Chhatwal, G. S. Invasion Mechanisms of Gram-positive Pathogenic Cocci. *Thromb. Haemost.* **2007**, 98 (3), 488–496.
 72. Cortez-San Martin, M.; González-Contreras, A.; Avendaño-Herrera, R. Infectivity Study of *Streptococcus phocae* to Seven Fish and Mammalian Cell Lines by Confocal Microscopy. *J. Fish Dis.* **2012**, 35 (6), 431–436, doi:10.1111/j.1365-2761.2012.01361.x.
 73. Eyngor, M.; Chilmonczyk, S.; Zlotkin, A.; Manuali, E.; Lahav, D.; Ghittino, C.; Shapira, R.; Hurvitz, A.; Eldar, A. Transcytosis of *Streptococcus iniae* through Skin Epithelial Barriers: An in Vitro Study. *FEMS microbiology letters*. England December 2007, pp 238–248, doi:10.1111/j.1574-6968.2007.00973.x.
 74. Shieh, H. S. An Extracellular Toxin Produced by Fish Kidney Disease Bacterium, *Renibacterium salmoninarum*. *Microbios Lett.* **1988**, 38 (149), 27–30.
 75. Ranger, B. S.; Mahrous, E. A.; Mosi, L.; Adusumilli, S.; Lee, R. E.; Colorni, A.; Rhodes, M.; Small, P. L. C. Globally Distributed Mycobacterial Fish Pathogens Produce a Novel Plasmid-Encoded Toxic Macrolide, Mycolactone F. *Infect. Immun.* **2006**, 74 (11), 6037–6045, doi:10.1128/IAI.00970-06.
 76. Skaar, E. P. The Battle for Iron between Bacterial Pathogens and Their Vertebrate Hosts. *PLoS Pathog.* **2010**, 6 (8), 1–2, doi:10.1371/journal.ppat.1000949.
 77. Goebel, W.; Chakraborty, T.; Kreft, J. Bacterial Hemolysins as Virulence Factors. *Antonie Van Leeuwenhoek* **1988**, 54 (5), 453–463, doi:10.1007/BF00461864.
 78. Locke, J. B.; Colvin, K. M.; Varki, N.; Vicknair, M. R.; Nizet, V.; Buchanan, J. T. *Streptococcus iniae* β -Hemolysin Streptolysin S Is a Virulence Factor in Fish Infection. *Dis. Aquat. Organ.* **2007**, 76 (1), 17–26, doi:10.3354/dao076017.
 79. Kim, M. S.; Choi, S. H.; Lee, E. H.; Nam, Y. K.; Kim, S. K.; Kim, K. H. α -Enolase, a Plasmin(Ogen) Binding and Cell Wall Associating Protein from a Fish Pathogenic *Streptococcus iniae* Strain. *Aquaculture* **2007**, 265 (1–4), 55–60, doi:10.1016/j.aquaculture.2007.01.034.
 80. Eberhard, T.; Kronvall, G.; Ullberg, M. Surface Bound Plasmin Promotes Migration of *Streptococcus pneumoniae* through Reconstituted Basement Membranes. *Microb. Pathog.* **1999**, 26 (3), 175–181, doi:10.1006/mpat.1998.0262.
 81. Green, E. R.; Mecsas, J. Bacterial Secretion Systems: An Overview. *Microbiol. Spectr.* **2016**, 4 (1), 1–4.
 82. Ribet, D.; Cossart, P. How Bacterial Pathogens Colonize Their Hosts and Invade Deeper Tissues. *Microbes Infect.* **2015**, 17 (3), 173–183.
 83. Abdallah, A. M.; Gey van Pittius, N. C.; Champion, P. A. D.; Cox, J.; Luirink, J.;

- Vandenbroucke-Grauls, C. M. J. E.; Appelmelk, B. J.; Bitter, W. Type VII Secretion--Mycobacteria Show the Way. *Nat. Rev. Microbiol.* **2007**, *5* (11), 883–891, doi:10.1038/nrmicro1773.
84. Bottai, D.; Brosch, R. Mycobacterial PE, PPE and ESX Clusters: Novel Insights into the Secretion of These Most Unusual Protein Families. *Mol. Microbiol.* **2009**, *73* (3), 325–328, doi:10.1111/j.1365-2958.2009.06784.x.
 85. Abdallah, A. M.; Verboom, T.; Hannes, F.; Safi, M.; Strong, M.; Eisenberg, D.; Musters, R. J. P.; Vandenbroucke-Grauls, C. M. J. E.; Appelmelk, B. J.; Luirink, J.; Bitter, W. A Specific Secretion System Mediates PPE41 Transport in Pathogenic Mycobacteria. *Mol. Microbiol.* **2006**, *62* (3), 667–679, doi:10.1111/j.1365-2958.2006.05409.x.
 86. Weerdenburg, E. M.; Abdallah, A. M.; Rangkuti, F.; El Ghany, M. A.; Otto, T. D.; Adroub, S. A.; Molenaar, D.; Ummels, R.; ter Veen, K.; van Stempvoort, G.; van der Sar, A. M.; Ali, S.; Langridge, G. C.; Thomson, N. R.; Pain, A.; Bitter, W. Genome-Wide Transposon Mutagenesis Indicates That *Mycobacterium marinum* Customizes Its Virulence Mechanisms for Survival and Replication in Different Hosts. *Infect. Immun.* **2015**, *83* (5), 1778–1788, doi:10.1128/IAI.03050-14.
 87. Gröschel, M. I.; Sayes, F.; Simeone, R.; Majlessi, L.; Brosch, R. ESX Secretion Systems: Mycobacterial Evolution to Counter Host Immunity. *Nat. Rev. Microbiol.* **2016**, *14* (11), 677–691, doi:10.1038/nrmicro.2016.131.
 88. Abdallah, A. M.; Verboom, T.; Weerdenburg, E. M.; Gey van Pittius, N. C.; Mahasha, P. W.; Jimenez, C.; Parra, M.; Cadieux, N.; Brennan, M. J.; Appelmelk, B. J.; Bitter, W. PPE and PE_PGRS Proteins of *Mycobacterium marinum* Are Transported via the Type VII Secretion System ESX-5. *Mol. Microbiol.* **2009**, *73* (3), 329–340, doi:10.1111/j.1365-2958.2009.06783.x.
 89. Brennan, M. J.; Delogu, G.; Chen, Y.; Bardarov, S.; Kriakov, J.; Alavi, M.; Jacobs, W. R. J. Evidence That Mycobacterial PE_PGRS Proteins Are Cell Surface Constituents That Influence Interactions with Other Cells. *Infect. Immun.* **2001**, *69* (12), 7326–7333, doi:10.1128/IAI.69.12.7326-7333.2001.
 90. Banu, S.; Honoré, N.; Saint-Joanis, B.; Philpott, D.; Prévost, M.-C.; Cole, S. T. Are the PE-PGRS Proteins of *Mycobacterium tuberculosis* Variable Surface Antigens? *Mol. Microbiol.* **2002**, *44* (1), 9–19, doi:10.1046/j.1365-2958.2002.02813.x.
 91. Delogu, G.; Pusceddu, C.; Bua, A.; Fadda, G.; Brennan, M. J.; Zanetti, S. Rv1818c-Encoded PE_PGRS Protein of *Mycobacterium tuberculosis* Is Surface Exposed and Influences Bacterial Cell Structure. *Mol. Microbiol.* **2004**, *52* (3), 725–733, doi:10.1111/j.1365-2958.2004.04007.x.
 92. Abdallah, A. M.; Savage, N. D. L.; van Zon, M.; Wilson, L.; Vandenbroucke-Grauls, C. M. J. E.; van der Wel, N. N.; Ottenhoff, T. H. M.; Bitter, W. The ESX-5 Secretion System of *Mycobacterium marinum* Modulates the Macrophage Response . *J. Immunol.* **2008**, *181* (10), 7166–7175, doi:10.4049/jimmunol.181.10.7166.
 93. Weerdenburg, E. M.; Abdallah, A. M.; Mitra, S.; De Punder, K.; Van der Wel, N. N.; Bird, S.; Appelmelk, B. J.; Bitter, W.; Van der Sar, A. M. ESX-5-Deficient *Mycobacterium marinum* is Hypervirulent in Adult Zebrafish. *Cell. Microbiol.* **2012**, *14* (5), 728–739, doi:10.1111/j.1462-5822.2012.01755.x.
 94. Zhang, W.; Rong, C.; Chen, C.; Gao, G. F. Type-IVC Secretion System: A Novel

- Subclass of Type IV Secretion System (T4SS) Common Existing in Gram-positive Genus *Streptococcus*. *PLoS One* **2012**, 7 (10), doi:10.1371/journal.pone.0046390.
95. Flano, E.; Kaattari, S. L.; Razquin, B.; Villena, A. J. Histopathology of the Thymus of Coho Salmon *Oncorhynchus kisutch* Experimentally Infected with *Renibacterium salmoninarum*. *Dis. Aquat. Org.* **1996**, 26 (1), 11–18, doi:10.3354/dao026011.
 96. Rose, A. S.; Levine, R. P. Complement-Mediated Opsonisation and Phagocytosis of *Renibacterium salmoninarum*. *Fish Shellfish Immunol.* **1992**, 2 (3), 223–240, doi:10.1016/S1050-4648(05)80061-0.
 97. Bruno, D. W. Histopathology of Bacterial Kidney Disease in Laboratory Infected Rainbow Trout, *Salmo gairdneri* Richardson, and Atlantic Salmon, *Salmo salar* L., with Reference to Naturally Infected Fish. *J. Fish Dis.* **1986**, 9 (6), 523–537, doi:10.1111/j.1365-2761.1986.tb01049.x.
 98. Gao, L.-Y.; Laval, F.; Lawson, E. H.; Groger, R. K.; Woodruff, A.; Morisaki, J. H.; Cox, J. S.; Daffe, M.; Brown, E. J. Requirement for KasB in Mycobacterium Mycolic Acid Biosynthesis, Cell Wall Impermeability and Intracellular Survival: Implications for Therapy. *Mol. Microbiol.* **2003**, 49 (6), 1547–1563, doi:10.1046/j.1365-2958.2003.03667.x.
 99. Ooyama, T.; Kera, A.; Okada, T.; Inglis, V.; Yoshida, T. The Protective Immune Response of Yellowtail *Seriola quinqueradiata* to the Bacterial Fish Pathogen *Lactococcus garvieae*. *Dis. Aquat. Organ.* **1999**, 37 (2), 121–126, doi:10.3354/dao037121.
 100. Buchanan, J. T.; Colvin, K. M.; Vicknair, M. R.; Patel, S. K.; Timmer, A. M.; Nizet, V. Strain-Associated Virulence Factors of *Streptococcus iniae* in Hybrid-Striped Bass. *Vet. Microbiol.* **2008**, 131 (1–2), 145–153, doi:10.1016/j.vetmic.2008.02.027.
 101. Raghunathan, A.; Reed, J.; Shin, S.; Palsson, B.; Daefler, S. Constraint-Based Analysis of Metabolic Capacity of *Salmonella* Typhimurium during Host-Pathogen Interaction. *BMC Syst. Biol.* **2009**, 3, 1–16, doi:10.1186/1752-0509-3-38.
 102. Slauch, J. M. How Does the Oxidative Burst of Macrophages Kill Bacteria? Still an Open Question. *Mol. Microbiol.* **2011**, 80 (3), 580–583, doi:10.1111/j.1365-2958.2011.07612.x.
 103. Uribe-Quero, E.; Rosales, C. Control of Phagocytosis by Microbial Pathogens. *Front. Immunol.* **2017**, 8 (OCT), 1–23, doi:10.3389/fimmu.2017.01368.
 104. Ordal, E. J.; Earp, B. J. Cultivation and Transmission of Etiological Agent of Kidney Disease in Salmonid Fishes. *Proc. Soc. Exp. Biol. Med.* **1956**, 92 (1), 85–88, doi:10.3181/00379727-92-22392.
 105. Campos-Pérez, J. J.; Ellis, A. E.; Secombes, C. J. Investigation of Factors Influencing the Ability of *Renibacterium salmoninarum* to Stimulate Rainbow Trout Macrophage Respiratory Burst Activity. *Fish Shellfish Immunol.* **1997**, 7 (8), 555–566, doi:10.1006/fsim.1997.0106.
 106. Ellis, A. E. Immunity to Bacteria in Fish. *Fish Shellfish Immunol.* **1999**, 9 (4), 291–308, doi:10.1006/fsim.1998.0192.
 107. Gutenberger, S. K.; Duimstra, J. R.; Rohovec, J. S.; Fryer, J. L. Intracellular Survival of *Renibacterium salmoninarum* in Trout Mononuclear Phagocytes. *Dis. Aquat. Org.* **1997**, 28 (2), 93–106, doi:10.3354/dao028093.
 108. Grayson, T. H.; Gilpin, M. L.; Evenden, A. J.; Munn, C. B. Evidence for the Immune

- Recognition of Two Haemolysins of *Renibacterium salmoninarum* by Fish Displaying Clinical Symptoms of Bacterial Kidney Disease (BKD). *Fish Shellfish Immunol.* **2001**, *11* (4), 367–370, doi:10.1006/fsim.2000.0317.
109. Evenden, A. J.; Gilpin, M. L.; Munn, C. B. The Cloning and Expression of a Gene Encoding Haemolytic Activity from the Fish Pathogen *Renibacterium salmoninarum*. *FEMS Microbiol. Lett.* **1990**, *59* (1–2), 31–34, doi:10.1016/0378-1097(90)90028-o.
 110. McIntosh, D.; Flaño, E.; Grayson, T. H.; Gilpin, M. L.; Austin, B.; Villena, A. J. Production of Putative Virulence Factors by *Renibacterium salmoninarum* Grown in Cell Culture. *Microbiology* **1997**, *143* (10), 3349–3356, doi:10.1099/00221287-143-10-3349.
 111. Elanco. *An Overview of Emerging Diseases in the Salmonid Farming Industry*; 2018.
 112. Pascho, R. J.; Elliott, D. G.; Chase, D. M. Comparison of Traditional and Molecular Methods for Detection of *Renibacterium salmoninarum*. 2002; pp 157–209, doi:10.1007/978-94-017-2315-2_7.
 113. Stamm, L. M.; Morisaki, J. H.; Gao, L. Y.; Jeng, R. L.; McDonald, K. L.; Roth, R.; Takeshita, S.; Heuser, J.; Welch, M. D.; Brown, E. J. *Mycobacterium marinum* Escapes from Phagosomes and Is Propelled by Actin-Based Motility. *J. Exp. Med.* **2003**, *198* (9), 1361–1368, doi:10.1084/jem.20031072.
 114. Weddle, E.; Agaisse, H. Principles of Intracellular Bacterial Pathogen Spread from Cell to Cell. *PLoS Pathog.* **2018**, *14* (12), 1–8, doi:10.1371/journal.ppat.1007380.
 115. Garin, J.; Diez, R.; Kieffer, S.; Dermine, J. F.; Duclos, S.; Gagnon, E.; Sadoul, R.; Rondeau, C.; Desjardins, M. The Phagosome Proteome: Insight into Phagosome Functions. *J. Cell Biol.* **2001**, *152* (1), 165–180, doi:10.1083/jcb.152.1.165.
 116. Gauthier, D. T.; Vogelbein, W. K.; Ottinger, C. A. Ultrastructure of *Mycobacterium marinum* Granuloma in Striped Bass *Morone saxatilis*. *Dis. Aquat. Organ.* **2004**, *62* (1–2), 121–132, doi:10.3354/dao062121.
 117. Chen, S. C.; Adams, A.; Thompson, K. D.; Richards, R. H. Electron Microscope Studies of the *in vitro* Phagocytosis of *Mycobacterium* Spp. by Rainbow Trout *Oncorhynchus mykiss* Head Kidney Macrophages. *Dis. Aquat. Organ.* **1998**, *32* (2), 99–110, doi:10.3354/dao032099.
 118. El-Etr, S. H.; Yan, L.; Cirillo, J. D. Fish Monocytes as a Model for Mycobacterial Host-Pathogen Interactions. *Infect. Immun.* **2001**, *69* (12), 7310–7317, doi:10.1128/IAI.69.12.7310-7317.2001.
 119. Walburger, A.; Koul, A.; Ferrari, G.; Nguyen, L.; Prescianotto-Baschong, C.; Huygen, K.; Klebl, B.; Thompson, C.; Bacher, G.; Pieters, J. Protein Kinase G from Pathogenic Mycobacteria Promotes Survival within Macrophages. *Science (80-)*. **2004**, *304* (5678), 1800–1804.
 120. Braunstein, M.; Espinosa, B. J.; Chan, J.; Belisle, J. T.; Jacobs, W. R. J. SecA2 Functions in the Secretion of Superoxide Dismutase A and in the Virulence of *Mycobacterium tuberculosis*. *Mol. Microbiol.* **2003**, *48* (2), 453–464, doi:10.1046/j.1365-2958.2003.03438.x.
 121. Jensen, K.; Ranganathan, U. D. K.; Van Rompay, K. K. A.; Canfield, D. R.; Khan, I.; Ravindran, R.; Luciw, P. A.; Jacobs, W. R. J.; Fennelly, G.; Larsen, M. H.; Abel,

- K. A Recombinant Attenuated *Mycobacterium tuberculosis* Vaccine Strain Is Safe in Immunosuppressed Simian Immunodeficiency Virus-Infected Infant Macaques. *Clin. Vaccine Immunol.* **2012**, *19* (8), 1170–1181, doi:10.1128/CVI.00184-12.
122. Watkins, B. Y.; Joshi, S. A.; Ball, D. A.; Leggett, H.; Park, S.; Kim, J.; Austin, C. D.; Paler-Martinez, A.; Xu, M.; Downing, K. H.; Brown, E. J. *Mycobacterium marinum* SecA2 Promotes Stable Granulomas and Induces Tumor Necrosis Factor Alpha *in vivo*. *Infect. Immun.* **2012**, *80* (10), 3512–3520, doi:10.1128/IAI.00686-12.
 123. Sullivan, J. T.; Young, E. F.; McCann, J. R.; Braunstein, M. The *Mycobacterium tuberculosis* SecA2 System Subverts Phagosome Maturation to Promote Growth in Macrophages. *Infect. Immun.* **2012**, *80* (3), 996–1006, doi:10.1128/IAI.05987-11.
 124. van der Woude, A. D.; Stoop, E. J. M.; Stiess, M.; Wang, S.; Ummels, R.; van Stempvoort, G.; Piersma, S. R.; Cascioferro, A.; Jiménez, C. R.; Houben, E. N. G.; Luirink, J.; Pieters, J.; van der Sar, A. M.; Bitter, W. Analysis of SecA2-Dependent Substrates in *Mycobacterium marinum* Identifies Protein Kinase G (PknG) as a Virulence Effector. *Cell. Microbiol.* **2014**, *16* (2), 280–295, doi:10.1111/cmi.12221.
 125. Parikka, M.; Hammarén, M. M.; Harjula, S. K. E.; Halfpenny, N. J. A.; Oksanen, K. E.; Lahtinen, M. J.; Pajula, E. T.; Iivanainen, A.; Pesu, M.; Rämetsä, M. *Mycobacterium marinum* Causes a Latent Infection That Can Be Reactivated by Gamma Irradiation in Adult Zebrafish. *PLoS Pathog.* **2012**, *8* (9), doi:10.1371/journal.ppat.1002944.
 126. Bhavsar, A. P.; Guttman, J. A.; Finlay, B. B. Manipulation of Host-Cell Pathways by Bacterial Pathogens. *Nature* **2007**, *449* (7164), 827–834, doi:10.1038/nature06247.
 127. Southwood, D.; Ranganathan, S. *Host-Pathogen Interactions*; Elsevier Ltd., 2018; Vol. 1–3, doi:10.1016/B978-0-12-809633-8.20088-5.
 128. Kehl-Fie, T. E.; Skaar, E. P. Nutritional Immunity beyond Iron: A Role for Manganese and Zinc. *Curr. Opin. Chem. Biol.* **2010**, *14* (2), 218–224, doi:10.1016/j.cbpa.2009.11.008.
 129. Hood, M. I.; Skaar, E. P. Nutritional Immunity: Transition Metals at the Pathogen-Host Interface. *Nat. Rev. Microbiol.* **2012**, *10* (8), 525–537, doi:10.1038/nrmicro2836.
 130. Wilson, B. R.; Bogdan, A. R.; Miyazawa, M.; Hashimoto, K.; Tsuji, Y. Siderophores in Iron Metabolism: From Mechanism to Therapy Potential. *Trends Mol. Med.* **2016**, *22* (12), 1077–1090, doi:10.1016/j.molmed.2016.10.005.
 131. Andreini, C.; Bertini, I.; Cavallaro, G.; Holliday, G. L.; Thornton, J. M. Metal Ions in Biological Catalysis: From Enzyme Databases to General Principles. *J. Biol. Inorg. Chem.* **2008**, *13* (8), 1205–1218, doi:10.1007/s00775-008-0404-5.
 132. Miethke, M.; Marahiel, M. A. Siderophore-Based Iron Acquisition and Pathogen Control. *Microbiol. Mol. Biol. Rev.* **2007**, *71* (3), 413–451, doi:10.1128/mmbr.00012-07.
 133. Weinberg, E. D. Iron and Infection. *Microbiol. Rev.* **1978**, *42* (1), 45–66.
 134. Barber, M. F.; Elde, N. C. Buried Treasure: Evolutionary Perspectives on Microbial Iron Piracy. *Trends Genet.* **2015**, *31* (11), 627–636, doi:10.1016/j.tig.2015.09.001.
 135. Litwin, C. M.; Calderwood, S. B. Role of Iron in Regulation of Virulence Genes. *Clin. Microbiol. Rev.* **1993**, *6* (2), 137–149, doi:10.1128/CMR.6.2.137.

136. Grayson, T. H.; Bruno, D. W.; Evenden, A. J.; Gilpin, M. L.; Munn, C. B. Iron Acquisition by *Renibacterium salmoninarum*: Contribution of Iron Reductase. *Dis. Aquat. Organ.* **1995**, *22* (2), 157–162, doi:10.3354/dao022157.
137. Bethke, J.; Poblete-Morales, M.; Irgang, R.; Yáñez, A.; Avendaño-Herrera, R. Iron Acquisition and Siderophore Production in the Fish Pathogen *Renibacterium salmoninarum*. *J. Fish Dis.* **2016**, *39* (11), 1275–1283, doi:10.1111/jfd.12456.
138. Adams, T. J.; Vartivarian, S.; Cowart, R. E. Iron Acquisition Systems of *Listeria monocytogenes*. *Infect. Immun.* **1990**, *58* (8), 2715–2718, doi:10.1128/iai.58.8.2715-2718.1990.
139. Johnson, W.; Varner, L.; Poch, M. Acquisition of Iron by *Legionella pneumophila*: Role of Iron Reductase. *Infect. Immun.* **1991**, *59* (7), 2376–2381, doi:10.1128/iai.59.7.2376-2381.1991.
140. Bethke, J.; Arias-Muñoz, E.; Yáñez, A.; Avendaño-Herrera, R. *Renibacterium salmoninarum* Iron-Acquisition Mechanisms and ASK Cell Line Infection: Virulence and Immune Response. *J. Fish Dis.* **2019**, *42* (9), 1283–1291, doi:10.1111/jfd.13051.
141. Bethke, J.; Yáñez, A. J.; Avendaño-Herrera, R. Comparative Genomic Analysis of Two Chilean *Renibacterium salmoninarum* Isolates and the Type Strain ATCC 33209T. *Genome Biol. Evol.* **2018**, *10* (7), 1816–1822, doi:10.1093/gbe/evy138.
142. Nobles, C. L.; Maresso, A. W. The Theft of Host Heme by Gram-positive Pathogenic Bacteria. *Metallomics* **2011**, *3* (8), 788–796, doi:10.1039/c1mt00047k.
143. Allen, C. E.; Burgos, J. M.; Schmitt, M. P. Analysis of Novel Iron-Regulated, Surface-Anchored Hemin-Binding Proteins in *Corynebacterium diphtheriae*. *J. Bacteriol.* **2013**, *195* (12), 2852–2863, doi:10.1128/JB.00244-13.
144. Banner, C. R.; Rohovec, J. S.; Fryer, J. L. A New Value for Mol Percent Guanine + Cytosine of DNA for the Salmonid Fish Pathogen *Renibacterium salmoninarum*. *FEMS Microbiol. Lett.* **1991**, *63* (1), 57–59, doi:10.1016/0378-1097(91)90527-h.
145. Andrews, S. C.; Robinson, A. K.; Rodríguez-Quiñones, F. Bacterial Iron Homeostasis. *FEMS Microbiol. Rev.* **2003**, *27* (2–3), 215–237, doi:10.1016/S0168-6445(03)00055-X.
146. Retamales, J.; González-Contreras, A.; Salazar, S.; Toranzo, A. E.; Avendaño-Herrera, R. Iron Utilization and Siderophore Production by *Streptococcus phocae* Isolated from Diseased Atlantic Salmon (*Salmo salar*). *Aquaculture* **2012**, *364–365*, 305–311, doi:10.1016/j.aquaculture.2012.08.047.
147. Brown, J. S.; Holden, D. W. Iron Acquisition by Gram-positive Bacterial Pathogens. *Microbes Infect.* **2002**, *4* (11), 1149–1156, doi:10.1016/S1286-4579(02)01640-4.
148. Metzger, D. C.; Elliott, D. G.; Wargo, A.; Park, L. K.; Purcell, M. K. Pathological and Immunological Responses Associated with Differential Survival of Chinook Salmon Following *Renibacterium salmoninarum* Challenge. *Dis. Aquat. Organ.* **2010**, *90* (1), 31–41, doi:10.3354/dao02214.
149. Eslamloo, K.; Kumar, S.; Caballero-Solares, A.; Gnanagobal, H.; Santander, J.; Rise, M. L. Profiling the Transcriptome Response of Atlantic Salmon Head Kidney to Formalin-killed *Renibacterium salmoninarum*. *Fish Shellfish Immunol.* **2020**, *98* (September 2019), 937–949, doi:10.1016/j.fsi.2019.11.057.
150. Gnanagobal, H.; Cao, T.; Hossain, A.; Dang, M.; Hall, J. R.; Kumar, S.; Van Cuong,

- D.; Boyce, D.; Santander, J. Lumpfish (*Cyclopterus lumpus*) is Susceptible to *Renibacterium salmoninarum* Infection and Induces Cell-mediated Immunity in the Chronic Stage . *Frontiers in Immunology* . 2021, p 4647.
151. Liu, C.; Hu, X.; Cao, Z.; Sun, Y.; Chen, X.; Zhang, Z. Construction and Characterization of a DNA Vaccine Encoding the SagH against *Streptococcus iniae*. *Fish Shellfish Immunol.* **2019**, *89* (December 2018), 71–75, doi:10.1016/j.fsi.2019.03.045.
 152. Jiang, J.; Miyata, M.; Chan, C.; Ngoh, S. Y.; Liew, W. C.; Saju, J. M.; Ng, K. S.; Wong, F. S.; Lee, Y. S.; Chang, S. F.; Orbán, L. Differential Transcriptomic Response in the Spleen and Head Kidney Following Vaccination and Infection of Asian Seabass with *Streptococcus iniae*. *PLoS One* **2014**, *9* (7), 1–14, doi:10.1371/journal.pone.0099128.
 153. Salazar, S.; Oliver, C.; Yáñez, A. J.; Avendaño-Herrera, R. Comparative Analysis of Innate Immune Responses to *Streptococcus phocae* Strains in Atlantic Salmon (*Salmo salar*) and Rainbow Trout (*Oncorhynchus mykiss*). *Fish Shellfish Immunol.* **2016**, *51*, 97–103, doi:10.1016/j.fsi.2016.02.005.
 154. Ziklo, N.; Colorni, A.; Gao, L. Y.; Du, S. J.; Ucko, M. Humoral and Cellular Immune Response of European Seabass *Dicentrarchus labrax* Vaccinated with Heat-killed *Mycobacterium marinum* (iipA::Kan Mutant). *J. Aquat. Anim. Health* **2018**, *30* (4), 312–324, doi:10.1002/aah.10042.
 155. Zhang, Q.; Wang, X.; Zhang, D.; Long, M.; Wu, Z.; Feng, Y.; Hao, J.; Wang, S.; Liao, Q.; Li, A. *De novo* Assembly and Analysis of Amur Sturgeon (*Acipenser schrenckii*) Transcriptome in Response to *Mycobacterium marinum* Infection to Identify Putative Genes Involved in Immunity. *J. Microbiol. Biotechnol.* **2019**, *29* (8), 1324–1334, doi:10.4014/jmb.1903.03034.
 156. Matsumoto, M.; Araki, K.; Hayashi, K.; Takeuchi, Y.; Shiozaki, K.; Suetake, H.; Yamamoto, A. Adjuvant Effect of Recombinant Interleukin-12 in the Nocardiosis Formalin-killed Vaccine of the Amberjack *Seriola dumerili*. *Fish Shellfish Immunol.* **2017**, *67*, 263–269, doi:10.1016/j.fsi.2017.06.025.
 157. Byadgi, O.; Chen, C. W.; Wang, P. C.; Tsai, M. A.; Chen, S. C. De Novo Transcriptome Analysis of Differential Functional Gene Expression in Largemouth Bass (*Micropterus salmoides*) after Challenge with *Nocardia seriolae*. *Int. J. Mol. Sci.* **2016**, *17* (8), 1–16, doi:10.3390/ijms17081315.
 158. Byadgi, O.; Chen, Y. C.; Barnes, A. C.; Tsai, M. A.; Wang, P. C.; Chen, S. C. Transcriptome Analysis of Grey Mullet (*Mugil cephalus*) after Challenge with *Lactococcus garvieae*. *Fish Shellfish Immunol.* **2016**, *58*, 593–603, doi:10.1016/j.fsi.2016.10.006.
 159. Boltaña, S.; Roher, N.; Goetz, F. W.; MacKenzie, S. A. PAMPs, PRRs and the Genomics of Gram-negative Bacterial Recognition in Fish. *Dev. Comp. Immunol.* **2011**, *35* (12), 1195–1203, doi:https://doi.org/10.1016/j.dci.2011.02.010.
 160. Sahoo, B. R. Structure of Fish Toll-like Receptors (TLR) and NOD-like Receptors (NLR). *Int. J. Biol. Macromol.* **2020**, *161*, 1602–1617, doi:10.1016/j.ijbiomac.2020.07.293.
 161. Palti, Y. Toll-like Receptors in Bony Fish: From Genomics to Function. *Dev. Comp. Immunol.* **2011**, *35* (12), 1263–1272, doi:10.1016/j.dci.2011.03.006.

162. Foster, S. L.; Hargreaves, D. C.; Medzhitov, R. Gene-Specific Control of Inflammation by TLR-Induced Chromatin Modifications. *Nature* **2007**, *447* (7147), 972–978, doi:10.1038/nature05836.
163. Iwasaki, A.; Medzhitov, R. Regulation of Adaptive Immunity by the Innate Immune System. *Science* **2010**, *327* (5963), 291–295, doi:10.1126/science.1183021.
164. Takeuchi, O.; Akira, S. Pattern Recognition Receptors and Inflammation. *Cell* **2010**, *140* (6), 805–820, doi:10.1016/j.cell.2010.01.022.
165. Qi, Z.; Wu, P.; Zhang, Q.; Wei, Y.; Wang, Z.; Qiu, M.; Shao, R.; Li, Y.; Gao, Q. Transcriptome Analysis of Soiny Mullet (*Liza haematocheila*) Spleen in Response to *Streptococcus dysgalactiae*. *Fish Shellfish Immunol.* **2016**, *49*, 194–204, doi:10.1016/j.fsi.2015.12.029.
166. Zhang, J.; Kong, X.; Zhou, C.; Li, L.; Nie, G.; Li, X. Toll-like Receptor Recognition of Bacteria in Fish: Ligand Specificity and Signal Pathways. *Fish Shellfish Immunol.* **2014**, *41* (2), 380–388, doi:10.1016/j.fsi.2014.09.022.
167. Meijer, A. H.; Krens, S. F. G.; Rodriguez, I. A. M.; He, S.; Bitter, W.; Snaar-Jagalska, B. E.; Spaink, H. P. Expression Analysis of the Toll-like Receptor and TIR Domain Adaptor Families of Zebrafish. *Mol. Immunol.* **2004**, *40* (11), 773–783.
168. Miettinen, M.; Sareneva, T.; Julkunen, I.; Matikainen, S. IFNs Activate Toll-like Receptor Gene Expression in Viral Infections. *Genes Immun.* **2001**, *2* (6), 349–355, doi:10.1038/sj.gene.6363791.
169. Pietretti, D.; Wiegertjes, G. F. Ligand Specificities of Toll-like Receptors in Fish: Indications from Infection Studies. *Dev. Comp. Immunol.* **2014**, *43* (2), 205–222, doi:10.1016/j.dci.2013.08.010.
170. Liu, F.; Su, B.; Fu, Q.; Shang, M.; Gao, C.; Tan, F.; Li, C. Identification, Characterization and Expression Analysis of TLR5 in the Mucosal Tissues of Turbot (*Scophthalmus maximus* L.) Following Bacterial Challenge. *Fish Shellfish Immunol.* **2017**, *68*, 272–279, doi:10.1016/j.fsi.2017.07.021.
171. Eslamloo, K.; Caballero-Solares, A.; Inkpen, S. M.; Emam, M.; Kumar, S.; Bouniot, C.; Avendaño-Herrera, R.; Jakob, E.; Rise, M. L. Transcriptomic Profiling of the Adaptive and Innate Immune Responses of Atlantic Salmon to *Renibacterium salmoninarum* Infection. *Front. Immunol.* **2020**, *11* (October), doi:10.3389/fimmu.2020.567838.
172. Sullivan, C.; Charette, J.; Catchen, J.; Lage, C. R.; Giasson, G.; Postlethwait, J. H.; Millard, P. J.; Kim, C. H. The Gene History of Zebrafish Tlr4a and Tlr4b Is Predictive of Their Divergent Functions. *J. Immunol.* **2009**, *183* (9), 5896–5908.
173. Hwang, S. D.; Kondo, H.; Hirono, I.; Aoki, T. Molecular Cloning and Characterization of Toll-like Receptor 14 in Japanese Flounder, *Paralichthys olivaceus*. *Fish Shellfish Immunol.* **2011**, *30* (1), 425–429.
174. Ford, M. J. Molecular Evolution of Transferrin: Evidence for Positive Selection in Salmonids. *Mol. Biol. Evol.* **2001**, *18* (4), 639–647, doi:10.1093/oxfordjournals.molbev.a003844.
175. Lee, J. H.; Pooley, N. J.; Mohd-Adnan, A.; Martin, S. A. M. Cloning and Characterisation of Multiple Ferritin Isoforms in the Atlantic Salmon (*Salmo salar*). *PLoS One* **2014**, *9* (7), doi:10.1371/journal.pone.0103729.
176. Buhler, D. R. Studies on Fish Hemoglobins. *J. Biol. Chem.* **1962**, *238* (5).

177. Wicher, K. B.; Fries, E. Haptoglobin, a Hemoglobin-Binding Plasma Protein, Is Present in Bony Fish and Mammals but Not in Frog and Chicken. *Proc. Natl. Acad. Sci. U. S. A.* **2006**, *103* (11), 4168–4173, doi:10.1073/pnas.0508723103.
178. Hirayama, M.; Kobiyama, A.; Kinoshita, S.; Watabe, S. The Occurrence of Two Types of Hemopexin-like Protein in Medaka and Differences in Their Affinity to Heme. *J. Exp. Biol.* **2004**, *207* (8), 1387–1398, doi:10.1242/jeb.00897.
179. Zhou, Z.; Feng, C.; Liu, X.; Liu, S. 3nLcn2, a Teleost Lipocalin 2 That Possesses Antimicrobial Activity and Inhibits Bacterial Infection in Triploid Crucian Carp. *Fish Shellfish Immunol.* **2020**, *102* (January), 47–55, doi:10.1016/j.fsi.2020.04.015.
180. Zou, J.; Secombes, C. J. The Function of Fish Cytokines. *Biology (Basel)*. **2016**, *5* (2), doi:10.3390/biology5020023.
181. Nemeth, E.; Tuttle, M. S.; Powelson, J.; Vaughn, M. B.; Donovan, A.; Ward, D. M.; Ganz, T.; Kaplan, J. Hepcidin Regulates Cellular Iron Efflux by Binding to Ferroportin and Inducing Its Internalization. *Science* **2004**, *306* (5704), 2090–2093, doi:10.1126/science.1104742.
182. Nemeth, E.; Ganz, T. Regulation of Iron Metabolism by Hepcidin. *Annu. Rev. Nutr.* **2006**, *26*, 323–342.
183. Bury, N.; Grosell, M. Iron Acquisition by Teleost Fish. *Comp. Biochem. Physiol.* **2003**, *135* (Part C), 97–105, doi:10.1016/S1532-0456.
184. Torti, F. M.; Torti, S. V. Regulation of Ferritin Genes and Protein. *Blood* **2002**, *99* (10), 3505–3516, doi:10.1182/blood.V99.10.3505.
185. Walker, R. L.; Fromm, P. O. Metabolism of Iron by Normal and Iron Deficient Rainbow Trout. *Comp. Biochem. Physiol. A. Comp. Physiol.* **1976**, *55* (4A), 311–318, doi:10.1016/0300-9629(76)90052-9.
186. Ganz, T. Iron and Infection. *Int. J. Hematol.* **2018**, *107* (1), 7–15, doi:10.1007/s12185-017-2366-2.
187. Neves, J. V.; Caldas, C.; Vieira, I.; Ramos, M. F.; Rodrigues, P. N. S. Multiple Hepcidins in a Teleost Fish, *Dicentrarchus labrax*: Different Hepcidins for Different Roles. *J. Immunol.* **2015**, *195* (6), 2696–2709.
188. Lauth, X.; Babon, J. J.; Stannard, J. A.; Singh, S.; Nizet, V.; Carlberg, J. M.; Ostland, V. E.; Pennington, M. W.; Norton, R. S.; Westerman, M. E. Bass Hepcidin Synthesis, Solution Structure, Antimicrobial Activities and Synergism, and *in vivo* Hepatic Response to Bacterial Infections. *J. Biol. Chem.* **2005**, *280* (10), 9272–9282, doi:10.1074/jbc.M411154200.
189. Neves, J. V.; Ramos, M. F.; Moreira, A. C.; Silva, T.; Gomes, M. S.; Rodrigues, P. N. S. Hamp1 but Not Hamp2 Regulates Ferroportin in Fish with Two Functionally Distinct Hepcidin Types. *Sci. Rep.* **2017**, *7* (1), 1–14.
190. Hirono, I.; Hwang, J.-Y.; Ono, Y.; Kurobe, T.; Ohira, T.; Nozaki, R.; Aoki, T. Two Different Types of Hepcidins from the Japanese Flounder *Paralichthys olivaceus*. *FEBS J.* **2005**, *272* (20), 5257–5264, doi:10.1111/j.1742-4658.2005.04922.x.
191. Bayne, C. J.; Gerwick, L. The Acute Phase Response and Innate Immunity of Fish. *Dev. Comp. Immunol.* **2001**, *25* (8–9), 725–743, doi:10.1016/S0145-305X(01)00033-7.
192. Sussman, M. Iron and Infection. In *Iron in Biochemistry and Medicine*; Jacobs, A., Worwood, M., Eds.; Academic Press: New York, 1974; pp 649–679.

193. Suzumoto, B. K.; Schreck, C. B.; McIntyre, J. D. Relative Resistances of Three Transferrin Genotypes of Coho Salmon (*Oncorhynchus kisutch*) and Their Hematological Responses to Bacterial Kidney Disease. *J. Fish. Res. Board Canada* **1977**, *34*, 1–8.
194. Winter, G. W.; Schreck, C. B.; McIntyre, J. D. Resistance of Different Stocks and Transferrin Genotypes of Coho Salmon, *Oncorhynchus kisutch*, and Steelhead Trout, *Salmo gairdneri*, to Bacterial Kidney Disease and Vibriosis. *Fish. Bull.* **1980**, *77*, 795–802.
195. Stafford, J. L.; Belosevic, M. Transferrin and the Innate Immune Response of Fish: Identification of a Novel Mechanism of Macrophage Activation. *Dev. Comp. Immunol.* **2003**, *27* (6–7), 539–554, doi:10.1016/S0145-305X(02)00138-6.
196. Clifton, M. C.; Corrent, C.; Strong, R. K. Siderocalins: Siderophore-Binding Proteins of the Innate Immune System. *Biometals* **2009**, *22* (4), 557–564, doi:10.1007/s10534-009-9207-6.
197. Subramanian, S.; MacKinnon, S. L.; Ross, N. W. A Comparative Study on Innate Immune Parameters in the Epidermal Mucus of Various Fish Species. *Comp. Biochem. Physiol. B. Biochem. Mol. Biol.* **2007**, *148* (3), 256–263, doi:10.1016/j.cbpb.2007.06.003.
198. Brogden, G.; Propsting, M.; Adamek, M.; Naim, H. Y.; Steinhagen, D. Isolation and Analysis of Membrane Lipids and Lipid Rafts in Common Carp (*Cyprinus carpio* L.). *Comp. Biochem. Physiol. B. Biochem. Mol. Biol.* **2014**, *169*, 9–15, doi:10.1016/j.cbpb.2013.12.001.
199. Ben Hamed, S.; Tavares Ranzani-Paiva, M. J.; Tachibana, L.; de Carla Dias, D.; Ishikawa, C. M.; Esteban, M. A. Fish Pathogen Bacteria: Adhesion, Parameters Influencing Virulence and Interaction with Host Cells. *Fish Shellfish Immunol.* **2018**, *80* (July), 550–562, doi:10.1016/j.fsi.2018.06.053.
200. Grayson, T. H.; Cooper, L. F.; Wrathmell, A. B.; Roper, J.; Evenden, A. J.; Gilpin, M. L. Host Responses to *Renibacterium salmoninarum* and Specific Components of the Pathogen Reveal the Mechanisms of Immune Suppression and Activation. *Immunology* **2002**, *106* (2), 273–283, doi:10.1046/j.1365-2567.2002.01420.x.
201. Pandey, A. K.; Yang, Y.; Jiang, Z.; Fortune, S. M.; Coulombe, F.; Behr, M. A.; Fitzgerald, K. A.; Sasseti, C. M.; Kelliher, M. A. NOD2, RIP2 and IRF5 Play a Critical Role in the Type I Interferon Response to *Mycobacterium tuberculosis*. *PLoS Pathog.* **2009**, *5* (7), e1000500, doi:10.1371/journal.ppat.1000500.
202. Leong, J. C.; Trobridge, G. D.; Kim, C. H.; Johnson, M.; Simon, B. Interferon-Inducible Mx Proteins in Fish. *Immunol. Rev.* **1998**, *166*, 349–363, doi:10.1111/j.1600-065x.1998.tb01275.x.
203. Kim, C. H.; Johnson, M. C.; Drennan, J. D.; Simon, B. E.; Thomann, E.; Leong, J. A. DNA Vaccines Encoding Viral Glycoproteins Induce Nonspecific Immunity and Mx Protein Synthesis in Fish. *J. Virol.* **2000**, *74* (15), 7048–7054, doi:10.1128/jvi.74.15.7048-7054.2000.
204. Collet, B.; Secombes, C. J. The Rainbow Trout (*Oncorhynchus mykiss*) Mx1 Promoter. Structural and Functional Characterization. *Eur. J. Biochem.* **2001**, *268* (6), 1577–1584.
205. Rhodes, L. D.; Wallis, S.; Demlow, S. E. Genes Associated with an Effective Host

- Response by Chinook Salmon to *Renibacterium salmoninarum*. *Dev. Comp. Immunol.* **2009**, *33* (2), 176–186, doi:10.1016/j.dci.2008.08.006.
206. Elliott, D. G.; Wiens, G. D.; Hammell, K. L.; Rhodes, L. D. Vaccination against Bacterial Kidney Disease. *Fish Vaccin.* **2014**, *9780470674*, 255–272, doi:10.1002/9781118806913.ch22.
 207. Munang'andu, H. Intracellular Bacterial Infections: A Challenge for Developing Cellular-mediated Immunity Vaccines for Farmed Fish. *Microorganisms* **2018**, *6* (2), 33, doi:10.3390/microorganisms6020033.
 208. Sami, S.; Fischer-Scherl, T.; Hoffmann, R. W.; Pfeil-Putzien, C. Immune Complex-Mediated Glomerulonephritis Associated with Bacterial Kidney Disease in the Rainbow Trout (*Oncorhynchus mykiss*). *Vet. Pathol.* **1992**, *29* (2), 169–174, doi:10.1177/030098589202900210.
 209. Lumsden, J. S.; Russell, S.; Huber, P.; Wybourne, B. A.; Ostland, V. E.; Minamikawa, M.; Ferguson, H. W. An Immune-Complex Glomerulonephritis of Chinook Salmon, *Oncorhynchus tshawytscha* (Walbaum). *J. Fish Dis.* **2008**, *31* (12), 889–898, doi:10.1111/j.1365-2761.2008.00952.x.
 210. Kaattari, S. L.; Piganelli, J. D. Immunization with Bacterial Antigens: Bacterial Kidney Disease. *Dev. Biol. Stand.* **1997**, *90*, 145–152.
 211. Hardie, L. J.; Ellis, A. E.; Secombes, C. J. *In vitro* Activation of Rainbow Trout Macrophages Stimulates Inhibition of *Renibacterium salmoninarum* Growth Concomitant with Augmented Generation of Respiratory Burst Products. *Dis. Aquat. Organ.* **1996**, *25* (3), 175–183, doi:10.3354/dao025175.
 212. Campos-Perez, J. J.; Ward, M.; Grabowski, P. S.; Ellis, A. E.; Secombes, C. J. The Gills Are an Important Site of INOS Expression in Rainbow Trout *Oncorhynchus mykiss* after Challenge with the Gram-positive Pathogen *Renibacterium salmoninarum*. *Immunology* **2000**, *99* (1), 153–161, doi:10.1046/j.1365-2567.2000.00914.x.
 213. Jansson, E.; Hongslo, T.; Johannisson, A.; Pilström, L.; Timmusk, S.; Norrgren, L. Bacterial Kidney Disease as a Model for Studies of Cell-mediated Immunity in Rainbow Trout (*Oncorhynchus mykiss*). *Fish Shellfish Immunol.* **2003**, *14* (4), 347–362.
 214. Sakai, M.; Atsuta, S.; Kobayashi, M. Protective Immune Response in Rainbow Trout, *Oncorhynchus mykiss*, Vaccinated with β -Haemolytic Streptococcal Bacterin. *Fish Pathol.* **1989**, *24* (3), 169–173.
 215. Jiang, J.; Fisher, E. M.; Murasko, D. M. CD8 T Cell Responses to Influenza Virus Infection in Aged Mice. *Ageing Res. Rev.* **2011**, *10* (4), 422–427, doi:10.1016/j.arr.2011.02.001.
 216. Raberg, L.; Sim, D.; Read, A. F. Disentangling Genetic Variation for Resistance and Tolerance to Infectious Diseases in Animals. *Science* **2007**, *318* (5851), 812–814, doi:10.1126/science.1148526.
 217. Sako, H. Acquired Immunity of Yellowtail, *Seriola quinqueradiata* Recovered from Experimental Infection with β -Hemolytic *Streptococcus* Sp. *Aquac. Sci.* **1992**, *40* (4), 389–392.
 218. Purcell, M. K.; McKibben, C. L.; Pearman-Gillman, S.; Elliott, D. G.; Winton, J. R. Effects of Temperature on *Renibacterium salmoninarum* Infection and Transmission

- Potential in Chinook Salmon, *Oncorhynchus tshawytscha* (Walbaum). *J. Fish Dis.* **2016**, *39* (7), 787–798, doi:10.1111/jfd.12409.
219. Yanong, R. P. E.; Francis-floyd, R. Streptococcal Infections of Fish. *Univ. Florida* **2013**, 1–5.
 220. Rozas-Serri, M.; Lobos, C.; Correa, R.; Ildefonso, R.; Vásquez, J.; Muñoz, A.; Maldonado, L.; Jaramillo, V.; Coñuecar, D.; Oyarzún, C. Atlantic Salmon Pre-Smolt Survivors of *Renibacterium salmoninarum* Infection Show Inhibited Cell-mediated Adaptive Immune Response and a Higher Risk of Death during the Late Stage of Infection at Lower Water Temperatures. *Front. Immunol.* **2020**, *11*, 1378.
 221. Horzinek, M. C.; Schijns, V. E. C.; Denis, M.; Desmettre, P.; Babiuk, L. A. General Description of Vaccines. *Vet. Vaccinology. Amsterdam Elsevier* **1997**, 131–152.
 222. Kum, C.; Sekki, S. The Immune System Drugs in Fish: Immune Function, Immunoassay, Drugs. *Recent Adv. Fish Farms* **2011**, doi:10.5772/26869.
 223. Ma, J.; Bruce, T. J.; Jones, E. M.; Cain, K. D. A Review of Fish Vaccine Development Strategies: Conventional Methods and Modern Biotechnological Approaches. *Microorganisms* **2019**, *7* (11), 569.
 224. Salonijs, K.; Siderakis, C.; MacKinnon, A. M.; Griffiths, S. G. Use of *Arthrobacter davidanieli* as a Live Vaccine against *Renibacterium salmoninarum* and *Piscirickettsia salmonis* in Salmonids. *Dev. Biol. (Basel)*. **2005**, *121*, 189–197.
 225. Sun, Y.; Hu, Y.; Liu, C.; Sun, L. Construction and Analysis of an Experimental *Streptococcus iniae* DNA Vaccine. *Vaccine* **2010**, *28* (23), 3905–3912.
 226. Sun, Y.; Sun, L.; Xing, M.; Liu, C.; Hu, Y. SagE Induces Highly Effective Protective Immunity against *Streptococcus iniae* Mainly through an Immunogenic Domain in the Extracellular Region. *Acta Vet. Scand.* **2013**, *55* (1), 1–9.
 227. Sheng, X.; Liu, M.; Liu, H.; Tang, X.; Xing, J.; Zhan, W. Identification of Immunogenic Proteins and Evaluation of Recombinant PDHA1 and GAPDH as Potential Vaccine Candidates against *Streptococcus iniae* Infection in Flounder (*Paralichthys olivaceus*). *PLoS One* **2018**, *13* (5), e0195450.
 228. Fields, K. A.; Straley, S. C. LcrV of *Yersinia pestis* Enters Infected Eukaryotic Cells by a Virulence Plasmid-Independent Mechanism. *Infect. Immun.* **1999**, *67* (9), 4801–4813, doi:10.1128/IAI.67.9.4801-4813.1999.
 229. Hill, J.; Leary, S. E. C.; Griffin, K. F.; Williamson, E. D.; Titball, R. W. Regions of *Yersinia pestis* V Antigen That Contribute to Protection against Plague Identified by Passive and Active Immunization; 1997; Vol. 65.
 230. Overheim, K. A.; DePaolo, R. W.; Debord, K. L.; Morrin, E. M.; Anderson, D. M.; Green, N. M.; Brubaker, R. R.; Jabri, B.; Schneewind, O. LcrV Plague Vaccine with Altered Immunomodulatory Properties. *Infect. Immun.* **2005**, *73* (8), 5152–5159, doi:10.1128/IAI.73.8.5152-5159.2005.
 231. Vernazza, C.; Lingard, B.; Flick-Smith, H. C.; Baillie, L. W. J.; Hill, J.; Atkins, H. S. Small Protective Fragments of the *Yersinia pestis* V Antigen. *Vaccine* **2009**, *27* (21), 2775–2780, doi:10.1016/j.vaccine.2009.03.011.
 232. Sudheesh, P. S.; Al-Ghabshi, A.; Al-Mazrooei, N.; Al-Habsi, S. Comparative Pathogenomics of Bacteria Causing Infectious Diseases in Fish. *Int. J. Evol. Biol.* **2012**, *2012*, 1–16, doi:10.1155/2012/457264.
 233. Chukwu-Osazuwa, J.; Cao, T.; Vasquez, I.; Gnanagobal, H.; Hossain, A.;

- Machimbirike, V. I.; Santander, J. Comparative Reverse Vaccinology of *Piscirickettsia salmonis*, *Aeromonas salmonicida*, *Yersinia ruckeri*, *Vibrio anguillarum*, and *Moritella viscosa*, Frequent Pathogens of Atlantic Salmon and Lumpfish Aquaculture. *Vaccines* **2022**, *10* (3), 473.
234. Yoshida, T.; Sakai, M.; Kitao, T.; Khlil, S. M.; Araki, S.; Saitoh, R.; Ineno, T.; Inglis, V. Immunomodulatory Effects of the Fermented Products of Chicken Egg, EF203, on Rainbow Trout, *Oncorhynchus mykiss*. *Aquaculture* **1993**, *109* (3–4), 207–214, doi:10.1016/0044-8486(93)90163-S.
235. Sakai, M.; Yoshida, T.; Kobayashi, M. Influence of the Immunostimulant, EF203, on the Immune Responses of Rainbow Trout, *Oncorhynchus mykiss*, to *Renibacterium salmoninarum*. *Aquaculture* **1995**, *138* (1–4), 61–67.

Chapter 3. Lumpfish susceptibility and immune response to *R. salmoninarum* infection

The research described in Chapter 3 was published in *Frontiers in Immunology* as: Gnanagobal, H., Cao, T., Hossain, A., Dang, M., Hall, J., Kumar, S., Cuong, D. V., Boyce, D., and Santander. J. (2021). Lumpfish (*Cyclopterus lumpus*) is Susceptible to *Renibacterium salmoninarum* Infection and Induces Cell-Mediated Immunity in the Chronic Stage. *Frontiers in immunology* 22(12): 733266. doi: 10.3389/fimmu.2021.733266.

3.1. Abstract

Renibacterium salmoninarum is a Gram-positive, intracellular pathogen that causes Bacterial Kidney Disease (BKD) in several fish species in freshwater and seawater. Lumpfish (*Cyclopterus lumpus*) is utilized as a cleaner fish to biocontrol sea lice infestation in Atlantic salmon (*Salmo salar*) farms. Atlantic salmon are susceptible to *R. salmoninarum* and can transfer the infection to other fish species. Although BKD outbreaks have not been reported in lumpfish, its susceptibility and immune response to *R. salmoninarum* are unknown. In this study, we evaluated the susceptibility and immune response of lumpfish to *R. salmoninarum* infection. Groups of lumpfish were intraperitoneally (i.p.) injected with either *R. salmoninarum* (1×10^7 , 1×10^8 , or 1×10^9 cells dose⁻¹) or PBS (control). *R. salmoninarum* infection kinetics and mortality were followed for 98 days post-infection (dpi). Transcript expression levels of 33 immune-relevant genes were measured in the head kidney ($n = 6$) of fish infected with 1×10^9 cells/dose and compared to the control at 28 and 98 dpi. Infected lumpfish displayed characteristic clinical signs of BKD. Lumpfish infected with high, medium, and low doses had a survival rate of 65%, 93%, and 95%, respectively. Mortality in the high-dose infected group stabilized after 50 dpi, but *R. salmoninarum* persisted in the fish tissues until 98 dpi. Cytokines (*il1b*, *il8a*, *il8b*), pattern recognition receptors (*tlr5a*), interferon-induced effectors (*rsad2*, *mx**a*, *mx**b*, *mx**c*), iron regulation (*hamp*), and acute phase reactant (*saa5*) related genes were upregulated at 28 dpi. In contrast, cell-mediated adaptive immunity-related genes (*cd4a*, *cd4b*, *ly6g6f*, *cd8a*, *cd74*) were down-regulated at 28 dpi, revealing the immune suppressive nature of *R. salmoninarum*. However, significant upregulation of *cd74* at 98 dpi suggests induction of

cell-mediated immune response. This study showed that *R. salmoninarum* infected lumpfish in a similar fashion to salmonid fish species and caused a chronic infection, enhancing cell-mediated adaptive immune response.

Keywords: Bacterial Kidney Disease (BKD), Gram-positive pathogen, *Renibacterium salmoninarum*, lumpfish, cell-mediated immunity

3.2. Introduction

Bacterial Kidney Disease (BKD) caused by *Renibacterium salmoninarum* is a chronic disease of wild and cultured fish, including Atlantic salmon (*Salmo salar*), chinook salmon (*Oncorhynchus tshawytscha*), rainbow trout (*Oncorhynchus mykiss*), Arctic char (*Salvelinus alpinus* L.), Pacific herring (*Clupea pallasii pallasii*), sablefish (*Anoplopoma fimbria*), fathead minnow (*Pimephales promelas*), North Pacific hake (*Merluccius productus*), ayu (*Plecoglossus altivelis*), eel (*Anguilla anguilla*), as well as in bivalve molluscs, in both fresh and marine waters [1–7]. *R. salmoninarum* has primarily adapted to infect and persist in salmonids [8]. However, *R. salmoninarum* experimentally infected and caused mortality in non-salmonids, including sablefish and Pacific herring, shiner perch (*Cymatogaster aggregate*), common shiner (*Notropis cornutus*), and fathead minnow, and it caused mortality events in minnow (*Phoxinus phoxinus*) and three-spined stickleback (*Gasterosteus aculeatus*) [2,9–12].

R. salmoninarum is a Gram-positive, slow-growing, fastidious, and facultative intracellular pathogen [7,13] with high persistence within wild and farmed fish populations [2]. *R. salmoninarum* is the only marine bacterial pathogen that has been documented of both horizontal (i.e., from fish to fish) and vertical (i.e., from parent to progeny)

transmission [2]. *R. salmoninarum* has caused substantial losses in the salmonid aquaculture industry, affecting up to 80% and 40% of the Pacific and Atlantic salmon stocks, respectively [8]. The poor efficacy of antibiotics and vaccines in BKD prophylaxis has stymied the control of this pathogen [14,15].

Lumpfish (*Cyclopterus lumpus*), a globiform teleost native to the North Atlantic, is used as an eco-friendly cleaner fish to biocontrol sea lice (e.g., *Lepeophtheirus salmonis*) infestations in the Atlantic salmon aquaculture [16]. Lumpfish reduces the utilization of chemotherapeutants against sea lice in Atlantic salmon farms, consequently, its annual demands have significantly increased in the North Atlantic [17]. Lumpfish health is critical for its optimal performance and elimination of the potential risk of disease transmission between lumpfish and salmon [18,19]. *Pasteurella* sp., *Piscirickettsia salmonis*, *Vibrio anguillarum*, *Vibrio ordalii*, *Aeromonas salmonicida*, *Pseudomonas anguilliseptica*, *Moritella viscosa*, and *Tenacibaculum maritimum* have been reported to be primary bacterial pathogens in lumpfish [17]. Although *R. salmoninarum* outbreaks have not been reported in lumpfish, due to the broad host-range of *R. salmoninarum* (i.e., salmonid and non-salmonid fishes, as well as bivalve molluscs) and its horizontal transmission ability [20,21], it is important to determine the susceptibility of lumpfish to *R. salmoninarum* and its potential risk for BKD. The risk of *R. salmoninarum* infection in lumpfish is significant because sea lice, like other blood-sucking ectoparasites, act as *R. salmoninarum* vectors and could transfer *R. salmoninarum* from salmon to lumpfish and vice versa [22–24]. *R. salmoninarum* transmission may occur as a result of the dynamic interplay between a susceptible host and virulent *R. salmoninarum* in an environmental context that facilitates such disease conditions (i.e., environmental stressors in the marine environment, high

stocking densities in cultured conditions or parasitic infestations) [25,26]. For instance, horizontal transmission of *R. salmoninarum* between fish species like sockeye salmon (*Oncorhynchus nerka*) and chinook salmon (*O. tshawytscha*) has been reported [20,21], and high biomass within sea cages and the free movement of seawater in and out of cages could increase the opportunity for disease transmission [27]. Cleaner fish, like lumpfish, pose a moderate risk of disease transmission to salmon [28]. Transmission of the amoebic parasite (*Paramoeba perurans*) from lumpfish to Atlantic salmon was demonstrated under controlled conditions [29]. Though the anticipated risk of infected lumpfish transmitting the bacterial disease to salmon is low, Atlantic salmon showed susceptibility to a lumpfish isolate of *M. viscosa* [28,30]. Thus, lumpfish could possibly act as an asymptomatic carrier and transmit disease threat to salmon [19]. Several studies on the fish immune response to *R. salmoninarum* infection have been conducted in salmonids [31–34]. However, the lumpfish susceptibility and immune response to *R. salmoninarum* infection are unknown. In addition, lumpfish is becoming an accessible model to study marine infectious diseases and teleost immunity [35].

Here, we evaluated the lumpfish susceptibility to a type strain of *R. salmoninarum* (ATCC 33209) and immune response at early and chronic infection stages. We determined that lumpfish are susceptible to *R. salmoninarum*, causing mortality and a chronic infection in the surviving individuals, similar to salmonid fish. The immune response profile of the lumpfish head kidney at early and chronic infection stages showed that *R. salmoninarum* dysregulates the expression of transcripts with functional annotations related to pattern recognition, inflammation, cytokines, iron regulation, and cell-mediated adaptive immunity.

3.3. Materials and Methods

3.3.1. *Renibacterium salmoninarum* culture conditions and inoculum preparation

R. salmoninarum type strain (ATCC [American Type Culture Collection] 33209) was cultured in complex KDM2 broth (1.0% (w/v) peptone (Difco), 0.05% (w/v) yeast (Difco), 0.05% (w/v) L-cysteine HCl (Sigma-Aldrich, St. Louis, MO, USA), 10% (v/v) fetal bovine serum (Gibco, Thermofisher, Waltham, CA, USA), 1.5% (v/v) nurse medium contained filter-sterilized supernatant from *R. salmoninarum* cultures) [36] at 15 °C with aeration in an orbital shaker (180 rpm). When required, KDM2 broth was supplemented with 1.8% (w/v) agar (Difco), and cycloheximide (0.005% (w/v); Sigma-Aldrich), D-cycloserine (0.00125% (w/v); Sigma-Aldrich), polymyxin-B sulfate (0.0025% (w/v); Sigma-Aldrich), and oxolinic acid (0.00025% (w/v); Sigma-Aldrich) to make *R. salmoninarum* selective KDM2 plates (SKDM2) [37]. Bacterial growth was monitored by spectrophotometry (Genova Nano, Jenway, UK), flow cytometry (BD FACS Aria II flow cytometer and BD FACS Diva v7.0 software, BD Biosciences, San Jose, CA, USA) and/or by colony forming units (CFU) plate counting [38]. The purity and integrity of bacterial cells were evaluated and confirmed by Gram-staining [39] (Figure 3.1A) and PCR [40,41].

The bacterial infection inoculum was prepared as described previously [42], with modification for *R. salmoninarum*. Briefly, bacterial cells were cultured in 1 L of KDM2 at 15 °C for 10 days and harvested at mid-logarithmic phase (Optical Density (O.D.) 600 nm = 0.8 ~1x10⁸ CFU mL⁻¹) (Figure 3.1B) by centrifugation at 6,000 rpm for 10 min at 4 °C and washed once with sterile phosphate-buffered saline (PBS, pH 7.0; 136 mM NaCl, 2.7 mM KCl, 10.1 mM Na₂HPO₄, 1.5 mM KH₂PO₄) [43]. The bacterial pellet was

resuspended in 100 ml of PBS and subjected to bacterial enumeration using a bacteria counting kit (Invitrogen) and flow cytometry according to manufacturers' instructions. The number of bacterial cells in the inoculum was calculated by dividing the number of signals in the bacterial frame by the number of signals in the microsphere frame (Figure 3.1C). The bacterial cells suspension was normalized to 3×10^{10} cells ml^{-1} and serially diluted in PBS to the final infection doses of 1×10^9 cells dose^{-1} (high dose), 1×10^8 cells dose^{-1} (medium dose), and 1×10^7 cells dose^{-1} (low dose).

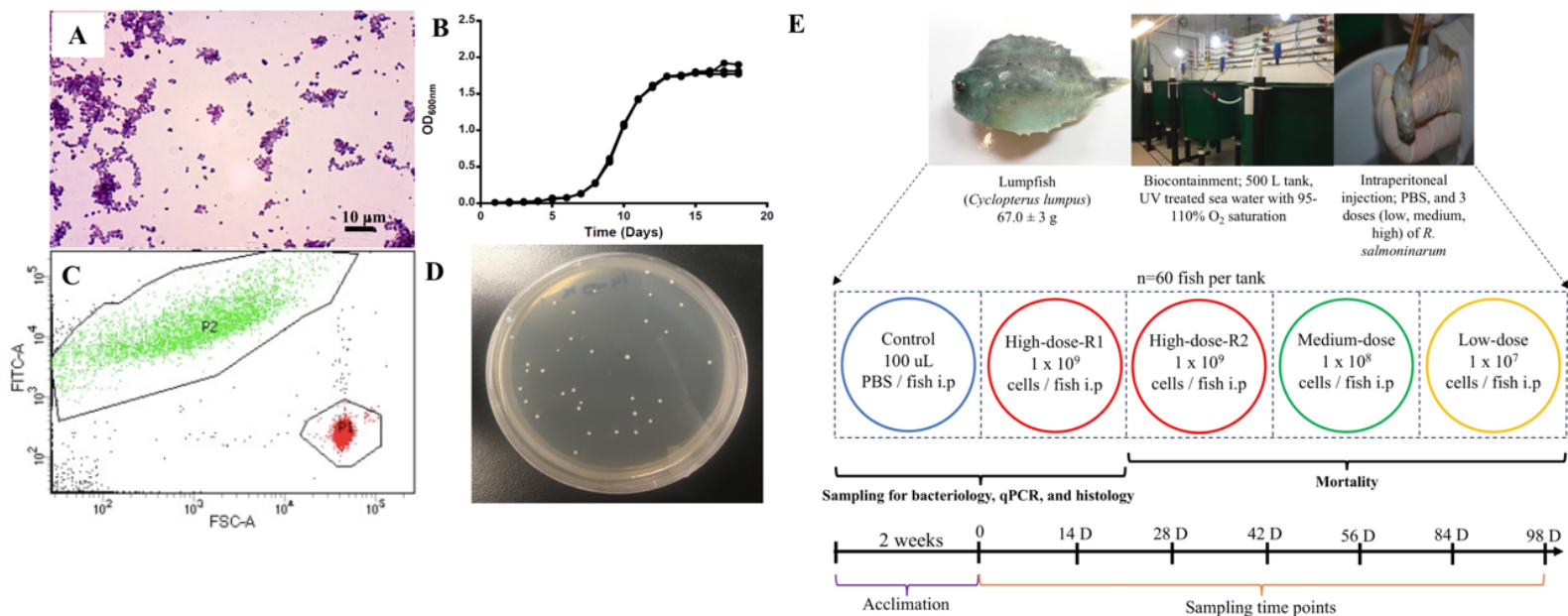


Figure 3.1. *R. salmoninarum* infection in lumpfish. **A.** Characterization of *R. salmoninarum* by Gram staining; **B.** *R. salmoninarum* growth curve in KDM2 broth; **C.** Flow cytometric enumeration of *R. salmoninarum*. FSC: Forward Scatter; FITC: Green Fluorescence. In this plot of forward scatter versus fluorescence, green signals in the upper left-hand frame represent bacteria stained with the SYTO BC bacterial stain; red signals in the lower right-hand frame represent microspheres particles, which serve as the standard used to indicate sample volume. P1: Number of signals in the microsphere frame; P2: Number of signals in the bacterial frame. **D.** *R. salmoninarum* colonies growing on an SKDM2 spread plate inoculated for the quantitative culture of the bacterium from fish head kidney; **(E)** Experimental design for this study. 300 lumpfish (average weight: 67.0 ± 3

g) were divided into 5 tanks (60 fish per tank) at the biocontainment facility. Fish from the control tank were i.p. with 100 μ l of PBS. Fish from the high (2 tanks for high dose; R1 and R2), medium, and low dose tanks were intraperitoneally injected with 100 μ l of 10^9 , 10^8 , and 10^7 cells per fish of *R. salmoninarum*, respectively. The mock-infected tank (PBS control) and 3 experimental tanks [low, medium, and high (R2 tank) doses of *R. salmoninarum*] were monitored for mortality. Fish for the sampling of the spleen, liver, and head kidney were collected from the mock-infected tank and high dose R1 tank. Sampling time points were 0, 14, 28, 42, 56, 84, and 98 dpi, and 6 fish were sampled at each time point.

3.3.2. Lumpfish

All animal protocols required for this research were reviewed and approved by the Institutional Animal Care Committee and the Biosafety Committee at Memorial University of Newfoundland (MUN) (<https://www.mun.ca/research/about/acs/acc/>) based on the guidelines of the Canadian Council on Animal Care (<https://ccac.ca/>). Experiments were conducted under protocols #18-01-JS, #18-03-JS, and biohazard license L-01.

Specific pathogen-free lumpfish (67.0 ± 3.0 g; mean \pm SD) were produced and cultivated at the Joe Brown Aquatic Research Building (JBARB; Ocean Sciences Centre, St. John's, NL, Canada). Infection studies were conducted in the aquatic level 3 (AQ3) biocontainment unit at the Cold-Ocean Deep-Sea Research Facility (CDRF; Ocean Sciences Centre, St. John's, NL, Canada). Fish were distributed into five 500 L tanks (60 fish per tank) at a biomass of 25 kg m^{-3} and acclimated for 2 weeks at $10 \text{ }^{\circ}\text{C}$ before *R. salmoninarum* infection. Prior to and throughout the experimental study, fish were kept at optimal conditions (500 L tanks with flow-through (7.5 L min^{-1}) filtered and UV-treated ($8\text{-}10 \text{ }^{\circ}\text{C}$) seawater, 95-110% air saturation, and ambient photoperiod (12 h light:12 h dark)). The fish were fed daily at a rate of 0.5% of their body weight per day with the commercial aquafeed Skretting - Europa 15 (55% crude protein, 15% crude lipid, and 1.5% crude fiber, 3% calcium, 2% phosphorus, 1% sodium, 5000 IU/kg vitamin A, 3000 IU kg^{-1} vitamin D, and 200 IU kg^{-1} vitamin E).

3.3.3. *Renibacterium salmoninarum* infection in lumpfish

Lumpfish were i.p. injected with 100 μl of 10^7 , 10^8 , or 10^9 cells of *R. salmoninarum* dose $^{-1}$, similar to infection studies in salmonids and other fish species [9,44–48]. A

duplicate group of lumpfish i.p. injected with 10^9 cells dose⁻¹ was utilized for tissue sampling. Lumpfish i.p. injected with PBS were used as a control group (Figure 3.1E). Fish were monitored daily for mortality and clinical signs until 98 days post-injection (dpi) (Figure 3.1E). The survival rate was calculated according to Survival rate (%) = (Survivors at the end of the experiment / Initial individuals) \times 100 [49].

Samples of the spleen, liver, and head kidney were taken at 14, 28, 42, 56, 84, and 98 dpi from six lumpfish infected with 10^9 cells of *R. salmoninarum* dose⁻¹ and PBS-injected lumpfish groups (Figure 3.1E). Before sampling, lumpfish were netted and euthanized with an overdose of MS222 (400 mg L⁻¹; Syndel Laboratories, Vancouver, BC, Canada). Each tissue was aseptically collected and consistently subsampled for bacteriology, histology, and immune-relevant transcript expression analyses. For bacteriology analysis, 30-100 mg of tissue was individually placed into a sterile homogenizer bag (Nasco whirl-pak[®], USA), kept on ice, and processed soon after harvesting (< 1 h). For histology, tissue sections were fully submerged into 15 mL falcon tubes containing 10% neutral-buffered formalin. For transcript expression analyses, 50-100 mg of tissue was placed in a 1.5 mL RNase-free tube, flash-frozen using liquid nitrogen, and stored at -80 °C until RNA preparation.

3.3.4. Determination of bacterial load in lumpfish tissues

To study *R. salmoninarum* kinetics in lumpfish tissues, bacterial loads per g of tissue of infected lumpfish ($n = 6$, from high dose infected group) were determined at 14, 28, 42, 56, 84, and 98 dpi according to previously described procedures for *R. salmoninarum* isolation from the salmonid kidney [50] with modifications. Briefly, tissues were kept cold

on ice after extraction and during all the procedures. Tissue samples were aseptically weighed in the sterile homogenizer bag, suspended in PBS peptone (PBS [pH 7.4]; 0.1% peptone) in the ratio of 1 mL PBS peptone per 0.1 g of tissue, and mechanically homogenized. Tissue homogenates were then transferred into sterile 1.5 mL centrifuge tubes and centrifuged at 2500 x g for 20 minutes at 4 °C. The absence of bacteria in the supernatant was confirmed by sub-culturing 10 µL on SKDM2 plates. The pellet was resuspended in PBS peptone at a ratio of 1:1 (w/v) (i.e., 0.1 g of tissue was resuspended in 100 µl of PBS peptone) and mixed using Vortex mixer (Corning, Life Sciences, USA). The suspension was serially diluted in PBS peptone (1:10), and either 10 µl of the tissue homogenate or 10 µl of the serial 10-fold dilution was spread onto SKDM2 agar plates (Figure 3.1D). The plates were sealed with paraffin film to prevent desiccation and incubated at 15 °C for up to 4-8 weeks. In each sampling point, the *R. salmoninarum* recovered on SKDM2 agar plates from lumpfish tissues were pure, and the observed *R. salmoninarum* colonies showed a homogenous morphology (Figure 3.1D). Also, the inocula obtained from these colonies were confirmed as *R. salmoninarum* by Gram-staining (i.e., presence of pure, Gram-positive diplobacilli) and PCR (i.e., positive amplification with the *R. salmoninarum* specific primers [40,41]). *R. salmoninarum* loads (CFU g of tissue⁻¹) were quantified by dividing the number of colonies by the weight of tissue plated (i.e., for a starting tissue weight of 0.1 g, 10 µl of the homogenate was spread onto SKDM2, then the tissue plated was equivalent to 0.01 g).

3.3.5. Histopathological examination

Tissue samples of spleen, liver, and head kidney collected at 14, 28, 42, and 98 dpi from PBS-control and high dose *R. salmoninarum* infected lumpfish groups were analyzed for histopathology. Tissues were fixed in 10% PBS-buffered formalin for three days at room temperature. The formalin was then removed, and the fixed tissues were preserved in PBS at 4 °C until processing for paraffin embedded tissue block according to established procedures [51]. Tissue sections of 5 µm thickness were stained with hematoxylin and eosin (Leica Biosystems) using established protocols [52,53] and observed for histopathological changes under the light microscope (Olympus CX40, USA).

3.3.6. RNA preparation

To study the lumpfish immune response to *R. salmoninarum* chronic infection, head kidney samples ($n = 6$ per group) extracted at 28 and 98 dpi from control (PBS-injected group) and infected lumpfish (10^9 cells dose⁻¹) groups were selected for real-time quantitative polymerase chain reaction (qPCR) analyses. Approximately 80-100 mg of tissue was added to a 1.5 mL RNase-free centrifuge tube containing 500 µl of TRIzol reagent (Invitrogen) and homogenized using a motorized RNase-Free Pellet Pestle Grinder (Fisherbrand, Fisher Scientific, USA). Then, an additional 500 µl of TRIzol were added, mixed by pipetting, and RNA extractions were completed following the manufacturer's instructions. Extracted RNA samples were then purified using RNeasy MinElute Cleanup Kit (QIAGEN, Mississauga, ON, Canada) following the manufacturer's instructions. RNA samples were treated with TURBO DNA-free™ Kit (Invitrogen) for complete digestion of DNA and removal of remaining DNase and divalent cations, such as magnesium and calcium. Purified RNA samples were quantified and verified for purity using a Genova

Nano microvolume spectrophotometer (Jenway, UK), and RNA integrity was tested by 1% agarose gel electrophoresis [43]. All RNA samples used in this study showed acceptable purity ratios ($A_{260}/A_{230} > 1.8$ and $A_{260}/A_{280} > 2.0$) and integrity (28S and 18S ribosomal RNA bands at a ~2:1 ratio).

3.3.7. cDNA synthesis and qPCR parameters

First-strand cDNA templates for qPCR were synthesized in 20 μ l reactions from 1 μ g purified RNA using SuperScript IV VILO Master Mix (Invitrogen) following the manufacturer's instructions.

PCR amplifications were performed in 13 μ l reactions using 1X Power SYBR Green PCR Master Mix (Applied Biosystems), 50 nM of both the forward and reverse primers, and the indicated cDNA quantity (see below). Amplifications were performed using the QuantStudio 6 Flex Real-Time PCR system (384-well format) (Applied Biosystems). The real-time analysis program consisted of 1 cycle of 50 °C for 2 min, 1 cycle of 95 °C for 10 min, 40 cycles of 95 °C for 15 sec, and 60 °C for 1 min, with fluorescence detection at the end of each 60 °C step and was followed by dissociation curve analysis.

3.3.8. Primer design and quality assurance testing

For each gene that was subjected to qPCR analyses, a group of transcripts (with associated TRINITY IDs) were obtained from the NCBI Sequence Read Archive (SRA) under accession number SRP238224 (Supplementary File S3.1). To confirm the identity of a given transcript, determine its orientation and identify the coding sequence (CDS), a BLASTx search of the non-redundant (nr) protein sequences database using a translated nucleotide query was performed between June and July 2019. A database of all confirmed

transcript sequences for a given gene was created using Vector NTI (Vector NTI Advance 11.5.4, Life Technologies). Next, for a given gene, multiple sequence alignments were performed for its corresponding transcripts using AlignX (Vector NTI Advance 11.5.4). These alignments were used to determine if the transcripts were identical, contained single nucleotide polymorphisms (SNPs)/sequencing errors, or represented different gene paralogues/isoforms. In the case of gene paralogues/isoforms, these alignments were also helpful to determine their percentage identity and to identify regions where paralogue/isoform-specific qPCR primers could be designed.

Primers were designed using Primer3 [54–56]. However, in the case of the gene paralogues/isoforms, some were custom-designed in paralogue/isoform-specific areas to ensure specificity. All primers are located in the CDS and in an area which overlapped with that of the best BLASTx-identified sequence. In the case of gene paralogues/isoforms, primers were designed in an area with ≥ 3 bp difference between them to ensure specificity. The amplicon size range was 90-160 bp. The sequences, amplicon sizes, and amplification efficiencies [57] for all primer pairs used in the qPCR analyses are presented in Table 3.1.

Each primer pair was quality tested to ensure that a single product was amplified (dissociation curve analysis) and that there was no primer-dimer present in the no-template control. Amplicons were electrophoretically separated on 2% agarose gels and compared with a 1 kb plus ladder (Invitrogen) to verify that the correct size fragment was being amplified using standard molecular methods [43]. Amplification efficiencies [57] were calculated for both control and immune-stimulated cDNA pools from head kidney samples. Standard curves were generated for both cDNA pools using a 5-point 1:3 dilution series

starting with cDNA representing 10 ng of input total RNA. The reported efficiencies are an average of the two values (Table 3.1).

3.3.9. Endogenous control (normalizer) selection

Expression levels of the genes of interest (GOIs) were normalized to expression levels of two endogenous gene controls. To select these endogenous controls, 5 genes [*60S ribosomal protein L32 (rpl32)*, *elongation factor 1-alpha (ef1a)*, *eukaryotic translation initiation factor 3 subunit D (etif3d)*, *polyadenylate-binding protein 1a (pabpc1a)* and *polyadenylate-binding protein 1b (pabpc1b)*] were analyzed. Briefly, the fluorescence threshold cycle (C_T) values of all 24 samples in the study were measured (in duplicate) for each of these transcripts using cDNA representing 4 ng of input total RNA and then analyzed using geNorm [58]. geNorm M values for all of the candidate normalizers were < 0.3 , suggesting stable expression; however, *pabpc1b* (geNorm M = 0.165) and *etif3d* (geNorm M = 0.168) were selected as the two endogenous controls as they were the most stably expressed.

Table 3.1. qPCR primers used in this study

Gene name (symbol)	Trinity ID (SRP238224)	Primer sequence (5' to 3')	R ²	Amplification efficiency (%)	Amplicon size (bp)
Genes of interest					
<i>C-C motif chemokine-like 19 (ccl19)</i>	DN10492_c0_g1_i4	F: GCTCAGGTACCAACGGACTG R: CGTGTCCTCCGATCTGTCTC	0.999	88.4	94
<i>cyclooxygenase-2 (cox2)</i>	DN750_c1_g1_i1	F: GAATCCTCACCTGGGTCAA R: ATGGCATCTCTGAGGAAGGA	0.994	90.6	122
<i>hepcidin anti-microbial peptide (hamp)</i>	DN2993_c0_g1_i4	F: GCTCGCCTTTATTTGCATTC R: ATATGCCGCAACTGGAGTGT	0.998	95.1	100
<i>HLA class II histocompatibility antigen gamma chain (cd74)</i>	DN13708_c0_g1_i6	F: ACGCCAAGACACCTCTGACT R: GGAAGGTCTCGTTGAACTGC	0.999	89.8	108
<i>immunoglobulin delta heavy chain (ighd)</i>	DN1665_c0_g2_i7	F: GGAGACAGTGTGTGCTGGA R: GGGCTTCAGGAAATTCAACA	0.999	88.4	121
<i>immunoglobulin heavy chain variable region a (igha)</i>	DN1665_c0_g3_i2	F: AGGACTGGAGTGGATTGGAA R: TGCATGGTCTGTCCGTTTAG	0.999	90.5	129
<i>immunoglobulin heavy chain b (ighb)</i>	DN1665_c0_g4_i1	F: GAATGGAACAAGGGGACAAA R: CGGTCGTTGAGTCTCTCCTC	0.999	89.6	108
<i>immunoglobulin mu heavy chain a (ighma)</i>	DN121_c0_g3_i3	F: CAGCTTCTGGATTAGACTTTGA R: GATGTTGTTACTGTTGTGTTGG	0.998	90.2	107
<i>immunoglobulin mu heavy chain b (ighmb)</i>	DN121_c0_g2_i2	F: CAGTCTCTAGGATATCATTAG R: GTGGGTACCATCGTCACTATT	0.992	92.1	101
<i>immunoglobulin mu heavy chain c (ighmc)</i>	DN121_c0_g3_i4	F: CAACATCCGGAATCACATTCAG R: GATTTTGAGGTCCCCTACTACCAT	0.998	87.7	112
<i>interleukin 1 beta (il1b)</i>	DN22448_c0_g2_i1	F: ATTGTGTTTCGAGCTCGGTTTC R: CGAACTATGGTCCGCTTCTC	0.996	97.4	98
<i>interleukin 8a (il8a)</i>	DN21169_c0_g1_i2	F: AAGTCATAGCCGACTGTCTG	0.999	96.3	109

<i>interleukin 8b (il8b)</i>	DN4613_c0_g1_i4	R: CCCTGCTGATGGAGTTGTCT F: GTCTGAGAAGCCTGGGAGTG	0.996	87.3	138
<i>interleukin 10 (il10)</i>	DN41536_c0_g1_i1	R: TCAGAGTGGCAATGATCTCG F: AACCAGTGCTGTCGTTTCGT	0.986	97.8	106
<i>serum amyloid A 5 (saa5)</i>	DN41536_c0_g1_i1	R: TGTCCAAGTCATCGTTTGCT F: AGAGTGGGTGCAGGAAAGAA	0.992	90.3	116
<i>T-cell surface glycoprotein CD4a (cd4a)</i>	DN9678_c0_g2_i9	R: GAAGTCCTGGTGGCCTGTAA F: CGTTAAGGTGCTGCAGATCA	0.995	84.9	122
<i>T-cell surface glycoprotein CD4b (cd4b)</i>	DN24146_c0_g1_i7	R: GCGGAAACCATTTTCAGTTGT F: TGTGGGGTTAGCTCCTTCAC	0.996	94.2	138
<i>lymphocyte antigen 6 complex locus protein G6f (ly6g6f)</i>	DN12606_c0_g1_i8	R: TGTTTGCGATCTCACCTTTG F: TCCATGTGGACGTGACTGTT	0.994	88.2	100
<i>T-cell surface glycoprotein CD8 alpha chain (cd8a)</i>	DN11791_c0_g1_i1	R: AACGGTGTCTGAGCCTGAGT F: GCTTTGCTCTCTGGGCATAC	0.996	89.6	104
<i>toll-like receptor 5a (tlr5a)</i>	DN29432_c0_g1_i1	R: TCCGGGTTCTTAAGTGGTTG F: TGGACGAGTTTCAGCAGTTG	0.988	95.6	129
<i>toll-like receptor 5b (tlr5b)</i>	DN55824_c0_g1_i5	R: AGACCCCTCACATGTCCAAG F: CCATCATGCACTTTGTACGG	0.999	88.6	127
<i>tumour necrosis factor alpha (tnfa)</i>	DN26791_c0_g1_i1	R: TGCTGTTGATCTCCCTGATG F: TTAGAAGGGAGCTGCGAAGA	0.982	90.1	119
<i>ATP-dependent RNA helicase lgp2 (lgp2)</i>	DN49186_c0_g1_i1	R: ATGACGATCCGGTTGTTCTC F: GCAACCTGGTGGTACGCTAT	0.998	84.9	104
<i>C-C motif chemokine-like 20 (ccl20)</i>	DN9266_c0_g1_i3	R: CTCGGCGACCACTGAATACT F: ATGGGCTACACCATCCAGAC	0.997	90.6	102
<i>interferon gamma (ifng)</i>	DN81754_c0_g1_i1	R: CCACTTGGATGAAGGGTCAG F: CTCTGGCTGGTTGTCTGTCA	0.996	90.7	105
		R: TCGCTCTCTCGATGGAATCT			

<i>interferon regulatory factor 7 (irf7)</i>	DN6933_c0_g1_i2	F: GGCTCATAGAGCAGGTGGAG R: CTGTCTTCGTCGTTGCAGTC	1.000	81.1	115
<i>interferon-induced GTP-binding protein a (mxα)</i>	DN526_c0_g1_i6	F: TGCACAGACTCAAGCAGAGC R: CCACACTTGAGCTCCTCTCC	0.999	89.6	144
<i>interferon-induced GTP-binding protein b (mxβ)</i>	DN526_c0_g1_i3	F: TTGCGGCTTGGA AAAATATC R: TCCACGGTACCTTCGTTTCAT	0.997	94.2	95
<i>interferon-induced GTP-binding protein c (mxγ)</i>	DN237_c1_g1_i1	F: GGAAGTGGCAGACATTGTGA R: CTGCTGCAATCTCCTTCTCC	0.999	93.5	131
<i>radical S-adenosyl methionine domain containing protein 2 / viperin (rsad2)</i>	DN16769_c0_g1_i1	F: AGGAGAGGGTGAAGGGAGAG R: ATCCAGAGGCAGGACAAATG	0.992	98.5	133
<i>signal transducer and activator of transcription 1 (stat1)</i>	DN3250_c2_g1_i2	F: CTCAAGATGCTGGACTGCAA R: ATGCTCTCGATCCACTTGCT	0.999	87.9	104
<i>toll-like receptor 3 (tlr3)</i>	DN30532_c0_g1_i1	F: AGAGGGCAGGGAATTTGAGT R: TGCACGAGTCATTCTCCAAG	0.999	92.9	101
<i>toll-like receptor 7 (tlr7)</i>	DN760_c1_g2_i1	F: GGCAA ACTGGAAGAATTGGA R: GAAGGGATTTGAGGGAGGAG	0.998	90.5	100
Candidate normalizers					
<i>60S ribosomal protein L32 (rpl32)</i>	DN3569_c0_g1_i2	F: GTAAGCCCAGGGGTATCGAC R: GGGCAGCATGTACTTGGTCT	0.999	92.9	107
<i>elongation factor 1 alpha (ef1α)</i>	DN12280_c0_g1_i3	F: CAAGGGATGGAAGATTGAGC R: TGTTCGATACTCCGATTT	0.996	94.3	151
<i>eukaryotic translation initiation factor 3 subunit D (etif3d) *</i>	DN7623_c0_g1_i5	F: AGCCAGATCAACCTGAGCAT R: AGGCTGTACACCCGAATCAC	1.000	90.3	134
<i>polyadenylate-binding protein 1 a (pabpc1a)</i>	DN6565_c0_g2_i3, DN6565_c0_g2_i4	F: CAAGAACTTTGGGGAGGACA R: TGACAAAGCCAAATCCCTTC	0.998	86.4	125
<i>polyadenylate-binding protein 1 b (pabpc1b) *</i>	DN6565_c0_g2_i5	F: GACTCAGGAGGCAGCTGAAC R: TCGCGCTCTTTACGAGATTT	0.998	92.0	102

Trinity IDs were associated with the groups of transcripts that were obtained from the NCBI Sequence Read Archive (SRA) under accession number SRP238224.

All T_m were set at 60 °C by default during primer design using Primer3.

Amplification efficiencies were calculated using a 5-point 1:3 dilution series starting with cDNA representing 10 ng of input total RNA. See methods for details.

* Expression levels of the transcripts of interest were normalized to expression levels of both *etif3d* and *pabpc1b*.

3.3.10. Experimental qPCR analyses

For experimental qPCR, head kidney samples from the control and the high dose *R. salmoninarum* infected fish at both 28 and 98 dpi were chosen to represent early (28 dpi) and chronic (98 dpi) infection stages of *R. salmoninarum* based on the survival and head kidney colonization data (i.e., fish showed mortality along with highest bacterial load at 28 dpi whereas fish mortality was stabilized even with the considerable amount of bacterial load at 98 dpi).

qPCR assays were designed for 33 transcripts with immune-relevant functional annotations (Table 3.1). These transcripts include pattern recognition receptors (e.g., *tlr3*, *tlr5a*, *tlr5b*, *tlr7*, *lgp2*), cytokines (e.g., *il1b*, *il8a*, *il8b*, *il10*, *ifng*, *tnfa*), chemokines (e.g., *ccl19*, *ccl20*), antimicrobial peptides (e.g., *hamp*), acute phase reactants (e.g., *saa5*), mediator of inflammation (e.g., *cox2*), interferon regulators (i.e., *irf7*, *stat1*), interferon-induced effectors (i.e., *rsad2*, *mx*a, *mx*b, *mx*c), humoral and cell-mediated adaptive immune response-related (i.e., *igha*, *ighb*, *ighd*, *ighma*, *ighmb*, *ighmc*, *cd4a*, *cd4b*, *ly6g6f*, *cd8a*, *cd74*) transcripts. An analysis of the expression of these transcripts related to innate and adaptive immunity would provide insight into host-pathogen interactions between lumpfish and *R. salmoninarum* at early and chronic infection stages.

The experimental qPCR analyses were conducted according to MIQE guidelines [59]. cDNA representing 4 ng of input RNA was used as a template in the PCR reactions. All samples were analyzed on a single plate (3 GOIs and the two endogenous controls per plate: 33 GOIs over 11 plates). On each plate, for every sample, the GOIs and endogenous controls were tested in triplicate, and a no-template control was included. The relative quantity (RQ) of each transcript was determined using the QuantStudio Real-Time PCR

Software (version 1.3) (Applied Biosystems) relative quantification study application, with normalization to both *pabpc1b* and *etif3d* transcript levels, and with amplification efficiencies incorporated. For each GOI, the sample with the lowest normalized expression (mRNA) level was set as the calibrator sample (i.e., assigned an RQ value = 1.0) (Supplementary Table S3.1). Also, transcript expression levels were determined using the comparative $2^{-\Delta\Delta C_t}$ method [60–62] (Supplementary Table S3.2). The levels of transcript expression data from the $2^{-\Delta\Delta C_t}$ and the RQ data analysis methods were used in the main (Figures 3.4-3.6) and the supplementary (Supplementary Figures S3.2-S3.4) graphs, respectively.

3.3.11. Statistical analysis

All data are expressed as mean \pm standard error (SE). Assumptions of normality and homoscedasticity were tested for the detected variances. Kaplan-Meier estimator was used to obtain survival fractions after the *R. salmoninarum* infection. The log-rank test was used to compare the survival curve trends ($p < 0.0001$), and a one-way ANOVA followed by Tukey's multiple comparison post hoc test was used to determine significant differences between the survival of control and infected groups. Also, one-way ANOVA followed by the Holm-Sidak post hoc test was conducted to compare differences between tissues and within fish individuals at a single time point, whereas a non-parametric Kruskal-Wallis test was performed to compare the tissue bacterial loads between various time points per organ. Transcript expression data were analyzed using a two-way ANOVA test, followed by the Sidak multiple comparisons post hoc test to identify significant differences between treatments (control and infected groups) at a single time point and for each treatment at different time points (i.e., 28 and 98 dpi). In all cases, $p < 0.05$ was considered statistically

significant. All statistical analyses were performed using GraphPad Prism 8.0 (GraphPad Software, La Jolla, CA, USA, www.graphpad.com).

3.4. Results

3.4.1. Lumpfish survival, *R. salmoninarum* infection kinetics and histopathology

BKD is a slowly progressing systemic infection depending on the virulence of the *R. salmoninarum* strain that correlates with their number of major soluble antigen (*msa*) gene copies [2,63]. In this study, we used the *R. salmoninarum* type strain ATCC 33209, which has only two *msa* copies [64] and it is known to exhibit lower pathogenicity, cause low mortality, and a chronic infection in salmonids [36,46,47]. Lumpfish infected with *R. salmoninarum* ATCC 33209 displayed characteristic clinical signs of a chronic BKD infection (Figure 3.2A). Mortality began at 20 dpi, gradually increased, and stabilized after 50 dpi in the high dose infected group (1×10^9 cells dose⁻¹) (Figure 3.2B). In the medium, (1×10^8 cells dose⁻¹) and low (1×10^7 cells dose⁻¹) dose groups, mortality began at 40 dpi and stabilized after 50 dpi as well (Figure 3.2B). External and internal BKD clinical signs and symptoms were observed in both dead and sampled fish. The clinical signs of *R. salmoninarum* infected lumpfish included hyper-pigmentation, lethargy, abdominal ascites, and hemorrhages in ventral sites. Examination of internal organs revealed splenomegaly, hydronephrosis, pale liver, pseudomembrane formation on internal organs, and ascites (Figure 3.2A). The survival rate for the high, medium, and low doses of *R. salmoninarum* groups was 65%, 93%, and 95%, respectively (Figure 3.2B).

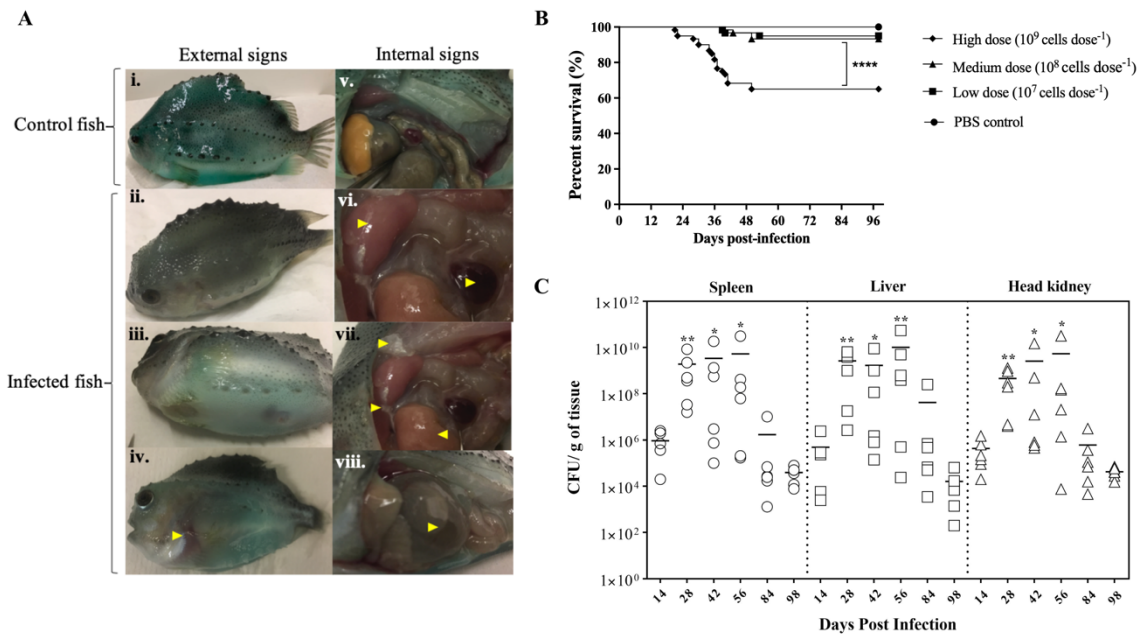


Figure 3.2. Bacterial Kidney Disease clinical signs, survival rates, and tissue colonization of *R. salmoninarum* infected lumpfish. **A.** Bacterial Kidney Disease signs and symptoms in lumpfish detected from 21 to 56 dpi. Pictures were randomly selected to visualize the external and internal disease signs in the infected fish compared to the i. exterior and v. interior views of control fish. Specific signs are indicated with yellow arrowheads. The external signs observed were ii. Skin darkening; iii. Abdominal distension due to ascites; iv. Hemorrhages in ventral sites. The internal signs observed were vi. Enlarged spleen and kidney; vii. Diffuse white membranous layer (pseudo membrane) on internal organs and pale liver; and viii. Accumulation of turbid fluid inside the abdominal sacs and cavities; **B.** Percent survival of lumpfish exposed to experimental infection with high (1×10^9 cells dose $^{-1}$), medium (1×10^8 cells dose $^{-1}$) or low (1×10^7 cells dose $^{-1}$) doses of *R. salmoninarum* compared to a PBS control; **** denotes the significant differences between infected and control groups ($p < 0.001$); **C.** *R. salmoninarum* tissue colonization in lumpfish. Bacterial loads in the spleen, liver, and head kidney of lumpfish ($n = 6$) infected with the high dose

(1×10^9 cells dose⁻¹) of *R. salmoninarum* after 14, 28, 42, 56, 84, and 98 dpi. Asterisks (*) represent significant differences ($*p < 0.05$, $**p < 0.01$) in the bacterial loads between time points (14, 28, 42, 56, and 84 dpi) per organ compared to the bacterial load at 98 dpi, as determined by the non-parametric Kruskal-Wallis test.

The cumulative number of fish mortalities (and mortality rate) observed during the experiment were 21 dead fish out of 60 total fish (35%), 4 dead out of 60 total fish (7%), and 3 dead out of 60 total fish (5%) for high, medium, and low *R. salmoninarum* doses, respectively. The mortality data often considered the fish deaths from the tanks assigned for mortality observation (i.e., sampled fish were not considered in the analyses) (Figure 3.1E). Significantly lower survival ($p<0.001$) was observed in the high dose *R. salmoninarum* infected group, whereas there were no significant differences in survival between PBS control low and medium dose fish groups.

R. salmoninarum colonized all of the organs sampled in the high dose infected lumpfish (Figure 3.2C; Supplementary Figure S3.1). Significantly higher bacterial loads were observed at 28, 42, and 56 dpi compared to 98 dpi (Figure 3.2C). A substantial decrease in the bacterial load was observed at 84 and 98 dpi. Tissue colonization results agreed with the mortality data (Figures 3.2B, C).

In contrast to the control fish, the spleen, liver, and head kidney of high dose infected fish at 14, 28, and 42 dpi showed apparent histopathological damages (Figures 3.3B-D, G-I, L-N). Tissue damage was observed in all three organs at 14, 28, and 42 dpi (Figures 3.3C, G, M, N). Hemorrhages were observed in the spleen and liver at 14 and 42 dpi (Figures 3.3B, D, G, I). The liver sections showed increased vacuolations in hepatocytes at 28 and 42 dpi (Figures 3.3H, I). Melanomacrophage centers were observed in the spleen and liver at 42 dpi (Figures 3.3D, I). Head kidney sections showed congested glomerulus with diffuse thickening of the basement membrane at 14 and 42 dpi (Figures 3L, N). Tissue sections of control fish and high dose infected fish at 98 dpi seemed similar without any significant histopathological damages (Figures 3A, E, F, J, K, O).

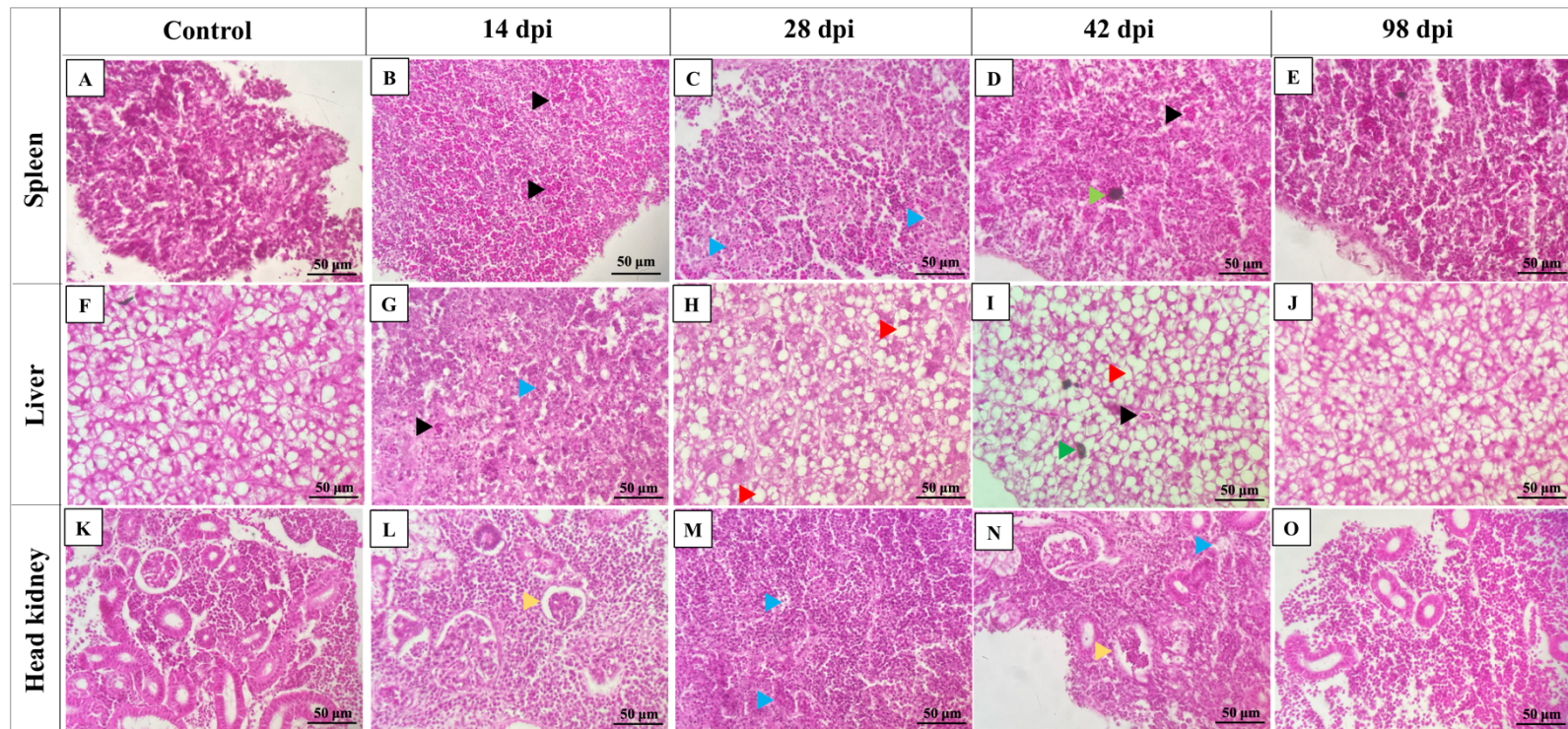


Figure 3.3. Histopathology changes in lumpfish tissues during *R. salmoninarum* infection. Lumpfish spleen, liver, and head kidney were collected from the high dose (1×10^9 cells dose⁻¹) infected group at 14, 28, 42, and 98 dpi and from the control (PBS-mock infected) group and stained with haematoxylin and eosin (H & E). Histopathological changes in lumpfish spleen: **A.** Spleen section from control fish; **B.** Spleen section from infected fish at 14 dpi, showing hemorrhages (black arrowhead); **C.** Spleen section from infected fish at 28 dpi, showing degenerations (blue arrowhead); **D.** Spleen section from infected fish at 42

dpi, showing hemorrhage (black arrowhead) and melanomacrophage center [MMC] (green arrowhead); **E.** Spleen section from infected fish at 98 dpi. Histopathological changes in lumpfish liver: **F.** Liver section from control fish; **G.** Liver section from infected fish at 14 dpi, showing hemorrhage (black arrowhead) and degeneration (blue arrowhead); **H.** Liver section from infected fish at 28 dpi, showing increased vacuolations (red arrowhead); **I.** Liver section from infected fish at 42 dpi, showing hemorrhage (black arrowhead), MMC (Green arrowhead), and vacuolation (red arrowhead); **J.** Liver section from infected fish at 98 dpi. Histopathological changes in lumpfish head kidney: **K.** Head kidney section from control fish; **L.** Head kidney section from infected fish at 14 dpi, showing congested glomerulus (yellow arrowhead); **M.** Head kidney section from infected fish at 28 dpi, showing degenerations (blue arrowhead); **N.** Head kidney section from infected fish at 42 dpi, showing degeneration (blue arrowhead) and congested glomerulus (yellow arrowhead); **O.** Head kidney section from infected fish at 98 dpi. Stain: H & E; Magnification: $\times 400$.

3.4.2. Lumpfish immune-related gene expression in response to *R. salmoninarum* infection

The immune response of lumpfish to *R. salmoninarum* infection was evaluated in the head kidney at 28 dpi and 98 dpi in 10^9 cells dose⁻¹ infected fish and compared to non-infected fish (PBS-control) at the same time points. Of the 33 genes (Table 3.1) that were evaluated, 12 genes were upregulated, and 4 genes were downregulated at both 28 and 98 dpi, whereas 17 genes were dissimilarly regulated.

Thirteen genes related to pattern recognition (Figures 3.4A-E) and cytokines (Figures 3.4F-M) were differentially regulated. *toll-like receptor 3 (tlr3)* and *toll-like receptor 7 (tlr7)* were significantly downregulated in infected fish compared to the control fish at 28 dpi (Figures 3.4A, D). *toll-like receptor 5a (tlr5a)* expression was significantly upregulated at 28 dpi compared to the respective control group (Figure 3.4B). *toll-like receptor 5b (tlr5b)* and *ATP-dependent RNA helicase lgp2 (lgp2)* showed no significant differences in their expression levels between control and infected fish at 28 dpi or 98 dpi (Figures 3.4C, E).

Canonical proinflammatory cytokine-encoding genes, including *interleukin 1 beta (il1b)*, *interleukin 8a (il8a)*, *interleukin 8b (il8b)*, and the anti-inflammatory cytokine *interleukin 10 (il10)*, showed significantly higher expression in infected fish at 28 dpi compared to the non-infected control fish (Figures 3.4F-I). The expression levels of *il1b*, *il8a*, *il8b*, and *il10* in infected fish were not significantly different at 98 dpi compared to the control fish (Figures 3.4F-I).

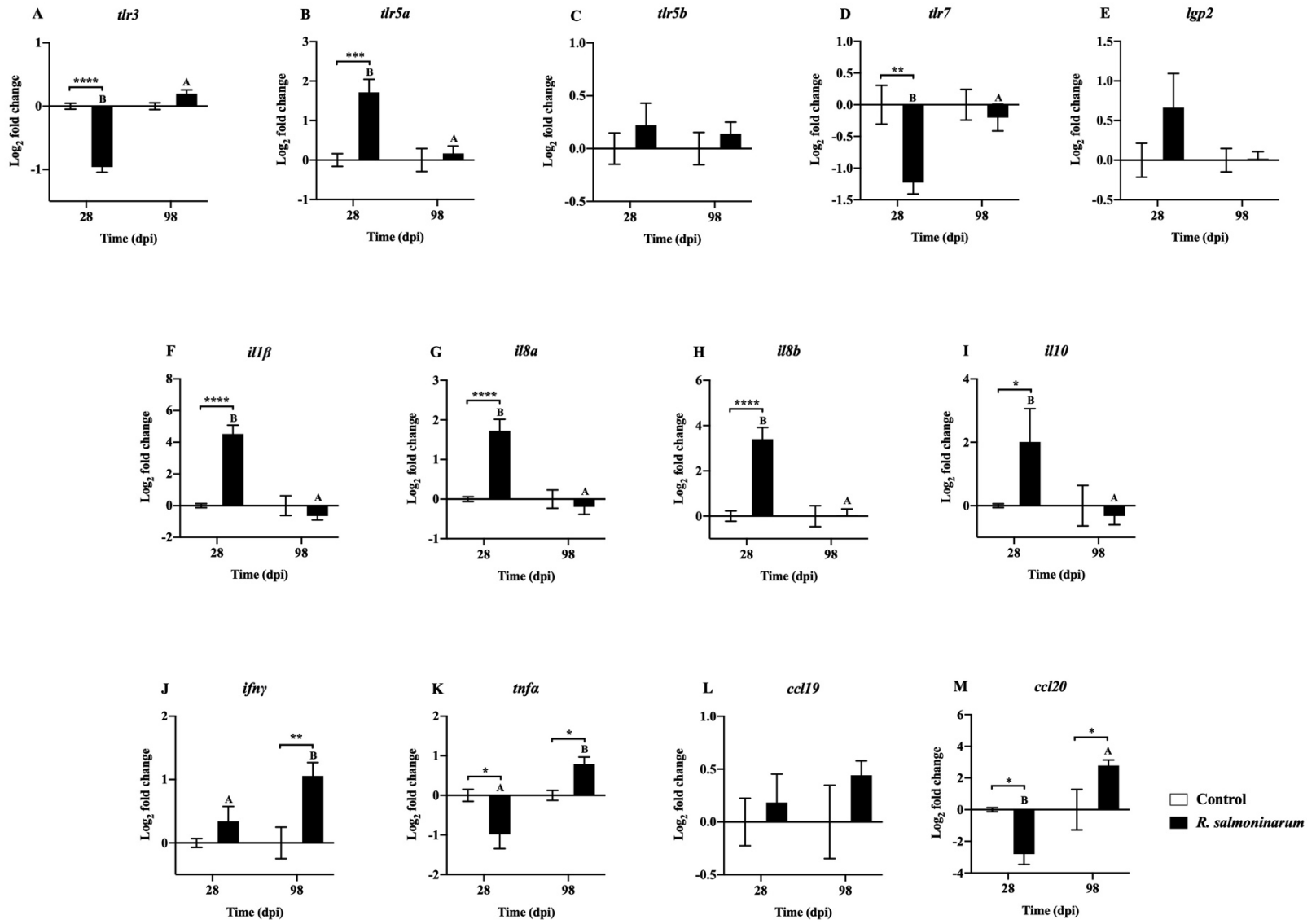


Figure 3.4. Expression of transcripts related to pattern recognition (A-E) and cytokines (F-M) in lumpfish head kidney in response to *R. salmoninarum* infection at 28 and 98 dpi. Transcript expression levels in the head kidney from the control (PBS-mock infected group) and infected [high dose (1×10^9 cells dose⁻¹) of *R. salmoninarum*] lumpfish at 28 and 98 dpi were analyzed using qPCR. Relative expression was calculated using the $2^{-\Delta\Delta C_t}$ method and log₂ transformed; *etif3d* and *pabpc1b* were the endogenous control genes. A two-way ANOVA test, followed by the Sidak multiple comparisons post hoc test, was used to identify significant differences between treatments (control and infected groups) at a single time point and for a given treatment at different time points (28 and 98 dpi). Asterisks (*) represent significant differences between treatments at each time point (* $p < 0.05$, ** $p < 0.01$, *** $p < 0.001$, **** $p < 0.0001$). Different letters represent significant differences between control (lower case) and infected (upper case) groups at 28 compared to 98 dpi. Each value is the mean \pm S.E.M ($n = 6$).

R. salmoninarum infection significantly downregulated *tumour necrosis factor alpha (tnfa)* and *C-C motif chemokine-like 20 (ccl20)* expression at 28 dpi (Figures 3.4K, M). In contrast, *interferon gamma (ifng)*, *tnfa*, and *ccl20* levels were significantly upregulated at 98 dpi compared to the respective non-infected fish group (Figures 3.4J, K, M).

Expression levels of 9 genes regulating the innate (Figures 3.5A-E) and inflammatory (Figures 3.5F-I) immune response were assessed. Gene expression levels of *hepcidin antimicrobial peptide (hamp)* and *serum amyloid A 5 (saa5)* were significantly upregulated in the head kidney of infected fish at 28 dpi compared to the respective non-infected control (Figures 3.5A, B).

At 28 dpi, *interferon regulatory factor 7 (irf7)* was significantly downregulated (Figure 3.5C). Conversely, interferon-induced effectors such as *radical S-adenosyl methionine domain-containing protein 2 / viperin (rsad2)* and three gene isoforms of *interferon-induced GTP-binding protein (mxg, mxh, and mxj)* were significantly upregulated compared to the control fish at 28 dpi (Figures 3.5D, G-I). *cyclooxygenase-2 (cox2)* expression was significantly upregulated in infected fish at 98 dpi compared to the control (Figure 3.5F).

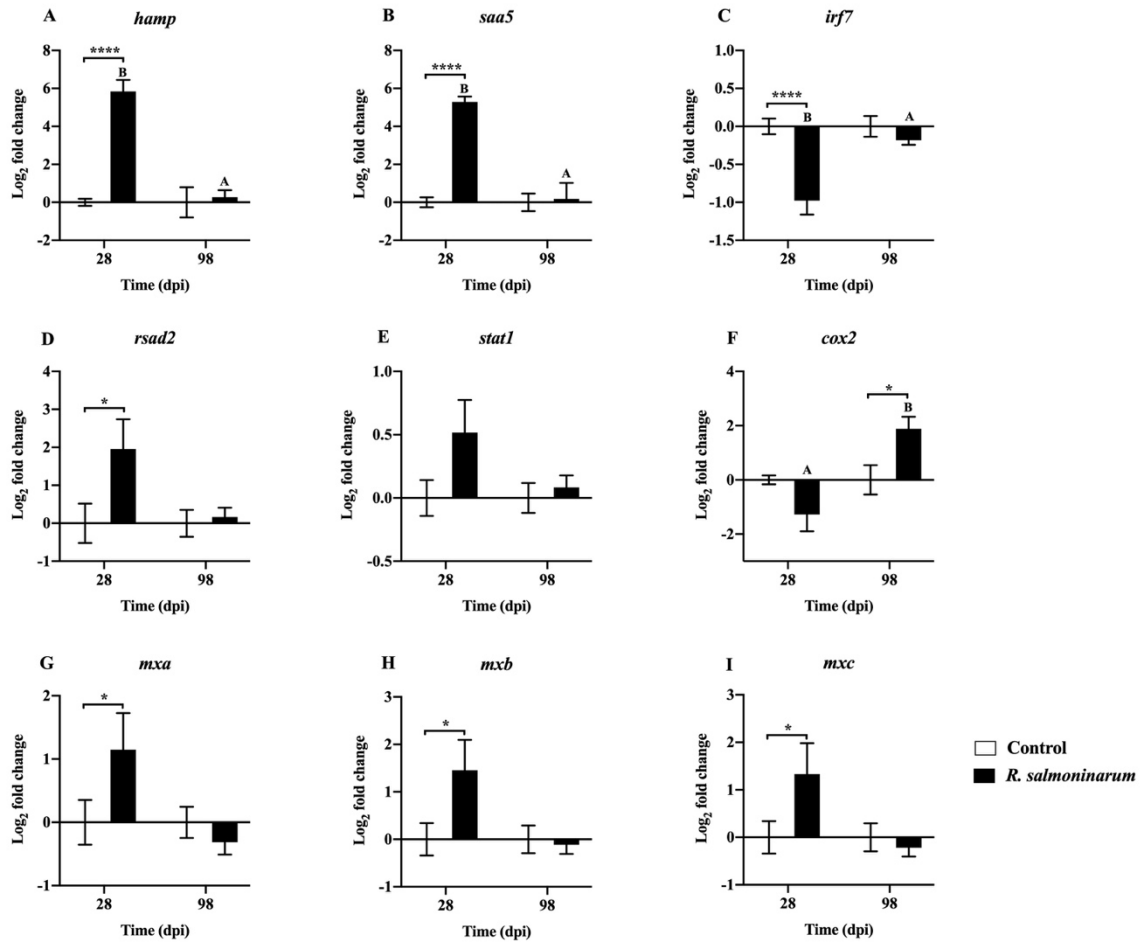


Figure 3.5. Expression of transcripts related to the regulation of the innate (A-E) and inflammatory (F-I) immune response in lumpfish head kidney in response to *R. salmoninarum* infection at 28 and 98 dpi. Transcript expression levels in the head kidney from the control (PBS-mock infected group) and infected [high dose (1×10^9 cells dose⁻¹) of *R. salmoninarum*] lumpfish at 28 and 98 dpi were analyzed using qPCR. Relative expression was calculated using the $2^{-\Delta\Delta C_t}$ method and log₂ transformed; *etif3d* and *pabpc1b* were the endogenous control genes. A two-way ANOVA test, followed by the Sidak multiple comparisons post hoc test, was used to identify significant differences between treatments (control and infected groups) at a single time point and for a given

treatment at different time points (28 and 98 dpi). Asterisks (*) represent significant differences between treatments at each time point (* $p < 0.05$, **** $p < 0.0001$). Different letters represent significant differences between control (lower case) and infected (upper case) groups at 28 compared to 98 dpi. Each value is the mean \pm S.E.M ($n = 6$).

The expression levels of 11 genes playing putative roles in humoral (Figures 3.6A-F) and cellular-mediated adaptive immunity (Figures 3.6G-K) were assessed. Humoral (*immunoglobulin heavy chain variable region a (igha)*, *immunoglobulin delta heavy chain (ighd)*, *immunoglobulin mu heavy chain a (ighma)*, and *immunoglobulin mu heavy chain b (ighmb)*), and cellular-mediated (*T-cell surface glycoprotein CD4a (cd4a)*, *T-cell surface glycoprotein CD4b (cd4b)*, *lymphocyte antigen 6 complex locus protein G6f (ly6g6f)*, *T-cell surface glycoprotein CD8 alpha chain (cd8a)*, and *HLA class II histocompatibility antigen gamma chain (cd74)*) adaptive immunity-related genes showed significant downregulation at 28 dpi in the infected head kidney compared to the non-infected control (Figures 3.6A, C-E, G-K).

At 98 dpi, only one adaptive immune-related gene, *cd74*, was significantly upregulated in infected fish compared to the control (Figure 3.6K). Expression of most of the genes related to humoral and cellular-mediated immunity in infected fish at 98 dpi was restored to similar levels observed in the control fish (Figures 3.6B, D, E-K).

The qPCR results were similar between the $2^{-\Delta\Delta C_t}$ and the RQ data representation methods. However, a few differences in the significance levels were detected for *tlr3*, *tnfa*, *rsad2*, *ighma*, and *cd8a* expression at 28 or 98 dpi (Figures 3.4A, K; 3.5E; 3.6D, J and Supplementary Figures S3.2A, K; S3.3E; S3.4D, J).

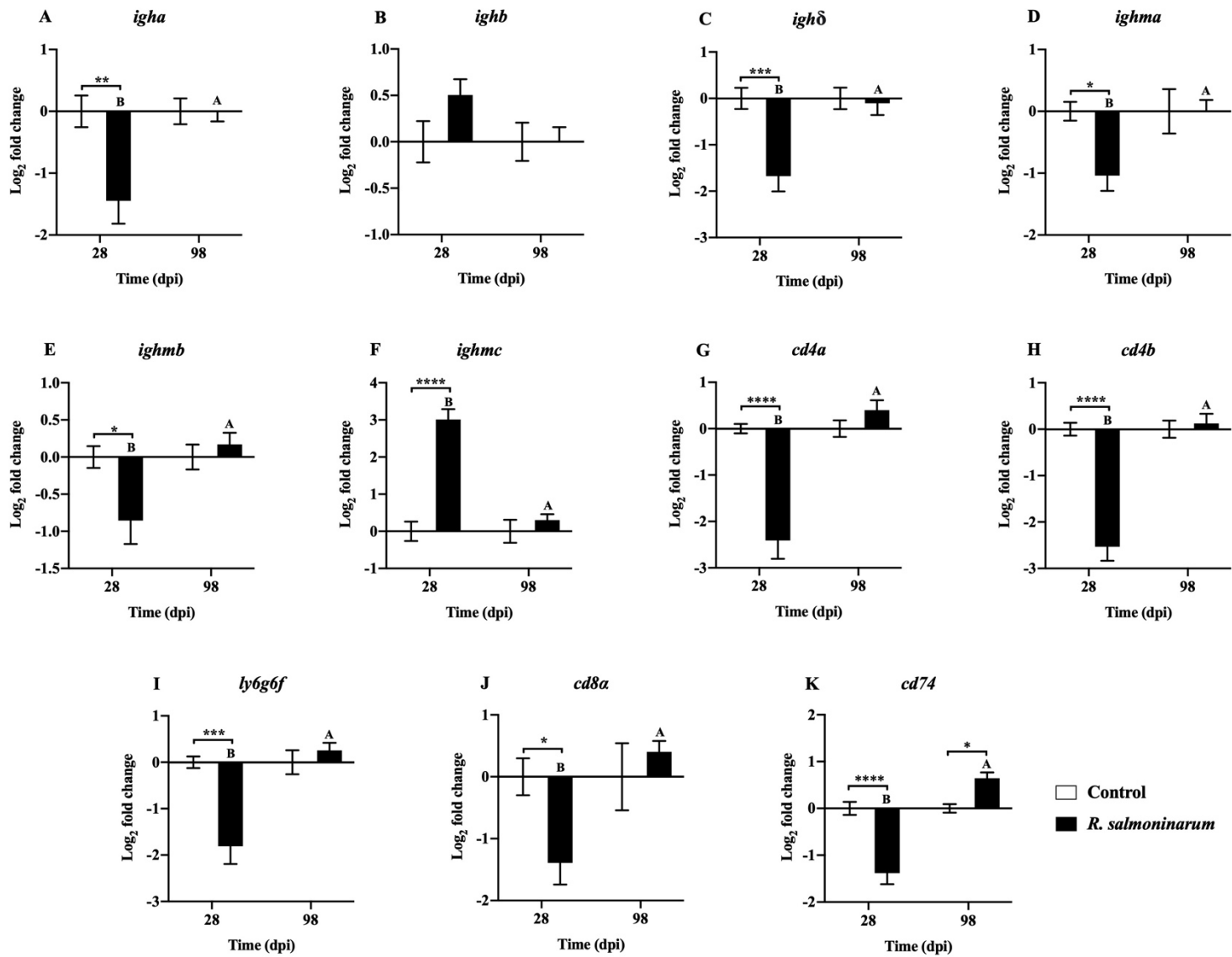


Figure 3.6. Expression of transcripts related to humoral (A-F) and cellular mediated (G-K) immunity in lumpfish head kidney in response to *R. salmoninarum* infection at 28 and 98 dpi. Transcript expression levels in the head kidney from the control (PBS-mock infected group) and infected [high dose (1×10^9 cells dose⁻¹) of *R. salmoninarum*] lumpfish at 28 and 98 dpi were analyzed using qPCR. Relative expression was calculated using the $2^{-\Delta\Delta Ct}$ method and log₂ transformed; *etif3d* and *pabpc1b* were the endogenous control genes. A two-way ANOVA test, followed by the Sidak multiple comparisons post hoc test, was used to identify significant differences between treatments (control and infected groups) at a single time point and for a given treatment at different time points (28 and 98 dpi). Asterisks (*) represent significant differences between treatments at each time point (* $p < 0.05$, ** $p < 0.01$, *** $p < 0.001$, **** $p < 0.0001$). Different letters represent significant differences between control (lower case) and infected (upper case) groups at 28 compared to 98 dpi. Each value is the mean \pm S.E.M ($n = 6$).

3.5. Discussion

As previously mentioned, lumpfish are in close contact with salmon when delousing sea lice in sea cage aquaculture [17,19], and this interaction could result in the horizontal transmission of infectious disease agents between both species, including *R. salmoninarum*. Atlantic salmon is susceptible to *R. salmoninarum*, and it could transfer this pathogen to other fish species [20,21]. It is believed that lumpfish could act as a non-symptomatic carrier and transmit disease to cohabitating salmon [19]. Haugland et al. (2017) confirmed the experimental transmission of amoebic parasite from lumpfish to salmon [29]. Also, Atlantic salmon susceptibility to a lumpfish isolate of *M. viscosa* reflects the disease risk to salmon [30]. Although BKD episodes have not been reported in lumpfish, its susceptibility and immune response to *R. salmoninarum* are unknown. Here, we examined the susceptibility of lumpfish to the *R. salmoninarum* (ATCC 33209) type strain, which has been utilized for several infection studies in different salmon species [36,47,65,66]. Using similar *R. salmoninarum* infection doses like other studies [9,44–48], we also determined the infection kinetics and lumpfish molecular immune response at early and late chronic infection with *R. salmoninarum*. This study is the first report of *R. salmoninarum* experimental infection in lumpfish and provides immune-relevant information on how the lumpfish respond to *R. salmoninarum*.

For the *R. salmoninarum* infection kinetics studies, we selected the plate counting method in SKDM2 over typical methods for *R. salmoninarum* quantification (e.g., FAT, ELISA, and PCR) because it directly enumerates viable bacteria [7]. Spleen and liver were also analyzed, in addition to the head kidney, to consider non-kidney *R. salmoninarum*

infections, which have been well described in salmonids [67,68]. In lumpfish, *R. salmoninarum* infection becomes evident at 2 weeks post-infection, similar to chinook salmon (*O. tshawytscha*) i.p. infected with 1×10^6 *R. salmoninarum* cells dose⁻¹ [66]. In an antibody capture ELISA and western blot-based analysis, Turaga *et al.* (1987) reported that levels of *R. salmoninarum* soluble antigens in infected coho salmon (*Oncorhynchus kisutch*) gradually increased during the course of infection and peaked at 20 dpi and thereafter, fish mortality was observed [69]. Although in the current study we did not measure *R. salmoninarum* soluble antigen levels, mortality of *R. salmoninarum* infected lumpfish started at 20 dpi, similar to coho salmon, i.p. infected with *R. salmoninarum* cells in the exponential phase of growth (O.D. 500 nm = 1.0) [69]. This suggests that mortality could be initiated by the accumulation of *R. salmoninarum* MSA in the infected lumpfish. Because increased MSA levels correlated with the severity of infection and mortality [69,70].

Lumpfish infected with a lethal dose of *R. salmoninarum* showed prominent BKD-associated clinical signs at 14, 28, and 56 dpi (Figure 3.2A), similar to clinical signs described in other fish species [7]. Bacterial loads in the spleen, liver, and head kidney at various time points indicated that *R. salmoninarum* established an infection in all infected individuals (Figure 3.2C). In contrast, carp (*Cyprinus carpio* L.), a non-salmonid like lumpfish, showed resistance to *R. salmoninarum* infection (4.8×10^7 and 4.8×10^8 cells dose⁻¹), and no bacteria were recovered from the head kidney after infection [44]. These results indicate that the lumpfish is susceptible to *R. salmoninarum* and could be a potential vector for this pathogen.

Significantly higher tissue bacterial loads at 28, 42, and 56 dpi agreed with higher mortality (Figures 3.2B, C). However, after fish mortality ended (Figure 3.2B), *R. salmoninarum* remained in the internal tissues (Figure 3.2C; Supplementary Figures S3.2E, F), indicating a pattern of chronic infection. Arctic charr [15], chinook salmon [63], lamprey [71] and carp [44] cleared *R. salmoninarum* infection after 175, 115, 92, and 38 days, respectively. *R. salmoninarum* persisted in lumpfish tissues for at least 98 dpi, which is consistent with studies in chinook salmon, where *R. salmoninarum* caused a chronic infection and persisted for up to 100 dpi [36]. However, if the current study had been extended, it is possible that lumpfish could have cleared the *R. salmoninarum* after 98-100 dpi, as seen in the Arctic charr [15] or remains in other tissues like gonads (i.e., *R. salmoninarum* in the ovarian fluid is an important source of infection for the eggs) to facilitate vertical transmission [7].

The lethal dose 50 (LD₅₀) of *R. salmoninarum* ATCC 33209 in various salmonid hosts ranged from 1.4×10^5 to 2.94×10^8 CFU dose⁻¹ [47]. We could not determine the LD₅₀ for *R. salmoninarum* ATCC 33209 in lumpfish because the fish infected with the highest dose (1×10^9 cells dose⁻¹), similar to other studies, showed only 35% mortality. In contrast, mortality reached 100% within 15 days in Atlantic salmon infected with 10^8 cells dose⁻¹ of highly virulent *R. salmoninarum* strains [72]. The LD₅₀ of *R. salmoninarum* type strain in lumpfish might be greater than 1×10^9 CFU dose⁻¹, and although 10^9 cells dose⁻¹ of *R. salmoninarum* ATCC 33209 was sufficient to invade, replicate and establish an infection in lumpfish, its lethality was lower than in salmonid species [36,73–76].

Differences in virulence between *R. salmoninarum* isolates from several geographical regions and fish hosts have been reported [47]. Rhodes et al. (2004)

demonstrated the positive correlation between the functional *msa* gene copy number per bacterial cell and virulence (i.e., increased mortality) [65]. The type strain *R. salmoninarum* ATCC 33209 used in this study has two *msa* gene copies, and both are essential for disease development and mortality [63,64]. Compared to other *R. salmoninarum* strains, *R. salmoninarum* ATCC 33209 has reduced virulence. For example, this strain showed lower virulence in chinook and coho salmon compared to the other isolates, and it is not capable of causing BKD in rainbow trout [46,47]. Furthermore, *R. salmoninarum* type strain does not infect the carp (*Epithelioma papillosum*) cell line, even with a dose of 1×10^9 cells, in contrast to more virulent strains of *R. salmoninarum* (e.g., FT10) that are capable of invading and proliferate in these cells [46,77]. *R. salmoninarum* ATCC 33209 type strain was isolated in 1974, and it has been subjected to extensive laboratory passages, which may have contributed to its relatively reduced virulence [65]. In the present study, *R. salmoninarum* ATCC 33209 was unable to kill all infected lumpfish even at a high dose, and this could be linked to the low virulence documented for *R. salmoninarum* ATCC 33209.

Histology observations in the sampled lumpfish infected with *R. salmoninarum* showed similarities with the histopathological characteristics of BKD in salmonids (Figure 3.3). For instance, glomerulopathy is related to antigen-antibody complex deposition in the glomeruli, which causes the thickening of the glomerular basement membrane [10,78]. In concordance with BKD histopathology, congested glomeruli were observed in the head kidney of infected lumpfish at 14 and 42 dpi (Figures 3.3L, N). Also, lysed and disrupted melanomacrophages resulting from the dispersal of pigments in tissues during BKD [79,80] were observed in the spleen and liver from infected

lumpfish at 42 dpi (Figures 3.3D, I). No histopathological differences were observed at 98 dpi (Figure 3.3). The persistence of *R. salmoninarum* in lumpfish tissues at 98 dpi was indicative of a chronic infection, and the bacterium may remain dormant or controlled by the fish immune system [81]. The lack of tissue inflammation and damage at 98 dpi could be explained by the known immune-suppressive nature of *R. salmoninarum* [8,10,82].

At 98 dpi, *R. salmoninarum* was isolated from the spleen, liver, and head kidney of the high dose infected lumpfish, which showed no external, internal, and histopathological disease signs (Figures 3.2C and 3.3). Similar to our results, *M. viscosa* was isolated from the kidneys of asymptomatic lumpfish at 27 days post-bath challenge [30]. This implies that lumpfish could be asymptomatic carriers for *R. salmoninarum*, and chronic infection could be a common strategy of marine bacterial pathogens.

The BKD-related histopathology observations in lumpfish coincided with the downregulation of immune-related genes in the lumpfish head kidney after *R. salmoninarum* infection. For instance, we observed that *R. salmoninarum* influenced the expression of genes related to pathogen recognition, immune signalling, antibacterial activity, and humoral and cell-mediated immunity in lumpfish (Figs 3.4-3.6).

TLR5 is associated with flagellin detection [83]. *tlr5a* was significantly upregulated at 28 dpi (Figure 3.4B). Increased expression of *tlr5a* in lumpfish upon exposure to Gram-positive, non-motile or non-flagellated bacteria like *R. salmoninarum* [84] is controversial. However, a similar upregulation of *tlr5* in response to both live and formalin-killed *R. salmoninarum* has been reported [48,85]. Also, increased expression of *tlr5a* and *tlr5b* was reported in turbot (*Scophthalmus maximus* L.) mucosal tissues (i.e., intestine and gills) in response to the Gram-positive non-flagellated pathogen *Streptococcus iniae* [86].

Therefore, the role of TLR5 beyond the recognition of flagellin, specifically in infection with non-flagellated bacteria in teleosts, warrants further investigation.

R. salmoninarum increased gene expression levels of the proinflammatory cytokine (*il1b*) and of the proinflammatory response-related chemokines (*il8a*, *il8b*) at 28 dpi (Figures 3.4F-H) in lumpfish, which coincided with a canonical innate immune response. Simultaneously, *il10*, an anti-inflammatory mediator, was significantly upregulated at 28 dpi (Figure 3.4I). This pattern strongly suggests an *R. salmoninarum*-induced immune suppression [8,82]. Similar to our results, IL-10 induction upon *R. salmoninarum* strain H-2 infection in Atlantic Salmon Kidney (ASK) cell line was observed by Bethke et al. (2019) [87]. IL10 counteracted the induced inflammatory immune responses (e.g., IL1 β , IL8), and as a result, the pathogen could possibly move forward in disease progression. However, as teleost fish IL-10 demonstrates immune suppressive function, *il10* expression upon pathogen infection could be the natural way for lumpfish to regulate its early innate immune responses [88]. Thus, IL-10 upregulation might be seen from a host point of view in which the host is trying to create a conducive environment to alleviate host-mediated pathology. For instance, IL-10 can promote tissue repair to overcome tissue damage due to disease progression [89].

IL-1 β was activated in fish leucocytes and macrophages and induced the expression of proinflammatory transcripts such as *cox2* and *tnfa* [90–92]. However, at 28 dpi, we observed that *cox2* and *tnfa* were not upregulated even with high expression of *il1b* (Figures 3.4F, K, and 3.5C). IL-1 β can also initiate an acute phase response and induce the synthesis of acute-phase proteins (APPs) such as Serum amyloid A5 (SAA5) upon invasion of the

pathogen [93,94]. We observed a significant upregulation of *saa5* at 28 dpi in lumpfish (Figure 3.5B), suggesting an inflammatory response to the infection [95].

TNF- α is associated with inflammation and chronic infections [96]. TNF- α can either improve the phagocytic activity of fish leucocytes or support the intracellular survival of pathogens [97–100]. In the current study, despite the high bacterial load in the fish tissues (Figure 3.2C), significant downregulation of *tnfa* at 28 dpi was observed in lumpfish (Figure 3.4K), which could affect the *tnfa*-dependent killing pathways, thereby facilitating the infection and intracellular survival of *R. salmoninarum* [32]. Also, this *tnfa* repression could reflect the immune-suppressive action of *R. salmoninarum* in lumpfish.

Reducing the availability of iron to bacteria as a means of nutritional immunity is one strategy used by vertebrates such as fish to control pathogens [101]. On the other hand, intracellular bacteria compete for iron for their survival [102]. HAMP is an antimicrobial peptide (AMP) that has anti-bacterial and immuno-modulatory functions and plays a role in iron homeostasis in fish [103]. Here, we found that *hamp* was significantly upregulated at 28 dpi (Figure 3.5A). Similar to our results, increased expression of *hamp* in the head kidney of Atlantic salmon has also been observed with *R. salmoninarum* infection [48,85]. Additionally, *transferrin*, an AMP-encoding gene and an acute phase protein [94], which has a putative role in iron sequestration from bacteria, is upregulated in response to *R. salmoninarum* in salmonid hosts [66] and is involved in BKD resistance in coho salmon (*O. kisutch*) [104]. Thus, *hamp* and *transferrin* in lumpfish might play an essential role in the BKD response.

IFN- γ is associated with adaptive immunity and has a role in both the early and late immune responses and in the host immune defense to intracellular bacteria [96,102]. *ifng*

stimulation in lumpfish at 28 dpi was not significant in our study. In contrast, significant upregulation of *ifng* was reported in Atlantic salmon and chinook salmon infected with *R. salmoninarum* [48,66]. Interferon-induced effectors (*rsad2*, *mx**a*, *mx**b*, and *mx**c*) were significantly upregulated at 28 dpi (Figures 3.4J and 3.5D, G-I). Similar to our results, upregulation of *rsad2* has also been observed in Atlantic salmon head kidney upon *R. salmoninarum* infection [48]. In addition, increased expression of mx genes *mx1*, *mx2*, and *mx3* in rainbow trout macrophages [32] and *mx1* in chinook salmon [66] after *R. salmoninarum* infection was also reported.

The immune-suppressive effects of *R. salmoninarum* were also observed in the adaptive immune response of lumpfish at 28 dpi. For instance, significant downregulation of humoral (*igha*, *ighd*, *ighma*, *ighmb*) (Figures 3.6A, C-E) and cell-mediated (*cd4a*, *cd4b*, *ly6g6f*, *cd8a*, *cd74*) (Figures 3.6G-K) adaptive immune-related transcripts at 28 dpi, was observed. Mortality in lumpfish during the early time points could be attributed to this immune suppressive function of *R. salmoninarum* observed at 28 dpi. Significant downregulation of *cd74* (an invariant polypeptide involved in major histocompatibility complex-II (MHC-II) formation and transport) (Figure 3.6K) in lumpfish head kidney at 28 dpi suggests that the T-cell responses could be modified towards an enhanced MHC-I and a reduced MHC-II dependent pathway, perhaps caused by an increased amount of MSA, similar to *R. salmoninarum* infection in rainbow trout [32,105]. This skewing towards the MHC-I pathway in lumpfish at the early stages of *R. salmoninarum* infection agrees with the BKD-dependent *major histocompatibility-1* (*mh1*) induction observed in Atlantic salmon at 13 dpi [48]. Further, Rozas-Serri et al. (2020) demonstrated that the humoral and cell-mediated adaptive immune responses against *R. salmoninarum* in

Atlantic salmon pre-smolts were significantly downregulated at the later stage of infection (55 dpi) [106], which agrees with our findings at 28 dpi. In contrast, while most of the humoral-immune genes showed strong down-regulation at 28 dpi (Figures 3.6A, C-E), only the *ighmc* was significantly upregulated (Figure 3.6F). This observation at 28 dpi is controversial but in line with the triggered humoral response against *R. salmoninarum* in salmonids, which does not necessarily correlate with immune protection [7,8,106].

R. salmoninarum persisted in the lumpfish tissues for at least 98 dpi (Figure 3.2C), which agrees with the chronic nature of BKD [2,107]. Significant upregulation of the eicosanoid *cox2* at 98 dpi (Figure 3.5F) could be related to the inflammatory response and supports the chronic persistence of *R. salmoninarum* in lumpfish tissues. *tnfa* was significantly upregulated at 98 dpi, which could be the result of MSA accumulation in infected lumpfish [32]. Chronic stimulation of *tnfa* is known to assist the chronic inflammatory pathology of BKD and contributed to the host-mediated destruction of the kidney tissues in rainbow trout [32]. In contrast, survivor lumpfish with considerable *R. salmoninarum* burden remaining in their internal tissues for at least 98 dpi (Figure 3.2C) did so in the absence of BKD clinical signs (Figures 3.3E, J, O) even with high expression of *tnfa* with respect to the control (Figure 3.4K). This immune pattern might be related to the chronic stage of *R. salmoninarum* infection. On the other hand, *tnfa* upregulation at 98 dpi (Figure 3.4K) could be linked to the low bacterial loads in lumpfish tissues at 98 dpi compared to 28 dpi (Figure 3.2C) because of the role of TNF- α in restricting the bacterial growth in infected macrophages and promoting macrophage survival in zebrafish (*Danio rerio*) infected with an intracellular pathogen, *Mycobacterium marinum* [108].

Most of the downregulated adaptive immune genes (*igha*, *ighd*, *ighma*, *ighmb*, *cd4a*, *cd4b*, *ly6g6f*, and *cd8a*) in infected lumpfish at 28 dpi returned to basal expression levels at 98 dpi (Figures 3.6A, C-E, 6G-J). Upregulation of *cd74* at 98 dpi (Figure 3.6K) could induce MHC-II expression. Also, significant stimulation of *ifng* at 98 dpi (Figure 3.4J) could enhance antigen presentation through MHC-I, as was observed in rainbow trout [109]. Thus, the interaction between this intracellular pathogen and teleost MHC-pathways warrants further investigation.

Based on gene expression results, *R. salmoninarum* could cause immune suppression of lumpfish at the early infection stages (28 dpi). In contrast, at a late stage (98 dpi), it seems that *R. salmoninarum* is partially controlled by the lumpfish immune system, which may be attributed to induced cell-mediated immunity. It is not clear whether the *R. salmoninarum* will be cleared or if it will persist and be horizontally transmitted or vertically transferred to the next generation of lumpfish. On the other hand, the majority of the lumpfish (65%) survived *R. salmoninarum* infection and presented the bacteria in the head kidney until 98 dpi. These observations suggest that lumpfish is susceptible to *R. salmoninarum*. Lumpfish susceptibility to high virulent strains of *R. salmoninarum* with multiple *msa* gene copies (i.e., *msa* gene copies ranged from two to five among 68 isolates) [110] and its transmission potential to other fish species warrants future research.

3.6. Conclusions

This study revealed that lumpfish is susceptible to *R. salmoninarum* ATCC 33209 i.p. infection, exhibiting a chronic infection pattern. *R. salmoninarum* caused immune suppression and modulated the lumpfish immune response towards the MHC-I pathway at 28 dpi. Lumpfish seemed to trigger a cell-mediated immune response against *R. salmoninarum* at the chronic stage of infection. Although *R. salmoninarum* persisted for at least 98 dpi in lumpfish tissues, it is not known whether lumpfish is able to clear the infection or if *R. salmoninarum* will persist and use lumpfish as a vector during cohabitation with salmon. Lumpfish susceptibility to more virulent *R. salmoninarum* strains or different routes of infection warrants further investigation.

3.7. References

1. Buller, N. B. Aquatic Animal Species and Organism Relationship. In *Bacteria and fungi from fish and other aquatic animals : a practical identification manual*; CABI: London, 2014; pp 368–373.
2. Evelyn, T. P. . Bacterial Kidney Disease – BKD. In *Bacterial Disease of Fish*; V., Roberts, R. J. and Bromage, N. R., Ed.; Blackwell Scientific: London, 1993; pp 177–195.
3. Kent, M. L.; Traxler, G. S.; Kieser, D.; Richard, J.; Dawe, S. C.; Shaw, R. W.; Prosperi-Porta, G.; Ketcheson, J.; Evelyn, T. P. T. Survey of Salmonid Pathogens in Ocean-Caught Fishes in British Columbia, Canada. *J. Aquat. Anim. Health* **1998**, *10* (2), 211–219, doi:10.1577/1548-8667(1998)010<0211:SOSPPIO>2.0.CO;2.
4. Starliper, C. E.; Morrison, P. Bacterial Pathogen Contagion Studies among Freshwater Bivalves and Salmonid Fishes. *J. Shellfish Res.* **2000**, *19* (1), 251–258.
5. Chambers, E. M.; Nagel, D. A.; Elloway, E. A.; Addison, K. L.; Barker, G. A.; Verner-Jeffreys, D. W.; Stone, D. M. Polymerase Chain Reaction Detection of *Renibacterium salmoninarum* in Fish: Validation of a Modified Protocol. *Aquaculture* **2009**, *287* (1–2), 35–39, doi:10.1016/j.aquaculture.2008.10.031.
6. Austin, B. and Austin, D. A. Aerobic Gram-positive Rods and Cocci. In *Bacterial Fish Pathogens*; Austin, Brian and Austin, D., Ed.; Springer: Germany, 2016, doi:10.1007/978-1-4020-6069-4.
7. Pascho, R. J.; Elliott, D. G.; Chase, D. M. Comparison of Traditional and Molecular Methods for Detection of *Renibacterium salmoninarum*; 2002; pp 157–209, doi:10.1007/978-94-017-2315-2_7.
8. Wiens, G. D. Bacterial Kidney Disease (*Renibacterium salmoninarum*). In *Fish Diseases and Disorders*; Woo, P. T. K., Bruno, D. W., Eds.; CABI: Wallingford, UK, 2011; pp 338–374.
9. Bell, G. R.; Hoffmann, R. W.; Brown, L. L. Pathology of Experimental Infections of the Sablefish, *Anoplopoma fimbria* (Pallas), with *Renibacterium salmoninarum*, the Agent of Bacterial Kidney Disease in Salmonids. *J. Fish Dis.* **1990**, *13* (5), 355–367.
10. Elliott, D. G. *Renibacterium salmoninarum*. In *Fish Viruses and Bacteria: Pathobiology and Protection*; Woo, P.T.K and Ciaprino, R. ., Ed.; CABI, U.K, 2017; pp 286–297.
11. Nagai, T.; Iida, Y. Occurrence of Bacterial Kidney Disease in Cultured Ayu. *Fish Pathol.* **2002**, *37* (2), 77–81, doi:10.3147/jsfp.37.77.
12. Wallace, I. S.; Munro, L. A.; Kilburn, R.; Hall, M.; Black, J.; Raynard, R. S.; Murray, A. G. *A Report on the Effectiveness of Cage and Farm-Level Following for the Control of Bacterial Kidney Disease and Sleeping Disease on Large Cage-Based Trout Farms in Scotland*; 2011; Vol. 2.
13. Fryer, J. L.; Lannan, C. N. The History and Current Status of *Renibacterium salmoninarum*, the Causative Agent of Bacterial Kidney Disease in Pacific Salmon. *Fish. Res.* **1993**, *17* (1–2), 15–33, doi:10.1016/0165-7836(93)90004-Q.
14. Boerlage, A. S.; Stryhn, H.; Sanchez, J.; Hammell, K. L. Case Definition for Clinical

- and Subclinical Bacterial Kidney Disease (BKD) in Atlantic Salmon (*Salmo salar* L.) in New Brunswick, Canada. *J. Fish Dis.* **2017**, *40* (3), 395–409, doi:10.1111/jfd.12521.
15. Gudmundsdóttir, S.; Kristmundsson; Árnason. Experimental Challenges with *Renibacterium salmoninarum* in Arctic Charr *Salvelinus alpinus*. *Dis. Aquat. Organ.* **2017**, *124* (1), 21–30, doi:10.3354/dao03107.
 16. Hvas, M.; Folkedal, O.; Imsland, A.; Oppedal, F. Metabolic Rates, Swimming Capabilities, Thermal Niche and Stress Response of the Lumpfish, *Cyclopterus lumpus*. *Biol. Open* **2018**, *7* (9), 1–9, doi:10.1242/bio.036079.
 17. Powell, A.; Treasurer, J. W.; Pooley, C. L.; Keay, A. J.; Lloyd, R.; Imsland, A. K.; Garcia de Leaniz, C. Use of Lumpfish for Sea-Lice Control in Salmon Farming: Challenges and Opportunities. *Rev. Aquac.* **2018**, *10* (3), 683–702, doi:10.1111/raq.12194.
 18. Murray, A. G. A Modelling Framework for Assessing the Risk of Emerging Diseases Associated with the Use of Cleaner Fish to Control Parasitic Sea Lice on Salmon Farms. *Transbound. Emerg. Dis.* **2016**, *63* (2), e270–e277, doi:10.1111/tbed.12273.
 19. Brooker, A. J.; Papadopoulou, A.; Gutierrez, C.; Rey, S.; Davie, A.; Migaud, H. Sustainable Production and Use of Cleaner Fish for the Biological Control of Sea Lice: Recent Advances and Current Challenges. *Vet. Rec.* **2018**, *183* (12), 383, doi:10.1136/vr.104966.
 20. Bell, G. R., Higgs, D. A. and Traxler, G. S. The Effect of Dietary Ascorbate, Zinc, and Manganese on the Development of Experimentally Induced Bacterial Kidney Disease in Sockeye Salmon (*Oncorhynchus nerka*). *Aquaculture* **1984**, *36*, 293–311.
 21. Murray, C.; Evelyn, T.; Beacham, T.; Bamer, L.; Ketcheson, J.; Prosperi-Porta, L. Experimental Induction of Bacterial Kidney Disease in Chinook Salmon by Immersion and Cohabitation Challenges. *Dis. Aquat. Organ.* **1992**, *12*, 91–96, doi:10.3354/dao012091.
 22. Richards, R. H., Roberts, R. J., and Schlotfeldt, H.-J. Bacterial Diseases of the Bony Fish. In *Basics of Fish pathology*; Roberts, R. J., and Schlotfeldt, H.-J., Ed.; Paul Parey: Hamburg, Germany, 1985; pp 174–207.
 23. Frerichs, G., and Roberts, R. *Fish Pathology*, Second edi.; Roberts, R., Ed.; Bailliere Tindall: London, 1989.
 24. Scientific Committee on Animal Health and Animal Welfare. *Bacterial Kidney Disease - BKD*; 1999.
 25. Snieszko, S. F. Nutritional Fish Diseases. In *Fish Nutrition*; Elsevier, 1972; pp 403–437, doi:10.1016/b978-0-12-319650-7.50014-6.
 26. Lafferty, K. D.; Harvell, C. D.; Conrad, J. M.; Friedman, C. S.; Kent, M. L.; Kuris, A. M.; Powell, E. N.; Rondeau, D.; Saksida, S. M. Infectious Diseases Affect Marine Fisheries and Aquaculture Economics. *Ann. Rev. Mar. Sci.* **2015**, *7* (1), 471–496, doi:10.1146/annurev-marine-010814-015646.
 27. Conlon, H.; Imsland, A. K. D. Lumpfish Habitat Development for Use in Salmon Farming. **2019**, No. May.
 28. Rimstad, E.; Basic, D.; Gulla, S.; Hjeltne, B.; Mortensen, S. Risk Assessment of Fish Health Associated with the Use of Cleaner Fish in Aquaculture. *Opin. panel Anim. Heal. Welf. Nor. Sci. Comm. Food Environ. VKM Rep.* **2017**, *32*.

29. Haugland, G. T.; Olsen, A.-B.; Rønneseth, A.; Andersen, L. Lumpfish (*Cyclopterus lumpus* L.) Develop Amoebic Gill Disease (AGD) after Experimental Challenge with *Paramoeba perurans* and Can Transfer Amoebae to Atlantic Salmon (*Salmo salar* L.). *Aquaculture* **2017**, *478*, 48–55.
30. Einarsdottir, T.; Sigurdardottir, H.; Bjornsdottir, T. S.; Einarsdottir, E. Moritella Viscosa in Lumpfish (*Cyclopterus lumpus*) and Atlantic Salmon (*Salmo salar*). *J. Fish Dis.* **2018**, *41* (11), 1751–1758.
31. Campos-Perez, J. J.; Ward, M.; Grabowski, P. S.; Ellis, A. E.; Secombes, C. J. The Gills Are an Important Site of INOS Expression in Rainbow Trout *Oncorhynchus mykiss* after Challenge with the Gram-positive Pathogen *Renibacterium salmoninarum*. *Immunology* **2000**, *99* (1), 153–161, doi:10.1046/j.1365-2567.2000.00914.x.
32. Grayson, T. H.; Cooper, L. F.; Wrathmell, A. B.; Roper, J.; Evenden, A. J.; Gilpin, M. L. Host Responses to *Renibacterium salmoninarum* and Specific Components of the Pathogen Reveal the Mechanisms of Immune Suppression and Activation. *Immunology* **2002**, *106* (2), 273–283, doi:10.1046/j.1365-2567.2002.01420.x.
33. Jansson, E.; Hongslo, T.; Johannisson, A.; Pilström, L.; Timmusk, S.; Norrgren, L. Bacterial Kidney Disease as a Model for Studies of Cell-mediated Immunity in Rainbow Trout (*Oncorhynchus mykiss*). *Fish Shellfish Immunol.* **2003**, *14* (4), 347–362.
34. Rhodes, L. D.; Wallis, S.; Demlow, S. E. Genes Associated with an Effective Host Response by Chinook Salmon to *Renibacterium salmoninarum*. *Dev. Comp. Immunol.* **2009**, *33* (2), 176–186, doi:10.1016/j.dci.2008.08.006.
35. Ellul, R. M.; Walde, C.; Haugland, G. T.; Wergeland, H.; Rønneseth, A. Pathogenicity of *Pasteurella* Sp. in Lumpsuckers (*Cyclopterus lumpus* L.). *J. Fish Dis.* **2019**, *42* (1), 35–46, doi:10.1111/jfd.12905.
36. Purcell, M. K.; Murray, A. L.; Elz, A.; Park, L. K.; Marcquenski, S. V.; Winton, J. R.; Alcorn, S. W.; Pascho, R. J.; Elliott, D. G. Decreased Mortality of Lake Michigan Chinook Salmon after Bacterial Kidney Disease Challenge: Evidence for Pathogen-Driven Selection? *J. Aquat. Anim. Health* **2008**, *20* (4), 225–235, doi:10.1577/H08-028.1.
37. Austin, B.; Embley, T. M.; Goodfellow, M. Selective Isolation of *Renibacterium salmoninarum*. *FEMS Microbiol. Lett.* **1983**, *17* (1–3), 111–114, doi:10.1111/j.1574-6968.1983.tb00383.x.
38. Valderrama, K.; Saravia, M.; Santander, J. Phenotype of *Aeromonas salmonicida* sp. *salmonicida* Cyclic Adenosine 3',5'-Monophosphate Receptor Protein (Crp) Mutants and Its Virulence in Rainbow Trout (*Oncorhynchus mykiss*). *J. Fish Dis.* **2017**, *40* (12), 1849–1856, doi:10.1111/jfd.12658.
39. Leboffe, M. J.; Pierce, B. E. *Microbiology: Laboratory Theory & Application*, 2nd editio.; Ferguson, D., Ed.; Morton Publishing, 2015.
40. Brown, L. L.; Iwama, G. K.; Evelyn, T. P. T.; Nelson, W. S.; Levine, R. P. Use of the Polymerase Chain Reaction (PCR) to Detect DNA from *Renibacterium salmoninarum* within Individual Salmonid Eggs. *Dis. Aquat. Organ.* **1994**, *18* (3), 165–171, doi:10.3354/dao018165.
41. Brown, L. L.; Evelyn, T. P.; Iwama, G. K.; Nelson, W. S.; Levine, R. P. Bacterial

- Species Other than *Renibacterium salmoninarum* Cross-React with Antisera against *R. salmoninarum* but Are Negative for the p57 Gene of *R. salmoninarum* as Detected by the Polymerase Chain Reaction (PCR). *Dis. Aquat. Organ.* **1995**, *21* (3), 227–231, doi:10.3354/dao021227.
42. Vasquez, I.; Cao, T.; Hossain, A.; Valderrama, K.; Gnanagobal, H.; Dang, M.; Leeuwis, R. H. J.; Ness, M.; Campbell, B.; Gendron, R.; Kao, K.; Westcott, J.; Gamperl, A. K.; Santander, J. *Aeromonas salmonicida* Infection Kinetics and Protective Immune Response to Vaccination in Sablefish (*Anoplopoma fimbria*). *Fish Shellfish Immunol.* **2020**, *104* (May), 557–566, doi:10.1016/j.fsi.2020.06.005.
 43. Sambrook, J. and Russel, W. *Molecular Cloning: A Laboratory Manual*, 2nd ed.; Cold Spring Harbor Laboratory Press: New York, 2001.
 44. Sakai, M.; Ogasawara, K.; Atsuta, S.; Kobayashi, M. Comparative Sensitivity of Carp, *Cyprinus carpio* L. and Rainbow Trout, *Salmo gairdneri* Richardson, to *Renibacterium salmoninarum*. *J. Fish Dis.* **1989**, *12* (4), 367–372, doi:10.1111/j.1365-2761.1989.tb00325.x.
 45. Sakai, M.; Atsuta, S.; Kobayashi, M. Susceptibility of Five Salmonid Fishes to *Renibacterium salmoninarum*. *Fish Pathol.* **1991**, *26* (3), 159–160, doi:10.3147/jsfp.26.159.
 46. McIntosh, D.; Flano, E.; Grayson, T. H.; Gilpin, M. L.; Austin, B.; Villena, A. J. Production of Putative Virulence Factors by *Renibacterium salmoninarum* Grown in Cell Culture. *Microbiology* **1997**, *143* (10), 3349–3356.
 47. Starliper, E. D. R. S. & T. S. Virulence of *Renibacterium salmoninarum* to Salmonids. **1997**, *9* (1), 37–41, doi:10.1577/1548-8667(1997)009.
 48. Eslamloo, K.; Caballero-Solares, A.; Inkpen, S. M.; Emam, M.; Kumar, S.; Bouniot, C.; Avendaño-Herrera, R.; Jakob, E.; Rise, M. L. Transcriptomic Profiling of the Adaptive and Innate Immune Responses of Atlantic Salmon to *Renibacterium salmoninarum* Infection. *Front. Immunol.* **2020**, *11*, 2487.
 49. Adewoye, S. O.; Ofawole, O. Growth Performance and Survival Rate of *Clarias gariepinus* Fed *Lactobacillus acidophilus* Supplemented Diets. **2013**, *3* (6), 45–50.
 50. U.S Geological Survey; Western Fisheries Research Centre, Seattle, WA, USA. Standard Operating Procedure (SOP): Culture of *Renibacterium salmoninarum* from Tissues and Ovarian Fluid. **2011**, 1–6.
 51. Chandler, D. E.; Roberson, R. W. Bioimaging: Current Concepts in Light and Electron Microscopy. **2009**.
 52. Luna, L. G. *Manual of Histologic Staining Methods of the Armed Forces Institute of Pathology.*, 3rd editio.; McGraw-Hill: New York, 1968.
 53. Bernet, D.; Schmidt, H.; Meier, W.; Burkhardt-Holm, P.; Wahli, T. Histopathology in Fish: Proposal for a Protocol to Assess Aquatic Pollution. *J. Fish Dis.* **1999**, *22* (1), 25–34, doi:10.1046/j.1365-2761.1999.00134.x.
 54. Koressaar, T.; Remm, M. Enhancements and Modifications of Primer Design Program Primer3. *Bioinformatics* **2007**, *23* (10), 1289–1291, doi:10.1093/bioinformatics/btm091.
 55. Untergasser, A.; Cutcutache, I.; Koressaar, T.; Ye, J.; Faircloth, B. C.; Remm, M.; Rozen, S. G. Primer3--New Capabilities and Interfaces. *Nucleic Acids Res.* **2012**, *40* (15), e115, doi:10.1093/nar/gks596.

56. Kõressaar, T.; Lepamets, M.; Kaplinski, L.; Raime, K.; Andreson, R.; Remm, M. Primer3_masker: Integrating Masking of Template Sequence with Primer Design Software. *Bioinformatics* **2018**, *34* (11), 1937–1938, doi:10.1093/bioinformatics/bty036.
57. Pfaffl, M. W. A New Mathematical Model for Relative Quantification in Real-Time RT-PCR. *Nucleic Acids Res.* **2001**, *29* (9), e45, doi:10.1093/nar/29.9.e45.
58. Vandesompele, J.; De Preter, K.; Pattyn, F.; Poppe, B.; Van Roy, N.; De Paepe, A.; Speleman, F. Accurate Normalization of Real-Time Quantitative RT-PCR Data by Geometric Averaging of Multiple Internal Control Genes. *Genome Biol.* **2002**, *3* (7), Research0034.
59. Bustin, S. A.; Benes, V.; Garson, J. A.; Hellemans, J.; Huggett, J.; Kubista, M.; Mueller, R.; Nolan, T.; Pfaffl, M. W.; Shipley, G. L.; Vandesompele, J.; Wittwer, C. T. The MIQE Guidelines: Minimum Information for Publication of Quantitative Real-Time PCR Experiments. *Clin. Chem.* **2009**, *55* (4), 611–622, doi:10.1373/clinchem.2008.112797.
60. Livak, K. J.; Schmittgen, T. D. Analysis of Relative Gene Expression Data Using Real-Time Quantitative PCR and the $2^{-\Delta\Delta CT}$ Method. *Methods* **2001**, doi:10.1006/meth.2001.1262.
61. Riedel, G.; Düker, U.; Fekete-Drimusz, N.; Manns, M.; Vondran, F.; Bock, M. An Extended ΔCT -Method Facilitating Normalisation with Multiple Reference Genes Suited for Quantitative RT-PCR Analyses of Human Hepatocyte-Like Cells. *PLoS One* **2014**, *9*, e93031, doi:10.1371/journal.pone.0093031.
62. Soto-Dávila, M.; Valderrama, K.; Inkpen, S. M.; Hall, J. R.; Rise, M. L.; Santander, J. Effects of Vitamin D2 (Ergocalciferol) and D3 (Cholecalciferol) on Atlantic Salmon (*Salmo salar*) Primary Macrophage Immune Response to *Aeromonas salmonicida* subsp. *salmonicida* Infection. *Front. Immunol.* **2020**, *10* (December 2019), 0–14, doi:10.3389/fimmu.2019.03011.
63. Coady, A. M.; Murray, A. L.; Elliott, D. G.; Rhodes, L. D. Both *msa* Genes in *Renibacterium salmoninarum* Are Needed for Full Virulence in Bacterial Kidney Disease. *Appl. Environ. Microbiol.* **2006**, *72* (4), 2672–2678, doi:10.1128/AEM.72.4.2672-2678.2006.
64. O'Farrell, C. L.; Strom, M. S. Differential Expression of the Virulence-Associated Protein p57 and Characterization of Its Duplicated Gene *msa* in Virulent and Attenuated Strains of *Renibacterium salmoninarum*. *Dis. Aquat. Organ.* **1999**, *38* (2), 115–123, doi:10.3354/dao038115.
65. Rhodes, L. D.; Coady, A. M.; Deinhard, R. K. Identification of a Third *msa* Gene in *Renibacterium salmoninarum* and the Associated Virulence Phenotype. *Appl. Environ. Microbiol.* **2004**, *70* (11), 6488–6494, doi:10.1128/AEM.70.11.6488-6494.2004.
66. Metzger, D. C.; Elliott, D. G.; Wargo, A.; Park, L. K.; Purcell, M. K. Pathological and Immunological Responses Associated with Differential Survival of Chinook Salmon Following *Renibacterium salmoninarum* Challenge. *Dis. Aquat. Organ.* **2010**, *90* (1), 31–41, doi:10.3354/dao02214.
67. Hoffmann, R.; Popp, W.; Van de Graaff, S. Atypical BKD Predominantly and Skin Lesions. *Bull. Eur. Assoc. Fish Pathol.* **1984**, *4* (1), 7–9.

68. Bruno, D. W.; Noguera, P. A.; Poppe, T. T. *A Colour Atlas of Salmonid Diseases*; Springer Netherlands, 2013, doi:10.1007/978-94-007-2010-7.
69. Turaga, P. S. D.; Wiens, G. D.; Kaattari, S. L. Analysis of *Renibacterium salmoninarum* Antigen Production in Situ. *Fish Pathol.* **1987**, 22 (4), 209–214.
70. Turaga, P.; Wiens, G.; Kaattari, S. Bacterial Kidney Disease: The Potential Role of Soluble Protein Antigen(s). *J. Fish Biol.* **1987**, 31 (sa), 191–194, doi:10.1111/j.1095-8649.1987.tb05312.x.
71. Bell, G. R.; Traxler, G. S. Resistance of the Pacific Lamprey, *Lampetra tridentata* (Gairdner), to Challenge by *Renibacterium salmoninarum*, the Causative Agent of Kidney Disease in Salmonids. *J. Fish Dis.* **1986**, 9 (3), 277–279, doi:10.1111/j.1365-2761.1986.tb01014.x.
72. Daly, J. G.; Griffiths, S. G.; Kew, A. K.; Moore, A. R.; Olivier, G. Characterization of Attenuated *Renibacterium salmoninarum* Strains and Their Use as Live Vaccines. *Dis. Aquat. Organ.* **2001**, 44 (2), 121–126, doi:10.3354/dao044121.
73. Withler, R. E.; Evelyn, T. P. T. Genetic Variation in Resistance to Bacterial Kidney Disease within and between Two Strains of Coho Salmon from British Columbia. *Trans. Am. Fish. Soc.* **1990**, 119, 1003–1009, doi:10.1577/1548-8659(1990)119.
74. Becham, T. D.; Evelyn, T. P. T. Population and Genetic Variation in Resistance of Chinook Salmon to Vibriosis, Furunculosis, and Bacterial Kidney Disease. *J. Aquat. Anim. Health* **1992**, 4 (September), 153–167.
75. Gjedrem, T.; Gjøen, H. M. Genetic Variation in Susceptibility of Atlantic Salmon, *Salmo salar* L., to Furunculosis, BKD and Cold Water Vibriosis. *Aquac. Res.* **1995**, 26 (2), 129–134, doi:10.1111/j.1365-2109.1995.tb00892.x.
76. Purcell, M. K.; Hard, J. J.; Neely, K. G.; Park, L. K.; Winton, J. R.; Elliott, D. G. Genetic Variation in Bacterial Kidney Disease (BKD) Susceptibility in Lake Michigan Chinook Salmon and Its Progenitor Population from the Puget Sound. *J. Aquat. Anim. Health* **2014**, 26 (1), 9–18, doi:10.1080/08997659.2013.860061.
77. McIntosh, D.; Austin, B. The Validity of Western Blotting for the Diagnosis of Bacterial Kidney Disease Based on the Detection of the P57 Antigen of *Renibacterium salmoninarum*. *J. Microbiol. Methods* **1996**, 25 (3), 329–335, doi:10.1016/0167-7012(96)00004-8.
78. Elliott, D. G.; Wiens, G. D.; Hammell, K. L.; Rhodes, L. D. Vaccination against Bacterial Kidney Disease. *Fish Vaccin.* **2014**, 9780470674, 255–272, doi:10.1002/9781118806913.ch22.
79. Bruno, D. W. Histopathology of Bacterial Kidney Disease in Laboratory Infected Rainbow Trout, *Salmo gairdneri* Richardson, and Atlantic Salmon, *Salmo salar* L., with Reference to Naturally Infected Fish. *J. Fish Dis.* **1986**, 9 (6), 523–537, doi:10.1111/j.1365-2761.1986.tb01049.x.
80. Flano, E.; Kaattari, S. L.; Razquin, B.; Villena, A. J. Histopathology of the Thymus of Coho Salmon *Oncorhynchus kisutch* Experimentally Infected with *Renibacterium salmoninarum*. *Dis. Aquat. Org.* **1996**, 26 (1), 11–18, doi:10.3354/dao026011.
81. Gutenberger SK, Duimstra JR, Rohovec JS, F. J. Intracellular Survival of *Renibacterium salmoninarum* in Trout Mononuclear Phagocytes. *Dis Aquat Org* **1997**, 28, 93–106.
82. Fredriksen, Å.; Endresen, C.; Wergeland, H. I. Immunosuppressive Effect of a Low

- Molecular Weight Surface Protein from *Renibacterium salmoninarum* on Lymphocytes from Atlantic Salmon (*Salmo salar* L.). *Fish Shellfish Immunol.* **1997**, 7 (4), 273–282, doi:10.1006/fsim.1997.0082.
83. Pietretti, D.; Wiegertjes, G. F. Ligand Specificities of Toll-like Receptors in Fish: Indications from Infection Studies. *Dev. Comp. Immunol.* **2014**, 43 (2), 205–222, doi:10.1016/j.dci.2013.08.010.
 84. Fryer, J. L.; Sanders, J. E. Bacterial Kidney Disease of Salmonid Fish. *Annu. Rev. Microbiol.* **1981**, 35, 273–298, doi:10.1146/annurev.mi.35.100181.001421.
 85. Eslamloo, K.; Kumar, S.; Caballero-Solares, A.; Gnanagobal, H.; Santander, J.; Rise, M. L. Profiling the Transcriptome Response of Atlantic Salmon Head Kidney to Formalin-killed *Renibacterium salmoninarum*. *Fish Shellfish Immunol.* **2020**, 98 (September 2019), 937–949, doi:10.1016/j.fsi.2019.11.057.
 86. Liu, F.; Su, B.; Fu, Q.; Shang, M.; Gao, C.; Tan, F.; Li, C. Identification, Characterization and Expression Analysis of TLR5 in the Mucosal Tissues of Turbot (*Scophthalmus maximus* L.) Following Bacterial Challenge. *Fish Shellfish Immunol.* **2017**, 68, 272–279, doi:10.1016/j.fsi.2017.07.021.
 87. Bethke, J.; Arias-Muñoz, E.; Yáñez, A.; Avendaño-Herrera, R. *Renibacterium salmoninarum* Iron-Acquisition Mechanisms and ASK Cell Line Infection: Virulence and Immune Response. *J. Fish Dis.* **2019**, 42 (9), 1283–1291, doi:10.1111/jfd.13051.
 88. Piazzon, M. C.; Savelkoul, H. F. J.; Pietretti, D.; Wiegertjes, G. F.; Forlenza, M. Carp Il10 Has Anti-Inflammatory Activities on Phagocytes, Promotes Proliferation of Memory T Cells, and Regulates B Cell Differentiation and Antibody Secretion. *J. Immunol.* **2015**, 194 (1), 187–199.
 89. King, A.; Balaji, S.; Le, L. D.; Crombleholme, T. M.; Keswani, S. G. Regenerative Wound Healing: The Role of Interleukin-10. *Adv. Wound Care* **2014**, 3 (4), 315–323, doi:10.1089/wound.2013.0461.
 90. Hong, S.; Zou, J.; Crampe, M.; Peddie, S.; Scapigliati, G.; Bols, N.; Cunningham, C.; Secombes, C. J. The Production and Bioactivity of Rainbow Trout (*Oncorhynchus mykiss*) Recombinant IL-1 β . *Vet. Immunol. Immunopathol.* **2001**, 81 (1–2), 1–14, doi:10.1016/S0165-2427(01)00328-2.
 91. Lu, D. Q.; Bei, J. X.; Feng, L. N.; Zhang, Y.; Liu, X. C.; Wang, L.; Chen, J. L.; Lin, H. R. Interleukin-1 β Gene in Orange-Spotted Grouper, *Epinephelus coioides*: Molecular Cloning, Expression, Biological Activities and Signal Transduction. *Mol. Immunol.* **2008**, 45 (4), 857–867, doi:10.1016/j.molimm.2007.08.009.
 92. Hong, S.; Li, R.; Xu, Q.; Secombes, C. J.; Wang, T. Two Types of TNF- α Exist in Teleost Fish: Phylogeny, Expression, and Bioactivity Analysis of Type-II TNF-A3 in Rainbow Trout *Oncorhynchus mykiss*. *J. Immunol.* **2013**, 191 (12), 5959–5972, doi:10.4049/jimmunol.1301584.
 93. Thorn, C. F.; Whitehead, A. S. Differential Transcription of the Mouse Acute Phase Serum Amyloid A Genes in Response to Pro-inflammatory Cytokines. *Amyloid* **2002**, 9 (4), 229–236, doi:10.3109/13506120209114098.
 94. Bayne, C. J.; Gerwick, L. The Acute Phase Response and Innate Immunity of Fish. *Dev. Comp. Immunol.* **2001**, 25 (8–9), 725–743, doi:10.1016/S0145-305X(01)00033-7.

95. Berliner, J. A.; Navab, M.; Fogelman, A. M.; Frank, J. S.; Demer, L. L.; Edwards, P. A.; Watson, A. D.; Lusis, A. J. Atherosclerosis: Basic Mechanisms. Oxidation, Inflammation, and Genetics. *Circulation* **1995**, *91* (9), 2488–2496, doi:10.1161/01.cir.91.9.2488.
96. Zou, J.; Secombes, C. J. The Function of Fish Cytokines. *Biology (Basel)*. **2016**, *5* (2), doi:10.3390/biology5020023.
97. Zou, J.; Peddie, S.; Scapigliati, G.; Zhang, Y.; Bols, N. C.; Ellis, A. E.; Secombes, C. J. Functional Characterisation of the Recombinant Tumor Necrosis Factors in Rainbow Trout, *Oncorhynchus mykiss*. *Dev. Comp. Immunol.* **2003**, *27* (9), 813–822, doi:10.1016/S0145-305X(03)00077-6.
98. García-Castillo, J.; Chaves-Pozo, E.; Olivares, P.; Pelegrín, P.; Meseguer, J.; Mulero, V. The Tumor Necrosis Factor Alpha of the Bony Fish Seabream Exhibits the *in vivo* Proinflammatory and Proliferative Activities of Its Mammalian Counterparts, yet It Functions in a Species-Specific Manner. *Cell. Mol. Life Sci.* **2004**, *61* (11), 1331–1340, doi:10.1007/s00018-004-4068-1.
99. Grayfer, L.; Walsh, J. G.; Belosevic, M. Characterization and Functional Analysis of Goldfish (*Carassius auratus* L.) Tumor Necrosis Factor-Alpha. *Dev. Comp. Immunol.* **2008**, *32* (5), 532–543, doi:10.1016/j.dci.2007.09.009.
100. Engele, M.; Stöbel, E.; Castiglione, K.; Schwerdtner, N.; Wagner, M.; Bölskei, P.; Röllinghoff, M.; Stenger, S. Induction of TNF in Human Alveolar Macrophages As a Potential Evasion Mechanism of Virulent *Mycobacterium tuberculosis*. *J. Immunol.* **2002**, *168* (3), 1328–1337, doi:10.4049/jimmunol.168.3.1328.
101. Skaar, E. P. The Battle for Iron between Bacterial Pathogens and Their Vertebrate Hosts. *PLoS Pathog.* **2010**, *6* (8), 1–2, doi:10.1371/journal.ppat.1000949.
102. Kaufman, S. H. E. Immunity to Intracellular Bacteria. In *Fundamental immunology*; Paul, W. E., Ed.; Philadelphia, 1999; pp 1335–1371.
103. Valero, Y.; Chaves-Pozo, E.; Meseguer, J.; Esteban, M. A.; Cuesta, A. *Biological Role of Fish Antimicrobial Peptides*; 2013.
104. Winter, G. W.; Schreck, C. B.; McIntyre, J. D. Resistance of Different Stocks and Transferrin Genotypes of Coho Salmon, *Oncorhynchus kisutch*, and Steelhead Trout, *Salmo gairdneri*, to Bacterial Kidney Disease and Vibriosis. *Fish. Bull.* **1980**, *77*, 795–802.
105. Cresswell, P. Assembly, Transport, and Function of MHC Class II Molecules. *Annu. Rev. Immunol.* **1994**, *12* (1), 259–291, doi:10.1146/annurev.iy.12.040194.001355.
106. Rozas-Serri, M.; Lobos, C.; Correa, R.; Ildefonso, R.; Vázquez, J.; Muñoz, A.; Maldonado, L.; Jaramillo, V.; Coñuecar, D.; Oyarzún, C. Atlantic Salmon Pre-Smolt Survivors of *Renibacterium salmoninarum* Infection Show Inhibited Cell-mediated Adaptive Immune Response and a Higher Risk of Death during the Late Stage of Infection at Lower Water Temperatures. *Front. Immunol.* **2020**, *11*, 1378.
107. Evenden, A. J.; Grayson, T. H.; Gilpin, M. L.; Munn, C. B. *Renibacterium salmoninarum* and Bacterial Kidney Disease - the Unfinished Jigsaw. *Annu. Rev. Fish Dis.* **1993**, *3* (C), 87–104, doi:10.1016/0959-8030(93)90030-F.
108. Clay, H.; Volkman, H. E.; Ramakrishnan, L. Tumor Necrosis Factor Signaling Mediates Resistance to Mycobacteria by Inhibiting Bacterial Growth and Macrophage Death. *Immunity* **2008**, *29* (2), 283–294,

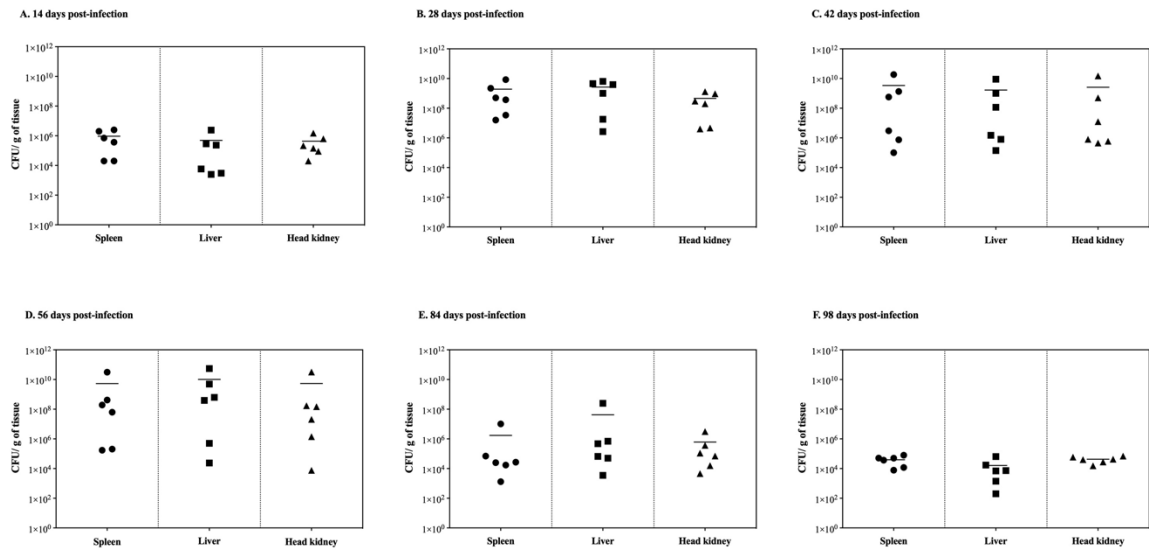
doi:10.1016/j.immuni.2008.06.011.

109. Martin, S. A. M.; Zou, J.; Houlihan, D. F.; Secombes, C. J. Directional Responses Following Recombinant Cytokine Stimulation of Rainbow Trout (*Oncorhynchus mykiss*) RTS-11 Macrophage Cells as Revealed by Transcriptome Profiling. *BMC Genomics* **2007**, *8*, 150, doi:10.1186/1471-2164-8-150.
110. Brynildsrud, O.; Gulla, S.; Feil, E. J.; Nørstebø, S. F.; Rhodes, L. D. Identifying Copy Number Variation of the Dominant Virulence Factors Msa and p22 within Genomes of the Fish Pathogen *Renibacterium salmoninarum*. *Microb. genomics* **2016**, *2* (4), e000055, doi:10.1099/mgen.0.000055.

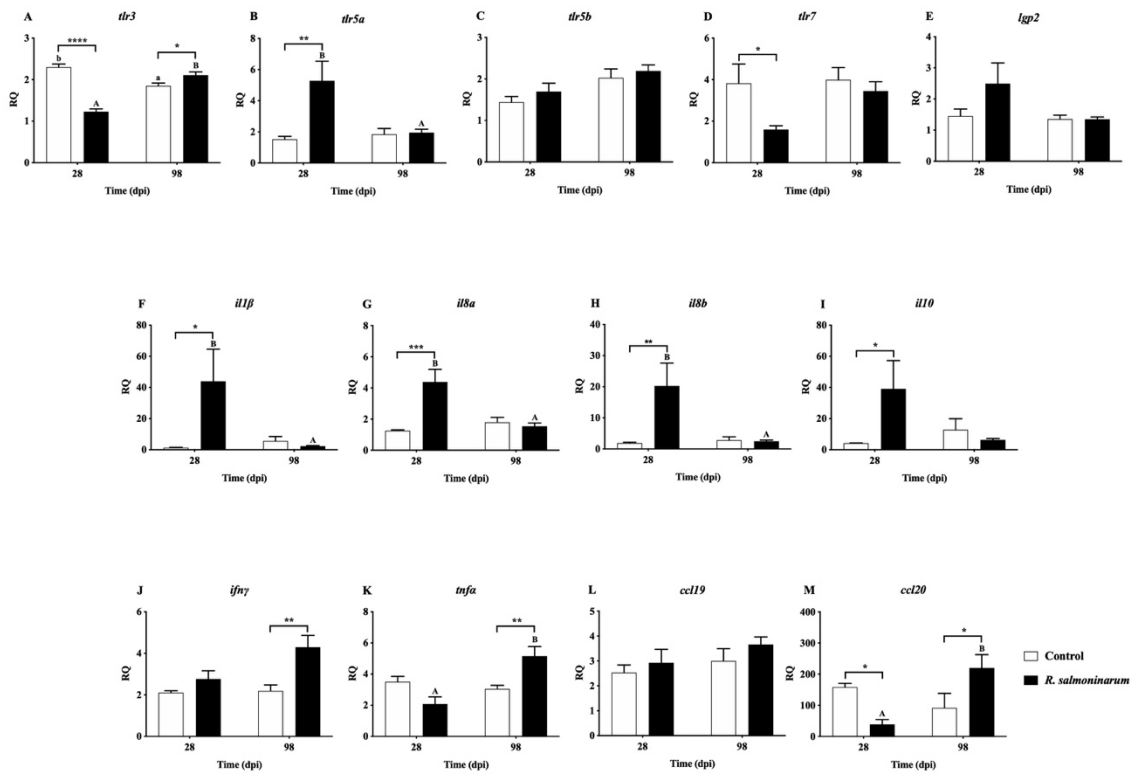
3.8. Supplementary Materials

The following URL leads to Supplementary File 3.1, Supplementary Tables S3.1 and S3.2:

<https://www.frontiersin.org/articles/10.3389/fimmu.2021.733266/full#supplementary-material>

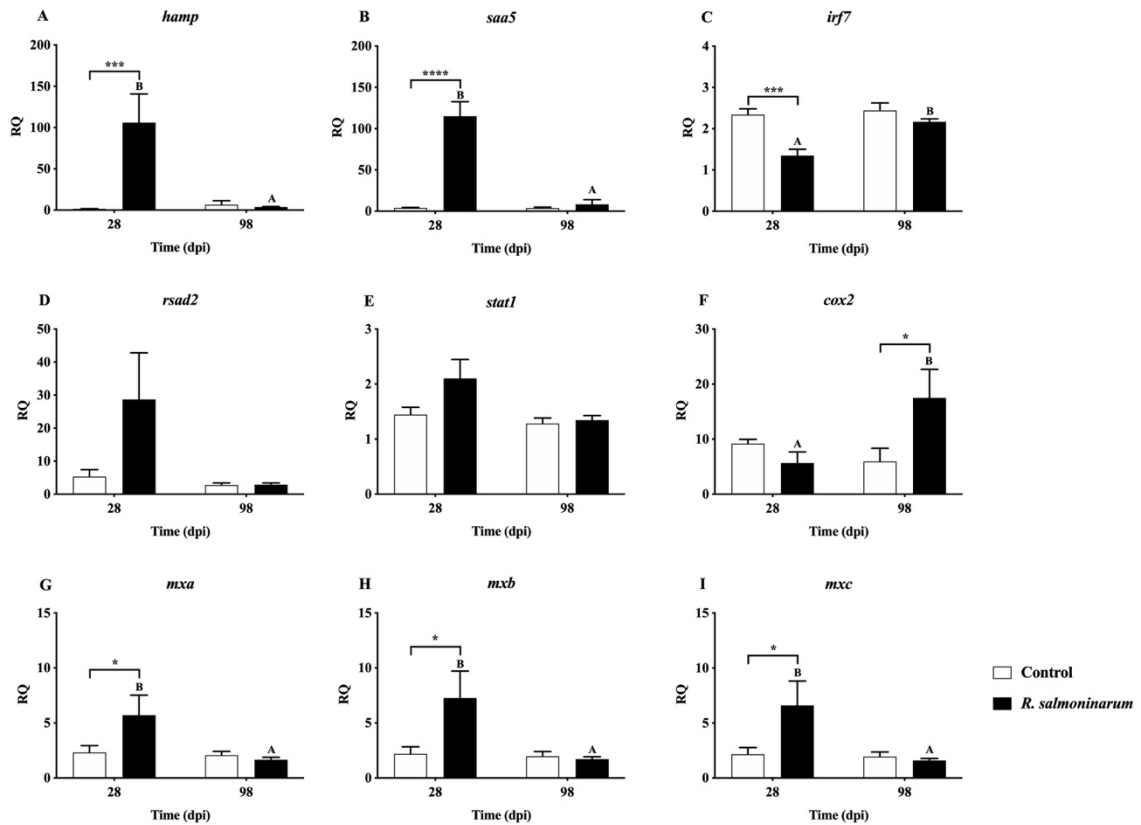


Supplementary Figure S3.1. *R. salmoninarum* colonization in high-dose infected lumpfish ($n = 6$) spleen, liver, and head kidney at **A.** 14, **B.** 28, **C.** 42, **D.** 56, **E.** 84, and **F.** 98 dpi. There were no significant differences in bacterial loads between the 3 tissues at each time point ($p < 0.05$), but differences between individual fishes were significant ($p < 0.05$) at all the time points except at 84 and 98 dpi, as determined by a one-way ANOVA test followed by the Holm-Sidak post hoc test to compare the differences between tissues, and within fish individuals, at a single time point.



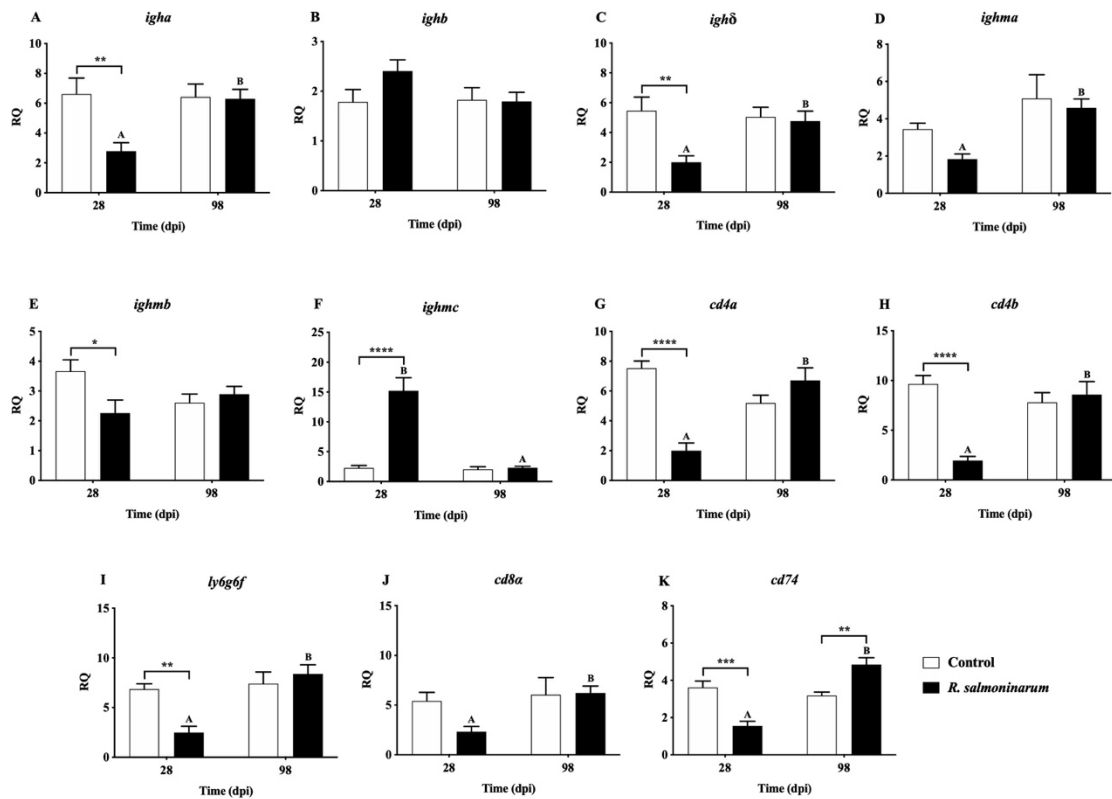
Supplementary Figure S3.2. Expression of transcripts related to pattern recognition (A-E) and cytokines (F-M) in lumpfish head kidney in response to *R. salmoninarum* infection at 28 and 98 dpi. Transcript expression levels in the head kidney from the control (PBS-mock infected group) and infected [high dose (1×10^9 cells dose⁻¹) of *R. salmoninarum*] lumpfish at 28 and 98 dpi were analyzed using qPCR. Transcript levels are presented as relative quantity (RQ) values (i.e., values for the transcript of interest were normalized to both *etif3d* and *pabpc1b* transcript levels and were calibrated to the individual with the lowest normalized expression level of that given transcript). A two-way ANOVA test, followed by the Sidak multiple comparisons post hoc test, was used to identify significant differences between treatments (control and infected groups) at a single time point and for a given treatment at different time points (28 and 98 dpi). Asterisks (*) represent significant differences between treatments at each time point (* $p < 0.05$, ** $p < 0.01$, *** $p < 0.001$,

**** $p < 0.0001$). Different letters represent significant differences between control (lower case) and infected (upper case) groups at 28 compared to 98 dpi. Each value is the mean \pm S.E.M ($n = 6$).



Supplementary Figure S3.3. Expression of transcripts related to the regulation of the innate (A-E) and inflammatory (F-I) immune response in lumpfish head kidney in response to *R. salmoninarum* infection at 28 and 98 dpi. Transcript expression levels in the head kidney from the control (PBS-mock infected group) and infected [high dose (1×10^9 cells dose⁻¹) of *R. salmoninarum*] lumpfish at 28 and 98 dpi were analyzed using qPCR. Transcript levels are presented as relative quantity (RQ) values (i.e., values for the transcript of interest were normalized to both *etif3d* and *pabpc1b* transcript levels and were calibrated to the individual with the lowest normalized expression level of that given transcript). A two-way ANOVA test, followed by the Sidak multiple comparisons post hoc test, was used to identify significant differences between treatments (control and infected groups) at a single time point and for a given treatment at different time points (28 and 98

dpi). Asterisks (*) represent significant differences between treatments at each time point (* $p < 0.05$, *** $p < 0.001$, **** $p < 0.0001$). Different letters represent significant differences between control (lower case) and infected (upper case) groups at 28 compared to 98 dpi. Each value is the mean \pm S.E.M ($n = 6$).



Supplementary Figure S3.4. Expression of transcripts related to humoral (A-F) and cellular mediated (G-K) immunity in lumpfish head kidney in response to *R. salmoninarum* infection at 28 and 98 dpi. Transcript expression levels in the head kidney from the control (PBS-mock infected group) and infected [high dose (1×10^9 cells dose⁻¹) of *R. salmoninarum*] lumpfish at 28 and 98 dpi were analyzed using qPCR. Transcript levels are presented as relative quantity (RQ) values (i.e., values for the transcript of interest were normalized to both *etif3d* and *pabpc1b* transcript levels and were calibrated to the individual with the lowest normalized expression level of that given transcript). A two-way ANOVA test, followed by the Sidak multiple comparisons post hoc test, was used to identify significant differences between treatments (control and infected groups) at a single time point and for a given treatment at different time points (28 and 98 dpi). Asterisks (*)

represent significant differences between treatments at each time point ($*p < 0.05$, $**p < 0.01$, $***p < 0.001$, $****p < 0.0001$). Different letters represent significant differences between control (lower case) and infected (upper case) groups at 28 compared to 98 dpi. Each value is the mean \pm S.E.M ($n = 6$).

Chapter 4. Transcriptome profiling of lumpfish (*Cyclopterus lumpus*) head kidney to *Renibacterium salmoninarum* at early and chronic infection stages

The research described in Chapter 5 was submitted to *Developmental and Comparative Immunology* as: Gnanagobal, H., Chakraborty, S., Vasquez, I., Chukwu-Osazuwa, J., Cao, T., Hossain, A., Dang, M., Valderrama, K., Kumar, S., Bindea, G., Hill, S., Boyce, D., Hall, J., and Santander. J. (2023). Transcriptome profiling of lumpfish (*Cyclopterus lumpus*) head kidney to *Renibacterium salmoninarum* at early and chronic infection stages.

4.1. Abstract

Renibacterium salmoninarum cause Bacterial Kidney Disease (BKD) in several fish species. Atlantic lumpfish, a cleaner fish, is susceptible to *R. salmoninarum*. To profile the transcriptome response of lumpfish to *R. salmoninarum* at early and chronic infection stages, fish were intraperitoneally (i.p.) injected with either a high dose of *R. salmoninarum* (1×10^9 cells dose⁻¹) or PBS (control). Head kidney tissue samples were collected at 28- and 98-days post-infection (dpi) for RNA sequencing. Transcriptomic profiling identified 1971 and 139 differentially expressed genes (DEGs) in infected compared with control samples at 28 and 98 dpi, respectively. At 28 dpi, *R. salmoninarum*-induced genes ($n=434$) mainly involved in innate and adaptive immune response-related pathways, whereas *R. salmoninarum*-suppressed genes ($n=1537$) were largely connected to amino acid metabolism and cellular processes. Cell-mediated immunity-related genes showed dysregulation at 98 dpi. Several immune-signalling pathways were dysregulated in response to *R. salmoninarum*, including apoptosis, alternative complement, JAK-STAT signalling, and MHC-I dependent pathways. In summary, *R. salmoninarum* causes immune suppression at early infection, whereas lumpfish induce a cell-mediated immune response at chronic infection. This study provides a complete depiction of diverse immune mechanisms dysregulated by *R. salmoninarum* in lumpfish and opens new avenues to develop immune prophylactic tools to prevent BKD.

Keywords: Bacterial Kidney Disease, *Renibacterium salmoninarum*, Immune suppressive pathogen, Lumpfish, RNA sequencing

4.2. Introduction

The primary fish health issue plaguing salmon aquaculture is infestation with sea lice (*Lepeophtheirus salmonis*) [1]. The use of cleaner fish is a popular non-chemical and biological sea lice control strategy [2]. Lumpfish (*Cyclopterus lumpus*), a native fish from the North Atlantic, is utilized as an eco-friendly cold-water cleaner fish (i.e., living pest remover) to manage sea lice infestations [3,4]. Lumpfish aquaculture is expanding to meet the industry's growing demands and to achieve self-sufficiency in Norway, the UK, and Atlantic Canada [2]. Due to its endurance in cold water, lumpfish are favored over wrasses (*Labridae* spp.) for biological delousing in Atlantic salmon (*Salmo salar*) farms [4]. Like all fish species, lumpfish encounter health challenges, and bacterial infections are the most common. Among primary pathogens associated with outbreaks in lumpfish, Gram-negatives are the most frequent, including atypical *Aeromonas salmonicida*, *Vibrio anguillarum*, *Pasteurella* sp., *Pseudomonas anguilliseptica*, *Tenacibaculum maritimum*, *Moritella viscosa*, and *Piscirickettsia salmonis* [3].

R. salmoninarum is a Gram-positive, non-motile, facultative intracellular pathogen that causes Bacterial Kidney Disease (BKD) in wild and cultured salmonids in fresh and marine waters across North America, South America, Europe, and Asia [5,6]. *R. salmoninarum* is more persistent in fish populations because of its ability for horizontal and vertical transmission [7]. *R. salmoninarum* has also been found in non-salmonids, including ayu (*Plecoglossus altivelis*), North Pacific hake (*Merluccius productus*), sablefish (*Anoplopoma fimbria*), Pacific herring (*Clupea pallasii pallasii*), sea lamprey (*Petromyzon marinus*) as well as bivalve molluscs [8–11]. While outbreaks of Gram-positive pathogens have not been documented in lumpfish, *R. salmoninarum* has recently been identified as a

pathogen that affects this species [12]. Lumpfish showed susceptibility to *R. salmoninarum*, and fish infected with higher dose (10^9 cells per fish) showed 35% mortality and characteristic clinical signs of BKD, such as hemorrhages around the ventral area, enlargement of the spleen and kidney, an accumulation of turbid fluid in the abdominal cavity, and pseudomembrane formation around the kidney [12]. Since lumpfish is an emerging aquaculture species, sufficient knowledge on its susceptibility and biology, including immune responses or functions, is still lacking [2,3,13].

The teleost immune system is highly diverse but physiologically similar to that of higher vertebrates and employs both innate and adaptive immunity [14,15]. Functional analyses of some lumpfish immune mechanisms, immune cells, and effector molecules have been reported [16,17]. For instance, innate immune processes such as phagocytosis and respiratory burst have been demonstrated to be functional in lumpfish [16]. Additionally, Rønneseth et al. (2015) reported the phagocytic propensity of IgM⁺ B cells, suggesting a crucial role for phagocytic B cells in lumpfish innate immunity [17]. Moreover, lumpfish is able to produce specific antibodies upon immunization, proving the species' adaptive immunity [17]. Previous studies have also revealed lumpfish immune responses to bacterial infections [12,18]. Canonical immune genes related to cytokines (i.e., *il8b*, *il10*, and *ifng*), chemokines (i.e., *ccl19*, *ccl20*), humoral (i.e., *igha*, *ighb*), and adaptive (i.e., *cd8a*, *cd74*) immunity were subtly stimulated in lumpfish larvae in response to oral immunization with bio-encapsulated *V. anguillarum* bacterin through live feed, *Artemia salina* [18]. Moreover, lumpfish significantly upregulated the cell-mediated adaptive immunity (i.e., *cd74*) in response to *R. salmoninarum* during the chronic infection [12].

RNA sequencing (RNA-seq) based fish transcriptomics utilizes high-throughput sequencing methods to provide insights on host-pathogen interactions during the course of infection [19,20]. Understanding the disease and developing effective immune prophylactic measures requires a thorough knowledge of how the host and the pathogen interact [11]. The RNA-seq research on fish immune responses to pathogens not only reveals the host-immune strategies that are triggered against the pathogen but also explains how the pathogen circumvents the host-mediated defense [20]. An RNA-seq-based *de novo* transcriptomics study has characterized the early innate immune responses of lumpfish head kidney leucocytes following *in vitro* exposure to *V. anguillarum* O1 at 6 and 24 hours post-exposure [15]. The complement system and TLR signalling pathway were shown to be the most highly upregulated innate immune responses in lumpfish, and according to differential expression analysis, highly upregulated cytokines were *il1b*, *il6*, *il8*, and *tnfa*. We have already used qPCR to study the immune response of lumpfish to *R. salmoninarum* infection in the head kidney at 28 and 98 dpi and examined the differential expression of 33 immune-relevant transcripts [12]. However, profiling the head kidney transcriptome of lumpfish using RNA-seq would be valuable to further the knowledge of host-pathogen interactions between lumpfish and the Gram-positive *R. salmoninarum* and to depict a comprehensive picture of the fish host's immune pathways involved.

There is a moderate risk of disease transfer from lumpfish to salmon or vice versa during cohabitation as the cleaner fish industry grows and the number of lumpfish interacting closely with salmon rises [21]. Also, lumpfish with a potential pathogen load could serve as an asymptomatic vector and spread disease to the cohabitating salmon [2,12]. *R. salmoninarum* primarily infects salmonids, and the Atlantic salmon head kidney

transcriptome response against live and dead *R. salmoninarum* has been reported using microarray analyses [6,22,23]. In contrast, the lumpfish transcriptome response to a Gram-positive pathogen like *R. salmoninarum* has yet to be documented. Therefore, in the present study, I profiled the lumpfish head kidney transcriptome response to *R. salmoninarum* at early (28 dpi) and chronic (98 dpi) infection stages using reference genome-guided RNA-seq analyses. I aimed to identify and compare the immune pathways differentially regulated in response to *R. salmoninarum* at 28 and 98 dpi, thus developing a better understanding of the genes and the molecular mechanisms associated with the lumpfish response to this pathogen. In addition, to understand the innate and adaptive immunity-related immune functions in lumpfish upon *R. salmoninarum* infection, we examined lysozyme activity and *R. salmoninarum* specific antibody titers in lumpfish serum at 14, 28, 42, 56, and 98 dpi. Overall, the findings of this study provide insights into lumpfish immunity against a Gram-positive pathogen and may serve as baseline knowledge to understand the host-pathogen interactions between lumpfish and *R. salmoninarum*.

4.3. Materials and Methods

4.3.1. *Renibacterium salmoninarum* culture

R. salmoninarum (type strain ATCC 33209) was cultured in 1 L of KDM-2 (1.0% peptone (Difco), 0.05% yeast (Difco), 0.05% L-cysteine HCl (Sigma-Aldrich, St. Louis, MO, USA), 10% fetal bovine serum (Gibco, Thermofisher, Waltham, CA, USA), 1.5% *R. salmoninarum* conditioned metabolite (i.e., nurse medium)) [24] at 15 °C with aeration at 180 rpm for 10-15 days. Bacterial inoculum for infection was prepared and enumerated as previously described [12]. Briefly, *R. salmoninarum* cells grown in KDM-2 were harvested at optical density (O.D. 600 nm) of 0.8 (~1x10⁸ CFU mL⁻¹) and washed with phosphate-

buffered saline (PBS, pH 7.0; 136 mM NaCl, 2.7 mM KCl, 10.1 mM Na₂HPO₄, 1.5 mM KH₂PO₄) [25] by centrifugation (6,000 rpm for 10 min at 4 °C). The bacterial pellet was then resuspended in PBS. Bacterial cells in suspension were quantified using flow cytometry and bacteria counting kit (Invitrogen, Thermofisher Scientific, Eugene, OR, USA) according to the manufacturers' instructions. The final dose for infection was prepared to have a concentration of 1×10⁹ cells dose⁻¹. A relatively high dose was used to ensure mortalities and strong lumpfish immune response to *R. salmoninarum* [12].

4.3.2. Lumpfish

Lumpfish were cultured and maintained at the Joe Brown Aquatic Research Building (JBARB; Ocean Sciences Centre, St. John's, NL, Canada). Lumpfish infection assays were carried out in the aquatic level 3 (AQ3) biocontainment unit at the Cold-Ocean Deep-Sea Research Facility (CDRF; Ocean Sciences Centre, St. John's, NL, Canada) conducted under protocols #18-01-JS, #18-03-JS, and biohazard license L-01. All animal-related procedures in this study were examined and approved by the Memorial University of Newfoundland's (MUN) (<https://www.mun.ca/research/about/acs/acc/>) Institutional Animal Care Committee and the Biosafety Committee in accordance with the guidelines of the Canadian Council on Animal Care (<https://ccac.ca/>).

Two weeks prior to infection, fish were transferred to 500 L tanks (60 fish per tank at a biomass of 25 kg m⁻³) supplied with filtered and UV-treated seawater (33 ppt) at flow-through of 7.5 L min⁻¹ and 95-110% air saturation, for acclimation at 8-10 °C. Fish were fed at 0.5% of their average body weight daily using commercial dry pellets (Skretting - Europa 15; 3-4 mm) and kept under 12 h light: 12 h dark photoperiod during the adaptation and the experimental period.

4.3.3. Infection and sampling

Lumpfish fasted for 24 h before injection and sampling. Each fish was i.p. injected with either 100 µl of 10^9 cells dose⁻¹ *R. salmoninarum* (infected group) or 100 µl of PBS (control group) (Figure 4.1A). Mortalities were recorded daily in the duplicate lumpfish group i.p. injected with the high dose. Mortalities started at 20 dpi, gradually increased, and remained steady after 50 dpi [12]. The cumulative mortality at 98 dpi was 35% (Figure 4.1B). Considering the mortality (Figure 4.1B) and head kidney colonization data from Gnanagobal et al. (2021) [12], we selected 28 and 98 dpi to represent early and chronic infection stages of *R. salmoninarum* in lumpfish, respectively, for sampling and transcriptome analyses. For instance, lumpfish showed mortality and high *R. salmoninarum* loads in the head kidney at 28 dpi. However, at 98 dpi, fish exhibited no mortality and a considerable amount of chronic *R. salmoninarum* loads in the head kidney.

Fish from infected and control tanks ($n = 5$ per tank) were sampled at 1, 14, 28, 42, 56, and 98 dpi. Fish were euthanized with MS222 (400 mg L⁻¹; Syndel Laboratories, Vancouver, BC, Canada). Blood samples (1 mL) were taken from all five fish by puncturing the caudal vein and centrifuged at 10,000 rpm for 5 min at 4 °C to collect serum. The serum samples were stored at -80 °C until lysozyme activity assay and ELISA were performed.

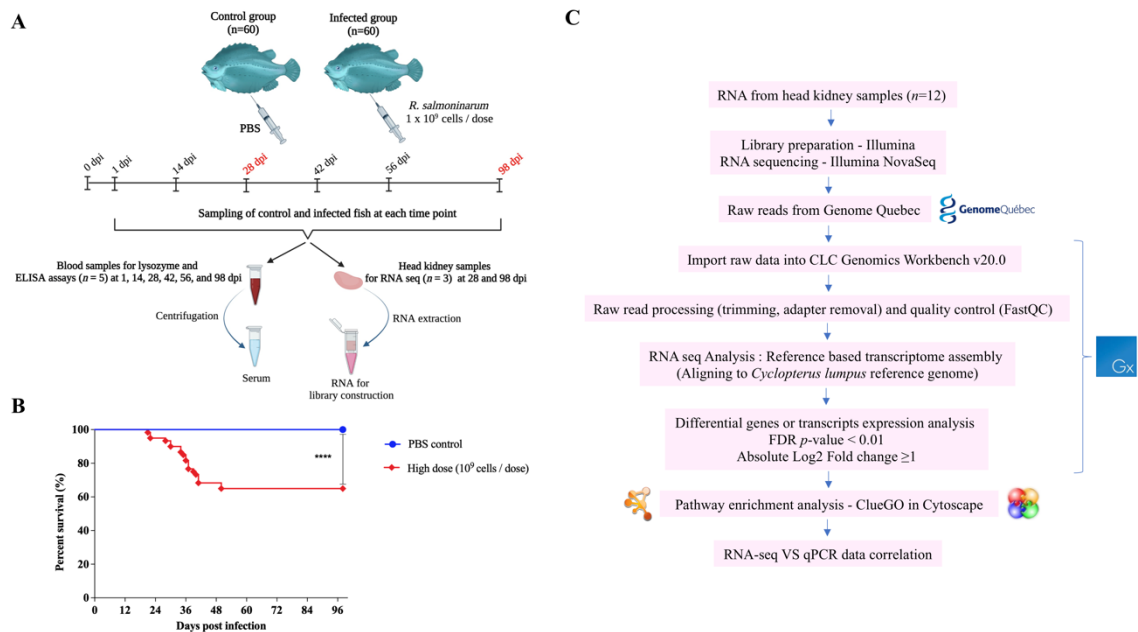


Figure 4.1. Overview of the experimental infection, cumulative mortality and RNA-seq-based transcriptomics. **A.** Experimental design for *R. salmoninarum* infection in lumpfish and sampling. **B.** Cumulative mortality in control and high-dose *R. salmoninarum* infected groups. **C.** RNA-seq-based transcriptomic assembly pipeline used in this study to profile lumpfish head kidney transcriptome.

In order to provide an understanding of the lumpfish head kidney transcriptome response to *R. salmoninarum* at early and chronic infection stages, head kidney samples (~50-100 mg of tissue) were aseptically collected from control ($n = 3$) and infected ($n = 3$) fish at 28 and 98 dpi, placed in a 1.5 mL RNase-free tube, flash-frozen using liquid nitrogen, and kept at -80°C until RNA extraction.

4.3.4. Lumpfish head kidney transcriptome profiling by RNA-sequencing

4.3.4.1. RNA extraction

Total RNA from head kidney samples was extracted using TRIzol reagent (Invitrogen) and purified with the RNeasy MinElute Cleanup Kit (QIAGEN, Mississauga, ON, Canada) following the manufacturer's instructions. Head kidney tissues (80-100 mg) were TRIzol-lysed using RNase-free motorized Pellet Pestle Grinder (Fisherbrand, Fisher Scientific, USA) prior to total RNA extraction. To remove residual genomic DNA, RNA samples were treated with TURBO DNA-free™ Kit (Invitrogen) following the manufacturer's recommendations. Purified RNA samples were quantified using a Genova Nano microvolume spectrophotometer (Jenway, UK) and assessed for integrity by 1% agarose gel electrophoresis. RNA samples used in transcriptome and qPCR analyses of this study showed acceptable integrity (i.e., tight 28S and 18S ribosomal RNA bands at a 2:1 ratio) and purity (i.e., $A_{260}/A_{230} > 1.8$ and $A_{260}/A_{280} > 2.0$).

4.3.4.2. Library preparation and RNA-seq

RNA from head kidney samples of 3 fish in the control group and 3 fish in the *R. salmoninarum* infected group at 28 and 98 dpi were subjected to RNA-seq analyses (i.e., 12 samples in total) (Figures 4.1A, C). RNA quality was determined using a NanoDrop spectrophotometer (Thermo Scientific) and Bioanalyzer 2100 (Agilent), and samples with

an RNA integrity number (RIN) of 8 or above were used to build the libraries (Supplementary Table S4.1). Genome Quebec, QC, Canada constructed cDNA libraries using the NEBNext® Multiplex Oligos for Illumina® and performed paired-end sequencing on an Illumina NovaSeq 6000 platform with 100 bp read length. The current study's RNA-seq raw data are submitted in NCBI Sequence Read Archive (SRA) database under the bioproject accession number PRJNA978536.

4.3.4.3. RNA-Seq data analyses

RNA-seq data were examined in CLC Genomics Workbench v20.0 (CLCGWB; Qiagen, Hilden, Germany) using settings similar to those previously reported [26]. Following the removal of poor-quality reads, clean paired reads were produced. Then, reads comprising adapters were trimmed employing the trim reads tool in CLCGWB. FastQC (<https://www.bioinformatics.babraham.ac.uk/projects/fastqc/>) and multiQC [27] were used for the quality assessment of reads prior to and following trimming, respectively. CLCGWB mapped the trimmed high-quality reads against the lumpfish reference genome (Accession: PRJNA625538) using the RNA-seq analysis program. Gene expression was measured and mapped read counts were normalized using the RESM and eXpress methods [28,29]. After normalization, the counts allocated to each transcript were then used to generate the transcript per million reads (TPM) values using the trimmed mean of M-values (TMM) [30]. Global correlation analysis (e.g., Pearson method) and hierarchical clustering were performed on each gene's log₂-transformed TPM values (x+1) under control and *R. salmoninarum*-infected conditions at 28 and 98 dpi. The differential expression tool in CLCGWB, which is based on a negative binomial general linear model (GLM), was used to analyze differential gene expression of abundance data [31]. Biologically significant

differentially expressed genes (DEGs) were identified using the standard cut-off values of \log_2 fold-change (FC) $\geq |1|$ and false discovery rate (FDR) $p \leq 0.01$ (Supplementary File 4.1A-D).

4.3.4.4. GO (Gene Ontology) enrichment analyses and visualization of GO term networks

To understand the biologically relevant lumpfish immune responses modulated by the Gram-positive pathogen *R. salmoninarum* at early (28 dpi) and chronic (98 dpi) infection stages, selected DEGs from the reference-based transcriptomic assembly were subjected to GO term enrichment analyses using ClueGO (v2.5.9) and CluePedia plugins in Cytoscape (v3.9.0) [32,33]. The ClueGO source file for lumpfish was used [26].

First, to obtain an overall host-centric point of view based on enriched GO terms at each infection stage (i.e., early and chronic), the enrichment (i.e., right-sided hypergeometric test) analysis was performed on lists of DEGs (i.e., 1971 DEGs at 28 dpi and 139 DEGs at 98 dpi) (Supplementary File 4.1C, D) using the Benjamini-Hochberg method for p -value corrections ($p < 0.001$ for 28 dpi and $p < 0.01$ for 98 dpi), kappa-statistics score threshold of 0.5, and medium network specificity in ClueGO.

ClueGO generates networks of terms with related functions by using kappa-statistics to link the enriched Biological Processes (BP) GO terms [34]. The kappa-statistics scores (i.e., kappa-coefficient), which are computed for each term-term association based on the common genes between them, were used to define functional groupings of strongly-linked terms within the GO networks [23,34]. Since the kappa-statistic score cutoff is set at 0.5, term-term relationships with coefficient values below 0.5 were considered non-significant. In addition, a GO term fusion approach was used to combine GO categories, reduce complexity, and build a functionally structured GO cluster network. The GO term

with the lowest p -value was selected as the main term in each functional group for each cluster (represented by different colors). By considering the higher number of DEGs ($n = 1971$) at the early infection stage, a lower p -value (0.001) and the GO term fusion option were used in the enrichment analyses at 28 dpi in order to minimize the complexity of networks and to obtain a clear visualization of enriched terms.

Next, as previously described in Eslamloo et al. (2020) [23] and Xue et al. (2021) [35], the enriched GO terms were classified into five functional themes (i.e., cellular process, localization, and structure; metabolic process; development; immune response; response to stress) using the Gene Ontology Browser (<http://www.informatics.jax.org>) to further analyze the resulting networks at 28 dpi. The GO terms were grouped according to the biological process to which they were related and/or their parent terms.

Third, to explore the immune genes or pathways involved in the lumpfish host immune response against *R. salmoninarum* pathogenesis at the early infection stage (i.e., 28 dpi), the enrichment analysis was carried out on DEG lists (i.e., upregulated ($n = 434$) and downregulated genes ($n = 1537$) at 28 dpi) (Supplementary File 4.1E, F) using a right-sided hypergeometric test with the Benjamini-Hochberg method for p -value corrections ($p < 0.001$), kappa-statistics score cutoff of 0.5, GO term fusion option, and medium network specificity in ClueGO.

4.3.4.5. Correlation between RNA-seq and qPCR data

I previously reported the expression of 30 immune-relevant genes, including pattern recognition receptors, cytokines, innate and inflammatory immune response regulators, and humoral and cell-mediated immunity-related genes using qPCR analyses (Chapter 3) [12]. Since I used the same RNA samples (i.e., 3 fish per time point from the control and infected

groups, Total $n=12$ samples) from my earlier qPCR study for the present RNA-seq, I compared the expression values from the RNA-seq data to the relative quantity (RQ) values obtained from qPCR to validate the results of the RNA-seq analysis. The QuantStudio Real-Time PCR Software-based (version 1.3) (Applied Biosystems) relative quantification study application was used to determine the RQ value of each sample for each gene after normalizing the C_T values to the levels of 2 reference genes (i.e., *pabpc1b* and *eif3d*). A correlation analysis was performed between the normalized counts (TPM+1) of RNA-seq data and the RQ values from qPCR analyses for the same 12 samples for the selected 30 genes. TPMs of RNA-seq data (\log_2 TPM+1 on the X axis) were plotted against RQs from qPCR (\log_2 RQ on the Y axis) on a scatter graph. Pearson correlation coefficients (R^2 ; $p < 0.05$) from simple linear regression analysis were used to compare the correlation between RNA-seq and q-PCR analyses.

4.3.5. Fluorescence-based lysozyme activity assay

Lysozyme levels in lumpfish serum at 1, 14, 28, 42, 56, and 98 dpi were determined using a fluorescence-based lysozyme activity assay kit (Abcam, Waltham, MA, USA) following the manufacturer's instructions. This ultrasensitive assay measures the lysozyme activity by using the ability of lysozyme (Muramidase or N-acetylmuramide glycanhydrolase) [36] to cleave a synthetic substrate (4-Methylumbelliferone: 4-MU) and release a free fluorophore which can be quantified at Excitation/Emission (Ex/Em) of 360/445 nm at 37 °C in a fluorescent microplate reader. The increase in the fluorescence yield is proportional to the amount of active lysozyme in the serum samples.

Standard curve dilutions ranging from 20 to 100 pmol/well in a final volume of 50 μ L were prepared in triplicate using a 10 μ M 4-MU standard. Serum samples were

centrifuged at $12,000 \times g$ for 5 min at 4 °C to discard any debris and diluted 1:10,000 in lysosome assay buffer to fit standard curve readings (i.e., sample readings should not be greater than that of the highest standard and must fall within the standard curve value range). Standards (50 μL), samples (40 μL), sample background controls (40 μL), reagent background control (40 μL), and positive control (40 μL) were randomly added to 96 well opaque white microplates (Falcon™, Fisher Scientific, Ottawa, ON, Canada). For substrate hydrolysis, 10 μL of the lysozyme substrate mix was added to each sample and positive control wells only and thoroughly mixed. Then, the plate was incubated at 37 °C for 60 min in the dark. After incubation, 50 μL of lysozyme stop buffer was added to all wells. The fluorescence was measured immediately on a fluorescent microplate reader (SpectraMax M5 Multi-Mode Microplate Reader, Molecular Devices, Sunnyvale, CA, USA) at Ex/Em of 360/445 nm at 37 °C in endpoint mode with 5 sec of plate shaking before reading.

Corrected fluorescence values were obtained by subtracting the mean fluorescence value of the blank (standard of 0 pmol/well) from standard and sample readings. In addition, sample background readings were also deducted from the sample readings. A standard curve was generated by plotting the readings of the standards ranging from 0 to 100 pmol/well and drawing the line of the best fit. The trend line equation that provided the most accurate fit was calculated in order to get the amount of 4-MU generated during the reaction. For example, the variation in the fluorescence of each sample after deducting blank and sample background control values was applied to the standard curve trend line equation to determine the amount of 4-MU in the sample well. Lysozyme activity (pmol/minute/mL) in each sample was calculated as follows:

$$\text{Lysozyme activity} = \left(\frac{B}{\Delta T \times V} \right) \times D$$

B = Amount of 4-MU in the sample well calculated from the standard curve (pmol); ΔT = Reaction time (min); V = Sample volume per well; D = Sample dilution factor

4.3.6. Indirect Enzyme-Linked Immunosorbent Assay (ELISA)

Indirect ELISA was used to measure the *R. salmoninarum*-specific lumpfish antibody titers at 14, 28, 42, 56, and 98 dpi. Initially, serum samples (5 control and 5 infected fish per time point) were incubated at 56 °C for 30 min in a water bath to inactivate the complement components. Subsequently, 100 μ L of chloroform were added to the heat-treated serum samples and kept for 10 min at room temperature to dissolve fats. Finally, samples were centrifuged at 4,000 \times g for 5 min at room temperature, supernatants were extracted and transferred into clean microfuge tubes. A new checkerboard titration by indirect ELISA method (as described below) was performed to identify the optimal antigen concentration (Formalin-killed *R. salmoninarum* cell antigen) to react with lumpfish serum [37]. The anti-*R. salmoninarum* antibodies in the lumpfish serum were determined using 6 different antigen concentrations (4, 2, 1, 0.5, 0.25, 0.125 μ g/mL) to react with 6 two-fold serial dilutions of a pool of serum from control and *R. salmoninarum* infected lumpfish (1:2 to 1:64). First, microplate wells were coated with different antigen concentrations and incubated overnight at 4 °C. The wells were washed 3 times with PBS-Tween and blocked with 150 μ L of ChonBlock™ for 1 h at 37 °C, washed 3 times, and incubated with different dilutions of control and *R. salmoninarum* infected lumpfish serum in PBS-Tween for 1 h at 37 °C. From the checkerboard titration, 4 μ g/mL was selected as an optimal antigen concentration for the experimental indirect ELISA.

For the experimental indirect ELISA, each well of the 96 well microtiter plates (Corning Costar, Waltham, MA, USA) was coated with 100 μ L (4 μ g/well) of formalin-killed *R. salmoninarum* cell antigen diluted in coating buffer (0.015 mM Na₂CO₃; 0.035 mM NaHCO₃; pH 9.8) and incubated at 4 °C overnight. Unbound antigen in the coated plates was removed by washing the wells 3 times with PBS containing 0.1% Tween-20 (PBS-Tween). To block antigen uncoated sites, 150 μ L of ChonBlock™ blocking buffer (Chondrex Inc, Woodinville, WA, USA) was added to each well and incubated for 1 h at 37 °C. After washing the plate 3 times with PBS-Tween, the wells were incubated with 8 two-fold serial dilutions of control ($n=5$) and *R. salmoninarum* infected ($n=5$) lumpfish serum (1:2 to 1:256 in PBS-Tween) for 1 h at 37 °C and washed 5 times with PBS-Tween. One hundred microliters of anti-lumpfish IgM chicken IgY (secondary antibody) diluted to 1:10,000 in PBS-Tween were subsequently added to all tested wells, incubated for 1 h at 37 °C, and washed 5 times with PBS-Tween. Later, 100 μ L of streptavidin-HRP (Southern Biotech, Birmingham, AL, USA) diluted to 1:10,000 in PBS-Tween was added to each well and incubated for 1 h at 37 °C. After washing 3 times with PBS-Tween at room temperature, 50 μ L of ultra TMB (1-Step™ Ultra TMB-ELISA substrate solution, Thermofisher Scientific, Rockford, IL, USA) was added to the wells, incubated at room temperature for 30 min, and the colorimetric reaction was stopped by adding 50 μ L of 2M H₂SO₄. The O.D. was read at 450 nm on a microplate reader (SpectraMax M5 Multi-Mode Microplate Reader, Molecular Devices, Sunnyvale, CA, USA). To choose the optimal serum dilution cut-off, the highest dilution of the serum, after which the O.D values started to increase with the increasing dilution factor, was taken as the specific antibody titer and normalized to logarithmic base two scale.

4.3.7. Statistical Analysis

Statistical analysis and data visualization were carried out in Prism package v7.0 (GraphPad Software, La Jolla, CA, USA), and a p -value ≤ 0.05 was regarded as statistically significant. Survival rates of control and *R. salmoninarum* infected groups were calculated using the Kaplan-Meier estimator and compared using the Log-rank test. Lysozyme activity and indirect ELISA results were analyzed using a two-way ANOVA test and Sidak multiple comparisons test to determine significant differences between treatments (i.e., control and infected groups) and time points (i.e., 14, 28, 42, 56, 98 dpi). Simple regression analysis was conducted to determine the correlation between TPM and RQ values.

4.4. Results

4.4.1. Global transcriptome profile of lumpfish head kidney at early and chronic *R. salmoninarum* infection stages

To study the lumpfish head kidney response to *R. salmoninarum* at early and chronic infection stages, the global transcriptomic profiles of lumpfish head kidney at 28 and 98 dpi were explored using RNA-seq. Information on RNA-seq data quality and sequencing statistics is provided in Supplementary Tables S4.1, S4.2, and Supplementary Figure S4.1A. Sequencing of RNA extracted from lumpfish head kidney samples of 3 fish in the control group and 3 fish in the *R. salmoninarum* infected group (10^9 cells dose⁻¹) at 28 and 98 dpi ($n = 12$ samples in total) resulted in approximately 223 million Illumina NovaSeq reads. After trimming, the RNA sequencing reads were subjected to reference-based transcriptome assembly analysis (Figure 4.1C).

Global correlation analyses showed a high degree of expression correlation under different experimental conditions, for instance, R^2 of 0.95 and 0.97 ($p < 0.0001$) were

observed between control and *R. salmoninarum* infected fish groups at 28 and 98 dpi, respectively (Supplementary Figures S4.1B, C). Principal component analysis (PCA) and hierarchical clustering analyses (i.e., heat map) showed clear differences between control and infected samples at 28 dpi (Figures 4.2A, C). Contrarily, despite the fact that the control and infected samples were segregated at 98 dpi, their clusters in the PCA had a minor overlap, which also matched the heat map (Figures 4.2B, D). The $\log_2 FC \geq |1|$ and $FDR p \leq 0.01$ were set as cut-off criteria to identify significant DEGs. The transcriptome dysregulations in the lumpfish head kidney were stronger and more extensive at 28 dpi (Figure 4.2E) compared to 98 dpi (Figure 4.2F).

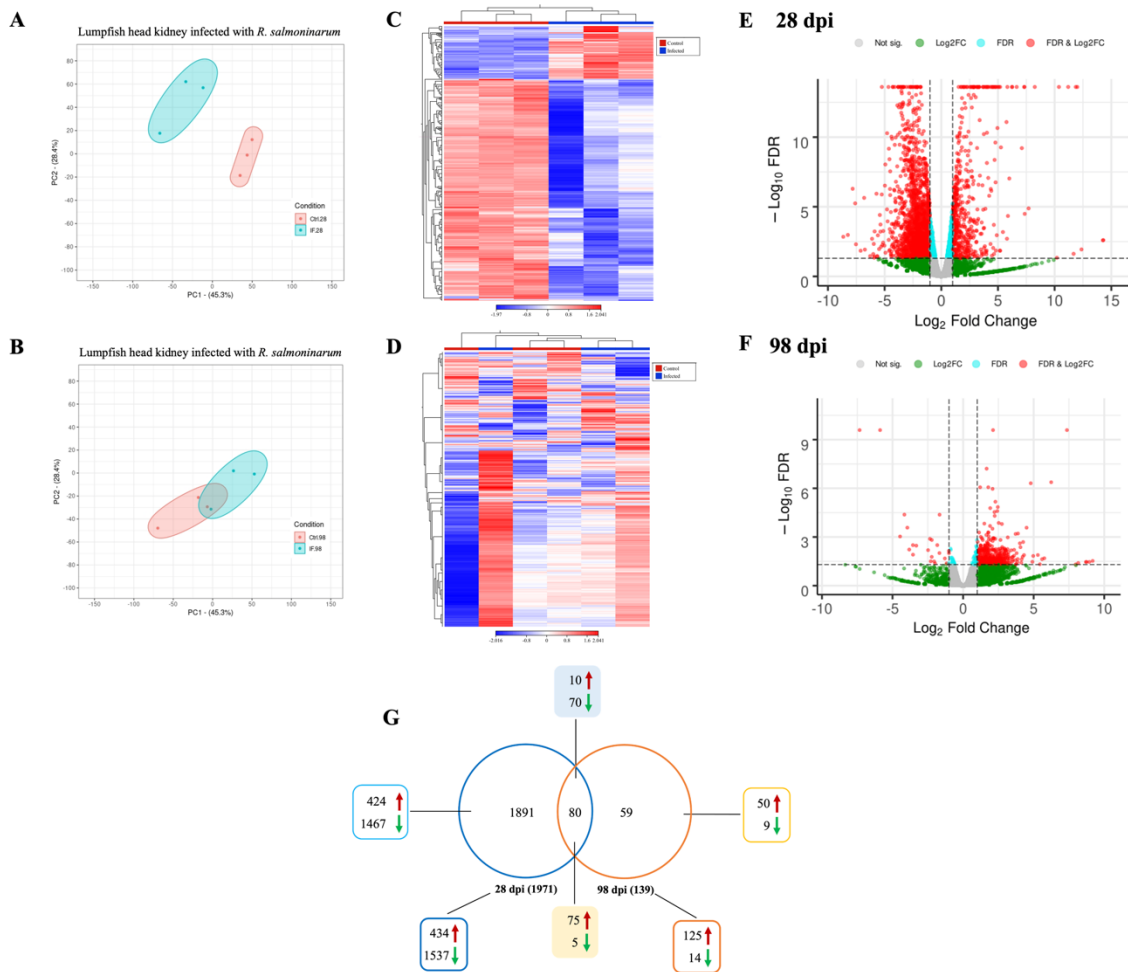


Figure 4.2. Global transcriptomic profiling of the lumpfish head kidney response to *R. salmoninarum* at early (28 dpi) and chronic (98 dpi) infection stages by RNA-seq. A total of 12 RNA libraries comprised of 3 biological replicates for 2 different conditions (control and *R. salmoninarum* infected head kidney samples at 28 and 98 dpi) were included in the RNA-seq analyses. Principal component analysis (PCA) of control (Ctrl) and *R. salmoninarum* infected (IF) head kidney samples at **A.** 28 dpi and **B.** 98 dpi. Hierarchical clustering of differentially expressed genes (DEGs); color bars below the horizontal cluster indicate control (red) and *R. salmoninarum* infected head kidney samples (blue) at **C.** 28

dpi and **D.** 98 dpi. Volcano plots of DEGs at **E.** 28 dpi and **F.** 98 dpi. Red dots indicate significant DEGs. **G.** Venn Diagram (Genes) showing an overview of RNA-seq results between early (28 dpi) and chronic infection (98 dpi) stages. Blue and orange circles represent 28 and 98 dpi, respectively, whereas red and green arrows indicate up- and down-regulated genes, respectively.

In agreement with this, the number of statistically significant DEGs in the lumpfish head kidney at 28 dpi (1971) was higher compared to 98 dpi (139) (Figure 4.2G). Among 1971 DEGs at 28 dpi, 434 genes were upregulated, and 1537 genes were downregulated. On the other hand, total DEGs at 98 dpi included 125 upregulated and 14 downregulated genes. As shown in the Venn diagram, there were 80 genes (10 up- and 70 down-regulated at 28 dpi, 75 up- and 5 down-regulated at 98 dpi) overlapping between gene lists at both time points 28 and 98 dpi (Figure 4.2G). Gene identifier, description, fold change, and FDR p -value at 28 and 98 dpi were listed in Supplementary File 4.1A-N.

4.4.2. Pathway enrichment analyses

To study host molecular pathways regulated by *R. salmoninarum* infection, I used ClueGO and identified the enriched GO terms related to biological processes (BP), molecular functions (MF), and cellular components (CC) of significant *R. salmoninarum*-responsive DEGs lists in lumpfish head kidney at 28 and 98 dpi.

First, I tested the BPs, MFs, and CCs over-represented in the total up- and down-regulated lists of DEGs at 28 ($n = 1971$) and 98 ($n = 139$) dpi (Supplementary File 4.1C, D) to obtain an overall host-centric point of view. The enriched GO terms identified herein for 28 dpi were further classified into functional themes using Gene Ontology Browser. For instance, we identified 167 GO terms enriched ($p < 0.001$) in *R. salmoninarum*-responsive genes in the lumpfish head kidney at 28 dpi (Figure 4.3A; Supplementary Table S4.3). These enriched GO terms were associated with cellular process, localization, and structure (63%), metabolic process (25%), immune response (7%), response to stress (3%), and development (2%) (Figure 4.3A). When examining BPs, MFs, and CCs over-represented in the total up- and down-regulated lists of DEGs ($n=139$) in the lumpfish head kidney at

98 dpi (Supplementary File 4.1D), we found only 21 GO terms enriched ($p < 0.01$) in *R. salmoninarum*-responsive genes (Figure 4.3B; Supplemental Table S4.4). Chronic infection with *R. salmoninarum* in lumpfish at 98 dpi triggered dysregulation of several BPs relevant to adaptive immunity. This involved immune response to tumor cells and its regulation (e.g., T cell-mediated cytotoxicity directed against tumor cell target, T cell-mediated immune response to tumor cell), and antigen presentation process (e.g., antigen processing and presentation of peptide antigen via MHC class I). In addition, other BPs enriched in the lumpfish head kidney at 98 dpi were involved in antioxidant activity (e.g., glutathione peroxidase activity), osmoregulation (e.g., regulation of water loss via skin), and organic substance metabolic process (e.g., glutathione metabolic process). The enriched GO terms associated with MFs at 98 dpi were related to transferase activity (e.g., glutathione transferase activity), protein or protein-containing complex binding (e.g., beta-2-microglobulin binding, T cell receptor binding), and oxidoreductase activity (e.g., oxidoreductase activity - acting on peroxide as acceptor). Finally, the GO term MHC class I protein complex, which is associated with CC, was enriched at 98 dpi.

Figure 4.3. Global view of ClueGO-based gene ontology enrichment networks in lumpfish head kidney at **A.** 28 and **B.** 98 dpi. The enrichment (i.e., right-sided hypergeometric test) analysis was performed on lists of DEGs (i.e., 1971 DEGs at 28 dpi and 139 DEGs at 98 dpi) that contain total up- and down-regulated genes using Benjamini-Hochberg method for p -value corrections ($p < 0.001$ for 28 dpi and $p < 0.01$ for 98 dpi), kappa-statistics score threshold of 0.5, and medium network specificity in ClueGO. A significantly enriched Gene Ontology (i.e., GO) is represented by each node. The functional groups and processes that share similar genes are visualized using the node color regime. Each functional group's most significantly enriched terms are denoted by a summary label (i.e., the leading GO term based on the highest significance is represented using a name label). The GO term shapes, ellipse, rounded rectangle, and octagon represent biological processes (BPs), molecular functions (MFs), and cellular components (CCs), respectively. The shape size corresponds to the significance of the GO term or enriched pathway. For instance, the larger the size of the shapes, the higher the significance. The complete lists of GO terms and statistics (over-represented BPs, MFs, and CCs) are tabulated in Supplementary Tables S4.3 and S4.4.

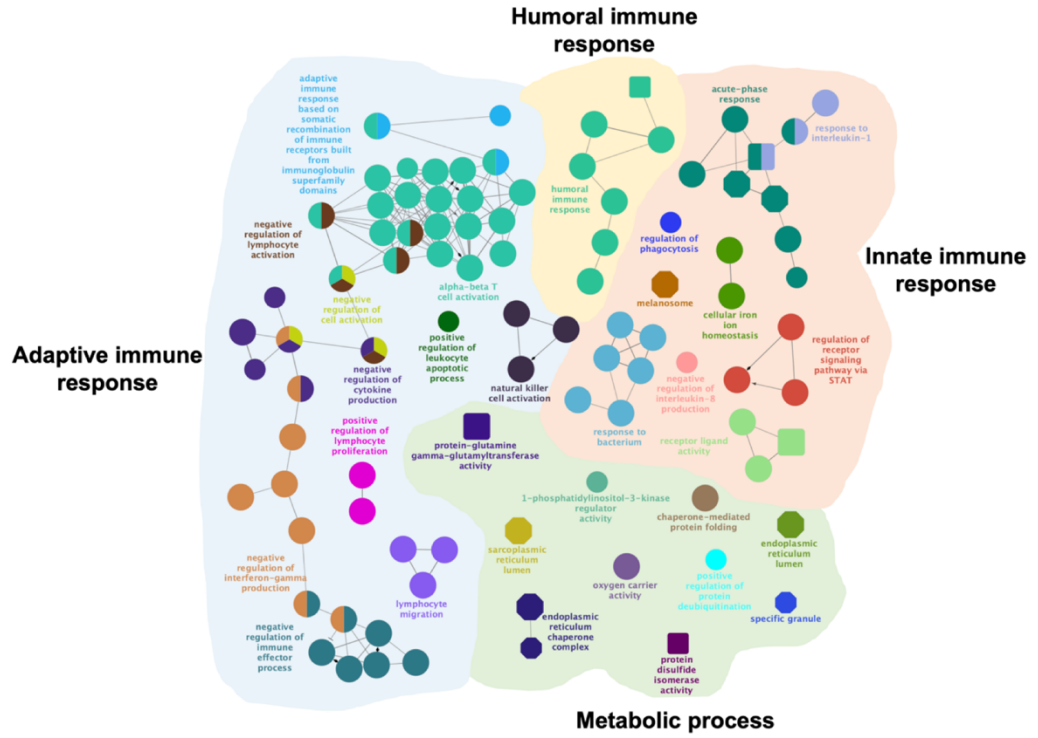
Second, I examined the BPs, MFs, and CCs over-represented in individual up- ($n=434$; Supplementary File 4.1E) and down-regulated ($n=1537$; Supplementary File 4.1F) DEG lists at 28 dpi to investigate specific immune pathways or genes involved in the lumpfish immune response against *R. salmoninarum* pathogenesis. Here, 93 and 160 GO terms were enriched ($p<0.001$) in the individual up- (Figure 4.4A; Supplementary Table S4.5) and down-regulated (Figure 4.4B; Supplementary Table S4.6) genes list, respectively, at 28 dpi.

Among the upregulated genes at 28 dpi, GO terms associated with several innate and adaptive immune processes were enriched (Figure 4.4A; Supplementary Table S4.5). A large number of BPs associated with the innate immune response (e.g., acute phase response, cytokine, and chemokine activity, complement activation, response to interleukin (IL)-1, defense response to bacterium) and regulation of immune response (e.g., negative regulation of IL-8 production, cellular iron ion homeostasis, regulation of nitric-oxide biosynthesis, regulation of phagocytosis, regulation of tumor necrosis factor superfamily cytokine production) were activated (Supplementary Table S4.5). The BPs enriched that were linked to the adaptive immune response include lymphocyte activation / differentiation / migration (e.g., natural killer cell activation and differentiation, negative regulation of T cell differentiation, CD4⁺, α - β T cell activation and differentiation involved in immune response and its positive regulation, lymphocyte chemotaxis, negative regulation of lymphocyte activation involved in immune response, negative regulation of leucocyte differentiation, mononuclear cell migration), adaptive immunity-related cytokine responses (e.g., negative regulation of interferon-gamma (IFN- γ) production, negative regulation of IL-6 production), B-cell, (e.g., antimicrobial humoral immune response,

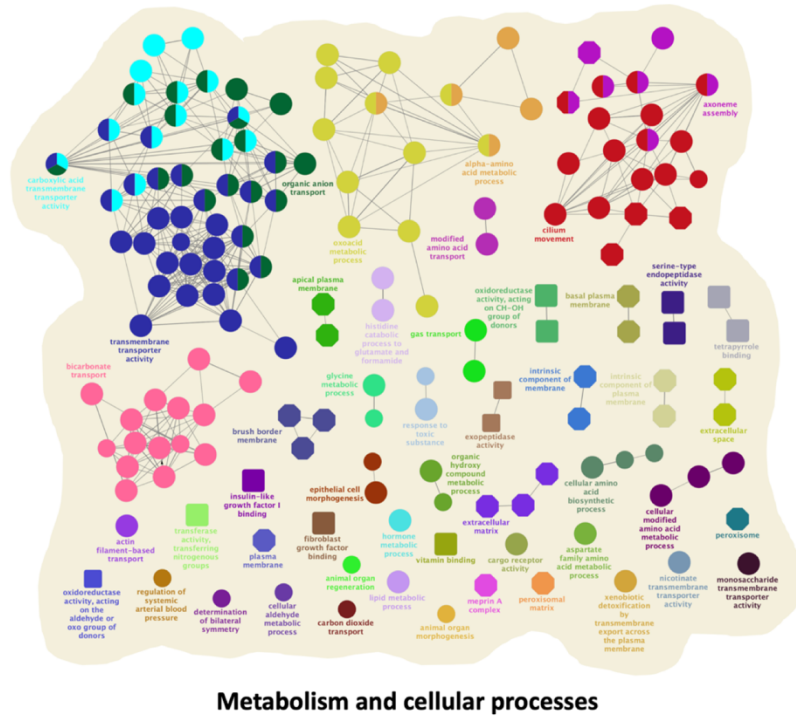
immunoglobulin (Ig) production and its regulation, positive regulation of B-cell proliferation, Ig-mediated immune response) and T-cell mediated (e.g., T-helper 1 type immune response, T-helper 17 type immune response, positive regulation of T cell proliferation) adaptive immune responses. Furthermore, I identified induction of immune pathways linked to complement activation (e.g., alternative pathway), cell death (e.g., positive regulation of leukocyte apoptotic process), and Janus kinase (JAK)-Signal transducer and activator of transcription (STAT) signalling (e.g., positive regulation of receptor signaling pathway via STAT, 1-phosphatidylinositol-3-kinase regulator activity) in response to *R. salmoninarum* infection at 28 dpi (Supplementary Table S4.5).

On the other hand, most of the BPs that were found to be enriched in the downregulated genes list at 28 dpi (Figure 4.4B; Supplementary Table S4.6) were associated with metabolism and cellular processes, particularly related to the amino acid metabolism (e.g., histidine catabolic process to glutamate and formamide / formate, the metabolic process of amino acid betaine / carnitine / glutamate / glycine / dicarboxylic acid / serine family amino acid / glutamine family amino acid / aspartate family amino acid / cellular aldehyde / cellular amino acid / cellular modified amino acid, the catabolic process of cellular amino acid / sulfur amino acid / alpha-amino acid / carboxylic acid, the biosynthetic process of cellular amino acid / alpha-amino acid).

A



B



Gene ontology: Biological Process Molecular function Cellular component

Node size significance: $p < 0.001$

Figure 4.4. ClueGO-based enriched gene ontology terms of all **A.** upregulated and **B.** downregulated genes in lumpfish head kidney at 28 dpi. The enrichment analysis was carried out on DEG lists (i.e., upregulated ($n = 434$) and downregulated genes ($n = 1537$) at 28 dpi) using a right-sided hypergeometric test with the Benjamini-Hochberg method for p -value corrections ($p < 0.001$), kappa-statistics score cutoff of 0.5, GO term fusion option, and medium network specificity in ClueGO. A significantly enriched Gene Ontology (i.e., GO) is represented by each node. The functional groups and processes that share similar genes are visualized using the node color regime. Each functional group's most significantly enriched terms are denoted by a summary label (i.e., the leading GO term based on the highest significance is represented using a name label). The GO term shapes, ellipse, rounded rectangle, and octagon represent biological processes (BPs), molecular functions (MFs), and cellular components (CCs), respectively. The significance of the GO term or enriched pathway is expressed by the size of the GO term shapes (i.e., the larger the size of the shapes, the higher the significance). The complete lists of GO terms and statistics (over-represented BPs, MFs, and CCs) are tabulated in Supplementary Tables S4.5 and S4.6.

Overall, in the lumpfish head kidney at the early infection stage (28 dpi), *R. salmoninarum*-induced (i.e., upregulated) genes were mainly involved in innate and adaptive immune response-related pathways, whereas *R. salmoninarum*-suppressed (i.e., downregulated) genes were largely connected to amino acid metabolism, cellular and developmental processes. On the other hand, *R. salmoninarum* dysregulated the genes involved in T-cell mediated cytotoxicity and MHC-I pathway in lumpfish head kidney at the chronic infection stage (98 dpi).

4.4.3. DEGs associated with the enriched GO terms of interest at 28 and 98 dpi

To generally understand the molecular pathways regulated by *R. salmoninarum* infection at the gene level, selected DEGs associated with enriched GO terms of interest from ClueGO analyses at 28 and 98 dpi are tabulated in Table 4.1.

In the enriched term “response to bacterium” at 28 dpi, *R. salmoninarum* infection upregulated pattern recognition receptors (PRR), including *toll-like receptor 5 (tlr5)*, *peptidoglycan recognition protein 6 (pglyrp6)*, and *C-type lectin domain family 4 member E (si:ch73-86n18.1)*. Interestingly, a mitogen-activated protein kinase (MAPK) or extracellular signal-regulated kinase (ERK) that mediate intracellular signalling, *MAP-kinase-activated protein kinase 3 (mapkapk3)* was upregulated, in contrast, a *regulator of G-protein signalling 3 isoform XI (si:ch211-152p11.4)*, which is a GTPase-activating protein that inhibits G-protein-mediated signal transduction, was downregulated. Moreover, *R. salmoninarum* downregulated the expression of *innate immunity activator protein (inavaa)*, which is crucial for PRR-induced signalling, cytokine release, and bacterial clearance.

Genes associated with cytokines or chemokines activity that were upregulated by *R. salmoninarum* infection in lumpfish head kidney at 28 dpi (Table 4.1; Supplementary Table S4.5) include *interleukin-1 beta-like* (*LOC117736885*), *interleukin-8 isoform X1* (*cxcl8a*), *interleukin-10* (*il10*), *C-X-C motif chemokine 19* (*cxcl19*), *C-C motif chemokine 13-like* (*LOC117736467*), and *IL-6 subfamily cytokine M17* (*m17*). *R. salmoninarum* was also found to induce the expression of genes involved in acute phase response [i.e., *amyloid protein A-like* (*LOC117728776*)], iron homeostasis [i.e., *hepcidin-1* (*hamp1*), *hemopexin b* (*hpxb*), *transferrin receptor 1b* (*tfr1b*)], complement activation - alternative pathway [i.e., *complement component C7* (*c7b*), *complement factor H-like* (*LOC117729317*), *complement component C6* (*c6*), *complement C3-like* (*LOC117745115*)], regulators of apoptosis and NFkB (nuclear factor kappa light chain enhancer of activated B cells) activation [i.e., *cell death-inducing p53-target protein 1 homolog* (*LOC117734930*), *caspase recruitment domain-containing protein 9* (*card9*), *B-cell lymphoma 3 protein homolog isoform X1* (*bcl3*)] and JAK-STAT signalling pathway [i.e., *interleukin-6-like* (*LOC117739248*), *interleukin-10 receptor subunit beta-like* (*LOC117750018*), *suppressor of cytokine signaling 3a* (*socs3a*), *cytokine-inducible SH2-containing protein* (*cish*)] in lumpfish at 28 dpi (Table 4.1).

Among the enriched GO terms associated with humoral and cell-mediated adaptive immunity at 28 dpi (Table 4.1; Supplementary Table S4.5), the genes play putative roles in the negative regulation of production of molecular mediators of immune response [e.g., *B-cell receptor CD22-like isoform X2* (*LOC117732554*)], negative regulation of T cell activation/differentiation [e.g., *cytotoxic T-lymphocyte protein 4-like* (*LOC117750771*)], regulation of immunoglobulin production [e.g., *sialic acid-binding Ig-like lectin 10 isoform*

X1 (LOC117727997)], regulation of phagocytosis [e.g., *tyrosine-protein kinase Mer isoform X2 (mertka)*], T-helper 1 type immune response [e.g., *interleukin-27 subunit beta (ebi3)*], and MHC-1 mediated antigen processing and presentation [e.g., *antigen peptide transporter 2a (tap2a)*] showed upregulation in response to *R. salmoninarum*. Further, *R. salmoninarum* caused the downregulation of many genes involved in amino acid metabolism (biosynthesis/degradation) (Table 4.1; Supplementary Table S4.6).

Compared to 28 dpi, where a larger number of genes and pathways were dysregulated, only a lesser number of genes and pathways were dysregulated at 98 dpi (Table 4.1; Supplementary Table S4.4). For instance, *R. salmoninarum* chronic infection upregulated genes involved in T-cell mediated cytotoxicity and MHC-1 pathway [e.g., *major histocompatibility complex class I-related gene protein-like isoform X2 (LOC117738775)*, *H-2 class I histocompatibility antigen, Q9 alpha chain-like (LOC117739375)*] in lumpfish head kidney at 98 dpi.

Table 4.1. Selected DEGs associated with enriched pathways of interest from ClueGO analyses at 28 and 98 dpi

Enriched pathway of interest	Gene Symbol	Log ₂ Fold change	FDR p-value	Putative protein product
28 dpi				
Response to bacterium	<i>tlr5</i>	2.40	4.2×10 ⁻⁶	Toll-like receptor 5
	<i>pglyrp6</i>	6.65	0	Peptidoglycan recognition protein 6
	<i>si:ch73-86n18.1</i>	1.45	6.3×10 ⁻⁷	C-type lectin domain family 4 member E
	<i>mapkapk3</i>	1.24	1.3×10 ⁻⁵	MAP kinase-activated protein kinase 3
	<i>si:ch211-152p11.4</i>	-2.06	5.0×10 ⁻⁴	Regulator of G-protein signaling 3 isoform X1
	<i>inavaa</i>	-2.17	8.9×10 ⁻⁴	Innate immunity activator protein
Cytokine / Chemokine activity	<i>LOC117736885</i>	6.24	0	Interleukin-1 beta-like
	<i>cxcl8a</i>	4.75	0	Interleukin-8 isoform X1
	<i>tnfsf12</i>	-2.47	1.7×10 ⁻¹²	Tumor necrosis factor ligand superfamily member 12
	<i>il10</i>	4.03	4.8×10 ⁻¹¹	Interleukin-10
	<i>LOC117727469</i>	-1.90	9.9×10 ⁻⁶	C-C motif chemokine 4-like
	<i>cxcl19</i>	1.72	5.6×10 ⁻⁵	C-X-C motif chemokine 19
	<i>LOC117736467</i>	2.95	1.4×10 ⁻⁴	C-C motif chemokine 13-like
	<i>m17</i>	1.84	2.6×10 ⁻⁴	IL-6 subfamily cytokine M17
Acute phase response	<i>LOC117728776</i>	14.26	2.6×10 ⁻³	Amyloid protein A-like
Cellular iron homeostasis	<i>LOC117728128</i>	11.99	0	Hepcidin-like
	<i>hamp</i>	7.32	0	Hepcidin-1
	<i>hpxb</i>	3.16	6.1×10 ⁻¹⁰	Hemopexin
	<i>tfr1b</i>	1.30	1.2×10 ⁻⁶	Transferrin receptor 1b
Complement activation, alternative pathway	<i>c7b</i>	4.52	0	Complement component C7
	<i>LOC117729317</i>	4.46	0	Complement factor H-like
	<i>LOC117742524</i>	4.02	7.2×10 ⁻⁹	Complement factor B-like
	<i>c6</i>	3.37	0	Complement component C6
	<i>LOC117745115</i>	2.43	8.6×10 ⁻³	Complement C3-like

Apoptosis	<i>card9</i>	1.08	6.0×10^{-6}	Caspase recruitment domain-containing protein 9
	<i>LOC117734930</i>	2.25	0	Cell death-inducing p53-target protein 1 homolog
	<i>bcl3</i>	1.61	3.7×10^{-8}	B-cell lymphoma 3 protein homolog isoform X1
Humoral and cell immunity	<i>LOC117732554</i>	1.04	3.0×10^{-3}	B-cell receptor CD22-like isoform X2
	<i>LOC117750771 / ctla4</i>	2.44	2.4×10^{-3}	Cytotoxic T-lymphocyte protein 4-like
	<i>LOC117727997 / siglec10</i>	1.29	6.8×10^{-6}	Sialic acid-binding Ig-like lectin 10 isoform X1
	<i>LOC117739425</i>	5.09	0	Tumor necrosis factor receptor superfamily member 6B-like
	<i>tnfaip3</i>	1.08	5.8×10^{-5}	Tumor necrosis factor alpha-induced protein 3 isoform X1
	<i>mertka</i>	1.42	1.1×10^{-10}	Tyrosine-protein kinase Mer isoform X2
	<i>ebi3</i>	1.97	1.8×10^{-4}	Interleukin-27 subunit beta
JAK-STAT signalling pathway	<i>tap2a</i>	1.27	9.0×10^{-6}	Antigen peptide transporter 2a
	<i>LOC117739248 / il6</i>	4.70	4.3×10^{-9}	Interleukin-6-like
	<i>LOC117750018 / il10rb</i>	1.18	7.4×10^{-7}	Interleukin-10 receptor subunit beta-like
	<i>socs3a</i>	3.96	0	Suppressor of cytokine signaling 3a
Amino acid metabolism	<i>cish</i>	3.92	0	Cytokine-inducible SH2-containing protein
	<i>hal</i>	-2.55	1.2×10^{-8}	Histidine ammonia-lyase
	<i>LOC117740696</i>	-5.88	5.9×10^{-4}	Betaine--homocysteine S-methyltransferase 1-like
	<i>adhfe1</i>	-2.23	9.3×10^{-14}	Hydroxyacid-oxoacid transhydrogenase, mitochondrial
	<i>gcshb</i>	-3.38	3.2×10^{-13}	Glycine cleavage system protein H (aminomethyl carrier), b
	<i>agxtb</i>	-2.61	8.8×10^{-8}	Alanine--glyoxylate and serine--pyruvate aminotransferase b
	<i>LOC117727751</i>	-3.13	8.7×10^{-4}	Rho GTPase-activating protein 11A-like
	<i>LOC117733571</i>	-4.10	0	Serine hydroxymethyltransferase, mitochondrial-like isoform X1
	<i>ddo</i>	-2.91	6.2×10^{-10}	D-aspartate oxidase
T cell-mediated immunity / MHC-class I	<i>got1</i>	-2.50	2.1×10^{-8}	Aspartate aminotransferase, cytoplasmic
	<i>gls2b</i>	-2.16	2.0×10^{-6}	Glutaminase 2b isoform X2
	98 dpi			
T cell-mediated immunity / MHC-class I	<i>LOC117738775</i>	2.29	6.7×10^{-6}	Major histocompatibility complex class I-related gene protein-like isoform X2
	<i>LOC117739375</i>	2.52	1.4×10^{-4}	H-2 class I histocompatibility antigen, Q9 alpha chain-like

	<i>LOC117725889</i>	1.92	1.7×10^{-5}	Microsomal glutathione S-transferase 1-like
Glutathione peroxidase activity	<i>gpx3</i>	1.32	7.0×10^{-3}	Glutathione peroxidase 3 isoform X1
	<i>gsta.1</i>	1.24	3.5×10^{-3}	Glutathione S-transferase, alpha tandem duplicate 1
	<i>gstt1a</i>	1.50	1.5×10^{-4}	Glutathione S-transferase theta-1a

4.4.4. qPCR validation analysis

To validate the current RNA-seq results, correlation analyses were performed between the \log_2 of the TPM values from the RNA-seq and the \log_2 of the RQ values from my previous qPCR [12] for 30 genes (Chapter 3). R^2 values of 0.8 or above are regarded as highly correlated [38]. R^2 values between 0.5 and 0.8 are regarded as having a medium level of correlation, while those below 0.5 are considered to have a low correlation. Among the 30 selected genes, 18 genes, such as *interleukin 8a (il8a)*, *interleukin 8b (il8b)*, *C-C motif chemokine-like 20 (ccl20)*, *hepcidin antimicrobial peptide (hamp)*, *toll-like receptor 5a (tlr5a)*, *HLA class II histocompatibility antigen gamma chain (cd74)*, *serum amyloid A 5 (saa5)*, *interleukin 1 beta (il1b)*, *lymphocyte antigen 6 complex locus protein G6f (ly6g6f)*, *interleukin 10 (il10)*, *radical S-adenosyl methionine domain-containing protein 2 / viperin (rsad2)*, *cyclooxygenase-2 (cox2)*, *interferon regulatory factor 7 (irf7)*, *T-cell surface glycoprotein CD8 alpha chain (cd8a)*, *interferon-induced GTP-binding protein a (mx a)*, *T-cell surface glycoprotein CD4a (cd4a)*, *T-cell surface glycoprotein CD4b (cd4b)*, and *interferon-induced GTP-binding protein c (mx c)* showed significantly high gene expression correlations (i.e., R^2 values ranged from 0.7987 to 0.9568; $p < 0.0001$), suggesting an overall high concordance between RNA-seq and qPCR data (Figure 4.5).

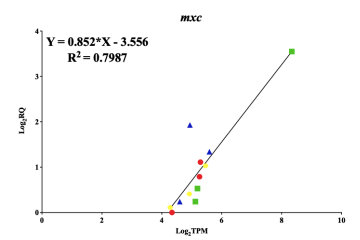
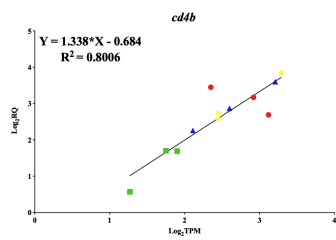
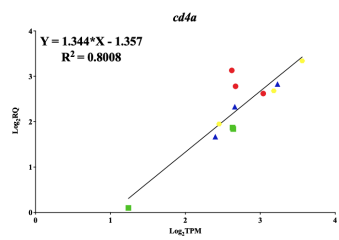
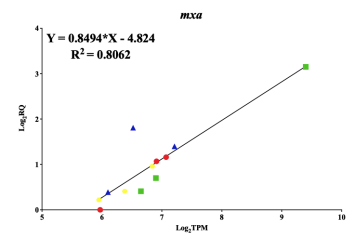
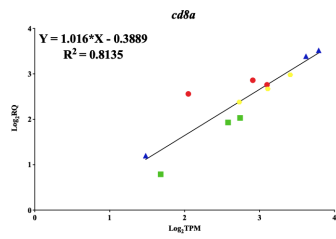
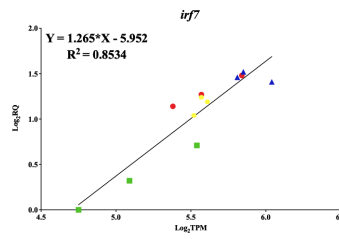
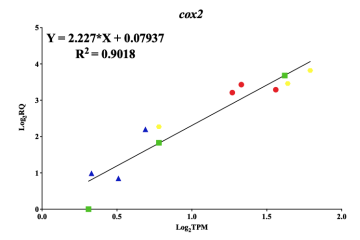
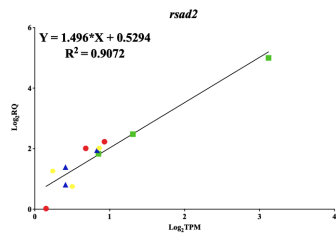
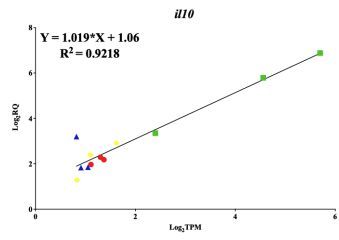
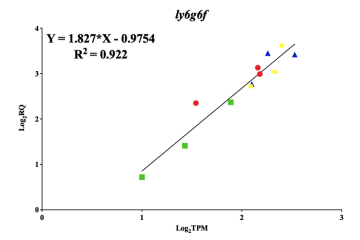
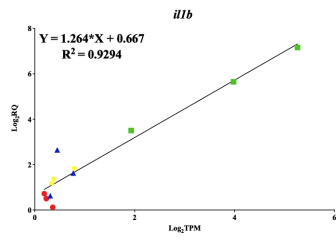
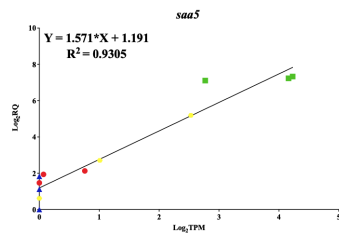
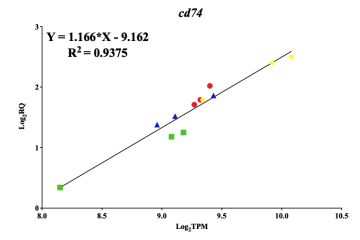
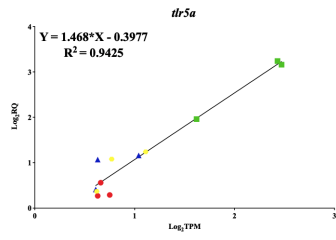
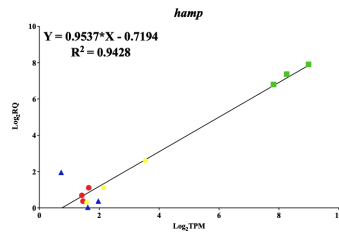
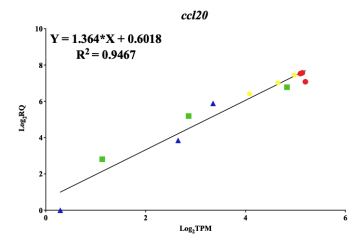
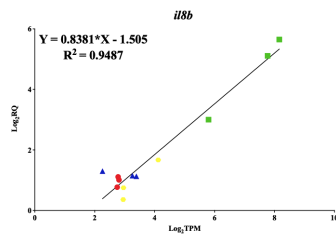
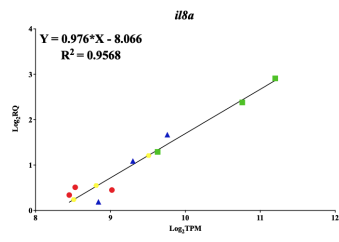


Figure 4.5. Gene expression correlation (high) between qPCR and RNA-seq data for 18 genes of interest. These 18 genes showed a significantly high correlation (level of significance: $p < 0.0001$ ****) with the current RNA-seq results. RNA-seq data are presented as \log_2 TPM (X axis). qPCR data are represented as \log_2 RQ (Y axis). The red circles represent control samples at 28 dpi; the green squares represent *R. salmoninarum*-infected samples at 28 dpi; the blue triangles represent control samples at 98 dpi; the yellow hexagons represent *R. salmoninarum*-infected samples at 98 dpi. Each symbol is an average of the three fish at a particular time point in the head kidney tissue. The linear regression equation and the correlation coefficient (R^2) are indicated for each gene expression correlation.

Significant medium gene expression correlations were observed for 7 genes (i.e., R^2 values ranged from 0.4904 to 0.7128; $p < 0.001$, $p < 0.01$, and $p < 0.05$), including *signal transducer and activator of transcription 1 (stat1)*, *ATP-dependent RNA helicase lgp2 (lgp2)*, *tumour necrosis factor alpha (tnfa)*, *interferon gamma (ifn γ)*, *toll-like receptor 5b (tlr5b)*, *toll-like receptor 7 (tlrl7)*, and *interferon-induced GTP-binding protein b (mxb)* (Supplemental Figure S4.2). Correlations between RNA-seq and qPCR data were poor and not significant for 5 genes (i.e., R^2 values ranged from 0.0922 to 0.2634), such as *C-C motif chemokine-like 19 (ccl19)*, *immunoglobulin mu heavy chain c (ighmc)*, *toll-like receptor 3 (tlr3)*, *immunoglobulin heavy chain variable region a (igha)*, and *immunoglobulin delta heavy chain (ighd)* (Supplemental Figure S4.2). Overall, 83% of the qPCR-studied genes showed significant correlations (i.e., 25 out of 30 genes showed significantly high to medium levels of correlation with R^2 values ranging from 0.5 to 0.96; R^2 values of 0.5 and above were considered as significant correlation) with the current RNA-seq results.

4.4.5. Lysozyme Activity in lumpfish serum

To determine changes in the lumpfish serum lysozyme levels during *R. salmoninarum* infection, a fluorescence-based lysozyme activity assay was used. The standard curve of the fluorescence-based activity assay is shown in Figure 4.6A. The linear regression equation and the correlation coefficient for the standard curve were $Y = 43.65X + 55.83$ and $R^2 = 0.9985$, respectively (Figure 4.6A). Figure 4.6B displays the measurements of active lysozyme in lumpfish serum at 1, 14, 28, 42, 56, and 98 dpi. The serum lysozyme levels of the infected fish at earlier sampling (i.e., 1 dpi) were significantly higher ($p < 0.05$) compared to the control fish at 1 dpi. Compared to the infected fish at 1 dpi, lysozyme activity in serum had significantly declined in the infected fish at 98 dpi.

However, on days 14, 28, 42, 56, and 98, lysozyme levels did not differ significantly between control and infected fish or between infected fish.

4.4.6. Specific serum antibody response

To examine the changes in the humoral antibody response in lumpfish serum during *R. salmoninarum* infection, specific serum antibody titers at 14, 28, 42, 56, and 98 dpi were measured using indirect ELISA. The \log_2 antibody titers were not significantly different between control and *R. salmoninarum* infected fish in all the tested time points (Figure 4.6C).

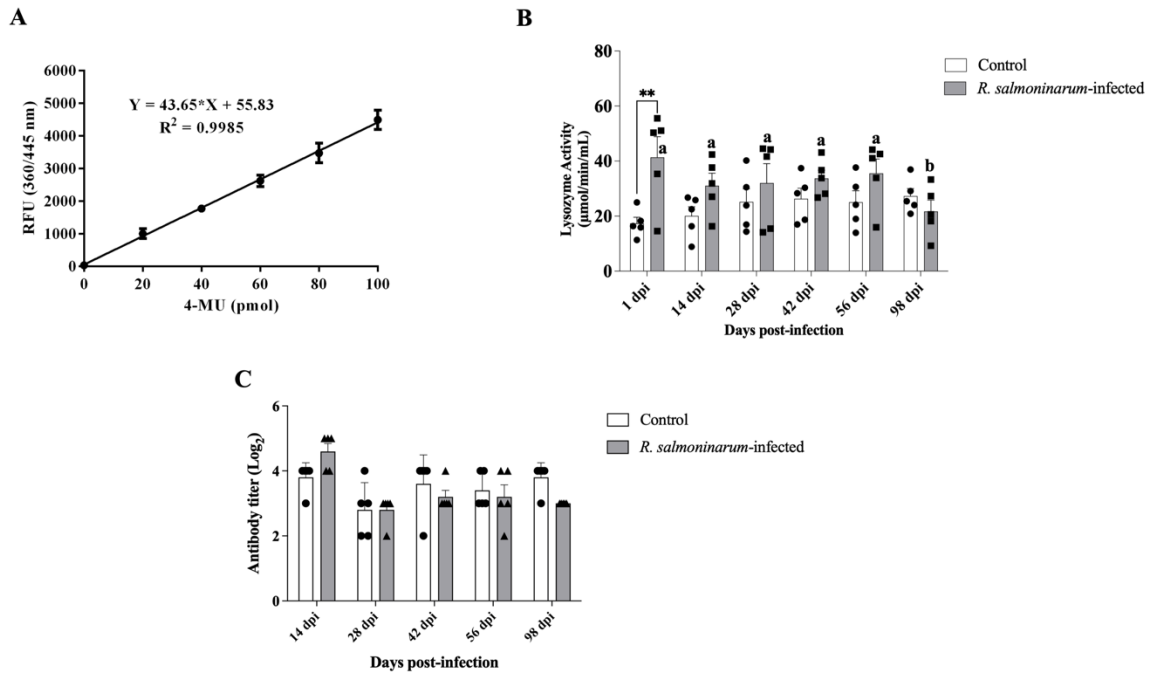


Figure 4.6. Lysozyme activity and antibody titers in lumpfish serum upon *R. salmoninarum* infection. **A.** Typical 4-Methylumbelliferon (4-MU) standard curve of the fluorometry-based lysozyme activity assay kit. **B.** Lysozyme enzyme activity of control and *R. salmoninarum*-infected lumpfish serum at 1-, 14-, 28-, 42-, 56-, and 98-dpi from control and *R. salmoninarum*-infected (1×10^9 cells dose⁻¹) fish groups. A two-way ANOVA test, followed by the Sidak multiple comparisons post hoc test, was used to identify significant differences between treatments (control and infected groups) at a single time point and for a given treatment at different time points (1, 14, 28, 42, 56, and 98 dpi). Asterisks (*) represent significant differences between treatments at each time point ($*p < 0.05$, $**p < 0.01$). Lowercase letters represent significant differences between the lysozyme activity of the infected group at different time points. Each value is the mean \pm S.E.M ($n = 5$). **C.** *R. salmoninarum*-specific antibody levels were measured by indirect ELISA in lumpfish

serum samples collected at 14-, 28-, 42-, 56-, and 98-days post-infection from control and *R. salmoninarum*-infected fish groups. Each value is the mean \pm S.E.M ($n = 5$).

4.5. Discussion

Lumpfish is a novel and economically important species for the salmon farming industry due to its use as cleaner fish to control sea lice [3]. However, high mortality caused by bacterial infections is a challenge for lumpfish aquaculture [2]. Expanding the knowledge of the lumpfish immune system and its host-pathogen interactions is crucial to provide a basis for the development of efficient immune prophylactic measures. The current study is the first to describe the transcriptome response of lumpfish head kidney to *R. salmoninarum* at early (28 dpi) and chronic (98 dpi) infection stages.

Fish immune mechanisms or signalling pathways that are triggered in response to several bacterial infections have been effectively studied using high-throughput transcriptomic or gene expression approaches, such as tag-based sequencing method, microarray, and RNA-Seq [20,39,40]. In the present study using RNA-seq, I identified 1971 (1537 up- and 434 down-regulated) and 139 (125 up- and 14 down-regulated) DEGs in lumpfish head kidney in response to *R. salmoninarum* at 28 and 98 dpi compared to the control fish (Figure 4.2G, Supplementary File 4.1). In contrast, a suppressive subtractive hybridization (SSH)-based investigation identified a total of 132 expressed sequence tags (ESTs) that showed differential expression in response to *R. salmoninarum* infection in chinook salmon (i.e., anterior kidney) [41]. Also, the Atlantic salmon head kidney transcriptome responses to formalin-killed and live *R. salmoninarum* were profiled using microarray-based analyses [22,23]. Atlantic salmon injected with inactivated *R. salmoninarum* at 24 hpi showed 379 differentially expressed probes (DEPs) in the head kidney when compared with the PBS-injected control fish [22]. On the other hand, a larger

number of DEPs (7729 and 6766 DEPs in the infected fish with higher and lower *R. salmoninarum* levels, respectively) were identified in Atlantic salmon head kidney infected with live *R. salmoninarum* at 13 dpi [23]. Moreover, RNA-seq was used to identify 412 and 467 DEGs at 7 and 14 dpi, respectively, in the Atlantic salmon head kidney in response to the Gram-negative *P. salmonis* infection [42]. RNA-seq-based approaches have also been successfully applied to study the lumpfish transcriptome response to Gram-negative bacterial pathogens. For instance, Eggestøl et al. (2018) elucidated the early immune responses of lumpfish leucocytes after an *in-vitro* exposure to *V. anguillarum* O1 and observed 9033 and 15225 DEGs at 6 and 24 hpi, respectively, using a *de-novo* transcriptome assembly [15]. In addition, Chakraborty et al. (2022) recently reported the transcriptome response of lumpfish spleen, liver, and head kidney to *A. salmonicida* infection at 3 and 10 dpi and found a total of 6246 DEGs using reference-genome guided transcriptome assembly [26]. Overall, the differences in the number of DEGs noticed between the current and the previous *R. salmoninarum*- or lumpfish-related studies may be due to variations in several factors, including host (i.e., species), bacterial pathogen (i.e., Gram-positive / Gram-negative and strains), host/pathogen-specific responses (i.e., live or killed bacteria), sampling time points (from hpi to dpi), experimental design, and transcriptomic approach (i.e., SSH, microarray, *de-novo*- or reference-based RNA-seq pipelines).

The current RNA-seq results found extensive *R. salmoninarum*-dependent dysregulation of several genes involved in immune responses, metabolism, cellular processes, development, and response to stress in lumpfish head kidney at 28 dpi compared to 98 dpi (Figures 4.2E, F and Figure 4.3A). To be specific, upregulated genes in response

to *R. salmoninarum* infection at 28 dpi were mainly involved in innate and adaptive immunity, whereas downregulated genes were mostly associated with amino acid metabolism (i.e., biosynthesis and degradation of amino acids), cellular and developmental processes (Figure 4.4). However, the lumpfish transcriptional response to this pathogen at 98 dpi was remarkably low, where *R. salmoninarum*-dependent dysregulation of genes was largely linked to cell-mediated adaptive immunity (Figure 4.3B). The samples from the control ($n = 3$) and *R. salmoninarum*-infected ($n = 3$) fish at 28 and 98 dpi (a total of 12 samples) used in the current RNA-seq analysis are the same ones I previously used in my qPCR study [12]. Thus, to validate the current lumpfish head kidney transcriptome, I used the prior qPCR results from Gnanagobal et al. (2021) for 30 selected genes. The correlation analysis revealed that 83% of the qPCR-studied genes showed significant correlations ($R^2 \geq 0.5$) between qPCR and RNA-seq data (Figure 4.5 and Supplementary Figure S4.2). Therefore, in general, the qPCR and RNA-seq results were in high agreement, proving the reliability of the transcriptome data reported in this study. My prior qPCR results also confirmed the induction of genes related to PRRs (e.g., *tlr5*), cytokines (e.g., *il1b*, *il8*, *il10*), iron homeostasis (e.g., *hamp*), and acute phase response (e.g., *saa5*) at 28 dpi, and cell-mediated adaptive immunity (e.g., *ifng*, *cd74*) at 98 dpi.

Innate immunity detects pathogens through a series of PRRs, which identify conserved pathogenic bacterial structures like flagellin and peptidoglycans and activate intracellular signalling pathways that result in inflammatory cytokines release and prime adaptive immunity. TLRs (Toll-like receptors), NLRs (NOD-like receptors), CLRs (C-type lectin receptors), and PGRP (peptidoglycan recognition proteins) are the 4 main types of PRRs found in fish [11]. Fish TLR5 sense flagellin [43]. *tlr5* was upregulated in the

lumpfish head kidney in response to *R. salmoninarum* infection at 28 dpi, which is also verified by qPCR (Table 4.1, Figure 4.5) [12]. Although TLR5 induction by a non-motile or non-flagellated Gram-positive *R. salmoninarum* is controversial [44], similar observations in TLR5 expression in response to *R. salmoninarum* and another non-motile Gram-positive pathogen, *Streptococcus iniae* were also reported in Atlantic salmon and turbot (*Scophthalmus maximus*), respectively [22,23,45]. Functional analyses are therefore required to understand the cross-talks between fish TLR5 and non-motile Gram-positive pathogens.

CLRs, which are calcium-dependent lectins that bind to carbohydrates (i.e., glycan structures of the pathogen), can activate several immune signalling pathways and have been implicated in complement activation, phagocytosis, cell death, inflammation, and antibacterial activities [46]. *clec4e* (*si:ch73-86n18.1*; *C-type lectin domain family 4 member E*) showed upregulation in the lumpfish head kidney at 28 dpi (Table 4.1). In contrast, Eslamloo et al. (2020) observed variable expression of the C-type lectin family domain (i.e., upregulation of *clec12b* and downregulation of *clec3a* and *clec4e*) in response to *R. salmoninarum* bacterin in Atlantic salmon head kidney [22]. Thus, C-type lectin family receptor induction in response to *R. salmoninarum* infection could be host-specific and vary between fish species. Little is known about CLR function in teleost fish, and the role of CLRs in lumpfish upon bacterial infection should be further explored at the gene or protein level to validate its variable expression between fish species.

PGRPs recognize the peptidoglycans (PGN) of the bacterial cell wall (i.e., binds strongly to murein PGN of Gram-positive bacteria) and kill Gram-positive pathogens by targeting their PGN biosynthesis [47]. PGRPs demonstrated bactericidal activity in

zebrafish (*Danio rerio*) and rockfish (*Sebastes schlegeli*) [48,49]. Gram-positive *R. salmoninarum* induced the expression of *pglyrp6* (*Peptidoglycan recognition protein 6*) in lumpfish at 28 dpi (Table 4.1). Similarly, Gram-positive *S. iniae* upregulated the PGRP gene (*Smpgrp2*) in mucosal tissues of turbot following challenge [50]. PGRP's involvement in intracellular immune signalling and lumpfish host defense is unknown and warrants future research.

Complement systems and antibodies, which identify and eliminate invading pathogens and stimulate inflammation, are the key humoral elements of innate immunity [51]. *R. salmoninarum* is known to activate the alternative complement pathway, where opsonin C3b directly binds to the bacterial surface and facilitates the intracellular invasion of bacteria into fish phagocytes [11,52]. Similarly, the current RNA-seq results indicated that *R. salmoninarum* activates alternative complement cascading and relevant genes, including complement C3-like gene (*LOC117745115*), at 28 dpi in lumpfish (Table 4.1; Supplementary Table S4.5). Complement activation in lumpfish was also reported against Gram-negative pathogens, *V. anguillarum* and *A. salmonicida* [15,26].

Nutritional immunity is a defense response against invading pathogens, where the host deprives the intracellular availability of critical nutrients, including iron, and amino acids, to limit bacterial proliferation [53–55]. Hepcidin (HAMP), a major iron metabolism regulator, is increased as a result of interleukin 6 (IL-6)-mediated hypoferric inflammatory response, which in turn inhibits iron exporters (i.e., ferroportin) and lowers the iron in tissues to a level below which the pathogen cannot proliferate and cause disease [11,56]. Teleost HAMP also presents antibacterial activity against Gram-positive bacteria [57,58]. In the present study, lumpfish significantly upregulated several hepcidin or hepcidin-like

genes (i.e., *hamp*, *LOC117728128*, and *LOC117728096*) in response to *R. salmoninarum* at 28 dpi. As in the RNA-seq results, my prior qPCR (Chapter 3) also showed statistically significant upregulation of *hamp* with a similar fold change [12] (Table 4.1 and Supplementary Table S4.3) and a significant correlation between TPM and RQ values (Figure 4.5). Similar to what I found in lumpfish, elevated expression levels of *hamp* were seen in other fish species in response to Gram-positive pathogens at early infection stages. These other fish species were Atlantic salmon (head kidney) following *R. salmoninarum* infection [22,23], hybrid striped bass (*Morone chrysops* × *Morone saxatilis*; liver) against *S. iniae* [59], and European sea bass (*Dicentrarchus labrax*; liver) following *Lactococcus garviae* and *Streptococcus parauberis* infection [58]. As lumpfish seem to have multiple hepcidin or hepcidin-like genes (Supplementary Table S4.3), future research on their structural and functional characterization and their involvement in the lumpfish antibacterial responses would be valuable.

Beyond the canonical lumpfish host immune-related response, I observed substantial dysregulation of the processes associated with amino acid metabolism; in particular, lumpfish downregulated genes involved in amino acid biosynthesis and degradation during the *R. salmoninarum* infection at 28 dpi (Table 4.1; Supplementary Table S4.6). Similar findings were also reported in Atlantic salmon in response to *R. salmoninarum* and another intracellular pathogen, *P. salmonis* [23,42]. For instance, Eslamloo et al. (2020b) observed extensive metabolic dysregulation of protein-related processes, including amino acid activation and cellular amino acid metabolism, in the Atlantic salmon head kidney upon *R. salmoninarum* infection at 13 dpi [23]. Both the Atlantic salmon (head kidney and spleen) and *P. salmonis* showed a greater number of

genes related to the amino acid metabolism when host and pathogen transcriptomes were analyzed simultaneously [42]. The authors also discovered that *P. salmonis* lacks certain amino acid biosynthesis pathways (e.g., valine, leucine, and isoleucine) and, therefore, is metabolically dependent on the amino acids present in its salmon host during infection [42]. According to Wiens et al. (2008), the *R. salmoninarum* type strain, which is used in the present study, lacks *de novo* biosynthesis of the amino acids serine, glycine, cysteine, asparagine, and methionine [60]. Intriguingly, the amino acid metabolism-related processes were downregulated in lumpfish upon *R. salmoninarum* infection at 28 dpi, including biosynthesis of glycine, serine, aspartate, cellular amino acids, and sulphur amino acids (i.e., cysteine and methionine) (Table 4.1; Supplementary Table S4.6). Therefore, like *P. salmonis*, *R. salmoninarum* may rely on the fish host's intracellular environment to uptake amino acids that its own cell machinery cannot synthesize. As a defense response, lumpfish potentially downregulated processes or genes related to amino acid biosynthesis and import to limit the availability of amino acids in fish tissues. Although amino acid metabolism is not a predominant transcriptome response in lumpfish in the current RNA-seq study, this scenario could be seen in the context of amino acid-based nutritional immunity induced by lumpfish to overcome *R. salmoninarum* during early infection stages. Research on how intracellular *R. salmoninarum* overcomes amino acid starvation within the host (i.e., nutritional virulence) or how it uses the host machinery to get amino acids from the host cell would be intriguing. Further, future *in-vitro* assays will be required to confirm the role of the critical amino acids in *R. salmoninarum* growth and metabolism.

Apoptosis or programmed cell death is a crucial defense mechanism against pathogens [61]. Caspase-associated recruitment domain (CARD) regulates caspase

activation during apoptosis and inflammation and NFkB activation during innate or adaptive immunity [62]. A positive regulator of apoptosis and NFkB activation, B cell lymphoma (BCL) 10 is an adaptor protein containing a CARD [63]. Association between CARDS from CARD-family proteins and B cell lymphoma 10 activates the NFkB pathway [64,65]. In teleost fish, genes for CARD-containing proteins implicated in NFkB activation have been identified [66,67]. According to the current RNA-seq results, induction of genes *card9*, *bcl3*, and *LOC117734930* in response to *R. salmoninarum* infection at 28 dpi suggests the activation of apoptosis and NFkB signalling pathways in lumpfish (Table 4.1). This might be how lumpfish facilitate the apoptotic clearance of infected cells. Further, Atlantic salmon also exhibited an abundance of BPs linked to cell death and increased expression of apoptotic caspase (*casp14*) against *R. salmoninarum* infection [23]. Studies on the structural and functional characterization of the lumpfish *card9* gene and examining its role in immune modulation would be interesting since it may be a promising biomarker for infection.

The JAK-STAT signalling pathway plays crucial roles in immune system orchestration, especially in mediating immune regulatory processes [68]. In mammals, a canonical JAK-STAT pathway is activated when the receptor binds to the ligand and deactivated when negative regulators are present [68]. Cytokines (i.e., ligands) IL-6, a pro-inflammatory cytokine, and IL-10, an anti-inflammatory cytokine, bind to their receptor, glycoprotein 130 (Gp130) and IL-10 receptor, respectively, and the ligand/receptor complex activates the JAK-STAT signalling cascade [68–70]. Suppressors of cytokine signalling (SOCS) and cytokine-inducible SH2 (Src homology 2) domain protein (CISH) are the negative regulators that function to inhibit JAK-STAT signalling [68]. Several

signalling molecules, including PI3 kinase (PI3K), MAPK, and ERK, participate in this pathway [68]. RNA-seq results presented in this study show that JAK-STAT signalling was found to be dysregulated by *R. salmoninarum* in lumpfish head kidney at 28 dpi, similar to what was reported in Atlantic salmon head kidney transcriptome profiling in response to this pathogen [23]. Thus, the JAK-STAT pathway may play a crucial role in the host-pathogen interactions between *R. salmoninarum* and lumpfish during early infection stages. To be specific, *R. salmoninarum* infection upregulated genes linked to JAK-STAT signalling (Table 4.1). For instance, the ligands *interleukin-6-like (LOC117739248)* and *interleukin-10 (il10)* were upregulated (Table 4.1; Supplementary Table S4.5). Significant pathogen-responsive induction expression of *il10* was also verified by qPCR (Figure 4.5). Interestingly, *R. salmoninarum* infection at 28 dpi also caused upregulation of the receptor, *il10 receptor subunit beta-like (LOC117750018)* and negative regulators, *socs3a*, and *cish*, suggesting the IL-10 mediated signal transduction (i.e., IL-10-JAK-STAT-Circuit), and suppression of JAK-STAT signalling, respectively. Inhibition of the JAK-STAT signalling pathway could be seen from both the host and the pathogen points of view. From the lumpfish point of view, the infection-induced IL-10-JAK-STAT module may balance the pro-inflammatory responses and prevent host-mediated immune hyperactivity [69]. But, from the pathogen perspective, *R. salmoninarum* may hijack the JAK-STAT module through IL-10, SOCS, and CISH upregulation to sabotage host immune responses and promote its intracellular survival [69]. It is important to note that the RNA-seq results presented herein only give an overview of up- and down-regulated genes in response to *R. salmoninarum* infection in lumpfish based on pathway enrichment analyses and offer speculations using the significantly dysregulated genes but do not reveal the exact

mechanisms of immune modulation. Thus, future studies are required to validate the lumpfish JAK-STAT signalling pathway and to functionally characterize the genes involved in this mechanism.

In teleost fish, cell-mediated adaptive immunity involves CD8⁺ T cells to kill intracellular pathogens [71]. As MHC-1 molecules present processed intracellular antigens to CD8⁺ T cells, they become cytotoxic T lymphocytes and release cytotoxic granules that cause infected cells to undergo apoptosis. Cytokines, such as IFN- γ , trigger CD4⁺ T cells to differentiate into T helper 1 (Th1) cells, which prime CD8⁺ cells [11,71]. At 28 dpi, a Th1-type immune response was seen, along with the upregulation of *tap2a*, which is linked to MHC-1-mediated antigen processing and presentation (Table 4.1 and Supplementary Table S4.5). Subsequently, at 98 dpi, genes related to T-cell mediated cytotoxicity and the MHC-1 pathway were stimulated. Eslamloo et al. (2020b) also noted interactions between *R. salmoninarum* and the MHC-1 pathway in Atlantic salmon [23], which is similar to what I saw in lumpfish. Infected lumpfish were dying at the early stage, but mortality was stabilized with persisted *R. salmoninarum* at the chronic infection stage (Figure 4.1B). Thus, *R. salmoninarum* may evade (i.e., escape into the cytosol from the phagosome) the MHC-1 antigen presentation pathway during early infection, while lumpfish survived chronic infection by limiting *R. salmoninarum* growth with induced cell-mediated immunity. Future studies are needed to understand how *R. salmoninarum* evades antigen presentation pathways or interacts with the MHC-1 pathway in teleosts.

Reactive oxygen species (ROS) (e.g., hydrogen peroxide and superoxide) are produced and released by host phagocytic cells to prevent bacterial infection [72,73]. Intracellular accumulation of ROS causes oxidative damage in the activated cells, including

DNA denaturation, apoptosis, and necrosis [74]. Glutathione peroxidase (GPx), an intracellular antioxidant enzyme, detoxifies hydrogen peroxide into water to counteract its potentially damaging effects and is present in most living organisms, including fish [75–77]. In the present study, lumpfish showed upregulation of genes involved in glutathione peroxidase activity in response to *R. salmoninarum* at 98 dpi (Table 4.1). *M. viscosa*, a Gram-negative bacterium, in contrast, downregulated the transcript expression of the gene encoding GPx (*gpx7*) in the skin of Atlantic salmon [78]. *R. salmoninarum* chronically persisted in the lumpfish tissues, and bacterial loads were significantly lower in lumpfish tissues at 98 dpi compared to 28 dpi [12]. ROS-mediated killing by lumpfish may be a cause of *R. salmoninarum*'s lower bacterial burden at 98 dpi. Through GPx activity, lumpfish may activate the anti-oxidant defence system to protect its own cells from ROS-mediated oxidative damage.

A crucial indicator of fish innate immunity is lysozyme activity [79]. Fish lysozyme is lytic against Gram-positive and Gram-negative bacteria [80]. It is present in mucus, serum, lymphoid tissues, and phagocytic cells of marine and freshwater fish [80]. Since fish appear to have a less developed specific immune system than mammals, non-specific antimicrobial compounds like lysozyme may be more significant in fish than in mammals [81]. Besides having bactericidal properties, lysozyme is opsonic and thus activates the complement pathway and phagocytes [80]. Increased levels of lysozyme at the first sampling point (1 dpi) were followed by no significant difference between infected and time-matched control samples at subsequent time points (14, 28, 42, 56, and 98 dpi) in the serum from *R. salmoninarum*-infected lumpfish compared to the control fish (Figure 4.6B). These findings corroborate those made in carp (*Cyprinus carpio*) infected with Gram-

negative *Pseudomonas alcaligenes* and *Aeromonas punctata* or tilapia (*Oreochromis niloticus*) infected with Gram-positive *Streptococcus agalactiae* [82,83]. Pathogen recognition initiates a rapid innate immune response, including lysozyme activity, and subsequently induces host immunity via multiple signalling pathways and defense mechanisms [84]. Therefore, earlier samplings, such as a few hours to a day after the challenge, may find elevated lysozyme levels. On the other hand, reduction in serum lysozyme activity at later time points means that the adaptive response or further defense mechanisms have been given the opportunity to take over [83].

An understanding of the humoral immune response elicited against bacterial infection can be gained by measuring the antibody titers in the serum of infected fish using ELISA. At all of the time points, no significant variations in \log_2 antibody titers between control and infected fish serum were seen (Figure 4.6C), indicating that the circulating antibody levels in lumpfish are not considerably impacted by *R. salmoninarum* infection. In other words, *R. salmoninarum*-infected fish showed a poor specific antibody response. This could be due to the immune suppressive protein p57 of *R. salmoninarum* adsorbing specific antibodies and forming antigen-antibody complexes or opsonization of such complexes [85–88]. In contrast, elevated levels of BKD-induced serum antibody titers were observed in Atlantic salmon and rainbow trout (*Oncorhynchus mykiss*) [89]. Therefore, various fish species may have varied humoral antibody responses to *R. salmoninarum*.

Figure 4.7 illustrates the putative immune pathways activated by *R. salmoninarum* infection in the lumpfish head kidney. Although *R. salmoninarum* infection affected many genes and pathways, particularly at 28 dpi, only a small percentage of them were associated with the immune response (7%) compared to the cellular (63%) and metabolic (25%)

processes in the global view (Figure 4.3A), suggesting that this pathogen may have suppressed the lumpfish immune system during the early stages of infection. As per RNA-seq and qPCR results, simultaneous upregulation of genes encoding canonical pro- and anti-inflammatory cytokines (*il1b*, *il8*, *il10*), downregulation of innate immunity activation (*inavaa*), negative regulation of BPs connected to adaptive immunity (i.e., negative regulation of interferon-gamma production, immune effector process, T cell activation/differentiation) and inhibition of JAK-STAT signalling (*socs3a*, and *cish*) also point to *R. salmoninarum*-induced immune suppression at the early infection stage (Figure 4.7A). On the other hand, at 98 dpi, lumpfish induced cell-mediated immunity related to the MHC-1 pathway suggests that *R. salmoninarum* may be present in the cytoplasm during intracellular infection.

These transcriptomics results provide valuable baseline information regarding the biological processes and molecular pathways underlying the lumpfish response to a Gram-positive fish pathogen, *R. salmoninarum*, during the early and chronic infection stages (Figure 4.7B). Knowledge of immune genes or pathways dysregulated in lumpfish during *R. salmoninarum* infection from the present study will be valuable for immunoprophylaxis. For instance, vaccine design with pertinent intracellular antigens that target cell-mediated immunity (CD8+ T-cells), and MHC-1 antigen presentation pathway may induce protection against this intracellular pathogen. Future RNA-seq analyses that simultaneously compare the transcriptomes of salmon and lumpfish in a cohabitation *R. salmoninarum* infection model would be beneficial to identify comparative molecular biomarkers for BKD-related investigations. Furthermore, to improve the existing

understanding of the lumpfish immune system, it is crucial to characterize the functions of the important immune-relevant genes identified herein.

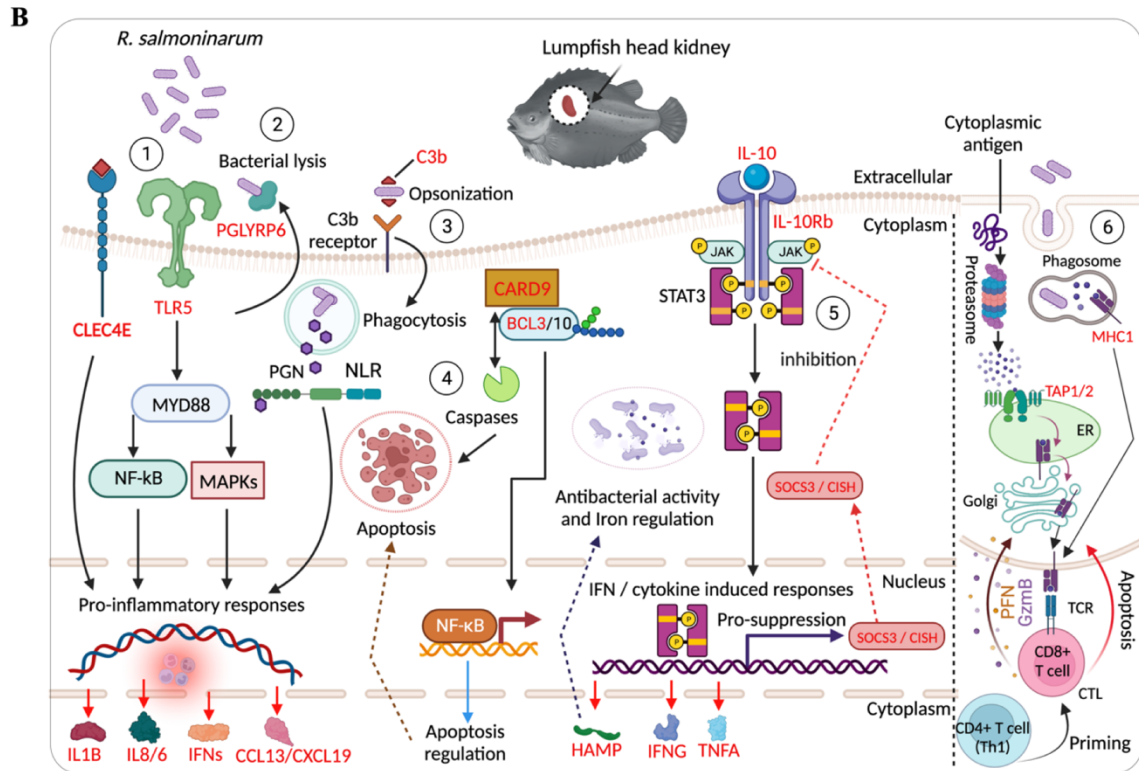
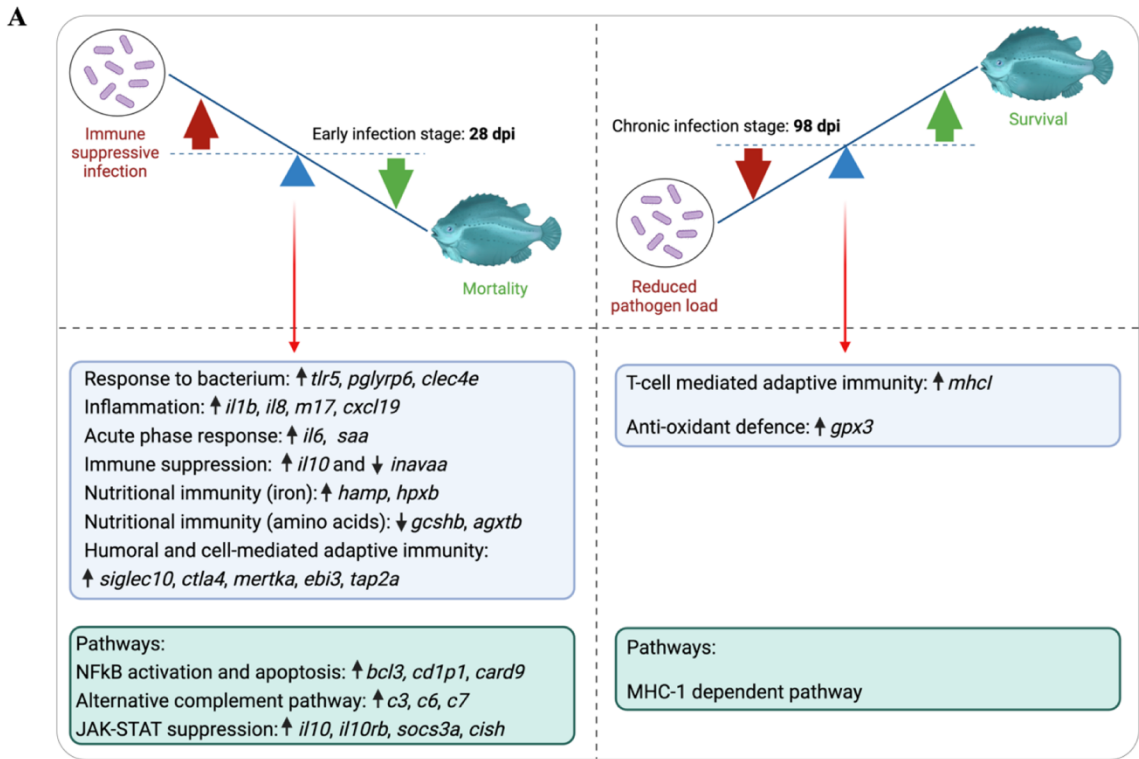


Figure 4.7. Lumpfish head kidney transcriptome response to *R. salmoninarum* at early (28 dpi) and chronic (98 dpi) infection stages. **A.** Immune genes and pathways dysregulated in lumpfish at 28 and 98 dpi. At earlier stages of infection (i.e., the onset of mortality), immune suppressive infection by *R. salmoninarum* caused mortality in lumpfish (i.e., *R. salmoninarum* took over the tug-of-war at 28 dpi). On the other hand, lumpfish survived at chronic stages of infection with induced cell-mediated immunity (i.e., lumpfish took over the tug-of-war at 98 dpi). ↑ and ↓ indicate up- and down-regulation of the genes, respectively (Table 1). **B.** Schematic representation of the host molecular pathways differentially regulated by *R. salmoninarum* in lumpfish. This figure was created using the genes found in this study (red fonts) and their regulatory pathways and functions in mammals, as described in the Discussion. **1.** TLR-mediated signalling and NFκB activation. **2.** Secreted peptidoglycan recognition proteins (PGLYRPs) interact with the bacterial peptidoglycan (PGN) and induce bacterial lysis. **3.** Complement pathway - C3b binding to the bacterial surface, followed by ligation to the C3b receptor and bacterial internalization by phagocytosis. Following degradation in the phagolysosome, PGN-derived small molecules are sensed by NOD-like receptors (NLRs) to induce pro-inflammatory cytokines. **4.** Apoptosis and NFκB activation through interactions between Caspase-associated recruitment domain (CARD) family proteins and B-cell lymphoma adaptor proteins (BCL3/10). **5.** JAK-STAT signalling (IL-10-JAK-STAT-Circuit) and its negative regulation (red-dotted arrows) by suppressors of cytokine signalling (SOCS) and cytokine-inducible SH2 domain protein (CISH). **6.** Interactions with the MHC-I dependent pathway. MHC-I molecules present processed intracellular antigens to CD8⁺ T cells. These CD8⁺ T cells become cytotoxic T-lymphocytes (CTL) and release perforins (PFN; form pores in

the plasma membrane) and granzymes (GZm; break down proteins and lyse the cells) into the infected cells and kill them. CD4⁺ T cells help CD8⁺ T cells priming to kill the intracellular pathogen. TLR, Toll-like receptor; MyD88, Myeloid differentiation primary response 88; NFkB, Nuclear factor kappa-B; MAPK, Mitogen-activated protein kinase; ILs, interleukin; IFNs, Interferons; CCL13, C-C motif chemokine; CXCL19, C-X-C motif chemokine 19; PGN, Peptidoglycans; PGLYRP6, Peptidoglycan recognition protein 6; NLR, NOD-like receptors; CLEC4E, C-type lectin domain family 4 member E; C3b, Complement B; CARD, Caspase-associated recruitment domain; BCL3, B-cell lymphoma 3; IL-10Rb, Interleukin-10 receptor subunit beta-like; JAK, Janus kinase; P, Phosphorylation; STAT, Signal transducer and activator of transcription; SOCS, Suppressors of cytokine signalling; CISH, Cytokine-inducible SH2 (Src homology 2) domain protein; HAMP, Hepcidin antimicrobial peptide; IFNG, Interferon gamma; TNFA, Tumor necrosis factor alpha; MHC1, Major histocompatibility complex I; TAP, Protein associated with antigen processing; ER, Endoplasmic reticulum protein; PFN, Perforin; GZm, Granzyme; TCR, T-cell receptor; CD, Cluster of differentiation; CTL, Cytotoxic T-lymphocytes. Figures A and B were created in BioRender (<https://biorender.com/>).

4.6. Conclusions

A global overview of the molecular mechanisms underlying lumpfish responses to *R. salmoninarum* during early (28 dpi) and chronic (98 dpi) infection stages was provided by this study, which used RNA-seq to profile the lumpfish head kidney transcriptome. Compared to 98 dpi, *R. salmoninarum* affected greater numbers of pathways and genes in lumpfish at 28 dpi. However, only a small percentage of them were related to immune responses, which might be attributed to the immune suppressive nature of this pathogen. At 28 dpi, *R. salmoninarum*-induced genes were linked to innate and adaptive immunity, and the pathways that were dysregulated include NFkB signaling, apoptosis, alternative complement cascading, and JAK-STAT signaling pathway. *R. salmoninarum*-suppressed genes in lumpfish at 28 dpi were associated with cellular and metabolic processes (e.g., amino acid biosynthesis/degradation). Lumpfish triggered MHC-1-related cell-mediated immunity against *R. salmoninarum* at 98 dpi, linked to its cytoplasmic location during intracellular infection. Lysozyme activity in infected lumpfish serum was higher at the earliest time point (1 dpi) and subsequently reduced at later time points (14, 28, 42, 56, and 98 dpi). *R. salmoninarum* infection did not significantly affect the antibody titers in lumpfish, according to ELISA. Overall, the present study is a combined approach of reference-based transcriptomic assembly and pathway enrichment analyses that provided gene repertoires and networks that regulate the host-pathogen interactions between lumpfish and *R. salmoninarum* and will act as a guide to understand host immunity and pathogen virulence.

4.7. References

1. Costello, M. J. The Global Economic Cost of Sea Lice to the Salmonid Farming Industry. *J. Fish Dis.* **2009**, *32* (1), 115–118, doi:10.1111/j.1365-2761.2008.01011.x.
2. Brooker, A. J.; Papadopoulou, A.; Gutierrez, C.; Rey, S.; Davie, A.; Migaud, H. Sustainable Production and Use of Cleaner Fish for the Biological Control of Sea Lice: Recent Advances and Current Challenges. *Vet. Rec.* **2018**, *183* (12), 383.
3. Powell, A.; Treasurer, J. W.; Pooley, C. L.; Keay, A. J.; Lloyd, R.; Imsland, A. K.; Garcia de Leaniz, C. Use of Lumpfish for Sea-lice Control in Salmon Farming: Challenges and Opportunities. *Rev. Aquac.* **2018**, *10* (3), 683–702.
4. Imsland, A. K.; Reynolds, P.; Eliassen, G.; Hangstad, T. A.; Foss, A.; Vikingstad, E.; Elvegård, T. A. The Use of Lumpfish (*Cyclopterus lumpus* L.) to Control Sea Lice (*Lepeophtheirus salmonis* Krøyer) Infestations in Intensively Farmed Atlantic Salmon (*Salmo salar* L.). *Aquaculture* **2014**, *424–425*, 18–23, doi:10.1016/j.aquaculture.2013.12.033.
5. Sanders, J. E.; Fryer, J. L. *Renibacterium salmoninarum* Gen. Nov., Sp. Nov., the Causative Agent of Bacterial Kidney Disease in Salmonid Fishes. *Int. J. Syst. Evol. Microbiol.* **1980**, *30* (2), 496–502.
6. Wiens, G. D. Bacterial Kidney Disease (*Renibacterium salmoninarum*). In *Fish Diseases and Disorders*; Woo, P. T. K., Bruno, D. W., Eds.; CABI: Wallingford, UK, 2011; pp 338–374.
7. Evelyn, T. P. Bacterial Kidney Disease – BKD. In *Bacterial Disease of Fish*; V., Roberts, R. J. and Bromage, N. R., Ed.; Blackwell Scientific: London, 1993; pp 177–195.
8. Pascho, R. J.; Elliott, D. G.; Chase, D. M. Comparison of Traditional and Molecular Methods for Detection of *Renibacterium salmoninarum*. 2002; pp 157–209, doi:10.1007/978-94-017-2315-2_7.
9. Eissa, A. E.; Elsayed, E. E.; McDonald, R.; Faisal, M. First Record of *Renibacterium salmoninarum* in the Sea Lamprey (*Petromyzon marinus*). *J. Wildl. Dis.* **2006**, *42* (3), 556–560, doi:10.7589/0090-3558-42.3.556.
10. Byford, G. J.; Faisal, M.; Tempelman, R. J.; Scribner, K. T. Prevalence and Distribution of *Renibacterium salmoninarum* in Non-salmonid Fishes from Laurentian Great Lakes and Inland Habitats. *J. Great Lakes Res.* **2020**, *46* (6), 1709–1715, doi:https://doi.org/10.1016/j.jglr.2020.09.014.
11. Gnanagobal, H.; Santander, J. Host-Pathogen Interactions of Marine Gram-Positive Bacteria. *Biology (Basel)*. **2022**, *11* (9), doi:10.3390/biology11091316.
12. Gnanagobal, H.; Cao, T.; Hossain, A.; Dang, M.; Hall, J. R.; Kumar, S.; Van Cuong, D.; Boyce, D.; Santander, J. Lumpfish (*Cyclopterus lumpus*) Is Susceptible to *Renibacterium salmoninarum* Infection and Induces Cell-Mediated Immunity in the Chronic Stage. *Frontiers in Immunology*. 2021, p 4647.
13. Rønneseth, A.; Haugland, G. T.; Colquhoun, D. J.; Brudal, E.; Wergeland, H. I. Protection and Antibody Reactivity Following Vaccination of Lumpfish (*Cyclopterus lumpus* L.) against Atypical *Aeromonas salmonicida*. *Fish Shellfish*

- Immunol.* **2017**, *64*, 383–391, doi:https://doi.org/10.1016/j.fsi.2017.03.040.
14. Uribe, C.; Folch, H.; Enríquez, R.; Moran, G. Innate and Adaptive Immunity in Teleost Fish: A Review. *Vet. Med. (Praha)*. **2011**, *56* (10), 486.
 15. Eggestøl, H. Ø.; Lunde, H. S.; Rønneseth, A.; Fredman, D.; Petersen, K.; Mishra, C. K.; Furmanek, T.; Colquhoun, D. J.; Wergeland, H. I.; Haugland, G. T. Transcriptome-Wide Mapping of Signaling Pathways and Early Immune Responses in Lumpfish Leukocytes upon *in vitro* Bacterial Exposure. *Sci. Rep.* **2018**, *8* (1), 5261, doi:10.1038/s41598-018-23667-x.
 16. Haugland, G. T.; Jakobsen, R. A.; Vestvik, N.; Ulven, K.; Stokka, L.; Wergeland, H. I. Phagocytosis and Respiratory Burst Activity in Lumpfish (*Cyclopterus lumpus* L.) Leucocytes Analysed by Flow Cytometry. *PLoS One* **2012**, *7* (10), e47909–e47909, doi:10.1371/journal.pone.0047909.
 17. Rønneseth, A.; Ghebretsaie, D. B.; Wergeland, H. I.; Haugland, G. T. Functional Characterization of IgM+ B Cells and Adaptive Immunity in Lumpfish (*Cyclopterus lumpus* L.). *Dev. Comp. Immunol.* **2015**, *52* (2), 132–143, doi:10.1016/j.dci.2015.05.010.
 18. Dang, M.; Cao, T.; Vasquez, I.; Hossain, A.; Gnanagobal, H.; Kumar, S.; Hall, J. R.; Monk, J.; Boyce, D.; Westcott, J.; Santander, J. Oral Immunization of Larvae and Juvenile of Lumpfish (*Cyclopterus lumpus*) against *Vibrio anguillarum* Does Not Influence Systemic Immunity. *Vaccines* **2021**, *9* (8), 819, doi:10.3390/vaccines9080819.
 19. Kukurba, K. R.; Montgomery, S. B. RNA Sequencing and Analysis. *Cold Spring Harb. Protoc.* **2015**, *2015* (11), 951–969, doi:10.1101/pdb.top084970.
 20. Sudhagar, A.; Kumar, G.; El-Matbouli, M. Transcriptome Analysis Based on RNA-Seq in Understanding Pathogenic Mechanisms of Diseases and the Immune System of Fish: A Comprehensive Review. *Int. J. Mol. Sci.* **2018**, *19* (1), 245, doi:10.3390/ijms19010245.
 21. Rimstad, E.; Basic, D.; Gulla, S.; Hjeltnes, B.; Mortensen, S. Risk Assessment of Fish Health Associated with the Use of Cleaner Fish in Aquaculture. *Opin. panel Anim. Heal. Welf. Nor. Sci. Comm. Food Environ. VKM Rep.* **2017**, *32*.
 22. Eslamloo, K.; Kumar, S.; Caballero-Solares, A.; Gnanagobal, H.; Santander, J.; Rise, M. L. Profiling the Transcriptome Response of Atlantic Salmon Head Kidney to Formalin-Killed *Renibacterium salmoninarum*. *Fish Shellfish Immunol.* **2020**, *98*, 937–949.
 23. Eslamloo, K.; Caballero-Solares, A.; Inkpen, S. M.; Emam, M.; Kumar, S.; Bouniot, C.; Avendaño-Herrera, R.; Jakob, E.; Rise, M. L. Transcriptomic Profiling of the Adaptive and Innate Immune Responses of Atlantic Salmon to *Renibacterium salmoninarum* Infection. *Front. Immunol.* **2020**, *11* (October), doi:10.3389/fimmu.2020.567838.
 24. Evelyn, T.; Prospero-Porta, L.; Ketcheson, J. Two New Techniques for Obtaining Consistent Results When Growing *Renibacterium salmoninarum* on KDM2 Culture Medium. *Dis. Aquat. Organ.* **1990**, *9*, 209–212, doi:10.3354/dao009209.
 25. Sambrook, J. and Russel, W. *Molecular Cloning: A Laboratory Manual*, 2nd ed.; Cold Spring Harbor Laboratory Press: New York, 2001.
 26. Chakraborty, S.; Hossain, A.; Cao, T.; Gnanagobal, H.; Segovia, C.; Hill, S.; Monk,

- J.; Porter, J.; Boyce, D.; Hall, J. R.; Bindea, G.; Kumar, S.; Santander, J. Multi-Organ Transcriptome Response of Lumpfish (*Cyclopterus lumpus*) to *Aeromonas salmonicida* subspecies *salmonicida* Systemic Infection. *Microorganisms*. 2022, doi:10.3390/microorganisms10112113.
27. Ewels, P.; Magnusson, M.; Lundin, S.; Källér, M. MultiQC: Summarize Analysis Results for Multiple Tools and Samples in a Single Report. *Bioinformatics* **2016**, *32* (19), 3047–3048, doi:10.1093/bioinformatics/btw354.
 28. Li, B.; Ruotti, V.; Stewart, R. M.; Thomson, J. A.; Dewey, C. N. RNA-Seq Gene Expression Estimation with Read Mapping Uncertainty. *Bioinformatics* **2010**, *26* (4), 493–500, doi:10.1093/bioinformatics/btp692.
 29. Teng, M.; Love, M. I.; Davis, C. A.; Djebali, S.; Dobin, A.; Graveley, B. R.; Li, S.; Mason, C. E.; Olson, S.; Pervouchine, D.; Sloan, C. A.; Wei, X.; Zhan, L.; Irizarry, R. A. Erratum to: A Benchmark for RNA-Seq Quantification Pipelines. *Genome Biol.* **2016**, *17* (1), 203, doi:10.1186/s13059-016-1060-7.
 30. Pereira, M. B.; Wallroth, M.; Jonsson, V.; Kristiansson, E. Comparison of Normalization Methods for the Analysis of Metagenomic Gene Abundance Data. *BMC Genomics* **2018**, *19* (1), 274, doi:10.1186/s12864-018-4637-6.
 31. Robinson, M. D.; McCarthy, D. J.; Smyth, G. K. EdgeR: A Bioconductor Package for Differential Expression Analysis of Digital Gene Expression Data. *Bioinformatics* **2010**, *26* (1), 139–140, doi:10.1093/bioinformatics/btp616.
 32. Shannon, P.; Markiel, A.; Ozier, O.; Baliga, N. S.; Wang, J. T.; Ramage, D.; Amin, N.; Schwikowski, B.; Ideker, T. Cytoscape: A Software Environment for Integrated Models of Biomolecular Interaction Networks. *Genome Res.* **2003**, *13* (11), 2498–2504, doi:10.1101/gr.1239303.
 33. Bindea, G.; Mlecnik, B.; Hackl, H.; Charoentong, P.; Tosolini, M.; Kirilovsky, A.; Fridman, W.-H.; Pagès, F.; Trajanoski, Z.; Galon, J. ClueGO: A Cytoscape Plug-in to Decipher Functionally Grouped Gene Ontology and Pathway Annotation Networks. *Bioinformatics* **2009**, *25* (8), 1091–1093, doi:10.1093/bioinformatics/btp101.
 34. Cohen, J. Weighted Kappa: Nominal Scale Agreement with Provision for Scaled Disagreement or Partial Credit. *Psychol. Bull.* **1968**, *70* (4), 213–220, doi:10.1037/h0026256.
 35. Xue, X.; Caballero-Solares, A.; Hall, J. R.; Umasuthan, N.; Kumar, S.; Jakob, E.; Skugor, S.; Hawes, C.; Santander, J.; Taylor, R. G.; Rise, M. L. Transcriptome Profiling of Atlantic Salmon (*Salmo salar*) Parr With Higher and Lower Pathogen Loads Following *Piscirickettsia salmonis* Infection. *Front. Immunol.* **2021**, *12*, 789465, doi:10.3389/fimmu.2021.789465.
 36. Ng, A.; Heynen, M.; Luensmann, D.; Subbaraman, L. N.; Jones, L. Optimization of a Fluorescence-Based Lysozyme Activity Assay for Contact Lens Studies. *Curr. Eye Res.* **2013**, *38* (2), 252–259, doi:10.3109/02713683.2012.757324.
 37. Crowther, J. R. The ELISA Guidebook. *Methods Mol. Biol.* **2000**, *149*, III–IV, 1–413, doi:10.1385/1592590497.
 38. Everaert, C.; Luypaert, M.; Maag, J. L. V.; Cheng, Q. X.; Dinger, M. E.; Hellemans, J.; Mestdagh, P. Benchmarking of RNA-Sequencing Analysis Workflows Using Whole-Transcriptome RT-qPCR Expression Data. *Sci. Rep.* **2017**, *7* (1), 1559.

39. Qian, X.; Ba, Y.; Zhuang, Q.; Zhong, G. RNA-Seq Technology and Its Application in Fish Transcriptomics. *OMICS* **2014**, *18* (2), 98–110, doi:10.1089/omi.2013.0110.
40. Martin, S. A. M.; Dehler, C. E.; Król, E. Transcriptomic Responses in the Fish Intestine. *Dev. Comp. Immunol.* **2016**, *64*, 103–117, doi:https://doi.org/10.1016/j.dci.2016.03.014.
41. Rhodes, L. D.; Wallis, S.; Demlow, S. E. Genes Associated with an Effective Host Response by Chinook Salmon to *Renibacterium salmoninarum*. *Dev. Comp. Immunol.* **2009**, *33* (2), 176–186, doi:10.1016/j.dci.2008.08.006.
42. Valenzuela-Miranda, D.; Gallardo-Escárate, C. Dual RNA-Seq Uncovers Metabolic Amino Acids Dependency of the Intracellular Bacterium *Piscirickettsia salmonis* Infecting Atlantic Salmon. *Front. Microbiol.* **2018**, *9*, 2877.
43. Pietretti, D.; Wiegertjes, G. F. Ligand Specificities of Toll-like Receptors in Fish: Indications from Infection Studies. *Dev. Comp. Immunol.* **2014**, *43* (2), 205–222, doi:10.1016/j.dci.2013.08.010.
44. Fryer, J. L.; Sanders, J. E. Bacterial Kidney Disease of Salmonid Fish. *Annu. Rev. Microbiol.* **1981**, *35*, 273–298, doi:10.1146/annurev.mi.35.100181.001421.
45. Liu, F.; Su, B.; Fu, Q.; Shang, M.; Gao, C.; Tan, F.; Li, C. Identification, Characterization and Expression Analysis of TLR5 in the Mucosal Tissues of Turbot (*Scophthalmus maximus* L.) Following Bacterial Challenge. *Fish Shellfish Immunol.* **2017**, *68*, 272–279, doi:10.1016/j.fsi.2017.07.021.
46. da Silva Lino, M. A.; Bezerra, R. F.; da Silva, C. D. C.; Carvalho, E.; Coelho, L. Fish Lectins: A Brief Review. *Adv. Zool. Res. Nov. Sci. Hauppauge* **2014**, 95–114.
47. Kang, D.; Liu, G.; Lundström, A.; Gelius, E.; Steiner, H. A Peptidoglycan Recognition Protein in Innate Immunity Conserved from Insects to Humans. *Proc. Natl. Acad. Sci. U. S. A.* **1998**, *95* (17), 10078–10082, doi:10.1073/pnas.95.17.10078.
48. Li, X.; Wang, S.; Qi, J.; Echtenkamp, S. F.; Chatterjee, R.; Wang, M.; Boons, G.-J.; Dziarski, R.; Gupta, D. Zebrafish Peptidoglycan Recognition Proteins Are Bactericidal Amidases Essential for Defense against Bacterial Infections. *Immunity* **2007**, *27* (3), 518–529, doi:https://doi.org/10.1016/j.immuni.2007.07.020.
49. Kim, M. Y.; Jang, J. H.; Lee, J.-W.; Cho, J. H. Molecular Cloning and Characterization of Peptidoglycan Recognition Proteins from the Rockfish, *Sebastes schlegeli*. *Fish Shellfish Immunol.* **2010**, *28* (4), 632–639, doi:https://doi.org/10.1016/j.fsi.2009.12.023.
50. Zhang, L.; Gao, C.; Liu, F.; Song, L.; Su, B.; Li, C. Characterization and Expression Analysis of a Peptidoglycan Recognition Protein Gene, SmPGRP2 in Mucosal Tissues of Turbot (*Scophthalmus maximus* L.) Following Bacterial Challenge. *Fish Shellfish Immunol.* **2016**, *56*, 367–373, doi:10.1016/j.fsi.2016.07.029.
51. Nakao, M.; Tsujikura, M.; Ichiki, S.; Vo, T. K.; Somamoto, T. The Complement System in Teleost Fish: Progress of Post-Homolog-Hunting Researches. *Dev. Comp. Immunol.* **2011**, *35* (12), 1296–1308, doi:10.1016/j.dci.2011.03.003.
52. Rose, A. S.; Levine, R. P. Complement-Mediated Opsonisation and Phagocytosis of *Renibacterium salmoninarum*. *Fish Shellfish Immunol.* **1992**, *2* (3), 223–240, doi:10.1016/S1050-4648(05)80061-0.
53. Hood, M. I.; Skaar, E. P. Nutritional Immunity: Transition Metals at the Pathogen-

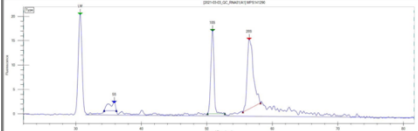
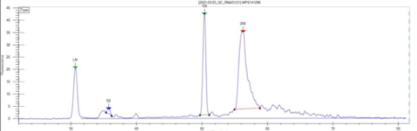
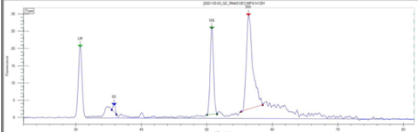
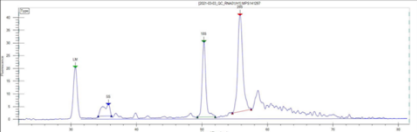
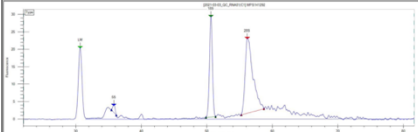
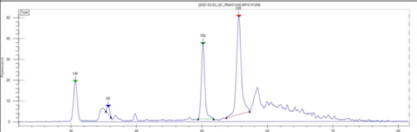
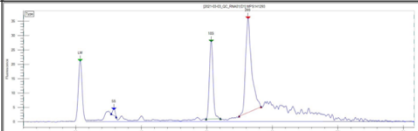
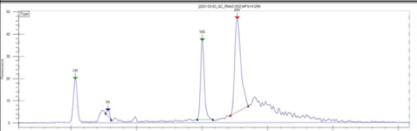
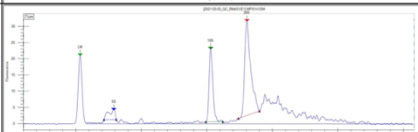
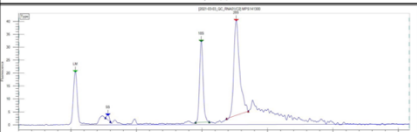
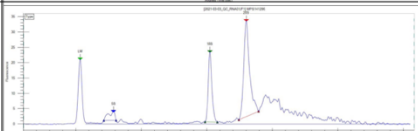
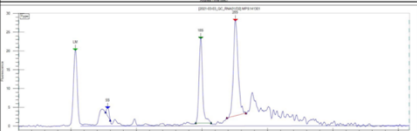
- Host Interface. *Nat. Rev. Microbiol.* **2012**, *10* (8), 525–537, doi:10.1038/nrmicro2836.
54. Abu Kwaik, Y.; Bumann, D. Microbial Quest for Food in Vivo: “Nutritional Virulence” as an Emerging Paradigm. *Cell. Microbiol.* **2013**, *15* (6), 882–890, doi:10.1111/cmi.12138.
 55. Barel, M.; Charbit, A. Francisella Tularensis Intracellular Survival: To Eat or to Die. *Microbes Infect.* **2013**, *15* (14), 989–997, doi:https://doi.org/10.1016/j.micinf.2013.09.009.
 56. Nemeth, E.; Ganz, T. Regulation of Iron Metabolism by Heparin. *Annu. Rev. Nutr.* **2006**, *26*, 323–342.
 57. Cai, L.; Cai, J. J.; Liu, H. P.; Fan, D. Q.; Peng, H.; Wang, K. J. Recombinant Medaka (*Oryzias melastigmus*) pro-Heparin: Multifunctional Characterization. *Comp. Biochem. Physiol. - B Biochem. Mol. Biol.* **2012**, *161* (2), 140–147, doi:10.1016/j.cbpb.2011.10.006.
 58. Neves, J. V.; Ramos, M. F.; Moreira, A. C.; Silva, T.; Gomes, M. S.; Rodrigues, P. N. S. Hamp1 but Not Hamp2 Regulates Ferroportin in Fish with Two Functionally Distinct Heparin Types. *Sci. Rep.* **2017**, *7* (1), 1–14.
 59. Lauth, X.; Babon, J. J.; Stannard, J. A.; Singh, S.; Nizet, V.; Carlberg, J. M.; Ostland, V. E.; Pennington, M. W.; Norton, R. S.; Westerman, M. E. Bass Heparin Synthesis, Solution Structure, Antimicrobial Activities and Synergism, and *in vivo* Hepatic Response to Bacterial Infections. *J. Biol. Chem.* **2005**, *280* (10), 9272–9282, doi:10.1074/jbc.M411154200.
 60. Wiens, G. D.; Rockey, D. D.; Wu, Z.; Chang, J.; Levy, R.; Crane, S.; Chen, D. S.; Capri, G. R.; Burnett, J. R.; Sudheesh, P. S.; Schipma, M. J.; Burd, H.; Bhattacharyya, A.; Rhodes, L. D.; Kaul, R.; Strom, M. S. Genome Sequence of the Fish Pathogen *Renibacterium salmoninarum* Suggests Reductive Evolution Away from an Environmental *Arthrobacter* Ancestor. *J. Bacteriol.* **2008**, *190* (21), 6970–6982, doi:10.1128/JB.00721-08.
 61. Miller, L. K. Baculovirus Interaction with Host Apoptotic Pathways. *J. Cell. Physiol.* **1997**, *173* (2), 178–182.
 62. Bouchier-Hayes, L.; Martin, S. J. CARD Games in Apoptosis and Immunity. *EMBO Rep.* **2002**, *3* (7), 616–621.
 63. Lucas, P. C.; Yonezumi, M.; Inohara, N.; McAllister-Lucas, L. M.; Abazeed, M. E.; Chen, F. F.; Yamaoka, S.; Seto, M.; Núñez, G. Bcl10 and MALT1, Independent Targets of Chromosomal Translocation in MALT Lymphoma, Cooperate in a Novel NF-KB Signaling Pathway*. *J. Biol. Chem.* **2001**, *276* (22), 19012–19019, doi:https://doi.org/10.1074/jbc.M009984200.
 64. Bhatt, D.; Ghosh, S. Regulation of the NF-KB-Mediated Transcription of Inflammatory Genes. *Front. Immunol.* **2014**, *5*, 71.
 65. Dubois, S. M.; Alexia, C.; Wu, Y.; Leclair, H. M.; Leveau, C.; Schol, E.; Fest, T.; Tarte, K.; Chen, Z. J.; Gavard, J.; Bidère, N. A Catalytic-Independent Role for the LUBAC in NF-KB Activation upon Antigen Receptor Engagement and in Lymphoma Cells. *Blood* **2014**, *123* (14), 2199–2203, doi:https://doi.org/10.1182/blood-2013-05-504019.
 66. Chang, M. X.; Chen, W. Q.; Nie, P. Structure and Expression Pattern of Teleost

- Caspase Recruitment Domain (CARD) Containing Proteins That Are Potentially Involved in NF-KappaB Signalling. *Dev. Comp. Immunol.* **2010**, *34* (1), 1–13, doi:10.1016/j.dci.2009.08.002.
67. Kono, T.; Sakai, T.; Sakai, M. Molecular Cloning and Expression Analysis of a Novel Caspase Recruitment Domain Protein (CARD) in Common Carp *Cyprinus carpio* L. *Gene* **2003**, *309* (1), 57–64, doi:https://doi.org/10.1016/S0378-1119(03)00494-3.
 68. Seif, F.; Khoshmirsafa, M.; Aazami, H.; Mohsenzadegan, M.; Sedighi, G.; Bahar, M. The Role of JAK-STAT Signaling Pathway and Its Regulators in the Fate of T Helper Cells. *Cell Commun. Signal.* **2017**, *15* (1), 1–13, doi:10.1186/s12964-017-0177-y.
 69. Carey, A. J.; Tan, C. K.; Ulett, G. C. Infection-Induced IL-10 and JAK-STAT. *Jak-Stat* **2012**, *1* (3), 159–167, doi:10.4161/jkst.19918.
 70. Lokau, J.; Schoeder, V.; Haybaeck, J.; Garbers, C. Jak-Stat Signaling Induced by Interleukin-6 Family Cytokines in Hepatocellular Carcinoma. *Cancers (Basel)*. **2019**, *11* (11), doi:10.3390/cancers11111704.
 71. Munang'andu, H. Intracellular Bacterial Infections: A Challenge for Developing Cellular Mediated Immunity Vaccines for Farmed Fish. *Microorganisms* **2018**, *6* (2), 33, doi:10.3390/microorganisms6020033.
 72. Mates, J. M. Effects of Antioxidant Enzymes in the Molecular Control of Reactive Oxygen Species Toxicology. *Toxicology* **2000**, *153* (1–3), 83–104.
 73. Brenot, A.; King, K. Y.; Janowiak, B.; Griffith, O.; Caparon, M. G. Contribution of Glutathione Peroxidase to the Virulence of *Streptococcus pyogenes*. *Infect. Immun.* **2004**, *72* (1), 408–413.
 74. Limón-Pacheco, J.; Gonsebatt, M. E. The Role of Antioxidants and Antioxidant-Related Enzymes in Protective Responses to Environmentally Induced Oxidative Stress. *Mutat. Res. Toxicol. Environ. Mutagen.* **2009**, *674* (1), 137–147, doi:https://doi.org/10.1016/j.mrgentox.2008.09.015.
 75. Margis, R.; Dunand, C.; Teixeira, F. K.; Margis-Pinheiro, M. Glutathione Peroxidase Family—an Evolutionary Overview. *FEBS J.* **2008**, *275* (15), 3959–3970.
 76. Abele, D.; Puntarulo, S. Formation of Reactive Species and Induction of Antioxidant Defence Systems in Polar and Temperate Marine Invertebrates and Fish. *Comp. Biochem. Physiol. part A Mol. Integr. Physiol.* **2004**, *138* (4), 405–415.
 77. Malandrakis, E. E.; Exadactylos, A.; Dadali, O.; Golomazou, E.; Kladoudatos, S.; Panagiotaki, P. Molecular Cloning of Four Glutathione Peroxidase (GPx) Homologs and Expression Analysis during Stress Exposure of the Marine Teleost *Sparus aurata*. *Comp. Biochem. Physiol. Part B Biochem. Mol. Biol.* **2014**, *168*, 53–61.
 78. Eslamloo, K.; Kumar, S.; Xue, X.; Parrish, K. S.; Purcell, S. L.; Fast, M. D.; Rise, M. L. Global Gene Expression Responses of Atlantic Salmon Skin to *Moritella viscosa*. *Sci. Rep.* **2022**, *12* (1), 4622.
 79. Bayne, C. J.; Gerwick, L. The Acute Phase Response and Innate Immunity of Fish. *Dev. Comp. Immunol.* **2001**, *25* (8–9), 725–743, doi:10.1016/S0145-305X(01)00033-7.
 80. Saurabh, S.; Sahoo, P. K. Lysozyme: An Important Defence Molecule of Fish Innate Immune System. *Aquac. Res.* **2008**, *39* (3), 223–239.

81. Grinde, B.; Lie, Ø.; Poppe, T.; Salte, R. Species and Individual Variation in Lysozyme Activity in Fish of Interest in Aquaculture. *Aquaculture* **1988**, *68* (4), 299–304.
82. Siwicki, A.; Studnicka, M. The Phagocytic Ability of Neutrophils and Serum Lysozyme Activity in Experimentally Infected Carp, *Cyprinus carpio* L. *J. Fish Biol.* **1987**, *31*, 57–60.
83. Biller, J. D.; Polycarpo, G. do V.; Moromizato, B. S.; Sidekerskis, A. P. D.; Silva, T. D. da; Reis, I. C. dos; Fierro-Castro, C. Lysozyme Activity as an Indicator of Innate Immunity of Tilapia (*Oreochromis niloticus*) When Challenged with LPS and *Streptococcus agalactiae*. *Rev. Bras. Zootec.* **2021**, *50*.
84. Janeway, C. A.; Medzhitov, R. Innate Immune Recognition. *Annu. Rev. Immunol.* **2002**, *20* (1), 197–216, doi:10.1146/annurev.immunol.20.083001.084359.
85. Turaga, P.; Wiens, G.; Kaattari, S. Bacterial Kidney Disease: The Potential Role of Soluble Protein Antigen(S). *J. Fish Biol.* **1987**, *31* (sa), 191–194, doi:10.1111/j.1095-8649.1987.tb05312.x.
86. Fredriksen, Å.; Endresen, C.; Wergeland, H. I. Immunosuppressive Effect of a Low Molecular Weight Surface Protein from *Renibacterium salmoninarum* on Lymphocytes from Atlantic Salmon (*Salmo salar* L.). *Fish Shellfish Immunol.* **1997**, *7* (4), 273–282, doi:10.1006/fsim.1997.0082.
87. Kaattari, S. L.; Piganelli, J. D. Immunization with Bacterial Antigens: Bacterial Kidney Disease. *Dev. Biol. Stand.* **1997**, *90*, 145–152.
88. Rømer Villumsen, K.; Dalsgaard, I.; Holten-Andersen, L.; Raida, M. K. Potential Role of Specific Antibodies as Important Vaccine Induced Protective Mechanism against *Aeromonas salmonicida* in Rainbow Trout. *PLoS One* **2012**, *7* (10), e46733, doi:10.1371/journal.pone.0046733.
89. Jansson, E.; Ljungberg, O. Detection of Humoral Antibodies to *Renibacterium salmoninarum* in Rainbow Trout *Oncorhynchus mykiss* and Atlantic Salmon *Salmo salar* Challenged by Immersion and in Naturally Infected Populations. *Dis. Aquat. Organ.* **1998**, *33* (2), 93–99.

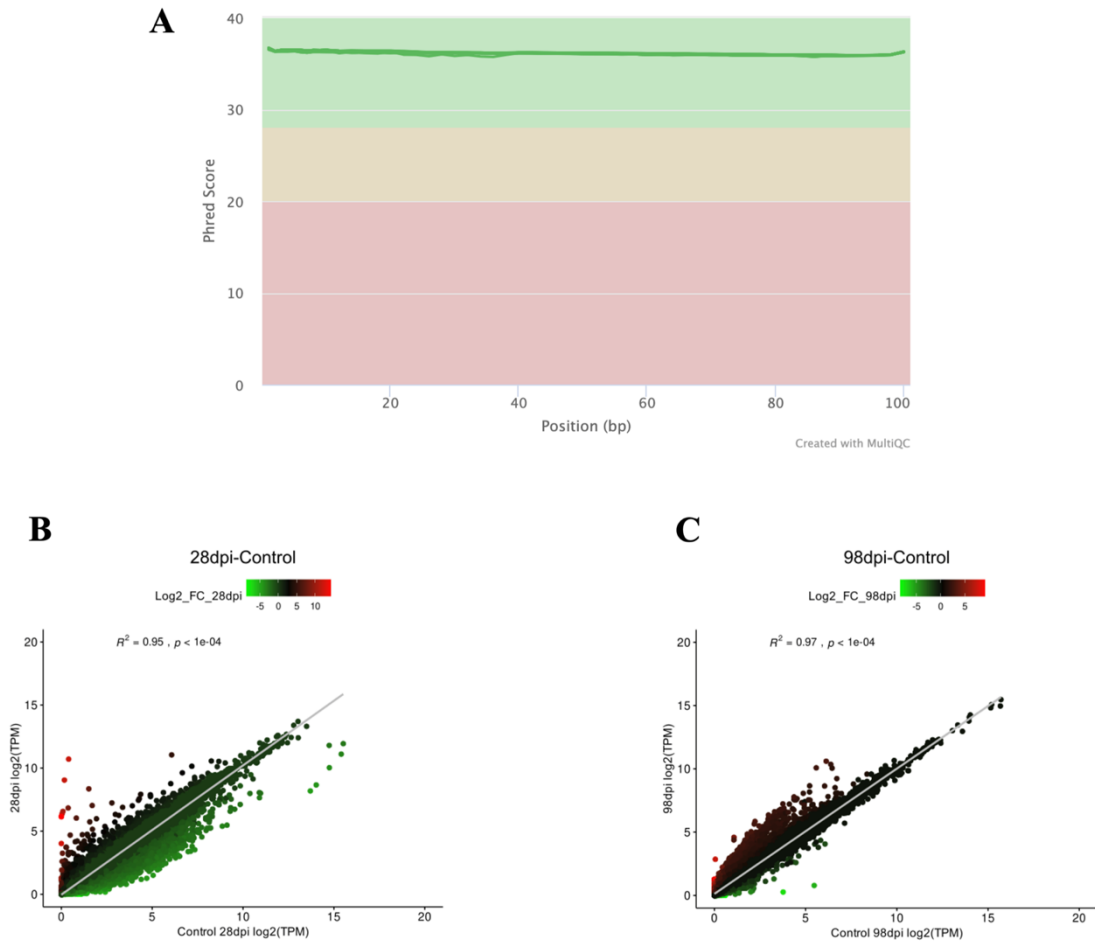
4.8. Supplementary Materials

Supplementary Table S4.1. Bioanalyzer data for the RNA samples ($n = 12$) used in the transcriptomic profiling of the lumpfish head kidney infected with *Renibacterium salmoninarum* at 28 and 98 days post-infection.

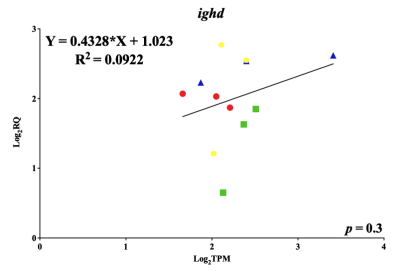
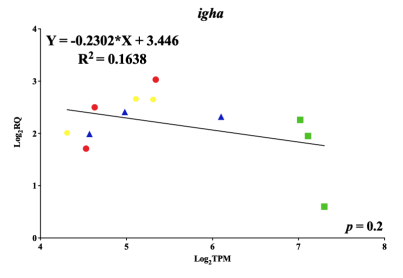
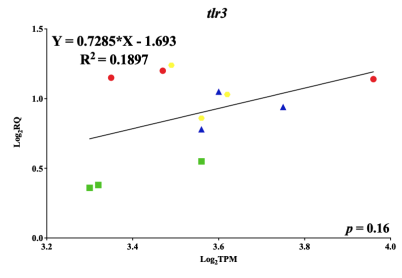
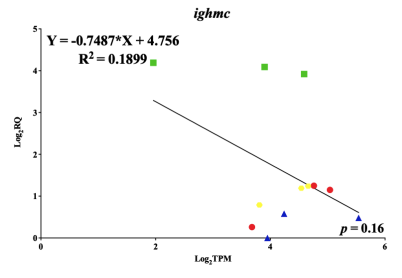
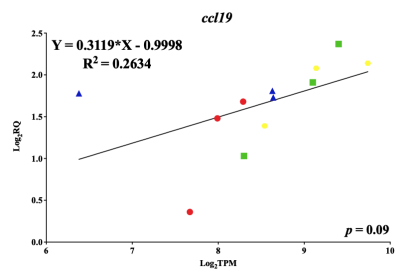
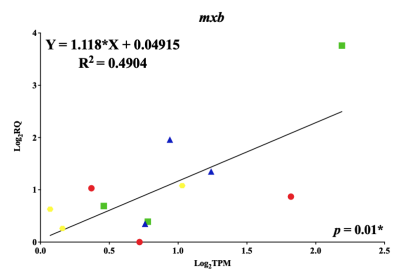
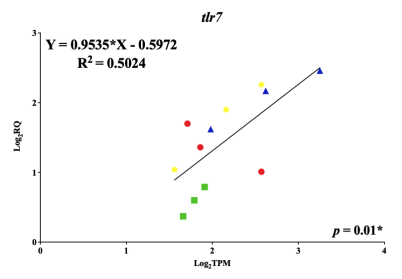
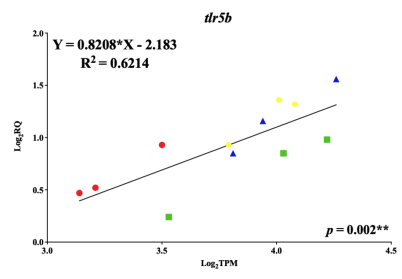
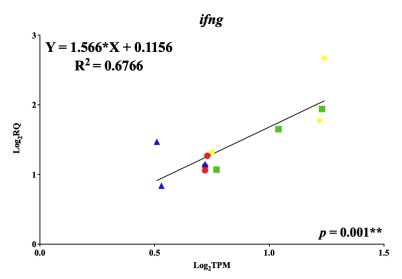
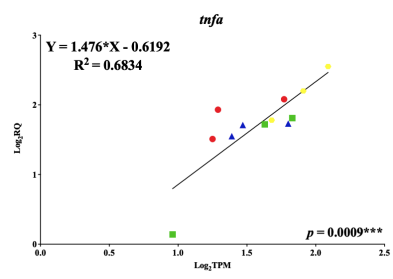
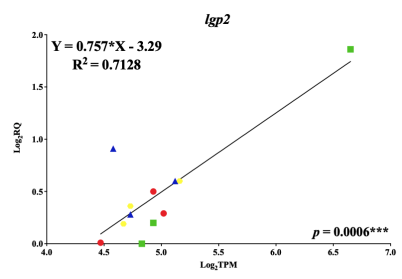
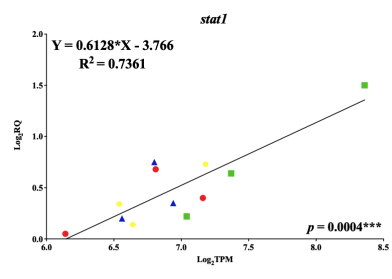
Samples ($n = 12$)	28 days-post-infection			98 days-post-infection		
	Electropherogram	28S/18S	RIN	Electropherogram	28S/18S	RIN
Control-Fish-1		0.87	8.4		0.80	8.7
Control-Fish-2		1.11	8.6		1.30	8.4
Control-Fish-3		0.76	8.7		1.32	8.2
Infected-Fish-1		1.23	8.4		1.23	8.4
Infected-Fish-2		1.34	8.6		1.23	8.7
Infected-Fish-3		1.40	8.6		1.18	8.2

Supplementary Table S4.2. Mapping Statistics of the RNA-seq data

Experimental conditions	Number of reads	Number of reads after trimming	Percentage (%) trimmed	Mapped reads	Percentage (%) reads mapped
Control fish 1 - 28 dpi	108,895,852	107,815,264	99.01	92,040,329	85.74
Control fish 2 - 28 dpi	104,988,352	103,432,706	98.52	88,252,280	85.91
Control fish 3 - 28 dpi	85,396,598	84,183,223	98.58	71,520,885	85.51
Infected fish 1 - 28 dpi	505,391,282	497,704,706	98.48	425,051,491	86.00
Infected fish 2 - 28 dpi	134,363,278	133,050,059	99.02	114,203,665	86.21
Infected fish 3 - 28 dpi	635,762,188	628,900,339	98.92	539,495,474	86.20
Control fish 1 - 98 dpi	84,443,932	83,464,290	98.84	71,278,852	85.86
Control fish 2 - 98 dpi	141,732,782	140,477,843	99.11	120,977,190	86.45
Control fish 3 - 98 dpi	104,924,338	103,299,974	98.45	88,953,090	86.72
Infected fish 1 - 98 dpi	114,646,580	113,224,414	98.76	96,560,104	85.76
Infected fish 2 - 98 dpi	85,096,384	83,868,468	98.56	70,730,675	84.90
Infected fish 3 - 98 dpi	123,766,998	121,728,135	98.35	103,870,732	85.98



Supplementary Figure S4.1. RNA-seq data quality. Sequence quality histogram with the mean quality scores from the MultiQC analysis. Scatter plot of RNA-seq expression under control and *R. salmoninarum*-infected conditions at **A.** 28 dpi and **B.** 98 dpi. Each dot represents a gene; where red, green and black represent up-, down-regulated and non-differentially expressed genes, respectively.



Supplementary Figure S4.2. Gene expression correlation (mid to low) between qPCR and RNA-seq data for 12 genes of interest. RNA-seq data are presented as \log_2 TPM (X axis). qPCR data are represented as \log_2 RQ (Y- axis). The red circles represent control samples at 28 dpi; the green squares represent *R. salmoninarum* infected samples at 28 dpi; the blue triangles represent control samples at 98 dpi; the yellow hexagons represent *R. salmoninarum* infected samples at 98 dpi. Each symbol is an average of the three fish at a particular time point in head kidney tissue. The linear regression equation, correlation coefficient (R^2) and level of significance ($p < 0.05^*$, $p < 0.01^{**}$, $p < 0.001^{***}$) are indicated for each gene expression correlation.

Chapter 5. Role of Riboflavin Biosynthesis Gene Duplication and Transporter in *Aeromonas salmonicida* Virulence in Lumpfish

The research described in Chapter 5 was published in *Virulence* as: Gnanagobal, H., Cao, T., Hossain, A., Vasquez, I., Chakraborty, S., Chukwu-Osazuwa, J., Boyce, D., Jesus Espinoza, M., García-Angulo, V. A. and Santander. J. (2023). Role of Riboflavin Biosynthesis Gene Duplication and Transporter in *Aeromonas salmonicida* Virulence in Marine Teleost Fish. *Virulence*, 14(1), 2187025. DOI: [10.1080/21505594.2023.2187025](https://doi.org/10.1080/21505594.2023.2187025).

5.1. Abstract

Active flavins derived from riboflavin (vitamin B₂) are essential for life. Bacteria biosynthesize riboflavin or scavenge it through uptake systems, and both mechanisms may be present. Because of riboflavin's critical importance, the redundancy of riboflavin biosynthetic pathway (RBP) genes might be present. *Aeromonas salmonicida*, the etiological agent of furunculosis, is a pathogen of freshwater and marine fish, and its riboflavin pathways have not been studied. This study characterized the *A. salmonicida* riboflavin provision pathways. Homology search and transcriptional orchestration analysis showed that *A. salmonicida* has a main riboflavin biosynthetic operon that includes *ribD*, *ribE1*, *ribBA*, and *ribH* genes. Outside the main operon, putative duplicated genes *ribA*, *ribB* and *ribE2*, and a *ribN* riboflavin importer encoding gene were found. Monocistronic mRNA *ribA*, *ribB*, and *ribE2* encode for their corresponding functional riboflavin biosynthetic enzyme. While the product of *ribBA* conserved the RibB function, it lacked the RibA function. Likewise, *ribN* encodes a functional riboflavin importer. Transcriptomics analysis indicated that external riboflavin affected the expression of a relatively small number of genes, including a few involved in iron metabolism. *ribB* was downregulated in response to external riboflavin, suggesting negative feedback. Deletion of *ribA*, *ribB*, and *ribE1* showed that these genes are required for *A. salmonicida* riboflavin biosynthesis and virulence in Atlantic lumpfish (*Cyclopterus lumpus*). *A. salmonicida* riboflavin auxotrophic attenuated mutants conferred low protection to lumpfish against virulent *A. salmonicida*. Overall, *A. salmonicida* has multiple riboflavin

endowment forms, and duplicated riboflavin provision genes are critical for *A. salmonicida* infection.

Keywords: Riboflavin biosynthesis, riboflavin transport, gene duplication, *Aeromonas salmonicida* virulence

5.2. Introduction

Riboflavin or vitamin B₂ is an essential micronutrient for all forms of life. Riboflavin derivatives, mainly flavin mononucleotide (FMN) and flavin adenine dinucleotide (FAD) (collectively known as flavins), are canonical cofactors for intracellular flavoprotein-mediated reduction/oxidation (RedOx) reactions and play a crucial role in oxidative metabolism [1,2]. Flavins may also be secreted to participate in extracellular RedOx processes related to bacterial physiology, such as iron reduction, electron transfer for extracellular respiration, the establishment of symbiotic interactions, and quorum-sensing signalling [3–6]. In pathogenic bacteria, riboflavin biosynthesis may also be crucial for virulence during infection [7].

Essential micronutrients are required for successful pathogen infection. Hosts may employ nutritional immunity to limit the availability of micronutrients, such as riboflavin, from systemic circulation and tissues [8,9]. For instance, approximately 60% of the riboflavin in the human plasma is withdrawn as a result of the acute phase response of the host to combat infection [10]. In return, pathogens could either synthesize this vitamin *de novo* through the riboflavin biosynthetic pathway (RBP) or scavenge it from host tissues using flavin transport systems to ensure their proliferation and survival [11]. Energy-wise, riboflavin biosynthesis is more expensive than the uptake [12]. For instance, 25 molecules

of ATP are required to synthesize 1 mole of riboflavin, but depending on the transport system, only two or even fewer molecules of ATP are required for uptake [4,13,14]. The RBP produces riboflavin from precursors guanosine-5-triphosphate (GTP) and ribulose-5-phosphate using the activities of five enzymes, GTP cyclohydrolase II (RibA according to the Gram-negative bacteria nomenclature), 3,4-dihydroxy-2-butanone-4-phosphate (3,4-DHBP) synthase (RibB), a bifunctional pyrimidine deaminase/reductase (RibD), riboflavin synthase (RibE) and 6,7-dimethyl-8-ribityllumazine (lumazine) synthase (RibH) [2,11,15–17]. Several bacterial riboflavin uptake systems have been described, and in some species, they coexist with the RBP [11,17,18]. Among them, the RibN transporter is present in Gram-negative proteobacteria such as *Vibrio cholerae* and *Rhizobium leguminosarum* [11,18].

Riboflavin provision pathways in bacteria appear to respond to species-specific metabolic needs of riboflavin [5,7]. When environmental riboflavin is present, riboflavin transporters may substitute for the RBP in riboflavin prototrophs [19–21]. Nonetheless, each riboflavin provision component may have specific, non-redundant functions. For example, in pathogens like *Listeria monocytogenes*, the transporter has been associated with the uptake of specific flavin species during host colonization [22]. So far, little is known about how intraspecies riboflavin supply pathways are coordinated to meet the flavin requirements in bacteria.

Significant differences exist amongst bacteria in the transcriptional organization of the RBP genes. Some species cluster all the RBP genes into a single operon, whereas other species disperse the RBP genes along the chromosome in various transcriptional units [11]. The expression of RBP and transporter genes may be regulated by the FMN riboswitch, a

genetic element found upstream of several *rib* operons and monocistronic *rib* genes [18,23–27]. FMN binds to the aptamer portion of the FMN riboswitch, inhibiting the transcription and or translation of the downstream genes [2,23].

In bacteria, some RBP enzymes may have duplicate or multiple gene copies. These gene duplications provide bacteria more flexibility in how they genetically manage their riboflavin supply [11]. In general, gene duplication events that are maintained in a population have benefits that surpass the fitness cost of carrying the duplication [28]. Intra-genome conserved multiple gene copies may confer adaptive advantages to the bacteria, such as improvements in their ability to adjust to changing environmental conditions (i.e., *ex vivo* and *in vivo*) [29]. Therefore, the extra copies of the RBP genes may have specific functions and provide adaptive benefits [11]. For instance, *Brucella abortus* has a second *ribH* gene outside the main RBP operon that is directly linked to intracellular survival and host colonization [7]. Overall, the variation in the assortment of copies of RBP genes and riboflavin importers may impact bacterial virulence and physiology.

The bacterial riboflavin provision pathways have been studied in some important human and animal pathogens, and the genes that encode for their RBP and riboflavin transporters have been identified [11,30–32]. However, this knowledge is lacking in marine pathogens of fish like *A. salmonicida*, which causes significant economic losses in finfish aquaculture. *A. salmonicida* is the etiological agent of furunculosis in various fish species [33,34], such as lumpfish (*Cyclopterus lumpus*), which is a cleaner fish employed to biologically control the sea lice (*Lepeophtheirus salmonis*) infestations in Atlantic salmon (*Salmo salar*) sea cages [35–38]. As a psychrotropic waterborne pathogen, *A. salmonicida* infects freshwater and marine fish [33,34]. The economic importance, suitability for genetic

manipulation, and relatively reproducible *in vivo* infection make *A. salmonicida* a good model organism to study psychrotropic marine pathogenesis [34,39–42]. Vaccines and antimicrobials have often been employed to prevent or control *A. salmonicida* disease outbreaks in aquaculture [43,44]. However, furunculosis still persists in some cultured fish species due to low vaccine or antimicrobial efficacy [45,46]. A better understanding of *A. salmonicida* physiology and virulence mechanisms is needed to design more adequate treatments or preferably, efficient vaccines to avoid its pernicious effects in aquaculture and spillbacks to wild fish. Given the importance and divergent effects of riboflavin in bacteria, in this study, I aimed to identify the riboflavin provision systems in *A. salmonicida* and their role in different physiological traits and virulence.

In the present study, I determined the presence and characterized the transcriptional organization of riboflavin supply pathways in *A. salmonicida* using genomic information and experimental characterization. A composite RBP featuring redundant functions and riboflavin uptake are present in *A. salmonicida*. The role of the different riboflavin provision components in virulence, the general regulatory effects of external riboflavin, and the possible use of flavin-impaired mutants as attenuated vaccines were also explored. Overall, this study characterizes the riboflavin provision pathways of *A. salmonicida* and starts elucidating their contribution to pathogenicity in a cold water marine teleost.

5.3. Materials and Methods

5.3.1. Bacterial strains, plasmids, media and reagents

A. salmonicida wild-type J223 strain isolated from Atlantic salmon was used in this study [40] (Table 5.1). This isolate served as the source for all genetically defined *A.*

salmonicida mutants constructed in this study (Table 5.1). Table 5.1 includes information about bacterial strains and plasmids. Media for bacteriology were from Difco (Franklin Lakes, NJ, USA). Sigma-Aldrich (St Louis, MO, USA) supplied the antibiotics, riboflavin, and reagents. Trypticase Soy Broth (TSB), M9 minimal media adapted for *A. salmonicida* growth (33 mM Na₂HPO₄, 22 mM KH₂PO₄, 20 mM NH₄Cl, 10mM NaCl, 1 mM MgSO₄, 0.1 mM CaCl₂, 10 mM glucose, 0.25 mM L-arginine and 0.25 mM L-methionine) [47], and Luria Bertani (LB) broth (tryptone 10 g; yeast extract 5 g; NaCl 10 g; dextrose 1 g; double distilled water, 1 L) [48] were routinely used. The media were supplemented as necessary with riboflavin (2 or 500 µM) [21], 1.5% agar, 10 % sucrose, Congo red (50 µg/mL), chloramphenicol (Cm; 25 µg/mL), kanamycin (Km; 50 µg/mL), gentamicin (Gm; 10 µg/mL), ampicillin (Amp; 100 µg/mL) or diaminopimelic acid (DAP; 50 µg/mL). *A. salmonicida* J223 and mutant strains were routinely cultured in TSB or modified M9 minimal media at 15 °C with aeration (180 rpm). *Escherichia coli* wild-type and mutant strains were cultured in LB at 37 °C with aeration (180 rpm). Spectrophotometry and/or agar plate counting were used to track bacterial growth. Primers used in this study (Supplementary Tables S5.1-S5.3) were synthesized by Integrated DNA Technologies (IDT, San Diego, CA, USA). Restriction endonucleases were from New England Biolabs (Whitby, ON, Canada). All PCR assays were conducted using GoTaq Green Master Mix from Promega (Madison, WI, USA). T4 ligase and T4 DNA polymerase were from Promega (Madison, WI, USA). Plasmid DNA was isolated, and gel DNA fragments and PCR products were purified using Qiagen products (Germantown, MD, USA).

5.3.2. *In-silico* characterization of riboflavin supply pathways and genes in *A. salmonicida*

A. salmonicida A449 and J223 genomes from the National Center for Biotechnology Information (NCBI) [49] and Kyoto Encyclopedia of Genes and Genomes (KEGG) [50] public databases were utilized for the search of RBP and transport genes and their organization within the genome. The RibEx tool was utilized to identify putative FMN riboswitches [51]. Amino acid sequences of the RBP proteins and their duplicated or multiplied copies were obtained in FASTA format from NCBI. Protein sequence alignments were performed in Jalview (Version 2.11.2.5) platform (www.jalview.org) [52] using web service function for Clustal Omega Multiple Sequence Alignment Program with default parameters, and sequence similarity values (i.e., percent identity and percent similarity) were obtained. Aligned sequences were rendered using the web-based interface of Easy Sequencing in PostScript (ESPrnt) [53]. The tridimensional (3D) protein structures of the RBP enzymes and their additional copies were modeled in HHpred [54] and visualized in Visual Molecular Dynamics (VMD; Version 1.9.1) [55]. Structure predictions for the duplicated enzymes were conducted using trRosetta modeling (<https://yanglab.nankai.edu.cn/trRosetta/>) [56]. 3D protein structures were compared and overlapped in VMD using the Structural Alignment of Multiple Proteins (STAMP) tool, and the structural homology values (Q_H) were generated.

Table 5.1. List of strains and plasmids used in this study

Strains/ plasmids	Characteristics	Source
<i>Aeromonas salmonicida</i>		
J223	Wild type	[40]
J412	$\Delta ribA$; J223 derivate	This study
J413	$\Delta ribB$; J223 derivate	This study
J414	$\Delta ribBA$; J223 derivate	This study
J415	$\Delta ribE1$; J223 derivate	This study
J416	$\Delta ribE2$; J223 derivate	This study
J417	$\Delta ribN$; J223 derivate	This study
J418	$\Delta ribA-\Delta ribE1$; J223 derivate	This study
<i>Escherichia coli</i>		
$\chi 7213$	<i>thr-1 leuB6 fhuA21 lacY1 glnV44 recA1 $\Delta asdA4$ $\Delta(zhf-2::Tn10)$ thi-1 RP4-2-Tc::Mu [λpir]; Km^r Tet^s Amp^s DAP⁻</i>	[57]
$\chi 7232$	<i>endA1 hsdR17 (r_k⁻, m_k⁺) supE44 thi-1 recA1 gyrA relA1 $\Delta(lacZYA-argF)$ U169 λpir deoR ($\phi 80dlac\Delta(lacZ)M15$); Nal^r UV^s Thi⁻ Lac⁻</i>	[58]
BW25113	Wild-type <i>Escherichia coli</i>	[59]
$\Delta ribB$	BW25113 $\Delta ribB::kan$	[18]
$\Delta ribA$	<i>E. coli</i> DH5 α $\Delta ribA::cat$	This study
Plasmids		
pR112	5173 bp, Suicide vector Cm, <i>sacB</i> , <i>oriV</i> , <i>oriT</i>	[58]
pMEG-375	8142 bp, Suicide vector, Cm, Amp, <i>lacZ</i> , R6K <i>ori</i> , <i>mob incP</i> , <i>sacR sacB</i>	[58]
TOPO	3.9 kb, pUC ori, Km ^r , Amp ^r	Invitrogen
pEZ323	pR112 derivate; $\Delta ribA$	This study
pEZ324	pR112 derivate; $\Delta ribB$	This study
pEZ325	pR112 derivate; $\Delta ribBA$	This study
pEZ326	pMEG-375 derivate; $\Delta ribE1$	This study
pEZ327	pMEG-375 derivate; $\Delta ribE2$	This study
pEZ328	pR112 derivate; $\Delta ribN$	This study
pEZ329	pTOPO- <i>ribBA</i> -Asal; Plasmid bearing <i>ribBA</i> of <i>A. salmonicida</i> , P _{lac} - <i>ribBA</i> , amp ^r Km ^r	This study
pEZ330	pTOPO- <i>ribB</i> -Asal; Plasmid bearing <i>ribB</i> of <i>A. salmonicida</i> , P _{lac} - <i>ribB</i> , amp ^r Km ^r	This study

pEZ331	pTOPO- <i>ribN</i> -Asal; Plasmid bearing <i>ribN</i> of <i>A. salmonicida</i> , P _{lac} - <i>ribN</i> , amp ^r Km ^r	This study
pKD46	Plasmid expressing the λ -red recombinase system, amp ^r	[59]
pKD3	Template plasmid bearing kanamycin resistance cassette, Km ^r	[59]
pG- <i>ribA</i> -Eco	Plasmid bearing <i>ribA</i> of <i>E. coli</i>	This study
pG- <i>ribB</i> -Vch	Plasmid bearing <i>ribB</i> of <i>Vibrio cholerae</i>	[21]

5.3.3. Experimental characterization of riboflavin supply pathways in *A. salmonicida*.

5.3.3.1. Bacterial growth in minimal media

Three milliliters of TSB were inoculated with a single colony of *A. salmonicida* J223 and incubated at 15 °C overnight in a roller drum (TC-7, New Brunswick Scientific Co, San Diego, NJ, USA). Then, 100 µL of the *A. salmonicida* overnight culture were transferred into 3 mL of modified M9 minimal media and allowed to grow for 2-3 days at 15 °C in a roller drum. Next, 30 µL of this minimal media culture were transferred into 3 mL of fresh minimal media and allowed to grow for another 2-3 days at 15 °C in a roller drum. Finally, the minimal media culture was centrifuged at 10,000 rpm for 2 minutes at 4 °C, the supernatant was discarded, the pellet was washed 3 times with minimal medium, and resuspended in 1 mL fresh minimal media. Three-hundred microliters of the resuspended cells were inoculated into three 50 mL individual flasks having 30 mL of fresh minimal media. Cultures were incubated at 15 °C with aeration (180 rpm) in an orbital shaker (MaxQ 4000, Thermo Fisher Scientific, MA, USA) until an optical density (OD_{600 nm}) of 0.7 (~1x10⁸ Colony Forming Units per mL (CFU/mL)). Next, these triplicate cultures were subjected to RNA extraction using established protocols [60].

5.3.3.2. Total RNA extraction, Reverse Transcription, and Polymerase Chain Reaction (RT-PCR)

Once the *A. salmonicida* cultures ($n = 3$) reached the desired OD_{600 nm}, cells were extracted by centrifugation (6000 rpm for 10 min) at 4 °C and twice washed with phosphate-buffered saline (PBS, pH 7.0; 136 mM NaCl, 2.7 mM KCl, 10.1 mM Na₂HPO₄, 1.5 mM KH₂PO₄) [61]. The cell pellets were used for RNA extraction. TRIzol reagent (Invitrogen) was used to extract total RNA, and the RNeasy MinElute Cleanup Kit was used to purify

it (Qiagen, Mississauga, ON, Canada) using the manufacturer's guidelines. RNA extracts were digested with TURBO DNA-free™ Kit (Invitrogen, Carlsbad, CA, USA). Purified RNA samples were measured using a Genova Nano microvolume spectrophotometer (Jenway, UK), and 1% agarose gel electrophoresis was used to verify the samples' integrity [61].

To experimentally depict the transcriptional orchestration of the *A. salmonicida* riboflavin supply genes, an RT-PCR was performed, as explained before by Cisternas et al. (2017). cDNA was synthesized using SuperScript Vilo IV Master Mix with reverse transcriptase (Invitrogen) as directed by the manufacturers' instructions with 1 µg RNA per reaction. PCR assays were carried out on these cDNAs using the primers (Supplementary Table S5.1) that amplify the putative gene junctions. For each sample ($n = 3$), a control reaction without reverse transcriptase (negative control) was added. Positive controls included PCR reactions on the *A. salmonicida* J223 genomic DNA with respective primers. Following the amplifications, the putative gene junctions tested were visualized in 1% agarose gel electrophoresis [61]. Positive PCR amplifications in this approach imply the joint of coding sequences in the same messenger RNA (mRNA), therefore, the genes are adjacent to each other and form an operon [21].

5.3.4. *A. salmonicida* gene functionality assays

5.3.4.1. Construction of complementation plasmids with *A. salmonicida* *ribB*, *ribBA*, *ribN*

The *A. salmonicida* genes *ribB*, *ribBA*, and *ribN* were independently cloned into high copy number plasmid (pCR™2.1-TOPO™) (Table 5.1) under P_{lac} control at the *AdhI* restriction site. Supplementary Table S5.3 provides the list of primers utilized to amplify the

corresponding genes under P_{lac} control. The resultant plasmids were used to complement the *E. coli* riboflavin auxotrophic mutant strains (Table 5.1).

5.3.4.2. Construction of *E. coli* $\Delta ribA$ mutant and complementation plasmid

The *E. coli* $\Delta ribA$ null mutant was constructed according to the mutagenesis by homologous recombination with PCR fragments protocol described before [59]. *E. coli* BW25113 bearing pKD46, previously grown at 30°C with arabinose, was electroporated with a PCR product obtained with primers *E. coli-ribA*-H1P1 and *E. coli-ribA*-H2P2 (Supplementary Table S5.3) and the pKD3 plasmid as template DNA. Candidate recombinant mutants were selected in LB plates with Cm and incubated overnight at 42 °C. The candidates obtained were screened by PCR for the replacement of *ribA* by the Km resistance cassette using primers flanking the recombination site *E. coli*-RibA-Fw and *E. coli*-RibA-Rv (Supplementary Table S5.3).

The plasmid pGEcoribA to complement *E. coli ribA* mutants was constructed by ligating a PCR product obtained with the set of primers *E. coli*-RibA-Fw / *E. coli*-RibA-Rv and wild-type *E. coli* genomic DNA in pGEM T Easy (Promega) in accordance with the manufacturer's protocol.

5.3.4.3. Functional complementation analysis in *E. coli* heterologous model

After transferring the complementing plasmid vectors into *E. coli* riboflavin auxotrophic mutants of $\Delta ribA$ and $\Delta ribB$ (Table 5.1), the phenotypic rescue of the *E. coli* mutants was evaluated either in LB or M9 minimal media agar plates in the presence and absence of riboflavin, to assess the functional complementation of riboflavin biosynthesis. Briefly, overnight cultures of *E. coli* wild-type and its derivative mutants and complemented strains grown in LB with 500 μ M riboflavin were washed twice with plain

LB or M9 and resuspended in fresh media without added riboflavin. These cultures were then serially diluted, and 5 μ L were spotted into LB or minimal media plates supplemented with 500 μ M riboflavin, 2 μ M riboflavin or without riboflavin. Plates were incubated at 37 $^{\circ}$ C overnight to observe growth.

5.3.5. *A. salmonicida* transcriptomics and qPCR analyses

5.3.5.1. Bacterial growth in minimal media with and without riboflavin, RNA extraction, and cDNA synthesis

Fifty milliliters of *A. salmonicida* wild-type J223 cultures grown with (2 μ M) and without riboflavin at 15 $^{\circ}$ C with shaking (180 rpm) to an OD_{600 nm} of 0.7 were subjected to TRIzol lysis, RNA extraction ($n = 6$), column-purification and DNase treatment, as previously described [60]. These RNA samples were used for RNA sequencing and RT-qPCR (Supplementary Figure S5.1). High-Capacity cDNA Reverse Transcription Kit (Thermofisher, Foster City, CA, USA) was used to obtain first-strand cDNA templates for qPCR from 1 μ g purified RNA in 20 μ L reactions, as instructed by the manufacturer.

5.3.5.2. Library preparation and RNA sequencing

For each experimental condition (Control ($n = 3$) and riboflavin-supplemented ($n = 3$) groups), there were 3 biological replicates (Total $n = 6$). Genome Quebec, Canada carried out the commercial library construction and RNA sequencing. Briefly, RNA quality was assessed using a Bioanalyzer 2100 (Agilent). rRNA was depleted using NEBNext[®] rRNA Depletion Kit (Bacteria). cDNA libraries were constructed using the adapters and primers of NEBNext[®] Multiplex Oligos for Illumina[®]. Sequencing was performed on a NovaSeq 6000 (Illumina) platform with a 100 bp paired-end protocol. Raw sequencing data have

been submitted to the NCBI Bio Project database under the accession number PRJNA909183.

5.3.5.3. RNA-seq data analyses

Data from RNA-seq were analyzed in CLC Genomics Workbench v22.0 (CLCGWB; Qiagen, Hilden, Germany) using comparable settings as those previously disclosed [62,63]. Low quality reads were removed, and clean paired reads were generated. The trim read tool in CLCGWB was used to trim the adapters with the default criteria. Quality control visualization of the reads was performed using FastQC (<https://www.bioinformatics.babraham.ac.uk/projects/fastqc/>) and multiQC [64] before and after trimming. The RNA-seq analysis program was used by CLCGWB to map good-quality trimmed reads to the *A. salmonicida* genome (Accession: PRJNA310296). The gene abundance of mapped reads was quantified and normalized using RSEM and eXpress approaches [65,66]. The transcript per million reads (TPM) values were then determined using the counts ascribed to each transcript [67]. A global correlation analysis, using the Pearson method to quantify the correlation, was performed on the Log₂ TPM values (x + 1) for each gene individually under the presence and absence of riboflavin conditions. Abundance data were consequently exposed to differential expression analysis in CLCGWB with negative binomial general linear model-based (GLM) normalization [68]. Biologically relevant differentially expressed genes (DEGs) were identified using the standard cut-off values of log₂ fold-change (FC) $\geq |1|$ and false discovery rate (FDR) $p \leq 0.05$. Selected DEGs were subjected to hierarchical cluster analysis in CLCGWB and visualized in the heat map. The expression fold-change values (in terms of TPM values) of significant DEGs from control and riboflavin-supplemented groups were compared and

visualized in bar plots using GraphPad Prism 7.0 (GraphPad Software, La Jolla, CA, USA). Operon mapper was used to predict whether the contiguous DEGs formed operons (http://biocomputo.ibt.unam.mx/operon_mapper/) [69].

5.3.5.4. Gradient PCR

Primers used for each gene (i.e., *ribA*, *ribBA*, *ribB*, *ribD*, *ribE1*, *ribE2*, *ribH*, and *ribN*) for the real-time quantitative PCR (RT-qPCR) analysis are stated in Supplementary Table S5.2. Gradient PCR was carried out to determine the ideal annealing or melting temperature (T_m) for each primer set, as described by Connors et al. (2019). Finally, specific amplicons for each primer set were visualized in 1% agarose gel. Gradient PCR demonstrated that all RT-qPCR primers (Supplementary Table S5.2) amplified a single amplicon at an ideal T_m of 55-60 °C (Supplementary Figure S5.2A).

5.3.5.5. RT-qPCR

To examine how the extracellular riboflavin affects the expression of the transcriptional units that encode for riboflavin supply pathways, the RT-qPCR amplifications were carried out, as previously mentioned [60]. Primer pairs for riboflavin supply genes were designed, and the standard curve approach was used to determine the primer efficiency and confirm the primer specificity (Supplementary Table S5.2). A cDNA pool made from control ($n = 3$) and riboflavin-supplemented (2 μ M; $n = 3$) *A. salmonicida* cultures in minimal media was used to analyze the primer efficiencies. Pooled cDNA was serially diluted with a 5-point 1:3 dilution series beginning at 20 ng/ μ L. Amplification efficiencies were estimated according to Pfaffl, 2001 [70]. Information on RT-qPCR primers are listed in Supplementary Table S5.2. Each pair of primers' melt curves had a

single peak, proving that they did not produce dimers and that they were specific for a single amplicon (Supplementary Figure S5.2B).

To select two endogenous control genes (i.e., reference genes) for RT-qPCR, 5 genes (i.e., *hfq*, *era*, *rpoB*, *recA*, and *fabD*) that had been reported in *A. salmonicida* to normalize transcriptional expression data were analyzed [60]. Raw threshold cycle (C_T) values of all 6 samples were determined in triplicates for each of these genes using cDNA equivalent to the input total RNA of 20 ng. The observed C_t value ranges were consistent and acceptable independent of the condition being tested (Supplementary Figure S5.2C). The geNorm tool in the Ref-Finder open-access portal (<http://www.heartcure.com.au/reffinder/>) was used to examine the stability of these genes' expression [71]. *era* and *hfq* (geNorm M = 0.223) were chosen as the two endogenous controls based on their constitutive expression.

All RT-qPCR reactions were performed using cDNA (5 ng/ μ L) and Power SYBR™ Green Master Mix (Applied Biosystems, Carlsbad, CA, USA) in QuantStudio 3 (Applied Biosystems) with the experimental qPCR parameters described in Connors et al. (2019). Each experimental condition was evaluated with biological ($n = 3$) and technical ($n = 3$) triplicates. Relative gene expression levels were estimated using the comparative $2^{-\Delta\Delta C_t}$ method [72,73].

To further evaluate the correlation between gene expression levels from RNA-seq and RT-qPCR data, a simple linear regression analysis was performed between the normalized counts (TPM) of RNA-seq data (Log_2 TPM on the X axis) and the C_t values from RT-qPCR (Log_2 C_t on the Y axis), and the Pearson correlation coefficients (r^2 ; $p < 0.05$) were calculated.

5.3.6. *A. salmonicida* mutants' construction and characterization

In-frame deletion of *ribA*, *ribB*, *ribBA*, *ribE1*, *ribE2*, *ribN* genes in *A. salmonicida* was accomplished using recombinant suicide vectors (Table 5.1) bearing the joined flanking regions, as previously reported [40,74]. A deletion with the ATG start codon but without the TAG or TAA stop codon is contained in the defined deletion mutations. Methods for PCR, DNA isolation, DNA cloning, restriction enzyme digestion, and plasmid construction are standard [61]. Supplementary Table S5.3 contains a list of all primers used for the mutant construction. Primer sets F1-R1 and F2-R2 were designed to amplify the up- and down-stream flanking regions, respectively. The flanking regions were amplified from *A. salmonicida* J223. Overlapping PCR was used to ligate the flanking regions. The PCR products containing in-frame deletion fragments of the selected genes were cloned into either pR112 or pMEG375 (Table 5.1) that had been digested with *Sph*I and *Xba*I. To construct *A. salmonicida* single deletion mutants ($\Delta ribA$, $\Delta ribB$, $\Delta ribBA$, $\Delta ribE1$, $\Delta ribE2$, $\Delta ribN$), the suicide plasmid was transferred from *E. coli* χ 7213 to *A. salmonicida* J223 by conjugation. To construct *A. salmonicida* double mutant ($\Delta ribA$ - $\Delta ribE1$), the suicide plasmid carrying in-frame deletion fragment of *ribA* gene (i.e., pEZ323; Table 5.1) was conjugationally transferred from *E. coli* χ 7213 to *A. salmonicida* J415 (i.e., $\Delta ribE1$). The transconjugants, in which the single-crossover plasmid insertions homologously recombined into the chromosome, were selected on TSA plates having Cm. The second recombination within homologous regions (i.e., allelic exchange) that results in the loss of suicide vector was selected by employing the “*sacB*-based sucrose sensitivity counter-selection system” adapted to *A. salmonicida* [40,75,76]. The colonies were chosen for Cm^r and screened by PCR with the use of primers F1 and R2.

Growth curve and biochemical profile assays were performed to characterize the phenotypic and biochemical differences in bacterial physiology between *A. salmonicida* J223 wild-type and mutant strains. Growth of *A. salmonicida* strains was evaluated in minimal media in the presence and absence of riboflavin at 15 °C in triplicates. Briefly, *A. salmonicida* strains were grown in 3 mL of M9 minimal media as previously described in section 2.3.1. Three-hundred microliters of these cultures were inoculated into 100 mL flasks containing 50 mL of fresh minimal media with and without riboflavin (2 µM) and incubated at 15 °C with shaking (180 rpm) for 15 days. Bacterial growth was monitored spectrophotometrically until the OD readings were stabilized (OD_{600nm} ~ 1 to 1.5). Biochemical and enzymatic profiles of *A. salmonicida* strains were determined using the API20E, API20NE, and APY-ZYM (BioMerieux, Marcy-l’Etoile, France) as instructed by the manufacturer. Stripes were incubated with *A. salmonicida* strains at 15 °C for 48 h, and the API WEB (BioMerieux) was used to examine the results.

5.3.7. Evaluation of *A. salmonicida* virulence in lumpfish (*C. lumpus*)

5.3.7.1. Bacterial inocula preparation

The bacterial inocula for infection and challenge were prepared according to the prior instructions with minor modifications [40]. Briefly, *A. salmonicida* J223 and mutant strains were cultured in 3 mL of TSB at 15 °C in a roller drum overnight. Three-hundred microliters of these cultures were inoculated into 100 mL flasks comprising 30 mL of fresh TSB and incubated at 15 °C with shaking (180 rpm) up to an OD_{600nm} of 0.7 (~1x10⁸ CFU/mL). By centrifuging at 6000 rpm for 10 min, at 4 °C, bacterial cells were collected, washed once with PBS, and resuspended in 300 µL of PBS. The bacterial cell suspension

was serially diluted in PBS (1:10) to achieve the final infection and challenge doses, at the same time, enumerated by plating on Trypticase Soy Agar (TSA) to determine CFU/mL.

5.3.7.2. Fish holding

This study was conducted using animal protocols that were approved by the Institutional Animal Care Committee and the Biosafety Committee at Memorial University of Newfoundland (MUN) (<https://www.mun.ca/research/about/acs/acc/>) in accordance with the guidelines set by the Canadian Council on Animal Care (<https://ccac.ca/>). The protocols #18-01-JS, #18-03-JS, and biohazard license L-01 were used for the fish experiments. Lumpfish (55.4 ± 5.6 ; mean \pm SD) were maintained at the Joe Brown Aquatic Research Building (JBARB), Department of Ocean Sciences (DOS), MUN and transferred to the aquatic level 3 (AQ3) biocontainment unit at the Cold-Ocean Deep-Sea Research Facility (CDRF), DOS, MUN for infection assays.

Fish were kept in ideal conditions before and during the experiment, including 500 L circular tanks with flow-through seawater system (7.5 L/min) using filtered, UV-treated seawater at 8-10 °C, 95-110% oxygen saturation and ambient photoperiod (12 h light: 12 h dark) (Supplementary Figure S5.3). Biomass density was kept at 25 kg per m³. Fish were fed daily with commercial aqua-feed (Skretting - Europa 15) at a rate of 0.5% of fish body weight per day.

5.3.7.3. Infection and Challenge

Lumpfish from JBARB were divided into nine 500 L tanks containing 60 fish per tank at CDRF and acclimatized for 2 weeks before infection. The fish were sedated in 40 mg/L of tricaine methane-sulphonate (MS-222; Syndel Laboratories, Vancouver, BC, Canada), and intraperitoneally (i.p.) infected with either 100 μ L of PBS or 100 μ L (10^4

CFU/dose) of wild-type *A. salmonicida* J223, and mutant strains (Supplementary Figure S5.3). Fish were observed daily for mortality and clinical signs until 30 days post-infection (dpi). Finally, surviving fish at 30 dpi were ip challenged with 10^3 CFU/dose (10 LD₅₀ (lethal dose 50%)) of *A. salmonicida* J223 wild-type.

5.3.7.4. Colonization of *A. salmonicida* wild-type and mutants in lumpfish tissues

A MS222 overdose (400 mg/L) was used to euthanize five lumpfish ($n = 5$) that were randomly selected at 3, 7, and 10 dpi. Samples of the spleen, liver, head kidney, and brain were aseptically removed and individually placed into sterile homogenizer bags (Nasco whirl-pak®, USA). Next, tissue samples were weighed, and homogenized in PBS to achieve a final volume of 1 mL (weight: volume; 0.1 g of tissue per 1 mL of PBS). These tissue suspensions were then serially diluted (1:10) and counted on TSA-Congo red (TSA-CR) plates. Likewise, 1 mL of blood was drawn, serially diluted, and plate counted onto TSA-CR. Wild-type *A. salmonicida* J223 or mutants CFU per g of tissue or per mL of blood were counted on the plates after 4-5 days of incubation at 15 °C.

5.3.8. Statistical analyses

The Prism program version 7.0 was used to conduct statistical analyses and visualize the data. A p -value ≤ 0.05 was considered statistically significant. Non-parametric one-way ANOVA Kruskal-Wallis test followed by Dunn's multiple comparison post hoc test was used to identify significant differences in the gene expression between groups (i.e., control and riboflavin-supplemented *A. salmonicida*). Kaplan-Meier estimator and Log-rank test were employed to obtain survival fractions following infection and to compare survival curve trends, respectively. A one-way ANOVA with a non-parametric Kruskal-Wallis test was used to compare the tissue colonization, and Dunn's multiple comparison

post hoc analysis was utilized to determine the significant differences in colonization between *A. salmonicida* J223 wild-type and mutant strains.

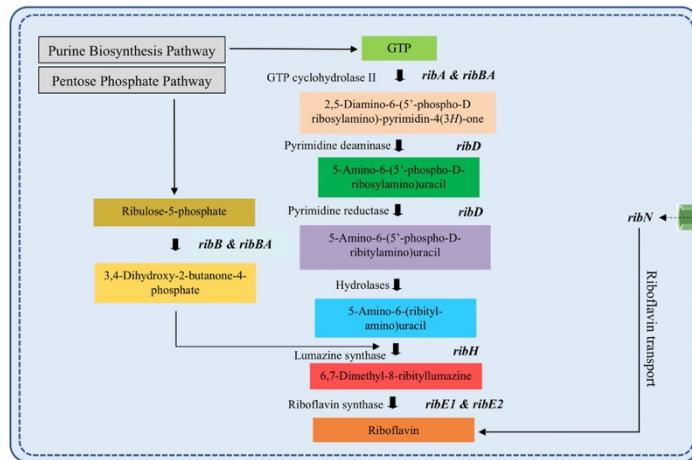
5.4. Results

5.4.1. *A. salmonicida* encodes a full RBP with additional *ribB* and *ribE* copies and a RibN riboflavin transporter.

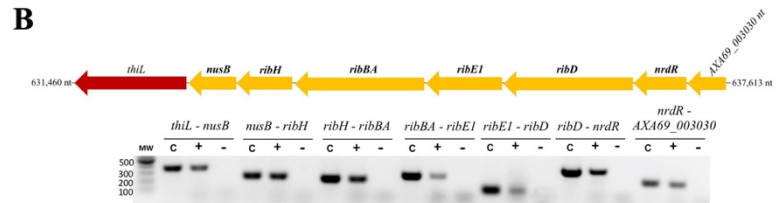
The enzymatic steps of the RBP and the associated catalytic enzymes are depicted in Figure 5.1A. The biochemical pathway of riboflavin synthesis utilizes one molecule of guanosine-5'-triphosphate (GTP) resulting from the purine biosynthesis pathway and two molecules of ribulose-5-phosphate from the pentose phosphate pathway to yield one molecule of riboflavin after a series of enzyme-catalyzed reactions (Figure 5.1A). To identify the riboflavin provision genes of *A. salmonicida* J223, we searched its genome in the NCBI and KEGG databases for RBP genes and riboflavin transporters and their functions, which are listed in Table 5.2. The results of this search indicated that *A. salmonicida* conserves a cluster of contiguous *ribD*, *ribE*, *ribBA*, *ribE1*, and *ribH* genes localized between *nusB* and *nrdR* (Figure 5.1B). Theoretically, this cluster would encode all enzymes required for riboflavin biosynthesis, with the *ribBA* gene product annotated as a fusion of the RibB and RibA proteins. In addition to this main cluster, a copy of *ribE*, denominated here as *ribE2*, and copies of independent *ribA*, *ribB*, and a *ribN* gene encoding a putative riboflavin transporter were identified in different regions of the chromosome (Figures 5.1C-F). Riboswitch prediction in the putative regulatory regions of the identified genes using RibEx [51] indicated that the upstream region of *ribB* contains a conserved FMN riboswitch (Figure 5.1D).

To experimentally characterize the transcriptional organization of the *A. salmonicida* riboflavin supply genes (Table 5.2), PCR analyses were conducted on cDNA obtained from RNA of *A. salmonicida* J223 cultured in minimal media with primers designed to amplify the gene junctions (Supplementary Table S5.1). Positive amplifications in the RT-PCR imply the joint of coding sequences in the same mRNA. Results revealed that the gene cluster composed of adjoining *nusB*, *ribH*, *ribBA*, *ribE1*, *ribD*, and *nrdR* was part of an operon (Figure 5.1B). Moreover, this operon also includes the genes *thiL* and AXA69_003030 (*NIPSNAP* [4-nitrophenyl phosphatase and non-neuronal SNAP25] family protein), which have putative roles in thiamine biosynthesis and vesicular transport, respectively, localized contiguous to *nusB* and *nrdR*, respectively (Figure 5.1B). This analysis showed that *ribA* comprises a monocistronic unit (Figure 5.1C) while *ribB* forms an operon with the downstream open reading frame (ORF) AXA69_001415 gene encoding a putative Lpp/OprI family alanine-zipper lipoprotein (Figure 5.1D). The second copy of the riboflavin synthase-encoding gene *ribE2*, located outside the main RBP operon, is a monocistronic unit (Figure 5.1E). Finally, this analysis showed that the riboflavin transporter *ribN* gene forms an operon with *purT*, which encodes a putative formate-dependent phosphoribosyl glycinamide formyl transferase (Figure 5.1F).

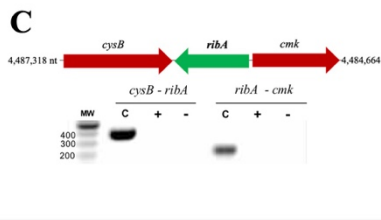
A



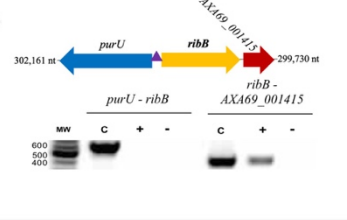
B



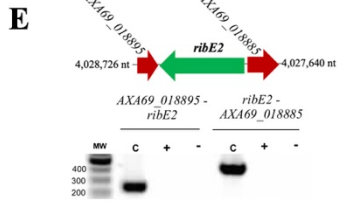
C



D



E



F

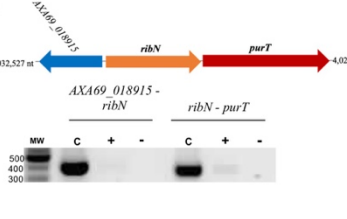


Figure 5.1. *In-silico* and experimental characterization of riboflavin supply pathways in *A. salmonicida*. A. Schematic illustration of riboflavin provision pathways: Riboflavin Biosynthetic Pathway (RBP) and RibN family transporter. (B-F). Evaluation of the transcriptional organization of *rib* genes in *A. salmonicida*. PCR reactions were performed on *A. salmonicida* cDNA using primers that amplify the specified gene junctions of *rib* genes and their adjacent genes at the loci encoding *ribD*, *ribE1*, *ribBA*, *ribH* (B), *ribA* (C), *ribB* (D), *ribE2* (E) and *ribN* (F). Each reaction was carried out 3 times separately with the same results. The

template cDNA from RT-PCR with reverse transcriptase is indicated by +, while the template cDNA from RT-PCR without reverse transcriptase is indicated by - (negative control). C implies PCR on chromosomal DNA as the template (positive control), and M stands for molecular weight marker in base pairs. The purple triangle between *purU* and *ribB* indicates the presence of FMN riboswitch.

Table 5.2. Riboflavin supply genes in *A. salmonicida*

Gene	Function	Location	Size (nt)	Locus tag
<i>ribA</i>	GTP cyclohydrolase II	Gene; 4485605..4486198	594	AXA69_020950
<i>ribB</i>	3,4-dihydroxy-2-butanone-4-phosphate synthase	Gene; complement 300198..300851	654	AXA69_001420
<i>ribBA</i>	Bifunctional 3,4-dihydroxy-2-butanone-4-phosphate synthase/GTP cyclohydrolase II	Operon; complement 633,551..634,660	1110	AXA69_003010
<i>ribD</i>	Bifunctional diamino hydroxy phosphoribosyl amino-pyrimidine deaminase/5-amino-6-(5 phosphoribosyl amino) uracil reductase ribD	Operon; complement 635,513..636,622	1110	AXA69_003020
<i>ribE1</i>	Riboflavin synthase	Operon; complement 634,804..635,457	654	AXA69_003015
<i>ribE2</i>	Riboflavin synthase	Gene; 4027977..4028594	618	AXA69_018890
<i>ribH</i>	6,7-dimethyl-8-ribityllumazine synthase	Operon; complement 632,949..633,419	471	AXA69_003005
<i>ribN</i>	DMT family transporter	Gene; complement 4,030,823..4,031,713	891	AXA69_018910
<i>nusB</i>	Transcription antitermination factor nusB	Operon; complement 632,521..632,934	414	AXA69_003000
<i>nrdR</i>	Transcriptional regulator nrdR	Operon; complement 636,697..637,146	450	AXA69_003025

According to the first insights from *in silico* and experimental analysis, *A. salmonicida* J223 possesses a full riboflavin biosynthetic pathway with possible duplications in RibA (GTP-cyclohydrolase II), RibB (3,4-DHBP synthase) and RibE (riboflavin synthase) activities, together with a RibN riboflavin transporter. To characterize the functionality of the possible duplicated genes, the protein sequences of putative orthologs were analyzed. First, the sequences of the RibBA fusion and the standalone RibB of *A. salmonicida* were aligned to the fully characterized *E. coli* RibB [77]. This alignment analysis indicated that *E. coli* RibB shares 51.69% identity with the amino half of the *A. salmonicida* RibBA fusion (amino acids 1 to 207). Both *A. salmonicida* RibBA and RibB conserve the critical residues for the 3,4-DHBP synthase activity characterized in RibB from *E. coli* (Figure 5.2A). Next, *A. salmonicida* RibBA and RibA were aligned together with RibA from *E. coli*. This alignment showed that *E. coli* RibA shares 31.40 % identity with the carboxyl-terminal domain of *A. salmonicida* RibBA (amino acids 204 to 369). Nonetheless, while the monofunctional *A. salmonicida* RibA protein conserves the 16 critical residues for GTP cyclohydrolase II activity described in *E. coli* RibA [78], the corresponding domain of *A. salmonicida* RibBA conserves only four of them (Figure 5.2B). Thus, *in-silico* sequence analysis suggests that the product of *A. salmonicida* *ribBA* (Figure 5.2C) in the main riboflavin biosynthetic operon possesses RibB activity but lacks RibA activity. Subsequently, we evaluated the ability of *A. salmonicida* *ribBA* fusion to complement *E. coli* *ribA* and *ribB* null mutants. Both *E. coli* Δ *ribA* and Δ *ribB* (Table 5.1) are riboflavin auxotroph strains that require a high riboflavin concentration (500 μ M) to grow in LB (Figure 5.2D). Control plasmids expressing *E. coli* *ribA* or *V. cholerae* *ribB* [79] complemented the growth of their respective *E. coli* riboflavin auxotroph mutant

strains in LB without added riboflavin (Figure 5.2D). In line with the insights obtained from the alignments, *A. salmonicida* RibBA fusion was able to complement the growth of the *E. coli* Δ *ribB* but not that of the Δ *ribA* (Figure 5.2D). Growth of *E. coli* *ribA* harboring the plasmid encoding *A. salmonicida* RibBA was only achieved in high riboflavin concentration (Figure 5.2D). These results indicated that the fusion annotated as RibBA in *A. salmonicida* does not conserve the GTP-cyclohydrolase II activity. Thus, this gene likely belongs to a family of previously identified genes encoded in RBP operons in different bacteria that encode for a fusion of a functional RibB and a domain of unknown function denominated RibBX [80,81]. Hence this gene was denominated *ribBX* hereafter.

A plasmid expressing the independent *E. coli* *ribA* gene complemented the growth of the *E. coli* *ribA* mutant (Figure 5.2D). Similarly, the plasmid containing *A. salmonicida* *ribB* rescued the growth of *E. coli* Δ *ribB* riboflavin auxotrophic phenotype without added riboflavin, confirming that there is redundancy in RibB activity in *A. salmonicida*, which is mediated by two different proteins (Figure 5.2E).

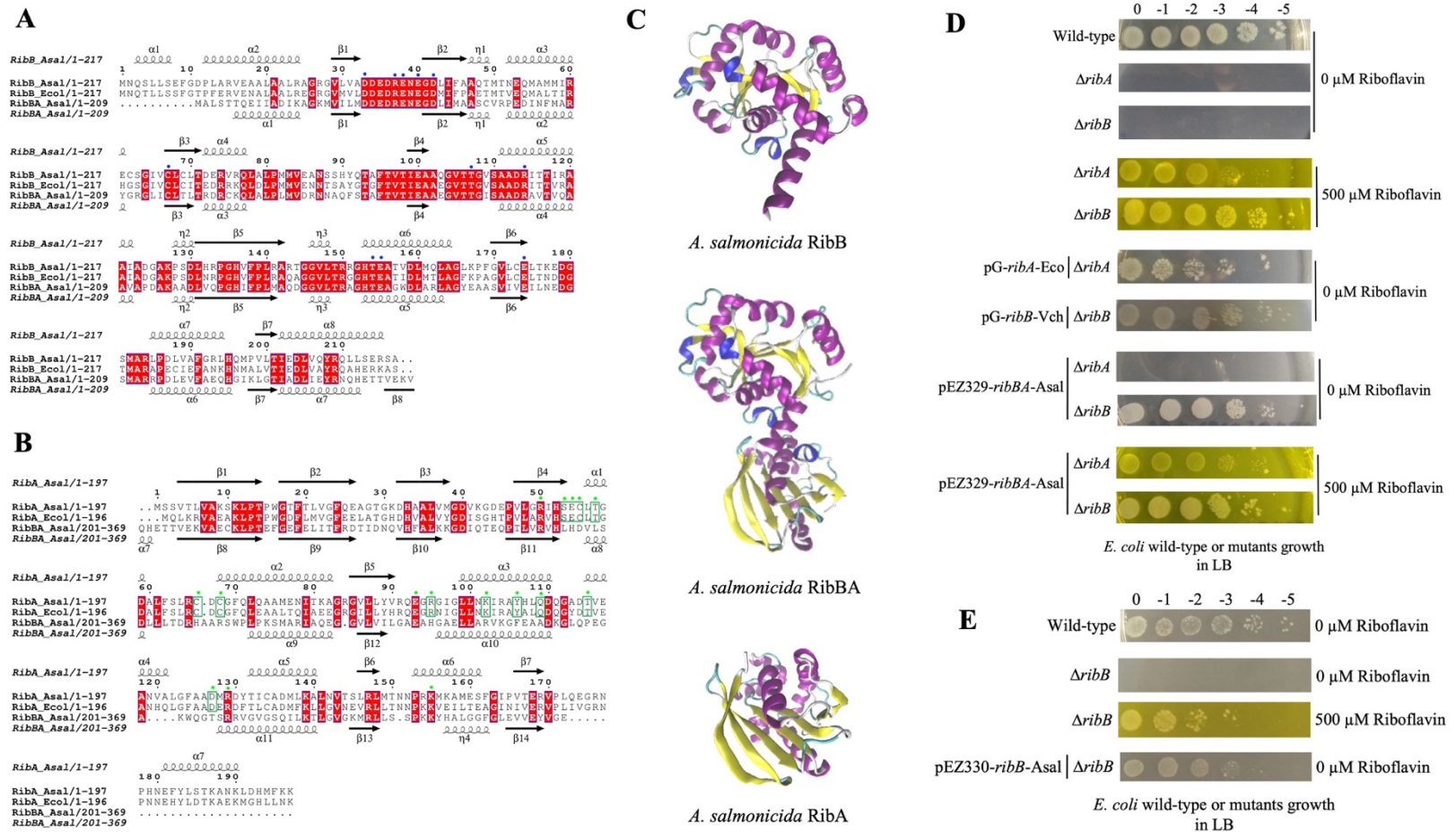


Figure 5.2. Sequence alignment, three-dimensional (3D) protein structures, and functionality of *ribB*, *ribA*, and *ribBA* (or *ribBX*) genes. Amino acid sequences of experimentally resolved RibA and RibB proteins from *E. coli* are used. RibA and RibB active

site residues are identified using reported literature. Conserved amino acid residues are highlighted in red. **A.** Multiple sequence alignment among RibB of *E. coli* (*Ecol*), RibB, and amino-terminal region of the RibBA fusion (amino acids 1 to 207) of *A. salmonicida* (*Asal*). The secondary structures at the top and bottom of the alignment correspond to the *A. salmonicida* RibB and RibBA, respectively (spirals represent α -helix; arrows represent β -sheet). The blue circles at the top of the aligned sequence indicated the key catalytic active site residues ($n=11$) that have been described in *E. coli* RibB, which are also present in *A. salmonicida* RibB and RibBA. **B.** Multiple sequence alignment among RibA of *E. coli* (*Ecol*), RibA, and carboxyl-terminal region of the RibBA fusion (amino acids 204 to 369) of *A. salmonicida* (*Asal*). The secondary structures at the top and bottom of the alignment correspond to the *A. salmonicida* RibA and RibBA, respectively. The green circles at the top of the aligned sequence indicated the key catalytic active site residues ($n=16$) that have been described in *E. coli* RibA. Out of these 16 active sites, 4 are conserved in both RibA and RibBA of *A. salmonicida*, while the remaining 12 are absent from *A. salmonicida* RibBA but conserved in RibA (highlighted with green squares). **C.** 3D protein structures of *A. salmonicida* RibB, RibBA, and RibA. 3D structures are predicted using the trRosetta protein structure prediction service and visualized in VMD. **D.** Complementation of *E. coli* *ribA* and *ribB* mutants with *ribBA* fusion gene of *A. salmonicida* in LB with no (0 μ M Riboflavin) and 500 μ M riboflavin. **E.** Complementation of *E. coli* *ribB* mutant with *ribB* of *A. salmonicida* in LB with no (0 μ M Riboflavin) and 500 μ M riboflavin.

Another *A. salmonicida* RBP gene showing possible duplication is RibE. To get insights into the functionality of the two putative *A. salmonicida* RibE homologs, RibE1 and RibE2 were aligned to *E. coli* and *Brucella abortus* RibE [82,83]. In this alignment, one critical residue required for the enzyme activity (Phe-2) and two other residues that provide significant enzyme activity improvement (Ser-41 and His-102) are indicated (Figure 5.3A). Residues that may be involved in substrate recognition (Met-1, Phe-2, Thr-3, Gly-4, Ile-5, and Ile-6 / Val-6) are also indicated in the amino-terminal section (Figure 5.3A). *A. salmonicida* RibE1 and RibE2 share 33.17 % identity. Both *A. salmonicida* RibE1 and RibE2 conserve the residues required for full activity (Phe-2, Ser-41, and His-102). Thus, sequence analysis suggests that *A. salmonicida* RibE1 and RibE2 function as riboflavin synthases.

Despite several attempts, our group could not obtain an *E. coli ribE* null mutant to perform complementation experiments. Thus, to obtain further information on the functionality of these proteins, their structures were predicted using trRosetta and compared to the reported *B. abortus* and *E. coli* RibE structures [82,83]. The predicted structures of RibE1 and RibE2 were highly similar to each other (Figure 5.3B). RibE1 and RibE2 structures overlapped with a good structural homology ($Q_H = 0.7219$). These structures were also highly similar to *B. abortus* and *E. coli* RibE (Figure 5.3B). *B. abortus* RibE arranges in trimers, with monomers showing two characteristic six-stranded β -barrels formed by the amino and carboxyl-terminal domains [83]. *A. salmonicida* RibE1 and RibE2 also formed these two β -barrel domains in the *in-silico* modelations (Figure 5.3B).

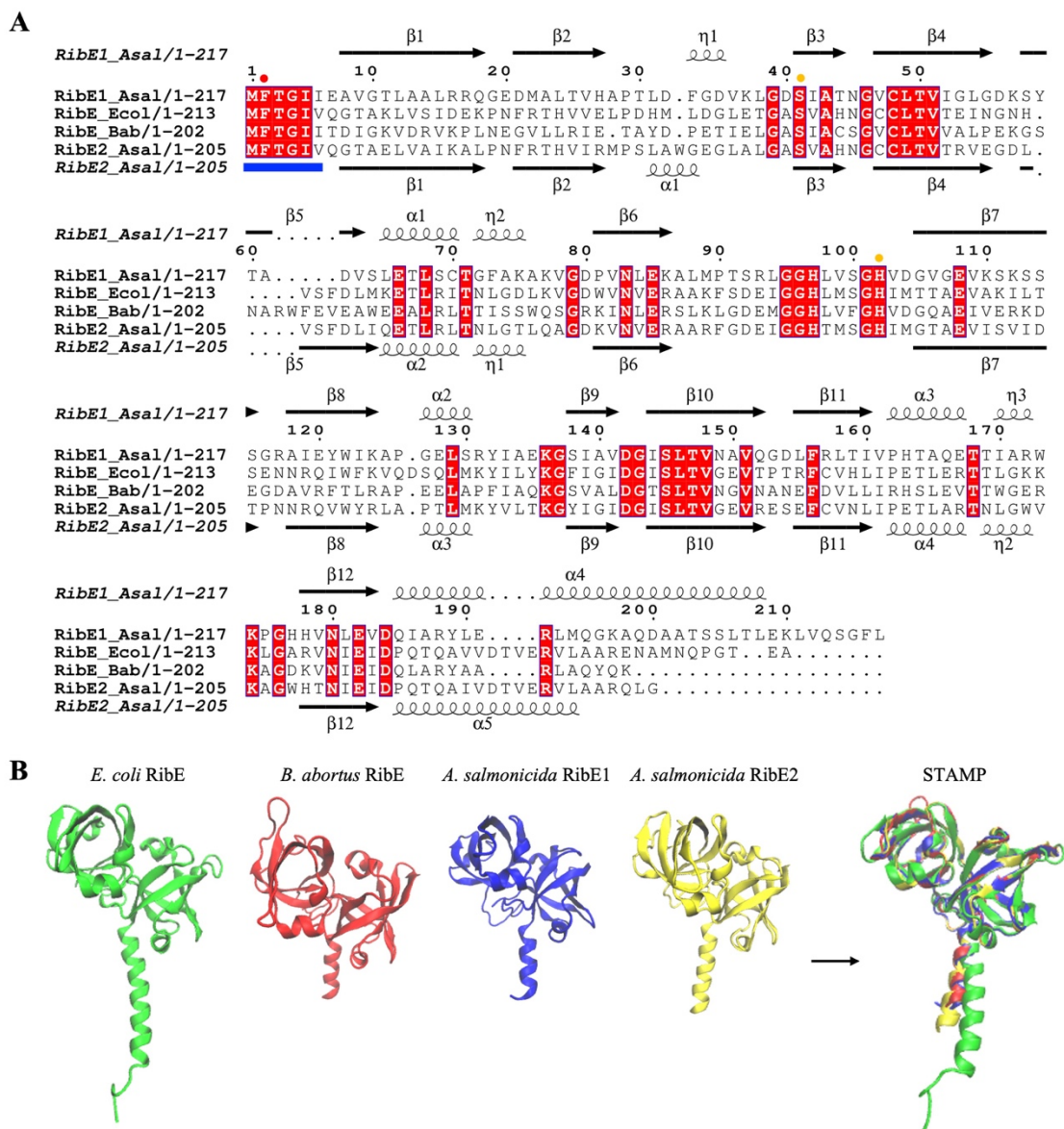


Figure 5.3. Sequence and structural alignments of *A. salmonicida* riboflavin synthases RibE1 and RibE2. **A.** Multiple sequence alignment of *E. coli* (*Ecol*), *B. abortus* (*Bab*), and *A. salmonicida* (*Asal*) RibE proteins. The secondary structures at the top and bottom of the alignment correspond to the *A. salmonicida* RibE1 and RibE2, respectively (spirals represent α -helix; arrows represent β -sheet). Conserved amino acid residues are highlighted in red. The circles indicated the one critical residue required for the enzyme activity (Phe-

2; red circle) and two other residues required for the significant enzyme activity improvement (Ser-41 and His-102; orange circle). Also, residues that may be involved in substrate recognition (Met-1, Phe-2, Thr-3, Gly-4, Ile-5, and Ile-6 / Val-6) are also indicated in the amino-terminal section with the blue line in the bottom of the alignment **B**. Structural alignment of RibE proteins from *E. coli*, *B. abortus*, and *A. salmonicida*. Sequence alignment of riboflavin synthases was performed in JAL view using Clustal Omega Multiple Sequence Alignment Program and rendered using the web-based interface of ESPript. 3D structures of *A. salmonicida* J223 riboflavin synthases were predicted using the trRosetta protein structure prediction service and visualized in VMD. Structural alignments of 3D protein structures of riboflavin synthases were performed using Structural Alignment of Multiple Proteins (STAMP) on VMD.

Therefore, structural models suggested that the *A. salmonicida* RibE1 and RibE2 are similar to a fully characterized RibE protein and likely possess riboflavin synthase activity.

The functionality of the putative *A. salmonicida* *ribN* gene was also assessed by complementing *E. coli* Δ *ribB* in M9 minimal media. *E. coli* Δ *ribB* did not grow in M9 or M9 supplemented with 2 μ M of riboflavin, but it grew in M9 supplemented with 500 μ M riboflavin (Figure 5.4). A plasmid expressing *ribN* from *A. salmonicida* rescued the *E. coli* Δ *ribB* phenotype in M9 with low riboflavin (Figure 5.4), strongly suggesting that RibN functions as a riboflavin importer.

Overall, these results indicate that *A. salmonicida* has a full RBP and a RibN transporter for riboflavin provision. Most of the genes required for the RBP are in the main operon, including *ribD*, *ribE*, *ribBX*, and *ribH*. The *ribA* gene and additional copies of *ribB* and *ribE* (*ribE2*) are encoded outside this operon.

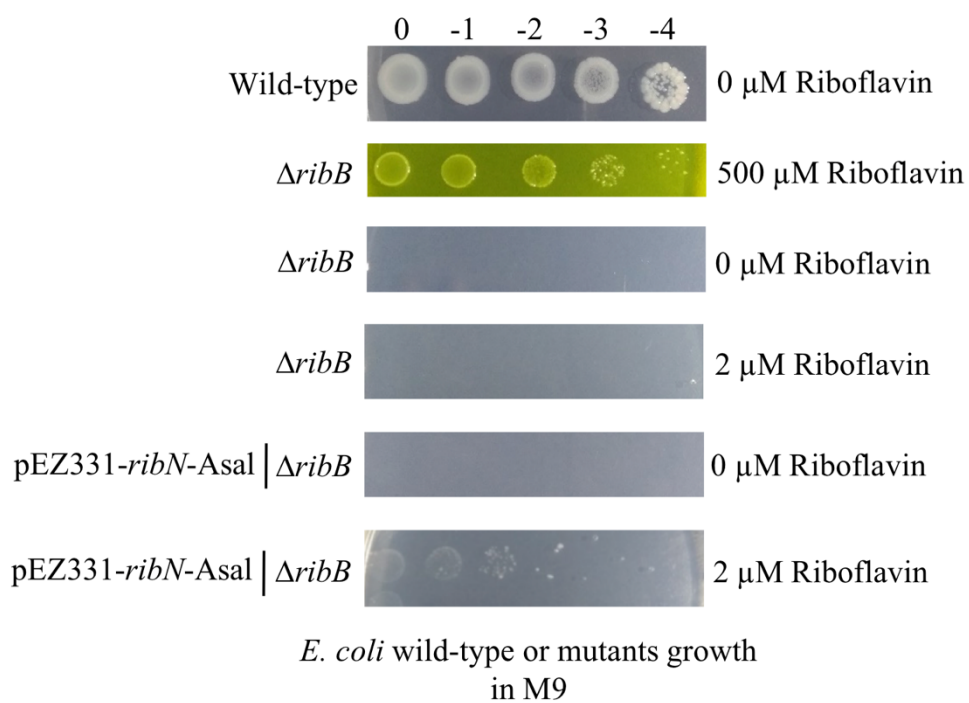


Figure 5.4. Functionality of *A. salmonicida* RibN family transporter is confirmed by complementing *E. coli ribB* mutant with the plasmid expressing the *A. salmonicida ribN*. Complementation assays were performed in minimal media (M9) plates supplemented with no (0 μM Riboflavin), low (2 μM Riboflavin), and high (500 μM Riboflavin) riboflavin.

5.4.2. Riboflavin influences the expression of a small set of genes, including *ribB*.

Being a riboflavin-prototroph that can also internalize riboflavin, it is intriguing how external riboflavin affects *A. salmonicida* physiology. To determine the effect of extracellular riboflavin on the genetic expression of *A. salmonicida*, global gene expression profiles of bacteria grown in M9 minimal media and M9 supplemented with 2 μ M riboflavin were determined by RNA-seq. Information on sequencing statistics is provided in Supplementary Table S5.4. Control and riboflavin-supplemented samples showed a highly significant positive correlation ($r^2 = 0.99$; $p < 0.0001$) according to the global expression correlation analysis (Figure 5.5A). Principal Component Analysis (PCA) and heat map with hierarchical clustering exhibited a clear segregation of control and riboflavin-supplemented samples (Figures 5.5B, C). A total variation of 71.3% in the expression data was explained by PC1 and PC2 (Figure 5.5B). The close distribution of samples under riboflavin-supplemented circumstances in comparison to the control samples demonstrates the impact of extracellular riboflavin on gene expression (Figure 5.5B). For the differential gene expression analysis, a \log_2 FC $\geq |1|$ and FDR p -value of 0.05 were used as the cut-off values. Only 19 genes were differentially expressed by *A. salmonicida* in response to extracellular riboflavin. Of these, 1 gene was upregulated, and 18 were downregulated (Figure 5.5D and Supplementary Figure S5.4A; Table 5.3; Supplementary File 5.1). The only upregulated gene encodes for a protein with putative transposase activity. Five of the downregulated genes are found to be part of a cluster in the genome. These genes were *cfa*, coding for a putative cyclopropane-fatty-acyl-phospholipid synthase, and the ORFs AXA69_RS13645 (nuclear transport factor 2 family protein), AXA69_RS13650 (short chain dehydrogenase family NAD(P)-dependent

oxidoreductase), AXA69_RS13655 (FAD-dependent oxidoreductase), AXA69_RS13660 (DUF1365 domain-containing protein), and AXA69_RS13670 (DUF2878 domain-containing protein). These genes are adjacent to each other, and an analysis using operon-mapper indicates that they are predicted to form an operon. Although no experimental information is available on the function of this cluster, the presence of *cfa* and other ORFs coding for enzymes involved in RedOx reactions suggests its involvement in fatty acid metabolism [84]. Riboflavin and iron have been proposed to reciprocally regulate their metabolic genes based on their common function as RedOx cofactors [85]. In this case, the AXA69_RS20570 ORF coding for a component of the ABC transport system of the amonabactin siderophore and *yedZ*, coding for a heme-cofactor subunit that works as an electron chain component of the MsrPQ (methionine sulfoxide reductase) system that repairs oxidized periplasmic proteins, were downregulated by external riboflavin (Table 5.3). Importantly, according to this transcriptomics analysis, the only riboflavin supply gene affected by external riboflavin was the monofunctional *ribB*, while neither any of the rest of the biosynthetic genes nor *ribN* was affected (Table 5.3). This agrees with the presence of a putative FMN riboswitch in *ribB*. The rest of the genes with a reduced expression included regulators, Lon protease substrate binding-like domain encoding gene, ATPase encoding gene involved in insertion sequences mobility, and mostly genes of unknown function (Table 5.3). In summary, results indicated that extracellular riboflavin impacts *A. salmonicida* J223 transcriptome response, mainly affecting a few genes probably involved in lipid metabolism, transposition, iron metabolism, and one involved in riboflavin supply.

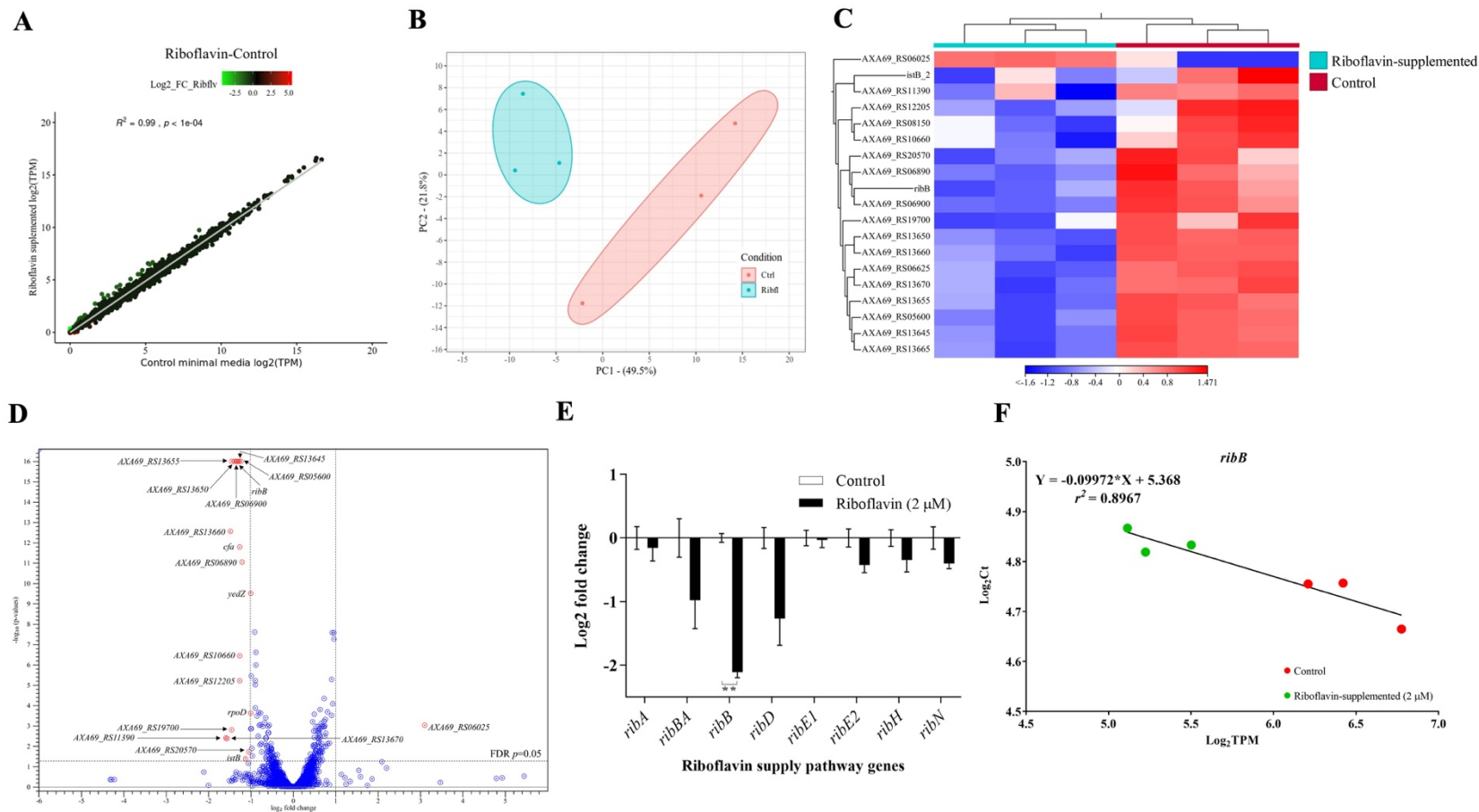


Figure 5.5. Effect of extracellular riboflavin on *A. salmonicida* J223 global transcriptomic response and expression of riboflavin supply pathway genes. *A. salmonicida* J223 grown in the presence and absence of riboflavin in minimal media. The RNA-Seq experiment involved 6 RNA libraries with three biological replicates for two distinct conditions; control (minimal media) versus

riboflavin supplemented (minimal media + riboflavin-2 μ M). **A.** Scatter plot of RNA-seq expression under control and riboflavin supplemented conditions. Red, green, and black dot colors stand for up-, down-, and non-differentially expressed genes, respectively, with each dot representing a gene. **B.** Principal component analysis (PCA) of *A. salmonicida* samples grown in the presence and absence of riboflavin in minimal media, based on the expression of all data sets. **C.** Hierarchical cluster analysis of RNA-seq results. DEGs are clustered on a heat map; the control (red) and riboflavin-supplemented (aqua) bacterial samples are indicated by the color bars below the horizontal cluster. **D.** Volcano plot of DEGs (Cut-off: Log_2 fold-change (FC) $\geq |1|$ and false discovery rate (FDR) $p \leq 0.05$). **E.** Relative expression of riboflavin supply pathway genes in *A. salmonicida* grown in minimal media with (2 μ M) and without riboflavin. Expression of genes *ribA*, *ribB*, *ribBA*, *ribD*, *ribE1*, *ribE2*, *ribH*, and *ribN* in cultures with and without riboflavin was assessed by RT-qPCR. The normalizers were *era* and *hfg*. Asterisks (*) represent the statistically significant differences ($***p < 0.01$) in the gene expression between control and riboflavin-supplemented *A. salmonicida* cultures, as determined by the non-parametric Kruskal-Wallis test, followed by Dunn's multiple comparison post hoc test. **F.** Correlation between gene expression levels of *ribB* from RT-qPCR and RNA-Seq data. A simple linear regression analysis was performed between the normalized counts (TPM) of RNA-seq data (Log_2 TPM on the X axis) and the Ct values from RT-qPCR (Log_2 Ct on the Y axis).

Table 5.3. Nineteen Differentially Expressed Genes (DEG) from transcriptomics

Locus Tag	Region	Gene Symbol	Putative Protein Product	Log ₂ Fold Change	FDR p-Value	Conserved Domain	Putative Function
AXA69_RS06025	1259692..1260842	-	IS3 family transposase	3.11	1.0×10^{-3}	Transpos_IS3	Transposase activity
AXA69_RS06625	Complement (1370582..1371214)	<i>yedZ</i>	Sulfoxide reductase heme-binding subunit YedZ	-1.00	3.2×10^{-10}	Cytochrome_b_N	Heme binding - protect from oxidative stress
AXA69_RS08150	Complement (1707332..1707850)	<i>rpoD</i>	Sigma-70 family RNA polymerase sigma factor	-1.01	2.0×10^{-4}	PRK09651	DNA binding and sigma factor activity
AXA69_RS20570	4389171..4390238	-	Amonabactin ABC transporter permease subunit 1	-1.05	1.9×10^{-2}	FecCD	Permease of amonabactin siderophore synthesis cluster
AXA69_RS01345	Complement (286176..286931)	<i>istB</i>	IS21-like element ISAs29 family helper ATPase	-1.13	4.1×10^{-2}	YlqF_related_GTPase	ATP binding
AXA69_RS06890	Complement (1431017..1431694)	-	ChrR family anti-sigma-E factor	-1.20	9.3×10^{-12}	Cupin_RmlC-like	Negative regulation of transcription
AXA69_RS05600	Complement (1172054..1172773)	-	SDR family NAD(P)-dependent oxidoreductase	-1.23	0	NADB_Rossmann	Oxidoreductase activity
AXA69_RS12205	Complement (2534814..2535632)	-	Hypothetical protein	-1.26	6.2×10^{-6}	N/A	Unknown
AXA69_RS10660	2232777..2233202	-	Hypothetical protein	-1.26	3.6×10^{-7}	N/A	Unknown
AXA69_RS13665	2851821..2853077	<i>cfa</i>	Cyclopropane-fatty-acyl-phospholipid synthase family protein	-1.26	1.6×10^{-12}	<i>cfa</i>	Methyl transferase in lipid biosynthesis / metabolism
AXA69_RS13645	2848535..2848963	-	Nuclear transport factor 2 family protein	-1.27	0	SnoaL_2	Protein transport into the nucleus and small GTPase binding

AXA69_RS01425	Complement (300198..300851)	<i>ribB</i>	3,4-dihydroxy-2- butanone-4- phosphate synthase	-1.32	0	DHBP_synthase	Riboflavin biosynthesis
AXA69_RS06900	Complement (1432389..1432955)	-	LON peptidase substrate-binding domain-containing protein	-1.35	0	LON	ATP-dependent peptidase activity
AXA69_RS13650	2848960..2849694	-	SDR family NAD(P)- dependent oxidoreductase	-1.39	0	NADB_Rossmann	Oxidoreductase activity
AXA69_RS19700	4189195..4189812	-	Hypothetical protein	-1.44	1.5×10^{-3}	P-loop_NTPase	Unknown
AXA69_RS13655	2849691..2850950	-	FAD-dependent oxidoreductase	-1.45	0	COG2907	FAD binding and oxidoreductase activity
AXA69_RS13660	2850947..2851699	-	DUF1365 domain- containing protein	-1.48	2.8×10^{-13}	DUF1365	Unknown
AXA69_RS11390	Complement (2375409..2375861)	-	Hypothetical protein	-1.56	4.4×10^{-3}	N/A	Unknown
AXA69_RS13670	2853080..2853559	-	DUF2878 domain- containing protein	-1.59	3.9×10^{-3}	DUF2878	Unknown

To validate the transcriptomics results and corroborate the effects of riboflavin on supply genes, the expression of genes of the RBP and *ribN* in the absence and presence of riboflavin was assessed by RT-qPCR. In accordance with the transcriptomics, a statistically significant two-fold repression of *ribB* expression was detected in RT-qPCR (Figure 5.5E), and a significant correlation ($r^2 = 0.8967$; $p < 0.05$) was observed between *ribB* gene expression levels from RNA-seq and RT-qPCR (Figure 5.5F). While other RBP genes showed some variability in expression, such differences did not reach statistical significance (Figure 5.5E), and the correlation between these genes' expression and the RNA-seq data is displayed in Supplementary Figure S5.4B.

5.4.3. Riboflavin biosynthesis genes *ribA*, *ribB*, and *ribE1* are required for *A. salmonicida* virulence in lumpfish

In order to assess whether riboflavin biosynthesis, its duplicated genes, and riboflavin uptake are required for virulence in *A. salmonicida*, the single mutant strains $\Delta ribA$, $\Delta ribB$, $\Delta ribBA$, $\Delta ribE1$, $\Delta ribE2$, and $\Delta ribN$ were constructed. In addition, a double $\Delta ribA$ - $\Delta ribE1$ mutant, combining deletions in a unique and in a duplicating main-operon riboflavin biosynthetic gene, was obtained. As an initial characterization, the growth of *A. salmonicida* J223 wild-type and its derivative mutants in minimal media in the presence and absence of 2 μ M riboflavin was assessed. *A. salmonicida* wild-type and mutants $\Delta ribB$, $\Delta ribBA$, $\Delta ribE1$, $\Delta ribE2$, and $\Delta ribN$ grew in the presence and absence of riboflavin with no significant differences (Figures 5.6A, D, E, G-J, L). In contrast, $\Delta ribA$ and $\Delta ribA$ - $\Delta ribE1$ mutants did not grow in M9 minimal media without riboflavin, and growth was restored by supplementing the M9 with a low concentration of riboflavin, indicating that they are riboflavin auxotrophs (Figures 5.6B-D). The riboflavin auxotrophic phenotype of

these mutants was confirmed by growth curves, where significantly higher growth of $\Delta ribA$ and $\Delta ribA-\Delta ribE1$ was observed in the presence of riboflavin (Figures 5.6F, K). Expectedly, the $\Delta ribN$ mutant has no growth defect in either condition as endogenous biosynthesis supplies the vitamin (Figure 5.6L). The requirement of external riboflavin for the growth of the $\Delta ribA$ strain confirmed that the RibBA protein does not display RibA activity and that the independent *riba* codes for the only GTP cyclohydrolase II in *A. salmonicida* (Figure 5.6F). Endogenous riboflavin provision is not compromised in the $\Delta ribB$ as the RibBA maintains RibB activity (Figure 5.6G). In the same way, the $\Delta ribE1$ strain not becoming riboflavin auxotroph supports the notion of that *ribE2* codes for a functional riboflavin synthase, and likewise, in the $\Delta ribE2$ mutant, the biosynthesis would be sustained by *ribE1* (Figures 5.6I, J).

A biochemical profile analysis using the API 20E and API 20NE showed few differences between the wild-type and mutants. *A. salmonicida* $\Delta ribA-\Delta ribE1$ displayed a negative reaction for the hydrolysis of L-arginine, while others displayed a positive reaction (Supplementary Tables S5.5 and S5.6). The *A. salmonicida* $\Delta ribB$ mutant showed a negative reaction for the naphthol-AS-BI-phosphohydrolase enzyme assay, while others showed positive reactions (Supplementary Table S5.7).

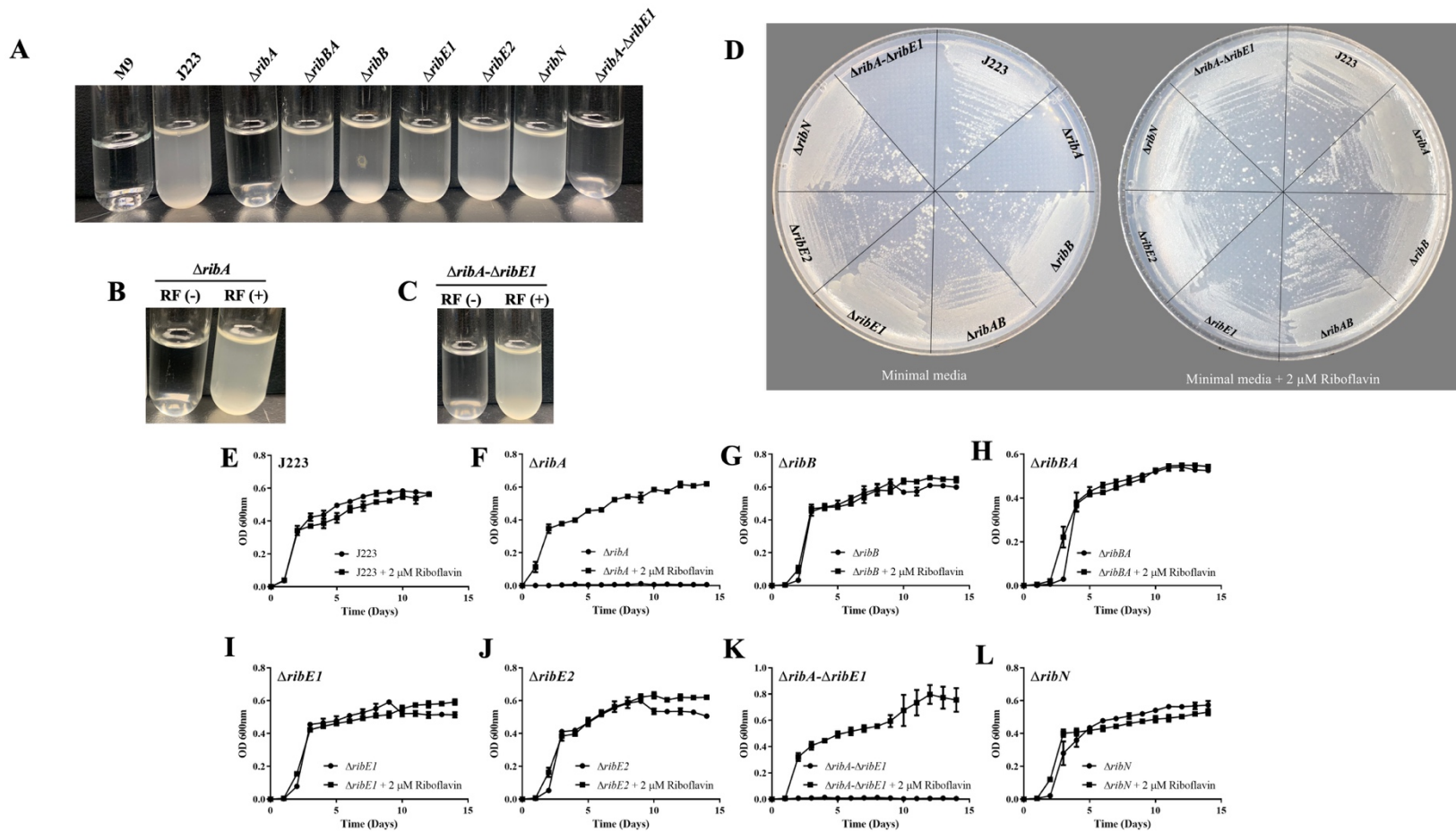


Figure 5.6. Growth of *A. salmonicida* J223 wild-type and mutant strains in M9 minimal media supplemented with (2 μ M) and without riboflavin (RF). **A.** Growth of J223 and mutants in M9. **B.** Growth of $\Delta ribA$ in M9 supplemented without RF(-) and with

RF(+) riboflavin. **C.** Growth of $\Delta ribA-\Delta ribE1$ in M9 supplemented without RF(-) and with RF(+) riboflavin. **D.** Growth of *A. salmonicida* J223 and mutants in M9 agar plates with and without riboflavin. Growth curves of **E.** *A. salmonicida* J223 wild-type, and *A. salmonicida* mutants **F.** $\Delta ribA$, **G.** $\Delta ribB$, **H.** $\Delta ribBA$, **I.** $\Delta ribE1$, **J.** $\Delta ribE2$, **K.** $\Delta ribA-\Delta ribE1$, and **L.** $\Delta ribN$ grown in minimal media in the presence (2 μ M) and absence of riboflavin at 15 °C in triplicates with aeration (180 rpm) for 15 days.

The virulence of *A. salmonicida* J223 wild-type and the mutants was evaluated in lumpfish using an intraperitoneal infection model [63]. Lumpfish were infected with 10^4 CFU/dose of wild-type or mutants, and their survival was recorded daily. Infected lumpfish showed classic clinical signs of furunculosis, including typical furuncles on the ventral part of the body (Figure 5.7A). All fish infected with the wild-type, the $\Delta ribBA$ or the $\Delta ribE2$ strains died within 10 dpi (Figure 5.7B). Lumpfish infected with *A. salmonicida* $\Delta ribN$ showed delayed mortality, reaching 100% after 21 dpi (Figure 5.7B). In contrast, the $\Delta ribA$, $\Delta ribB$, $\Delta ribE1$, and $\Delta ribA-\Delta ribE1$ mutant strains were fully attenuated as fish infected with these strains showed 100% survival (Figure 5.7B). The bacterial colonization of the spleen, liver, head kidney, brain, and blood was evaluated at 3, 7, and 10 dpi. In agreement with the survival levels, mutants $\Delta ribA$, $\Delta ribB$, $\Delta ribE1$, and $\Delta ribA-\Delta ribE1$ showed significantly lower levels of colonization than the *A. salmonicida* J223 wild-type (Figure 5.8). In contrast, the $\Delta ribBA$, $\Delta ribE2$, and $\Delta ribN$ mutants colonized tissues and blood at similar levels to the wild-type (Figure 5.8). In general, some of these attenuated mutants reached low levels of colonization in organs like the spleen, liver, and head kidney by 3 dpi but they were fully cleared from fish by 10 dpi (Figure 5.8).

To determine whether the infection with the attenuated mutants could confer immune protection to the lumpfish and to examine the mutants' utility as live attenuated vaccine, surviving fish from $\Delta ribA$, $\Delta ribB$, $\Delta ribE1$, and $\Delta ribA-\Delta ribE1$ infected groups were challenged with 10^3 CFU/dose (10 times the reported Lethal Dose 50 (LD₅₀) [63]) of *A. salmonicida* J223 wild-type after 30 dpi. All attenuated *A. salmonicida* mutants conferred low levels of protection, producing survival percentages ranging from 10 to 15 % (Figure 5.7C).

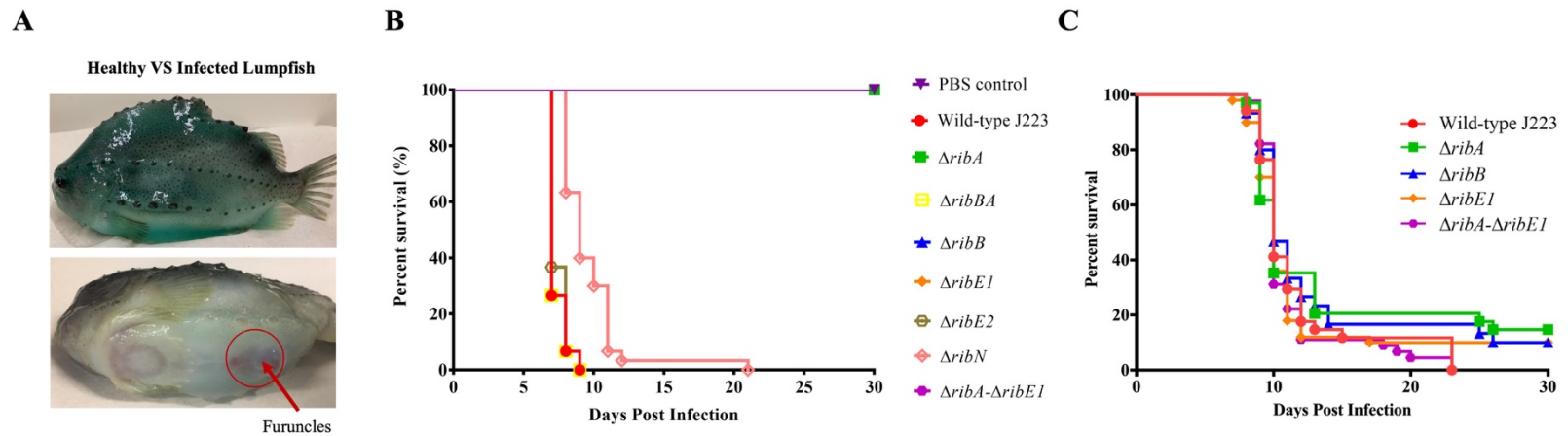


Figure 5.7. Virulence and immune protection of *A. salmonicida* mutants in lumpfish. **A.** Infected lumpfish showed furunculosis clinical signs compared to healthy fish. **B.** Lumpfish survival (%) after ip infection with 10^4 CFU/dose of *A. salmonicida* wild-type J223 and mutants. No significant difference was detected between PBS control, mutants $\Delta ribA$, $\Delta ribB$, $\Delta ribE1$, and $\Delta ribA-\Delta ribE1$. However, wild-type and mutants $\Delta ribBA$, $\Delta ribE2$, and $\Delta ribN$ infected fish groups showed significantly ($p < 0.0001$) lower survival compared to PBS control and mutants $\Delta ribA$, $\Delta ribB$, $\Delta ribE1$, and $\Delta ribA-\Delta ribE1$ infected fish groups. **C.** Survival (%) of lumpfish survivors from attenuated mutants; $\Delta ribA$, $\Delta ribB$, $\Delta ribE1$, and $\Delta ribA-\Delta ribE1$ infected groups, after ip challenge with 10^3 CFU/dose of wild-type *A. salmonicida*. These mutants did not significantly differ in their survival rates from one another.

Kaplan-Meier estimator and Log-rank test were used to obtain survival fractions after the infection and to compare survival curve trends, respectively.

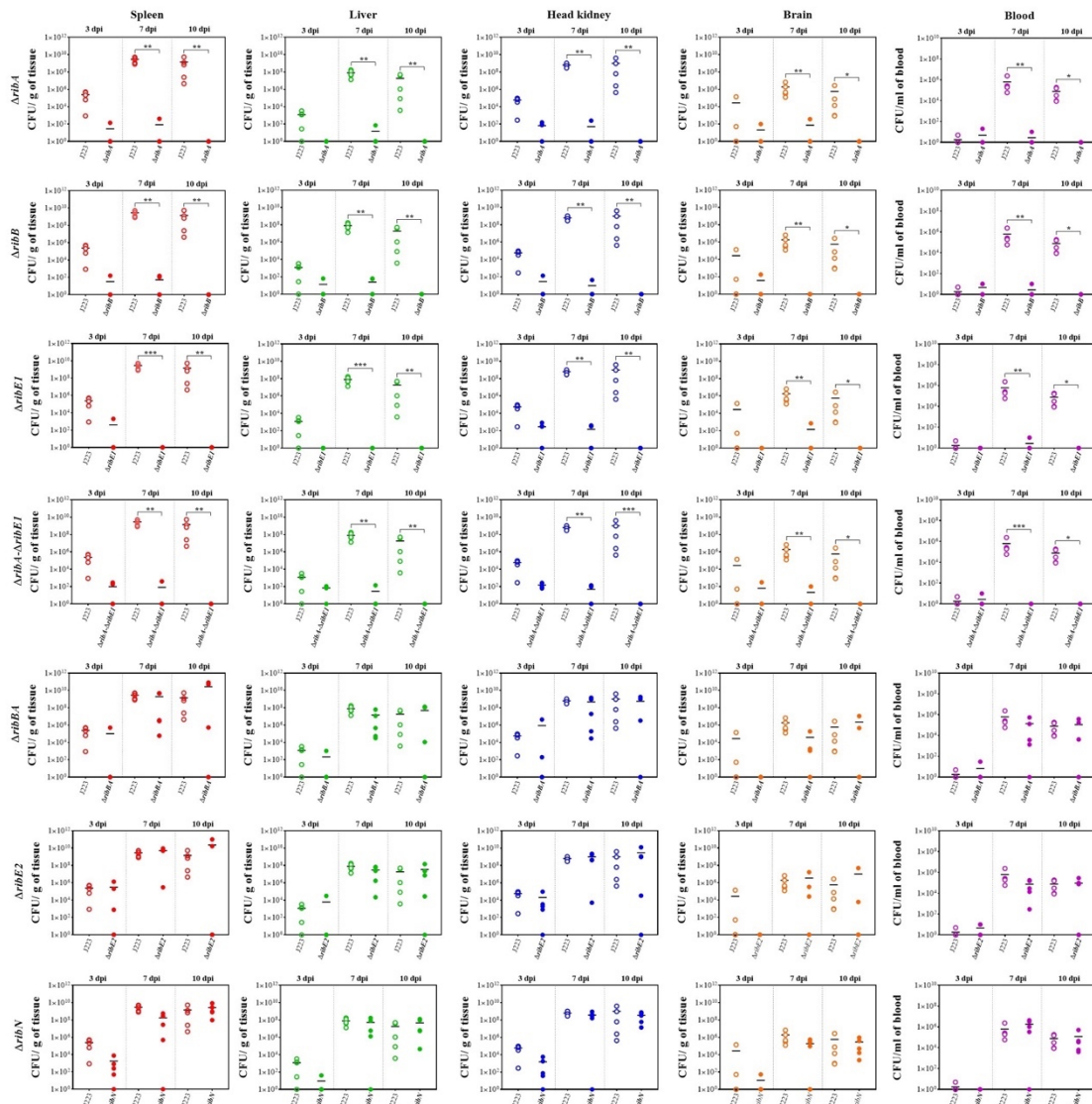


Figure 5.8. Lumpfish spleen, liver, head kidney, brain, and blood tissue colonization by *A. salmonicida* J223 wild-type versus mutant strains $\Delta ribA$, $\Delta ribB$, $\Delta ribE1$, $\Delta ribA-\Delta ribE1$, $\Delta ribBA$, $\Delta ribE2$, and $\Delta ribN$ at 3, 7, and 10 days post-infection. Five fish were sampled from each *A. salmonicida* strain infected fish group at each time point. Asterisks (*) represent the significant differences ($*p < 0.05$, $**p < 0.01$, $***p < 0.001$) in the tissue

colonization between wild type and each mutant strain per time point (3, 7, and 10 dpi), as determined by the non-parametric Kruskal-Wallis test, followed by Dunn's multiple comparison post hoc test.

5.5. Discussion

The results of this study show that *A. salmonicida* possesses both riboflavin biosynthesis and uptake functions by having an RBP and a RibN transporter, respectively. The coexistence of RBP and riboflavin transporters is relatively common in bacteria, like *Bacillus subtilis* and *Lactococcus lactis* [23,25,86,87], and seems to be conserved in fish pathogens like *A. salmonicida*.

The riboflavin provision genes landscape is highly variable among bacteria, with duplications or multiplications of functions present in many species. The initial search in *A. salmonicida* suggested that the main RBP operon included a *ribBA* gene coding for a bifunctional enzyme (Figure 5.1B). Nonetheless, alignments and functional complementation analysis further showed that its product conserves only RibB activity (Figures 5.2A, C). In other bacteria where similar genes for RibBX fusions have been identified, it has been reported that the putative RibA domain lacks critical residues for zinc binding and ring opening, which are essential for GTP cyclohydrolase II activity [80,81]. Functional complementation, sequence analysis, and phenotypic characterization of mutants revealed that conserved functional duplications are encoded by *ribB* and *ribE2* outside the main operon. In this regard, *A. salmonicida* riboflavin provision pathways are similar to those present in *Shewanella oneidensis* [80]. Notably, the X domain of *S. oneidensis* RibBX fusion lacks GTP-cyclohydrolase II activity, yet it regulates the activity of the associated N-terminal RibB domain by an unknown mechanism [80]. It has been hypothesized that *S. oneidensis* RibBX might have evolved when an alternative gene encoding a GTP cyclohydrolase II was acquired, releasing the original RibBA protein from

the selective pressure to keep its GTP cyclohydrolase II activity. In *A. salmonicida*, the GTP cyclohydrolase II activity is provided solely by the monocistronic *ribA*, as confirmed by the fact that a null mutation in this gene results in riboflavin auxotrophy, which suggests that the selective pressure to maintain the GTP cyclohydrolase II activity of the *A. salmonicida* RibBA protein may have been removed when this unique *ribA* gene was acquired.

Riboflavin synthase, which is encoded by *ribC* or *ribE* genes, catalyzes the last step of riboflavin biosynthesis (i.e., a dismutation reaction from 6,7-dimethyl-8-ribityllumazine to riboflavin) [2]. Since animals lack this enzyme and the majority of the pathogenic bacteria strictly rely on endogenous riboflavin biosynthesis, riboflavin synthase could be an interesting target for antimicrobial inhibitors, which may cause bacterial riboflavin auxotrophy or reduced virulence without putting the host at risk [7,88]. *A. salmonicida* encodes 2 *ribE* genes; *ribE1* is in the main RBP operon while *ribE2* is encoded outside of the main operon as a monocistronic unit (Figures 5.1B, E), similar to *S. oneidensis* and *Pseudomonas putida* [80]. Extracellular riboflavin had no significant effect on the expression of *ribE1* and *ribE2* in RNA-seq and qPCR (Supplementary File 5.1 and Figure 5.5E). Moreover, *A. salmonicida* Δ *ribE1* and Δ *ribE2* grew similarly to wild-type. Thus, it is possible that *ribE1* and *ribE2* are functionally equivalent and interchangeable when cultured in liquid media. *A. salmonicida* RibE1 and RibE2 monomers are predicted to fold very similarly with a good structural homology ($Q_H = 0.7219$) despite sharing only 33% of protein sequence identity.

Conservation of these highly similar riboflavin synthases with the same function in *A. salmonicida* is intriguing. However, we anticipate that the two *ribE* genes might be

differentially expressed inside the host. Strikingly, despite being functionally interchangeable *in vitro*, the $\Delta ribE1$ strain was fully attenuated while the $\Delta ribE2$ remained virulent in the lumpfish host (Figures 5.7B and 5.8). This indicates that *ribE1* is essential for *A. salmonicida* virulence and the provision of riboflavin within the host, while *ribE2* could be a redundant gene copy during host colonization but specifically required to grow in different yet unknown conditions. Additionally, the capacity of *ribE1* to compensate for the absence of *ribE2* may contribute to the virulence of *A. salmonicida* $\Delta ribE2$. Differential expression of these two genes inside the host cells may explain this effect. Similarly, differential effects of the two *B. abortus* *ribH* genes coding for lumazine synthases was demonstrated by Bonomi et al. (2010). In *B. abortus* either *ribH* is sufficient for *in vitro* growth, whereas *ribH2* is specifically required for intracellular proliferation and survival in murine macrophages [7]. It appears that vertical or horizontal gene transfer may cause the duplication of riboflavin synthases or lumazine synthases, which could provide positive fitness to bacteria in terms of virulence, pathogenicity, or other specific conditions. Moreover, results indicated that the extra copies of RBP genes in the genome seem not to be redundant.

Bacterial genomes encode riboflavin transporter proteins in addition to or in substitution of riboflavin biosynthetic genes [11,18]. *A. salmonicida* has a RibN transporter similar to those reported in *V. cholerae*, *Rhizobium leguminosarum*, and other proteobacteria [18,21], located independently from the main riboflavin biosynthesis genes. Previous studies have employed riboflavin auxotrophic strains to evaluate the functionality of riboflavin transporters, like RibN from *Rhizobium leguminosarum* [18] and RibM from *Streptomyces davawensis* [89] by growth complementation in low riboflavin concentration.

Similar to these described approaches, in this study, the growth of *E. coli ribB* mutant was rescued in M9 minimal media supplemented with 2 μ M riboflavin by the heterologous expression of the plasmid carrying *A. salmonicida ribN* (Figure 5.4), indicating the functionality of *A. salmonicida ribN* as riboflavin transporter. Extracellular riboflavin does not affect *A. salmonicida ribN* gene expression (Figure 5.5E). Similarly, *R. leguminosarum* and *V. cholerae* showed no differences in the *ribN* expression levels in the presence or absence of riboflavin [18,21]. The growth rate of *A. salmonicida Δ ribN* was identical to the wild-type, and no significant growth difference was observed in Δ *ribN* cultured with and without exogenous riboflavin (Figures 5.6E, L), similar to what was reported in *R. leguminosarum* [18]. Also, the Δ *ribN* mutant remained virulent in the lumpfish host, although it caused delayed mortality (Figure 5.7B). The *A. salmonicida ribN* mutant may have enough riboflavin supply via endogenous biosynthesis when grown in the absence of riboflavin in media and when it is inside the host. This could explain why no differences in growth rates were noticed (Figure 5.6L) and why the Δ *ribN* retained virulence (Figures 5.7B and 5.8). On the contrary, Garcia-Angulo et al. (2013) demonstrated that the RibN transporter of *R. leguminosarum* is required to enhance the colonization of the pea plant nodules [18]. Thus, the biological role of the RibN transporter may vary depending on the physiology of bacterial species.

This study assessed the response induced by the availability of riboflavin in *A. salmonicida* J223 grown in M9 minimal media. Our results showed that extracellular riboflavin has a moderate impact on gene expression in *A. salmonicida*. Transcriptomics analysis revealed that only 19 genes were differentially expressed (\log_2 FC \geq |1| and FDR $p \leq$ 0.05) in response to extracellular riboflavin (Table 5.3, Figures 5.5C, D),

suggesting that exogenous riboflavin is involved in very defined physiological functions. Concurrently, DEG analysis and RT-qPCR results showed that extracellular riboflavin downregulated the monocistronically encoded *ribB* while having no significant effect on the expression of genes in the main RBP operon (*ribH*, *ribBA*, *ribE1*, *ribD*) on which the other *ribB* homolog (i.e., *ribBA*) was encoded (Table 5.3; Figure 5.5E). Similar results were observed in *V. cholerae* N16961 cultured in T minimal media without and with riboflavin (2 μ M) in a transcriptomic-based approach [85], and in an RT-qPCR analysis [21]. Therefore, in the presence of exogenous riboflavin, *A. salmonicida* might still be able to display the riboflavin biosynthesis function.

In *V. cholerae* transcriptomic analysis (cut-off values of 1 fold change in expression and $p < 0.05$) performed by Cisternas et al. (2018), the number of genes affected by the elimination of riboflavin biosynthesis (*ribD* deletion, 142 DEGs) was substantially greater than the number of genes impacted by the presence of exogenous riboflavin (wild-type grown with 2 μ M riboflavin, 26 DEGs) or the elimination of riboflavin transport (*ribN* deletion, 71 DEGs) [85]. Interestingly, the number of genes impacted by extracellular riboflavin in wild-type *V. cholerae* is quite low (i.e., 26) and is comparable to our results (i.e., 19), which suggests the presence of external riboflavin affects only a small number of genes. Overall, findings from our transcriptomic study and that of Cisternas et al. (2018) suggest that the biosynthesis of riboflavin is more relevant for physiological functions than exogenous riboflavin [85].

The only upregulated ORF (AXA69_RS06025) in response to extracellular riboflavin in *A. salmonicida* encodes an IS3 family transposase (Table 5.3). DNA transposases are enzymes that transfer discrete DNA segments known as transposons from

one region of the genome to another region and are typically encoded by the mobile genetic element (i.e., insertion sequences; ISs) [90,91]. The *A. salmonicida* genome is rich in ISs, and ISs-mediated rearrangement events could cause a loss in the *A. salmonicida* virulence [92]. Concomitantly, the effect of ISs in the bacterial genome leads to “genomic plasticity,” which could aid in bacterial adaptation to changing environments, functional virulence, and acquisition of new metabolic capabilities [92–94]. Although the effect of the induction of this gene is not yet evident, it is interesting to investigate the probable role of riboflavin in the induction of genomic plasticity.

Riboflavin availability affects iron metabolism in bacteria, and there is a crucial regulatory crosstalk between these two important RedOx cofactors in many other species [3,85]. In line with this, exogenous riboflavin affected the expression of iron metabolism-related genes that are involved in heme binding (AXA69_RS06625) and siderophore synthesis (AXA69_RS20570) in *A. salmonicida* (Table 5.3). *A. salmonicida* produces siderophores such as acinetobactin and amonabactin under iron-limited conditions as one of its iron acquisition strategies [95]. Interestingly, amonabactin ABC transporter permease subunit 1, one of the genes in the gene cluster responsible for amonabactin synthesis and transport in *A. salmonicida*, was downregulated in response to riboflavin (Table 5.3) [95]. In contrast, the expression of other genes in this cluster, including the amonabactin ABC transporter permease subunit 2, was not affected by exogenous riboflavin [95].

The coexistence of *ribN* and a RBP with extra gene copies for *ribB* and *ribE* in *A. salmonicida* is intriguing (Figures 5.1B-F). The combined presence of functional duplications and transporter function may suggest that these individual biosynthetic and uptake genes are differentially regulated, presumably in response to the demand for flavins

that serve purposes distinct from nutritional requirements. For instance, flavins are involved in bacterial virulence [7]. It has been hypothesized before that RBP genes that have been duplicated or multiplied could have specific functions and provide adaptive benefits to the bacteria [11,28,29]. Thus, the role of the RBP genes and their additional copies and of the *ribN* transporter in the virulence and physiology of *A. salmonicida* is a question of biological relevance. To get insights into this, I constructed (Supplementary Figure S5.5) and characterized (Figure 5.6; Supplementary Tables S5.5-S5.7) $\Delta ribA$, $\Delta ribB$, $\Delta ribBA$, $\Delta ribE1$, $\Delta ribE2$, $\Delta ribN$, and $\Delta ribA-\Delta ribE1$ mutants and then examined their virulence in lumpfish infection model (Figures 5.7 and 5.8), which is a well-established marine teleost model to investigate bacterial pathogenesis [41,73,96,97]. This allowed us not only to determine the effects of the different RBP or transporter gene mutations on virulence but also to test the use of the mutants as live attenuated vaccine candidates for lumpfish.

Mutations in critical biosynthetic pathways (i.e., aromatic amino acids, purine, thymine, and riboflavin) of a pathogenic bacterium are known to attenuate and limit the growth or virulence of the pathogen *in vivo* [98]. When the riboflavin biosynthesis operon/gene of two mammal pathogens, *Rhodococcus equi* (i.e., $\Delta ribBA$) and *Actinobacillus pleuropneumoniae* (i.e., $\Delta ribGBAH$), were disrupted, both of these mutants became avirulent, making them potential live-attenuated vaccine candidates [99,100]. *A. salmonicida* $\Delta aroA$ mutants are attenuated because they lack biosynthesis of *p*-aminobenzoic acid, which is essential for folate (vitamin B₉) synthesis, and so this strain has been used as a vaccine in Atlantic salmon [101]. In our study, *A. salmonicida* mutants $\Delta ribA$, $\Delta ribB$, $\Delta ribE1$, and $\Delta ribA-\Delta ribE1$ were fully attenuated. Their colonization began at 3 dpi, it was significantly low at 7 dpi compared to the wild-type and the other virulent

mutants, and then bacteria were cleared from tissues and blood at 10 dpi (Figure 5.8). Therefore, it is evident that the attenuation facilitated host immune clearance. *A. salmonicida* attenuated mutants could not establish a systemic infection and extensive proliferation in lumpfish, probably due to the limited availability of riboflavin in the fish host milieu. Also, it appeared that *A. salmonicida* *ribA*, *ribB*, and *ribE1* genes are essential for the riboflavin supply during host colonization and influence virulence. Overall, riboflavin uptake cannot compensate for biosynthesis during infection; hence riboflavin biosynthesis is essential for *A. salmonicida* virulence and physiology. I next questioned whether the attenuated mutant strains retained immunogenicity and provided protection to lumpfish. However, after challenging the immunized lumpfish with the wild-type, I observed that these mutants confer only modest immune protection with low RPS (~ 10 to 15%) (Figure 5.7C). The lack of rounds of mutants' replication within the fish host may be a feasible explanation for why the *ribA*, *ribB*, *ribE1*, and *ribA-ribE1* mutants do not provide sufficient immune protection. In other words, mutants are simply too attenuated to adequately colonize at the appropriate time or in sufficient numbers to trigger a proper and protective memory immune response. Therefore, *A. salmonicida* riboflavin auxotrophic mutants of RBP (i.e., $\Delta ribA$ and $\Delta ribA-\Delta ribE1$) may not be useful in live-attenuated vaccine design against this pathogen due to their hyper-attenuation. On the other hand, the profound immune suppression imposed on lumpfish by *A. salmonicida* J223 strain may preclude protective immunity [63]. Further studies are required to improve the immunogenicity of the attenuated mutant strains, for instance, using a regulated-delayed attenuation strategy [102] or the overexpression of protective immunogenic antigens by these strains.

5.6. Conclusions

This study is the first report of riboflavin supply pathways in a marine fish bacterial pathogen, *A. salmonicida*, and comprises integral analyses investigating the host-pathogen-riboflavin interactions. Our results indicate that *A. salmonicida* has an RBP with extra gene copies for *ribB* and *ribE*, and *ribN* family transporter, which are encoded in five transcriptional units. Exogenous riboflavin affects the transcriptome response and differentially regulates the expression of riboflavin supply genes. Mutations in *ribA*, *ribB*, and *ribE1* have an impact on bacterial virulence, host colonization, and immune protection. The *ribE2* gene is redundant during lumpfish host colonization. In summary, we showed that riboflavin biosynthesis is essential for *A. salmonicida* virulence and physiology during lumpfish infection.

5.7 References

1. De Colibus, L.; Mattevi, A. New Frontiers in Structural Flavoenzymology. *Curr. Opin. Struct. Biol.* **2006**, *16* (6), 722–728, doi:<https://doi.org/10.1016/j.sbi.2006.10.003>.
2. Abbas, C. A.; Sibirny, A. A. Genetic Control of Biosynthesis and Transport of Riboflavin and Flavin Nucleotides and Construction of Robust Biotechnological Producers. *Microbiol. Mol. Biol. Rev.* **2011**, *75* (2), 321–360, doi:10.1128/MMBR.00030-10.
3. Crossley, R. A.; Gaskin, D. J. H.; Holmes, K.; Mulholland, F.; Wells, J. M.; Kelly, D. J.; van Vliet, A. H. M.; Walton, N. J. Riboflavin Biosynthesis is Associated with Assimilatory Ferric Reduction and Iron Acquisition by *Campylobacter jejuni*. *Appl. Environ. Microbiol.* **2007**, *73* (24), 7819–7825, doi:10.1128/AEM.01919-07.
4. Marsili, E.; Baron, D. B.; Shikhare, I. D.; Coursolle, D.; Gralnick, J. A.; Bond, D. R. *Shewanella* Secretes Flavins That Mediate Extracellular Electron Transfer. *Proc. Natl. Acad. Sci. U. S. A.* **2008**, *105* (10), 3968–3973, doi:10.1073/pnas.0710525105.
5. Yurgel, S. N.; Rice, J.; Domreis, E.; Lynch, J.; Sa, N.; Qamar, Z.; Rajamani, S.; Gao, M.; Roje, S.; Bauer, W. D. *Sinorhizobium meliloti* Flavin Secretion and Bacteria-Host Interaction: Role of the Bifunctional RibBA Protein. *Mol. Plant. Microbe Interact.* **2014**, *27* (5), 437–445, doi:10.1094/MPMI-11-13-0338-R.
6. Rajamani, S.; Bauer, W. D.; Robinson, J. B.; Farrow, J. M. 3rd; Pesci, E. C.; Teplitski, M.; Gao, M.; Sayre, R. T.; Phillips, D. A. The Vitamin Riboflavin and Its Derivative Lumichrome Activate the LasR Bacterial Quorum-sensing Receptor. *Mol. Plant. Microbe Interact.* **2008**, *21* (9), 1184–1192, doi:10.1094/MPMI-21-9-1184.
7. Bonomi, H. R.; Marchesini, M. I.; Klinke, S.; Ugalde, J. E.; Zylberman, V.; Ugalde, R. A.; Comerci, D. J.; Goldbaum, F. A. An Atypical Riboflavin Pathway is Essential for *Brucella abortus* Virulence. *PLoS One* **2010**, *5* (2), e9435, doi:10.1371/journal.pone.0009435.
8. Skaar, E. P. The Battle for Iron between Bacterial Pathogens and Their Vertebrate Hosts. *PLoS Pathog.* **2010**, *6* (8), 1–2, doi:10.1371/journal.ppat.1000949.
9. Gnanagobal, H.; Santander, J. Host-Pathogen Interactions of Marine Gram-positive Bacteria. *Biology (Basel)*. **2022**, *11* (9), doi:10.3390/biology11091316.
10. Prentice, A. M.; Ghattas, H.; Cox, S. E. Host-Pathogen Interactions: Can Micronutrients Tip the Balance? *J. Nutr.* **2007**, *137* (5), 1334–1337, doi:10.1093/jn/137.5.1334.
11. García-Angulo, V. A. Overlapping Riboflavin Supply Pathways in Bacteria. *Crit. Rev. Microbiol.* **2017**, *43* (2), 196–209, doi:10.1080/1040841X.2016.1192578.
12. Jaehme, M.; Slotboom, D. J. Structure, Function, Evolution, and Application of Bacterial Pnu-Type Vitamin Transporters. *Biol. Chem.* **2015**, *396* (9–10), 955–966.
13. Bacher, A.; Eberhardt, S.; Fischer, M.; Kis, K.; Richter, G. Biosynthesis of Vitamin B₂ (Riboflavin). *Annu. Rev. Nutr.* **2000**, *20* (1), 153–167, doi:10.1146/annurev.nutr.20.1.153.
14. Dauner, M.; Sonderegger, M.; Hochuli, M.; Szyperski, T.; Wüthrich, K.; Hohmann,

- H.-P.; Sauer, U.; Bailey, J. E. Intracellular Carbon Fluxes in Riboflavin-Producing *Bacillus subtilis* during Growth on Two-Carbon Substrate Mixtures. *Appl. Environ. Microbiol.* **2002**, *68* (4), 1760–1771, doi:10.1128/AEM.68.4.1760-1771.2002.
15. Fischer, M.; Bacher, A. Biosynthesis of Flavocoenzymes. *Nat. Prod. Rep.* **2005**, *22* (3), 324–350, doi:10.1039/b210142b.
 16. Haase, I.; Gräwert, T.; Illarionov, B.; Bacher, A.; Fischer, M. Recent Advances in Riboflavin Biosynthesis. *Methods Mol. Biol.* **2014**, *1146*, 15–40, doi:10.1007/978-1-4939-0452-5_2.
 17. Vitreschak, A. G.; Rodionov, D. A.; Mironov, A. A.; Gelfand, M. S. Regulation of Riboflavin Biosynthesis and Transport Genes in Bacteria by Transcriptional and Translational Attenuation. *Nucleic Acids Res.* **2002**, *30* (14), 3141–3151.
 18. Angulo, V. A. G.; Bonomi, H. R.; Posadas, D. M.; Serer, M. I.; Torres, A. G.; Zorreguieta, Á.; Goldbaum, F. A. Identification and Characterization of RibN, a Novel Family of Riboflavin Transporters from *Rhizobium leguminosarum* and Other Proteobacteria. **2013**, *195*, 4611–4619, doi:10.1128/JB.00644-13.
 19. Hemberger, S.; Pedrolli, D. B.; Stolz, J.; Vogl, C.; Lehmann, M.; Mack, M. RibM from *Streptomyces davawensis* Is a Riboflavin/Roseoflavin Transporter and May Be Useful for the Optimization of Riboflavin Production Strains. *BMC Biotechnol.* **2011**, *11* (1), 119, doi:10.1186/1472-6750-11-119.
 20. Jaehme, M.; Slotboom, D. J. Diversity of Membrane Transport Proteins for Vitamins in Bacteria and Archaea. *Biochim. Biophys. Acta* **2015**, *1850* (3), 565–576, doi:10.1016/j.bbagen.2014.05.006.
 21. Cisternas, I. S.; Torres, A.; Flores, A. F.; Angulo, V. A. G. Differential Regulation of Riboflavin Supply Genes in *Vibrio cholerae*. *Gut Pathog.* **2017**, *9* (1), 1–7, doi:10.1186/s13099-017-0159-z.
 22. Rivera-Lugo, R.; Light, S. H.; Garelis, N. E.; Portnoy, D. A. RibU Is an Essential Determinant of *Listeria* Pathogenesis That Mediates Acquisition of FMN and FAD during Intracellular Growth. *Proc. Natl. Acad. Sci.* **2022**, *119* (13), e2122173119, doi:10.1073/pnas.2122173119.
 23. Winkler, W. C.; Cohen-Chalamish, S.; Breaker, R. R. An mRNA Structure That Controls Gene Expression by Binding FMN. *Proc. Natl. Acad. Sci. U. S. A.* **2002**, *99* (25), 15908–15913, doi:10.1073/pnas.212628899.
 24. Vicens, Q.; Mondragón, E.; Batey, R. T. Molecular Sensing by the Aptamer Domain of the FMN Riboswitch: A General Model for Ligand Binding by Conformational Selection. *Nucleic Acids Res.* **2011**, *39* (19), 8586–8598, doi:10.1093/nar/gkr565.
 25. Gutiérrez-Preciado, A.; Gabriel Torres, A.; Merino, E.; Ruy Bonomi, H.; Alberto Goldbaum, F.; Antonio García-Angulo, V.; Moreno-Hagelsieb, G. Extensive Identification of Bacterial Riboflavin Transporters and Their Distribution across Bacterial Species. **2015**, doi:10.1371/journal.pone.0126124.
 26. Pedrolli, D.; Langer, S.; Hobl, B.; Schwarz, J.; Hashimoto, M.; Mack, M. The RibB FMN Riboswitch from *Escherichia coli* Operates at the Transcriptional and Translational Level and Regulates Riboflavin Biosynthesis. *FEBS J.* **2015**, *282* (16), 3230–3242, doi:10.1111/febs.13226.
 27. Vitreschak, A. G.; Rodionov, D. A.; Mironov, A. A.; Gelfand, M. S. Riboswitches: The Oldest Mechanism for the Regulation of Gene Expression? *Trends Genet.* **2004**,

- 20 (1), 44–50, doi:10.1016/j.tig.2003.11.008.
28. Adler, M.; Anjum, M.; Berg, O. G.; Andersson, D. I.; Sandegren, L. High Fitness Costs and Instability of Gene Duplications Reduce Rates of Evolution of New Genes by Duplication-Divergence Mechanisms. *Mol. Biol. Evol.* **2014**, *31* (6), 1526–1535, doi:10.1093/molbev/msu111.
 29. Maerk, M.; Johansen, J.; Ertesvåg, H.; Drabløs, F.; Valla, S. Safety in Numbers: Multiple Occurrences of Highly Similar Homologs among *Azotobacter vinelandii* Carbohydrate Metabolism Proteins Probably Confer Adaptive Benefits; 2014, doi:10.1186/1471-2164-15-192.
 30. Wilson, A. C.; Pardee, A. B. Regulation of Flavin Synthesis by *Escherichia coli*. *J. Gen. Microbiol.* **1962**, *28* (2), 283–303, doi:10.1099/00221287-28-2-283.
 31. Perkins, J. B., and J. G. P. Biosynthesis of Riboflavin , Biotin , Folic Acid , and Cobalamin. *Am. Soc. Microbiol.* **1993**, 391–394.
 32. Fuller, T. E.; Mulks, M. H. Characterization of *Actinobacillus pleuropneumoniae* Riboflavin Biosynthesis Genes. *J. Bacteriol.* **1995**, *177* (24), 7265–7270.
 33. Beaz-Hidalgo, R.; Figueras, M. J. *Aeromonas* spp. Whole Genomes and Virulence Factors Implicated in Fish Disease. *J. Fish Dis.* **2013**, *36* (4), 371–388, doi:10.1111/jfd.12025.
 34. Dallaire-Dufresne, S.; Tanaka, K. H.; Trudel, M. V; Lafaille, A.; Charette, S. J. Virulence, Genomic Features, and Plasticity of *Aeromonas salmonicida* subsp. *salmonicida*, the Causative Agent of Fish Furunculosis. *Vet. Microbiol.* **2014**, *169* (1–2), 1–7, doi:10.1016/j.vetmic.2013.06.025.
 35. Powell, A.; Treasurer, J. W.; Pooley, C. L.; Keay, A. J.; Lloyd, R.; Imsland, A. K.; Garcia de Leaniz, C. Use of Lumpfish for Sea-Lice Control in Salmon Farming: Challenges and Opportunities. *Rev. Aquac.* **2018**, *10* (3), 683–702, doi:10.1111/raq.12194.
 36. Imsland, A. K. D.; Hanssen, A.; Nytrø, A. V.; Reynolds, P.; Jonassen, T. M.; Hangstad, T. A.; Elvegård, T. A.; Urskog, T. C.; Mikalsen, B. It Works! Lumpfish Can Significantly Lower Sea Lice Infestation in Large-Scale Salmon Farming. *Biol. Open* **2018**, *7* (9), 1–6, doi:10.1242/bio.036301.
 37. Gulla, S.; Duodu, S.; Nilsen, A.; Fossen, I.; Colquhoun, D. J. *Aeromonas salmonicida* Infection Levels in Pre- and Post-Stocked Cleaner Fish Assessed by Culture and an Amended qPCR Assay. *J. Fish Dis.* **2016**, *39* (7), 867–877, doi:10.1111/jfd.12420.
 38. Rouleau, F. D.; Vincent, A. T.; Charette, S. J. Genomic and Phenotypic Characterization of an Atypical *Aeromonas salmonicida* Strain Isolated from a Lumpfish and Producing Unusual Granular Structures. *J. Fish Dis.* **2018**, *41* (4), 673–681, doi:10.1111/jfd.12769.
 39. Fast, M. D.; Tse, B.; Boyd, J. M.; Johnson, S. C. Mutations in the *Aeromonas salmonicida* subsp. *salmonicida* Type III Secretion System Affect Atlantic Salmon Leucocyte Activation and Downstream Immune Responses. *Fish Shellfish Immunol.* **2009**, *27* (6), 721–728, doi:10.1016/j.fsi.2009.09.009.
 40. Valderrama, K.; Saravia, M.; Santander, J. Phenotype of *Aeromonas salmonicida* sp. *salmonicida* Cyclic Adenosine 3',5'-Monophosphate Receptor Protein (Crp) Mutants and Its Virulence in Rainbow Trout (*Oncorhynchus mykiss*). *J. Fish Dis.*

- 2017, 40 (12), 1849–1856, doi:10.1111/jfd.12658.
41. Vasquez, I.; Cao, T.; Hossain, A.; Valderrama, K.; Gnanagobal, H.; Dang, M.; Leeuwis, R. H. J.; Ness, M.; Campbell, B.; Gendron, R.; Kao, K.; Westcott, J.; Gamperl, A. K.; Santander, J. *Aeromonas salmonicida* Infection Kinetics and Protective Immune Response to Vaccination in Sablefish (*Anoplopoma fimbria*). *Fish Shellfish Immunol.* **2020**, 104 (May), 557–566, doi:10.1016/j.fsi.2020.06.005.
 42. Gauthier, J.; Marquis, H.; Paquet, V. E.; Charette, S. J.; Levesque, R. C.; Derome, N. Genomic Perspectives on *Aeromonas salmonicida* subsp. *salmonicida* Strain 890054 as a Model System for Pathogenicity Studies and Mitigation of Fish Infections. *Front. Mar. Sci.* **2021**, 8 (November), 1–8, doi:10.3389/fmars.2021.744052.
 43. Inglis, V.; Robertson, D.; Miller, K.; Thompson, K. D.; Richards, R. H. Antibiotic Protection against Recrudescence of Latent *Aeromonas salmonicida* during Furunculosis Vaccination. *J. Fish Dis.* **1996**, 19 (5), 341–348.
 44. Sommerset, I.; Krossøy, B.; Biering, E.; Frost, P. Vaccines for Fish in Aquaculture. *Expert Rev. Vaccines* **2005**, 4 (1), 89–101, doi:10.1586/14760584.4.1.89.
 45. Gudding, R.; Van Muiswinkel, W. B. A History of Fish Vaccination: Science-Based Disease Prevention in Aquaculture. *Fish Shellfish Immunol.* **2013**, 35 (6), 1683–1688.
 46. Menanteau-Ledouble, S.; Krauss, I.; Santos, G.; Fibi, S.; Weber, B.; El-Matbouli, M. Effect of a Phytogenic Feed Additive on the Susceptibility of *Onchorhynchus mykiss* to *Aeromonas salmonicida*. *Dis. Aquat. Organ.* **2015**, 115 (1), 57–66.
 47. Nerland, A. H.; Høgh, B. T.; Olsen, A. B.; Jensen, H. B. *Aeromonas salmonicida* ssp. *salmonicida* Requires Exogenous Arginine and Methionine for Growth. *J. Fish Dis.* **1993**, 16 (6), 605–608, doi:10.1111/j.1365-2761.1993.tb00898.x.
 48. Bertani, G. Studies on Lysogenesis. I. The Mode of Phage Liberation by Lysogenic *Escherichia coli*. *J. Bacteriol.* **1951**, 62 (3), 293–300, doi:10.1128/jb.62.3.293-300.1951.
 49. Reith, M. E.; Singh, R. K.; Curtis, B.; Boyd, J. M.; Bouevitch, A.; Kimball, J.; Munholland, J.; Murphy, C.; Sarty, D.; Williams, J.; Nash, J. H.; Johnson, S. C.; Brown, L. L. The Genome of *Aeromonas salmonicida* subsp. *salmonicida* A449: Insights into the Evolution of a Fish Pathogen. *BMC Genomics* **2008**, 9 (1), 427, doi:10.1186/1471-2164-9-427.
 50. Kanehisa, M.; Sato, Y.; Kawashima, M.; Furumichi, M.; Tanabe, M. KEGG as a Reference Resource for Gene and Protein Annotation. *Nucleic Acids Res.* **2015**, 44, 457–462, doi:10.1093/nar/gkv1070.
 51. Abreu-Goodger, C.; Merino, E. RibEx: A Web Server for Locating Riboswitches and Other Conserved Bacterial Regulatory Elements. *Nucleic Acids Res.* **2005**, 33 (Web Server issue), W690-2, doi:10.1093/nar/gki445.
 52. Waterhouse, A. M.; Procter, J. B.; Martin, D. M. A.; Clamp, M.; Barton, G. J. Jalview Version 2—a Multiple Sequence Alignment Editor and Analysis Workbench. *Bioinformatics* **2009**, 25 (9), 1189–1191, doi:10.1093/bioinformatics/btp033.
 53. Gouet, P.; Robert, X.; Courcelle, E. ESPript/ENDscript: Extracting and Rendering Sequence and 3D Information from Atomic Structures of Proteins. **2003**,

- doi:10.1093/nar/gkg556.
54. Sö, J.; Biegert, A.; Lupas, A. N. The HHpred Interactive Server for Protein Homology Detection and Structure Prediction. **2005**, doi:10.1093/nar/gki408.
 55. Humphrey, W.; Dalke, A.; Schulten, K. VMD: Visual Molecular Dynamics. *J. Mol. Graph.* **1996**, *14* (1), 33–38, 27–28.
 56. Du, Z.; Su, H.; Wang, W.; Ye, L.; Wei, H.; Peng, Z.; Anishchenko, I.; Baker, D.; Yang, J. The TrRosetta Server for Fast and Accurate Protein Structure Prediction. *Nat. Protoc.* **2021**, *16* (12), 5634–5651, doi:10.1038/s41596-021-00628-9.
 57. Roland, K.; Curtiss, R. 3rd; Sizemore, D. Construction and Evaluation of a Delta Cya Delta Crp *Salmonella* Typhimurium Strain Expressing Avian Pathogenic *Escherichia coli* O78 LPS as a Vaccine to Prevent Airsacculitis in Chickens. *Avian Dis.* **1999**, *43* (3), 429–441.
 58. Santander, J.; Wanda, S. Y.; Nickerson, C. A.; Curtiss, R. Role of RpoS in Fine-Tuning the Synthesis of Vi Capsular Polysaccharide in *Salmonella enterica* Serotype Typhi. *Infect. Immun.* **2007**, *75* (3), 1382–1392, doi:10.1128/IAI.00888-06.
 59. Datsenko, K. A.; Wanner, B. L. One-Step Inactivation of Chromosomal Genes in *Escherichia coli* K-12 Using PCR Products. *Proc. Natl. Acad. Sci. U. S. A.* **2000**, *97* (12), 6640–6645, doi:10.1073/pnas.120163297.
 60. Connors, E.; Soto-Dávila, M.; Hossain, A.; Vasquez, I.; Gnanagobal, H.; Santander, J. Identification and Validation of Reliable *Aeromonas salmonicida* subspecies *salmonicida* Reference Genes for Differential Gene Expression Analyses. *Infect. Genet. Evol.* **2019**, *73*, doi:10.1016/j.meegid.2019.05.011.
 61. Sambrook, J. and Russel, W. *Molecular Cloning: A Laboratory Manual*, 2nd ed.; Cold Spring Harbor Laboratory Press: New York, 2001.
 62. Umasuthan, N.; Valderrama, K.; Vasquez, I.; Segovia, C.; Hossain, A.; Cao, T.; Gnanagobal, H.; Monk, J.; Boyce, D.; Santander, J. A Novel Marine Pathogen Isolated from Wild Cunnners (*Tautoglabrus adspersus*): Comparative Genomics and Transcriptome Profiling of *Pseudomonas* sp. Strain J380. *Microorganisms* **2021**, *9* (4), doi:10.3390/microorganisms9040812.
 63. Chakraborty, S.; Hossain, A.; Cao, T.; Gnanagobal, H.; Segovia, C.; Hill, S.; Monk, J.; Porter, J.; Boyce, D.; Hall, J. R.; Bindea, G.; Kumar, S.; Santander, J. Multi-Organ Transcriptome Response of Lumpfish (*Cyclopterus lumpus*) to *Aeromonas salmonicida* subspecies *salmonicida* Systemic Infection. *Microorganisms*. **2022**, doi:10.3390/microorganisms10112113.
 64. Ewels, P.; Magnusson, M.; Lundin, S.; Käller, M. MultiQC: Summarize Analysis Results for Multiple Tools and Samples in a Single Report. *Bioinformatics* **2016**, *32* (19), 3047–3048, doi:10.1093/bioinformatics/btw354.
 65. Li, B.; Ruotti, V.; Stewart, R. M.; Thomson, J. A.; Dewey, C. N. RNA-Seq Gene Expression Estimation with Read Mapping Uncertainty. *Bioinformatics* **2010**, *26* (4), 493–500, doi:10.1093/bioinformatics/btp692.
 66. Teng, M.; Love, M. I.; Davis, C. A.; Djebali, S.; Dobin, A.; Graveley, B. R.; Li, S.; Mason, C. E.; Olson, S.; Pervouchine, D.; Sloan, C. A.; Wei, X.; Zhan, L.; Irizarry, R. A. Erratum to: A Benchmark for RNA-Seq Quantification Pipelines. *Genome Biol.* **2016**, *17* (1), 203, doi:10.1186/s13059-016-1060-7.
 67. Pereira, M. B.; Wallroth, M.; Jonsson, V.; Kristiansson, E. Comparison of

- Normalization Methods for the Analysis of Metagenomic Gene Abundance Data. *BMC Genomics* **2018**, *19* (1), 274, doi:10.1186/s12864-018-4637-6.
68. Robinson, M. D.; McCarthy, D. J.; Smyth, G. K. EdgeR: A Bioconductor Package for Differential Expression Analysis of Digital Gene Expression Data. *Bioinformatics* **2010**, *26* (1), 139–140, doi:10.1093/bioinformatics/btp616.
 69. Taboada, B.; Estrada, K.; Ciria, R.; Merino, E. Operon-Mapper: A Web Server for Precise Operon Identification in Bacterial and Archaeal Genomes. *Bioinformatics* **2018**, *34* (23), 4118–4120, doi:10.1093/bioinformatics/bty496.
 70. Pfaffl, M. W. A New Mathematical Model for Relative Quantification in Real-Time RT-PCR. *Nucleic Acids Res.* **2001**, *29* (9), e45, doi:10.1093/nar/29.9.e45.
 71. Vandesompele, J.; De Preter, K.; Pattyn, F.; Poppe, B.; Van Roy, N.; De Paepe, A.; Speleman, F. Accurate Normalization of Real-Time Quantitative RT-PCR Data by Geometric Averaging of Multiple Internal Control Genes. *Genome Biol.* **2002**, *3* (7), 1–12.
 72. Livak, K. J.; Schmittgen, T. D. Analysis of Relative Gene Expression Data Using Real-Time Quantitative PCR and the $2^{-\Delta\Delta C(T)}$ Method. *Methods* **2001**, *25* (4), 402–408, doi:10.1006/meth.2001.1262.
 73. Gnanagobal, H.; Cao, T.; Hossain, A.; Dang, M.; Hall, J. R.; Kumar, S.; Van Cuong, D.; Boyce, D.; Santander, J. Lumpfish (*Cyclopterus lumpus*) is Susceptible to *Renibacterium salmoninarum* Infection and Induces Cell-mediated Immunity in the Chronic Stage. *Frontiers in Immunology* . 2021, p 4647.
 74. Santander, J.; Martin, T.; Loh, A.; Pohlenz, C.; Gatlin, D. M.; Curtiss, R. Mechanisms of Intrinsic Resistance to Antimicrobial Peptides of *Edwardsiella ictaluri* and Its Influence on Fish Gut Inflammation and Virulence. *Microbiology* **2013**, *159* (Pt 7), 1471–1486, doi:10.1099/mic.0.066639-0.
 75. Edwards, R. A.; Keller, L. H.; Schifferli, D. M. Improved Allelic Exchange Vectors and Their Use to Analyze 987P Fimbria Gene Expression. *Gene* **1998**, *207*, 149–157.
 76. Reyrat, J.; Pelicic, V.; Gicquel, B. Counterselectable Markers: Untapped Tools for Bacterial Genetics and Pathogenesis. *Infect. Immun.* **1998**, *66* (9), 4011–4017.
 77. Kelly, M. J. S.; Ball, L. J.; Krieger, C.; Yu, Y.; Fischer, M.; Schiffmann, S.; Schmieder, P.; Kühne, R.; Bermel, W.; Bacher, A.; Richter, G.; Oschkinat, H. The NMR Structure of the 47-KDa Dimeric Enzyme 3,4-Dihydroxy-2-Butanone-4-Phosphate Synthase and Ligand Binding Studies Reveal the Location of the Active Site. *Proc. Natl. Acad. Sci. U. S. A.* **2001**, *98* (23), 13025–13030, doi:10.1073/pnas.231323598.
 78. Ren, J.; Kotaka, M.; Lockyer, M.; Lamb, H. K.; Hawkins, A. R.; Stammers, D. K. GTP Cyclohydrolase II Structure and Mechanism. *J. Biol. Chem.* **2005**, *280* (44), 36912–36919, doi:10.1074/jbc.M507725200.
 79. Islam, Z.; Kumar, A.; Singh, S.; Salmon, L.; Karthikeyan, S. Structural Basis for Competitive Inhibition of 3,4-Dihydroxy-2-Butanone-4-Phosphate Synthase from *Vibrio cholerae*. *J. Biol. Chem.* **2015**, *290* (18), 11293–11308, doi:10.1074/jbc.M114.611830.
 80. Brutinel, E. D.; Dean, A. M.; Gralnick, J. A. Description of a Riboflavin Biosynthetic Gene Variant Prevalent in the Phylum Proteobacteria. *J. Bacteriol.*

- 2013, 195 (24), 5479–5486, doi:10.1128/JB.00651-13.
81. Nouwen, N.; Arrighi, J. F.; Gully, D.; Giraud, E. RibBX of *Bradyrhizobium* ORS285 Plays an Important Role in Intracellular Persistence in Various *Aeschynomene* Host Plants. *Mol. Plant-Microbe Interact.* **2021**, 34 (1), 88–99, doi:10.1094/MPMI-07-20-0209-R.
 82. Illarionov, B.; Kemter, K.; Eberhardt, S.; Richter, G.; Cushman, M.; Bacher, A. Riboflavin Synthase of *Escherichia coli*. Effect of Single Amino Acid Substitutions on Reaction Rate and Ligand Binding Properties. *J. Biol. Chem.* **2001**, 276 (15), 11524–11530, doi:10.1074/jbc.M008931200.
 83. Serer, M. I.; Bonomi, H. R.; Guimarães, B. G.; Rossi, R. C.; Goldbaum, F. A.; Klinke, S. Crystallographic and Kinetic Study of Riboflavin Synthase from *Brucella abortus*, a Chemotherapeutic Target with an Enhanced Intrinsic Flexibility. *Acta Crystallogr. D. Biol. Crystallogr.* **2014**, 70 (Pt 5), 1419–1434, doi:10.1107/S1399004714005161.
 84. Ma, Y.; Pan, C.; Wang, Q. Crystal Structure of Bacterial Cyclopropane-Fatty-Acyl-Phospholipid Synthase with Phospholipid. *J. Biochem.* **2019**, 166 (2), 139–147, doi:10.1093/jb/mvz018.
 85. Sepúlveda-Cisternas, I.; Lozano Aguirre, L.; Fuentes Flores, A.; Vásquez Solis de Ovando, I.; García-Angulo, V. A. Transcriptomics Reveals a Cross-modulatory Effect between Riboflavin and Iron and Outlines Responses to Riboflavin Biosynthesis and Uptake in *Vibrio Cholerae*. *Sci. Rep.* **2018**, 8 (1), 3149, doi:10.1038/s41598-018-21302-3.
 86. Gelfand, M. S.; Mironov, A. A.; Jomantas, J.; Kozlov, Y. I.; Perumov, D. A. A Conserved RNA Structure Element Involved in the Regulation of Bacterial Riboflavin Synthesis Genes. *Trends Genet.* **1999**, 15 (11), 439–442, doi:10.1016/s0168-9525(99)01856-9.
 87. Burgess, C. M.; Slotboom, D. J.; Geertsma, E. R.; Durkens, R. H.; Poolman, B.; Van Sinderen, D. The Riboflavin Transporter RibU in *Lactococcus lactis*: Molecular Characterization of Gene Expression and the Transport Mechanism. *J. Bacteriol.* **2006**, 188 (8), 2752–2760, doi:10.1128/JB.188.8.2752-2760.2006.
 88. Schott, K.; Kellermann, J.; Lottspeich, F.; Bacher, A. Riboflavin Synthases of *Bacillus subtilis*. Purification and Amino Acid Sequence of the Alpha Subunit. *J. Biol. Chem.* **1990**, 265 (8), 4204–4209.
 89. Grill, S.; Yamaguchi, H.; Wagner, H.; Zwahlen, L.; Kusch, U.; Mack, M. Identification and Characterization of Two *Streptomyces davawensis* Riboflavin Biosynthesis Gene Clusters. *Arch. Microbiol.* **2007**, 188 (4), 377–387, doi:10.1007/s00203-007-0258-1.
 90. Hickman, A. B.; Dyda, F. Mechanisms of DNA Transposition. *Microbiol. Spectr.* **2015**, 3 (2), MDNA3-2014, doi:10.1128/microbiolspec.MDNA3-0034-2014.
 91. Mahillon, J.; Chandler, M. Insertion Sequences. *Microbiol. Mol. Biol. Rev.* **1998**, 62 (3), 725–774, doi:10.1128/MMBR.62.3.725-774.1998.
 92. Tanaka, K. H.; Frenette, M.; Charette, S. J. IS-Mediated Loss of Virulence by *Aeromonas salmonicida*. *Mob. Genet. Elements* **2013**, 3 (1), e23498, doi:10.4161/mge.23498.
 93. Lysnyansky, I.; Calcutt, M. J.; Ben-Barak, I.; Ron, Y.; Levisohn, S.; Methé, B. A.;

- Yogev, D. Molecular Characterization of Newly Identified IS3, IS4 and IS30 Insertion Sequence-like Elements in *Mycoplasma bovis* and Their Possible Roles in Genome Plasticity. *FEMS microbiology letters*. England May 2009, pp 172–182, doi:10.1111/j.1574-6968.2009.01562.x.
94. Schmid-Appert, M.; Zoller, K.; Traber, H.; Vuilleumier, S.; Leisinger, T. Association of Newly Discovered IS Elements with the Dichloromethane Utilization Genes of Methylotrophic Bacteria. *Microbiology* **1997**, *143* (Pt 8, 2557–2567, doi:10.1099/00221287-143-8-2557.
 95. Balado, M.; Souto, A.; Vences, A.; Careaga, V. P.; Valderrama, K.; Segade, Y.; Rodríguez, J.; Osorio, C. R.; Jiménez, C.; Lemos, M. L. Two Catechol Siderophores, Acinetobactin and Amonabactin, are Simultaneously Produced by *Aeromonas salmonicida* subsp. *salmonicida* Sharing Part of the Biosynthetic Pathway. *ACS Chem. Biol.* **2015**, *10* (12), 2850–2860, doi:10.1021/acscchembio.5b00624.
 96. Chakraborty, S.; Cao, T.; Hossain, A.; Gnanagobal, H.; Vasquez, I.; Boyce, D.; Santander, J. Vibrogen-2 Vaccine Trial in Lumpfish (*Cyclopterus lumpus*) against *Vibrio anguillarum*. *J. Fish Dis.* **2019**, *42* (7), 1057–1064, doi:10.1111/jfd.13010.
 97. Dang, M.; Cao, T.; Vasquez, I.; Hossain, A.; Gnanagobal, H.; Kumar, S.; Hall, J. R.; Monk, J.; Boyce, D.; Westcott, J.; Santander, J. Oral Immunization of Larvae and Juvenile of Lumpfish (*Cyclopterus lumpus*) against *Vibrio anguillarum* Does Not Influence Systemic Immunity. *Vaccines* **2021**, *9* (8), 819, doi:10.3390/vaccines9080819.
 98. Fuller, T. E.; Thacker, B. J.; Mulks, M. H. A Riboflavin Auxotroph of *Actinobacillus pleuropneumoniae* is Attenuated in Swine. *Infect. Immun.* **1996**, *64* (11), 4659–4664.
 99. Lopez, A. M.; Townsend, H. G. G.; Allen, A. L.; Hondalus, M. K. Safety and Immunogenicity of a Live-Attenuated Auxotrophic Candidate Vaccine against the Intracellular Pathogen *Rhodococcus equi*. *Vaccine* **2008**, *26* (7), 998–1009, doi:10.1016/j.vaccine.2007.10.069.
 100. Fuller, T. E.; Thacker, B. J.; Duran, C. O.; Mulks, M. H. A Genetically-Defined Riboflavin Auxotroph of *Actinobacillus pleuropneumoniae* as a Live Attenuated Vaccine. *Vaccine* **2000**, *18* (25), 2867–2877, doi:10.1016/S0264-410X(00)00076-1.
 101. Vaughan, L. M.; Smith, P. R.; Foster, T. J. An Aromatic-Dependent Mutant of the Fish Pathogen *Aeromonas salmonicida* is Attenuated in Fish and Is Effective as a Live Vaccine against the Salmonid Disease Furunculosis. *Infect. Immun.* **1993**, *61* (5), 2172–2181, doi:10.1128/iai.61.5.2172-2181.1993.
 102. Swain, B.; Powell, C. T.; Curtiss, R. Pathogenicity and Immunogenicity of *Edwardsiella piscicida* Ferric Uptake Regulator (Fur) Mutations in Zebrafish. *Fish Shellfish Immunol.* **2020**, *107*, 497–510, doi:https://doi.org/10.1016/j.fsi.2020.10.029.

5.8. Supplementary Materials

The following URL leads to Supplementary File 5.1:

<https://www.tandfonline.com/doi/full/10.1080/21505594.2023.2187025>

Supplementary Table S5.1. Primers for Reverse Transcription PCR (RT-PCR) used to amplify gene junctions of *rib* gene operons

Primer name	Sequence (5' to 3')	Gene junction	Amplicon size (bp)
cysB-F	CAGCCAGCAACTGACACAAGGT	<i>cysB</i> - <i>ribA</i>	400
ribA-R	GAAAGCCTACCAGCGTGAA		
ribA-F	CCTCTCGACCAAAGCGAATAA	<i>ribA</i> - <i>cmk</i>	228
cmk-R	TGCCATGTTTGCCGATATAGAG		
3030-F	ATTGTTGCGCTGATCGAAGC	<i>nrdR</i> - AXA69_003030	246
nrdR-R	TATCAACCGCACTACAGAAAGG		
nrdR-F	ATGGATGAGCTCAAGAGCCTG	<i>ribD</i> - <i>nrdR</i>	413
ribD-R	CAGGGTCACATAAGCGGTAG		
ribD-F	ATCAAGGATGTGCGGCTGGTGG	<i>ribE1</i> - <i>ribD</i>	144
ribE1-R	GTTCCCACCGCTTCGATAAT		
ribE1-F	GTTATCTGGAGCGGCTGATG	<i>ribBA</i> - <i>ribE1</i>	304
ribBA-R	ATCCATCAGGATCACCATCTT		
ribBA-F	GTGGAATACGTCGGCGAATAA	<i>ribH</i> - <i>ribBA</i>	248
ribH-R	GTCCACCAAGCTTTCGTTGAT		
ribH-F	TACCAAGGCGGGTAACAAGG	<i>nusB</i> - <i>ribH</i>	254
nusB-R	AACAGCAGATCGCGGAAATA		
nusB-F	ACTGGACAAGGTGATCAAGAC	<i>thiL</i> - <i>nusB</i>	360
thiL-R	GGCGAGATCGGACAAATTGA		
8895-F	CGATGCGAATGGCCTCACA	AXA69_018895 - <i>ribE2</i>	244
ribE2-R	ATCACATGGGTGCGAAAGT		
ribE2-F	AACCTGGGTTGGGTCAAAG	<i>ribE2</i> - AXA69_018885	440
8885-R	ATCCCTCGGTGAGTTGAATG		
purU-F	TGTTGAGCTGGTGCTTGTAG	<i>purU</i> - <i>ribB</i>	600
ribB-R	GGGATCACCAAATTCAGTGTGTA		
ribB-F	TGAGCTGACCAAAGAAGATGG	<i>ribB</i> - AXA69_001415	439
1415-R	TTCCAGTTCGCTGGTGTTT		
8915-F	AGCCAGGAAGCCGTCTAT	AXA69_018915 - <i>ribN</i>	403
ribN-R	ATATTGGCTCAGACTGTTGAC		
ribN-F	CTGGCTGGCTGGTGTTT	<i>ribN</i> - <i>purT</i>	367
purT-R	TTGTGTGCCACCTGCAT		

Supplementary Table S5.2. RT-qPCR primers and primer efficiency

Gene	Forward primer (5' to 3')	T _m (°C)	Reverse primer (5' to 3')	T _m (°C)	Amplicon length (bp)	% Efficiency
<i>ribA</i>	CTGCGCCTGATGACCAATAA	55	GGTAGAACTCGTTGTGAGGATTG	55	115	98.85
<i>ribB</i>	CATGATGATCCGCGAGTGTT	55	GTCTGATAGTGGCTGGAGTTTG	55	111	91.45
<i>ribBA</i>	AAACTGCCACCGAGTTT	53	GGTCTGGATGTCACCTTTCTT	54	99	90.38
<i>ribE1</i>	GAATCTCGAGGTGGATCAGATAG	53	GACCAGTTTCTCCAGAGTCAG	54	100	94.91
<i>ribD</i>	GCCAAGCGGAACATCAATTC	54	GATAAAGCACCAGCTCATCCA	54	97	89.38
<i>ribE2</i>	GTGAAGTGCAGAGAGAGTGAAT	54	GGATCGATCTCGATATTGGTGTG	55	109	88.91
<i>ribH</i>	CAAGTCCAGGACAGCAATCT	54	TGGCATCGTATTGACCACTC	54	100	90.70
<i>ribN</i>	CCAGTTGCCTTTCATCAATAC	54	CGCAATTGGTTGGTCATCAG	54	99	104.84

Supplementary Table S5.3. Primers for mutants and plasmids construction

Primer	Sequence (5' to 3')
<i>ΔribBA A.sal (SphI)</i> F1	ACATGCATGCGGTGGGTGAGGTGAAGAGCAAGTCC
<i>ΔribBA A.sal (XhoI-PstI)</i> R1	CTCGAGCGGAAAACACTGCAGTTTTAGAGCGGGATCACAGAAAATCGTTT
<i>ΔribBA A.sal (XhoI-PstI)</i> F2	AAAACACTGCAGTTTTCCGCTCGAGTAAGCACGTGCCCCGCATGACATTG
<i>ΔribBA A.sal (XbaI)</i> R2	TCGTCTAGAGTGCCGCCACGGATGACGGTGCCCA
<i>ΔribE1 A.sal (SphI)</i> F1	ACATGCATGCACAAGGCGGCTGGCGACTGGCCTGA
<i>ΔribE1 A.sal (XhoI-PstI)</i> R1	CTCGAGCGGAAAACACTGCAGTTTTGCAGATCACCTTGATGATGACGGGG
<i>ΔribE1 A.sal (XhoI-PstI)</i> F2	AAAACACTGCAGTTTTCCGCTCGAGAACATAATTCTGTATCAAAGTGAGC
<i>ΔribE1 A.sal (XbaI)</i> R2	TCGTCTAGATGGCATCGGGCGCCACGGCGGCTG
<i>ΔribE2 A.sal (SphI)</i> F1	ACATGCATGCGGAGACAAAATGCGGGGGTGTCTT
<i>ΔribE2 A.sal (XhoI-PstI)</i> R1	CTCGAGCGGAAAACACTGCAGTTTTGTCTCTTCTCTCTGCTACGAAAAAAGGC
<i>ΔribE2 A.sal (XhoI-PstI)</i> F2	AAAACACTGCAGTTTTCCGCTCGAGGGTCAAAGCCGGTTGGCACACCAATAT
<i>ΔribE2 A.sal (XbaI)</i> R2	TCGTCTAGAGCTCAGATCCCTCGGTGAGTTGAAT
<i>ΔribA A.sal (SphI)</i> F1	ACATGCATGCTCGAGTTCACATCATGGTGCAAGG
<i>ΔribA A.sal (XhoI-PstI)</i> R1	CTCGAGCGGAAAACACTGCAGTTTTAGGTTGCTCCTTACTACAGCTGCTT
<i>ΔribA A.sal (XhoI-PstI)</i> F2	AAAACACTGCAGTTTTCCGCTCGAGTGAGCCTCACAACGAGGCCTGCCTTT
<i>ΔribA A.sal (XbaI)</i> R2	TCGTCTAGACAAAACCTATGTTCTGACTGGGCGTC
<i>ΔribB A.sal (SphI)</i> F1	ACATGCATGCCCATCTCTGTCATGATTCCGTTTGT
<i>ΔribB A.sal (XhoI-PstI)</i> R1	CTCGAGCGGAAAACACTGCAGTTTTGCAATATCTGTCTTATCCTCTTTCATC
<i>ΔribB A.sal (XhoI-PstI)</i> F2	AAAACACTGCAGTTTTCCGCTCGAGTGAGCCTCATAACGAAATTGTAATAAG
<i>ΔribB A.sal (XbaI)</i> R2	TCGTCTAGATGCAACATCAGCAGCAATCTTGGAT
<i>ΔribN A.sal (SphI)</i> F1	ACATGCATGCACGTTTCGTTTCAGGTTGTCACCACCG
<i>ΔribN A.sal (XhoI-PstI)</i> R1	CTCGAGCGGAAAACACTGCAGTTTTGGGATCCGGGTCGCTGGAAAAAAGT
<i>ΔribN A.sal (XhoI-PstI)</i> F2	AAAACACTGCAGTTTTCCGCTCGAGTGAGGTACGCCATGCGTGCCTCTTT
<i>ΔribN A.sal (XbaI)</i> R2	TCGTCTAGACTTGCTCAAGCTGTGCGAGGGTATC
<i>P_{lac-ribBA}</i> F	TTTACACTTTATGCTTCCGGCTCGTATGTTATGGCGCTGAGCACAAACCAGGAAA
<i>ribBA</i> R	TTATTCGCCGACGTATTCCACCACT
<i>P_{lac-ribE1}</i> F	TTTACACTTTATGCTTCCGGCTCGTATGTTATGTTTACCGBAATTATCGAAGCGG
<i>ribE1</i> R	TTACAGAAAAGCCGGACTGGACCAGT
<i>P_{lac-ribE2}</i> F	TTTACACTTTATGCTTCCGGCTCGTATGTTATGTTTACCGBGCATAGTGCAGGGGA
<i>ribE2</i> R	GATCAGGTTGACGCAAAATTCACTC
<i>P_{lac-ribA}</i> F	TTTACACTTTATGCTTCCGGCTCGTATGTTATGAGCAGCGTTACCCTCGTGGCCA
<i>ribA</i> R	TCACTTCTTGAACATGTGGTCCAAT
<i>P_{lac-ribB}</i> F	TTTACACTTTATGCTTCCGGCTCGTATGTTATGAATCAGTCTCTACTCAGTGAAT
<i>ribB</i> R	TCAGGCAGAACGTTCTGACAGCAAT
<i>P_{lac-ribN}</i> F	TTTACACTTTATGCTTCCGGCTCGTATGTTATGGCACCCCTCGCGCAGGCACTCTC
<i>ribN</i> R	TCAGGAAACAGATTGATGGGCGCGC
<i>E. coli-ribA-H1P1</i>	TATCTGGAGAATTTCATGCAGCTTAAACGTGTGGCAGAATGTAGGCTGGAGCTGCTTCG
<i>E. coli-ribA-H2P2</i>	AGCAAATGAATTACACAATGCAAGAGGGTTATTTGTTTACATATGAATATCCTCCTTAG
<i>E. coli-RibA-Fw</i>	ATTCTCGAGGCAATCGAACGCATGGCCTCTCC
<i>E. coli-RibA-Rv</i>	ATTAAGCTTTATGTTGAAGTAACAACACTATTTGC

Supplementary Table S5.4. Mapping Statistics of Transcriptomics

Experimental condition	Number of reads	Number of reads after trimming	Percentage (%) trimmed	Mapped reads	Percentage (%) reads mapped
ASAL_Control_1	138,818,018	138,757,015	99.96	137,107,214	98.85
ASAL_Control_2	124,141,028	124,075,517	99.95	122,783,010	99.00
ASAL_Control_3	125,508,488	125,396,689	99.91	123,806,818	98.81
ASAL_Riboflavin_1	121,754,142	121,658,530	99.92	120,190,512	98.86
ASAL_Riboflavin_2	172,517,820	172,340,374	99.90	170,258,416	98.89
ASAL_Riboflavin_3	115,788,490	115,727,832	99.95	114,385,936	98.89

Supplementary Table S5.5. Biochemical profiles of wild-type and mutants of *A. salmonicida* using the API 20E

Enzyme Assayed for	J223	$\Delta ribA$	$\Delta ribAB$	$\Delta ribB$	$\Delta ribE1$	$\Delta ribE2$	$\Delta ribN$	$\Delta ribA-\Delta ribE1$
β -Galactosidase	-	-	-	-	-	-	-	-
Indole production	-	-	-	-	-	-	-	-
Acetoin production	+	+	+	+	+	+	+	+
Citrate utilization	-	-	-	-	-	-	-	-
H ₂ S production	-	-	-	-	-	-	-	-
Urease	-	-	-	-	-	-	-	-
Hydrolysis of:								
L-Arginine	+	+	+	+	+	+	+	_*
L-Lysine	-	-	-	-	-	-	-	-
L-Ornithine	-	-	-	-	-	-	-	-
L-Tryptophane	-	-	-	-	-	-	-	-
Gelatinase	+	+	+	+	+	+	+	+
Assimilation of:								
D-Glucose	+	+	+	+	+	+	+	+
D-Mannitol	+	+	+	+	+	+	+	+
Inositol	-	-	-	-	-	-	-	-
D-Sorbitol	-	-	-	-	-	-	-	-
L-Rhamnose	-	-	-	-	-	-	-	-
D-Sucrose	-	-	-	-	-	-	-	-
D-Melibiose	-	-	-	-	-	-	-	-
Amygdalin	+	+	+	+	+	+	+	+
L-Arabinose	-	-	-	-	-	-	-	-
Oxidase	+	+	+	+	+	+	+	+

+ positive, -negative, * different reaction compared to wild-type and other mutant strains

Supplementary Table S5.6. Biochemical profiles of wild-type and mutants of *A. salmonicida* using the API 20NE

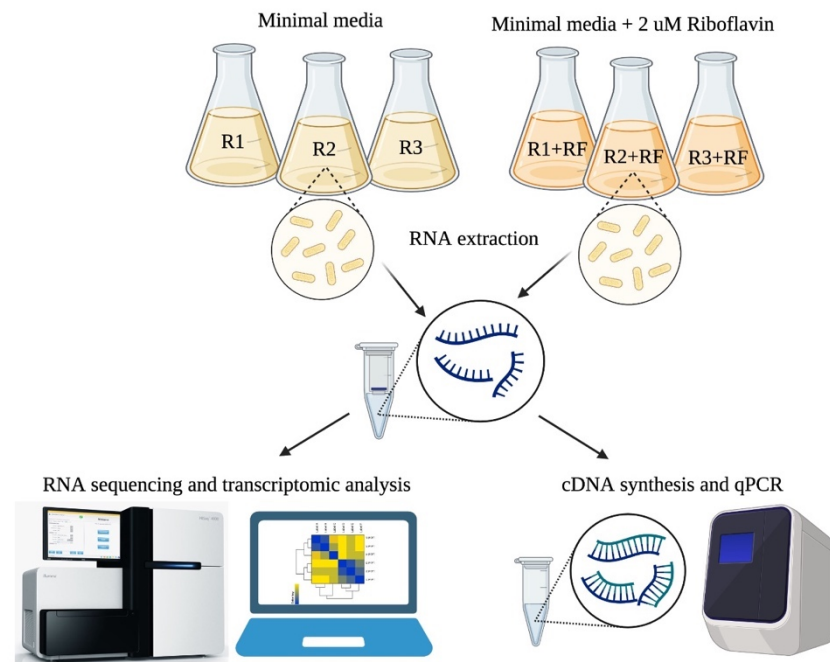
Enzyme Assayed for	J223	$\Delta ribA$	$\Delta ribAB$	$\Delta ribB$	$\Delta ribE1$	$\Delta ribE2$	$\Delta ribN$	$\Delta ribA-\Delta ribE1$
Reduction of nitrates to nitrites	+	+	+	+	+	+	+	+
Indole production	-	-	-	-	-	-	-	-
Glucose fermentation	+	+	+	+	+	+	+	+
Urease	-	-	-	-	-	-	-	-
β -Galactosidase	-	-	-	-	-	-	-	-
Hydrolysis of:								
Arginine	+	+	+	+	+	+	+	-*
Esculin	+	+	+	+	+	+	+	+
Gelatin	+	+	+	+	+	+	+	+
Assimilation of:								
D-glucose	+	+	+	+	+	+	+	+
L-arabinose	-	-	-	-	-	-	-	-
D-mannose	+	+	+	+	+	+	+	+
D-mannitol	+	+	+	+	+	+	+	+
N-acetyl-glucosamine	+	+	+	+	+	+	+	+
D-maltose	+	+	+	+	+	+	+	+
Potassium gluconate	-	-	-	-	-	-	-	-
Capric acid	-	-	-	-	-	-	-	-
Adipic acid	-	-	-	-	-	-	-	-
Malic acid	+	+	+	+	+	+	+	+
Trisodium citrate	-	-	-	-	-	-	-	-
Phenylacetic acid	-	-	-	-	-	-	-	-

+ positive, -negative, * different reaction compared to wild-type and other mutant strains

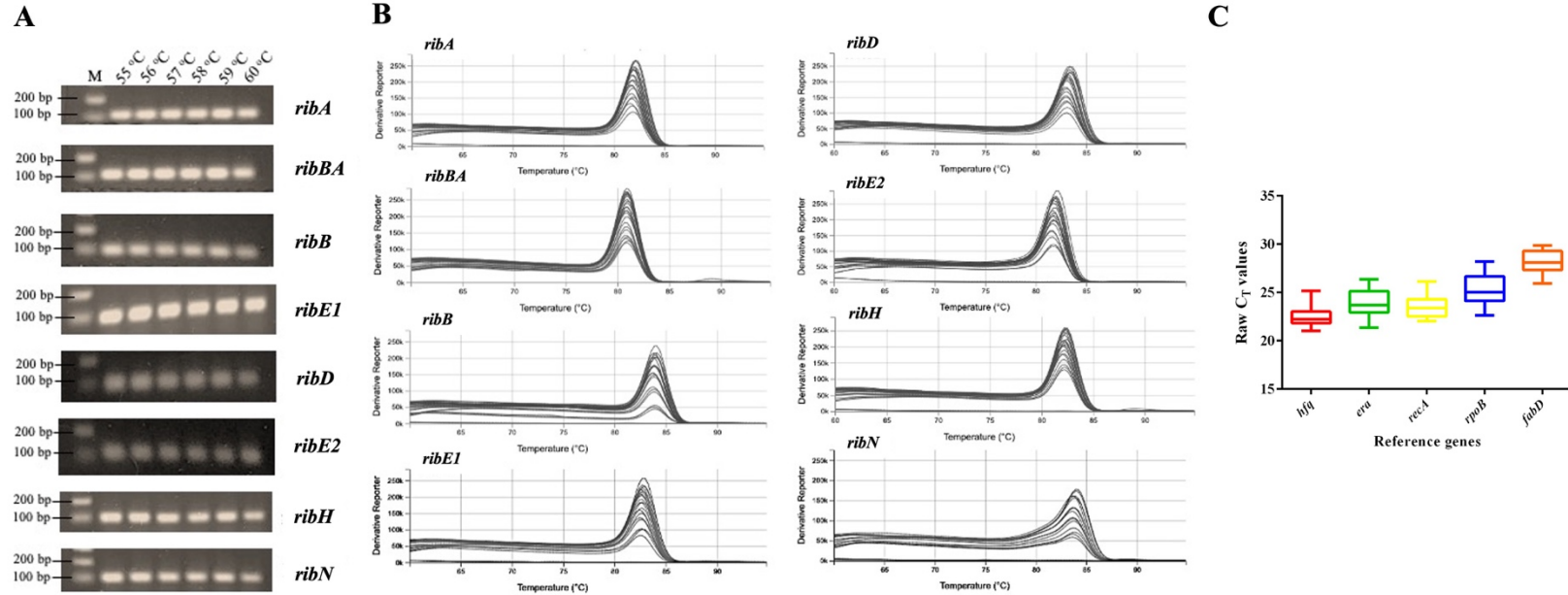
Supplementary Table S5.7. Enzymatic profiles of wild-type and mutants of *A. salmonicida* using the API-ZYM

Enzyme Assayed for	J223	$\Delta ribA$	$\Delta ribAB$	$\Delta ribB$	$\Delta ribE1$	$\Delta ribE2$	$\Delta ribN$	$\Delta ribA-\Delta ribE1$
Alkaline phosphatase	+	+	+	+	+	+	+	+
Esterase (C ₄)	+	+	+	+	+	+	+	+
Esterase lipase (C ₈)	+	+	+	+	+	+	+	+
Lipase (C ₁₄)	+	+	+	+	+	+	+	+
Leucine arylamidase	+	+	+	+	+	+	+	+
Valine arylamidase	±	±	±	±	±	±	±	±
Cystine arylamidase	-	-	-	-	-	-	-	-
Trypsin	-	-	-	-	-	-	-	-
α-Chymotrypsin	-	-	-	-	-	-	-	-
Acid Phosphatase	+	+	+	+	+	+	+	+
Naphthol-AS-BI-Phosphohydrolase	+	+	+	-*	+	+	+	+
α-galactosidase	-	-	-	-	-	-	-	-
β-galactosidase	-	-	-	-	-	-	-	-
β-glucuronidase	-	-	-	-	-	-	-	-
α-glucosidase	-	-	-	-	-	-	-	-
β-glucosidase	+	+	+	+	+	+	+	+
N-acetyl-β-glucosaminidase	+	+	+	+	+	+	+	+
α-mannosidase	-	-	-	-	-	-	-	-
α-fucosidase	-	-	-	-	-	-	-	-

+ positive, -negative, ± weak positive, * different reaction compared to wild-type and other mutant strains

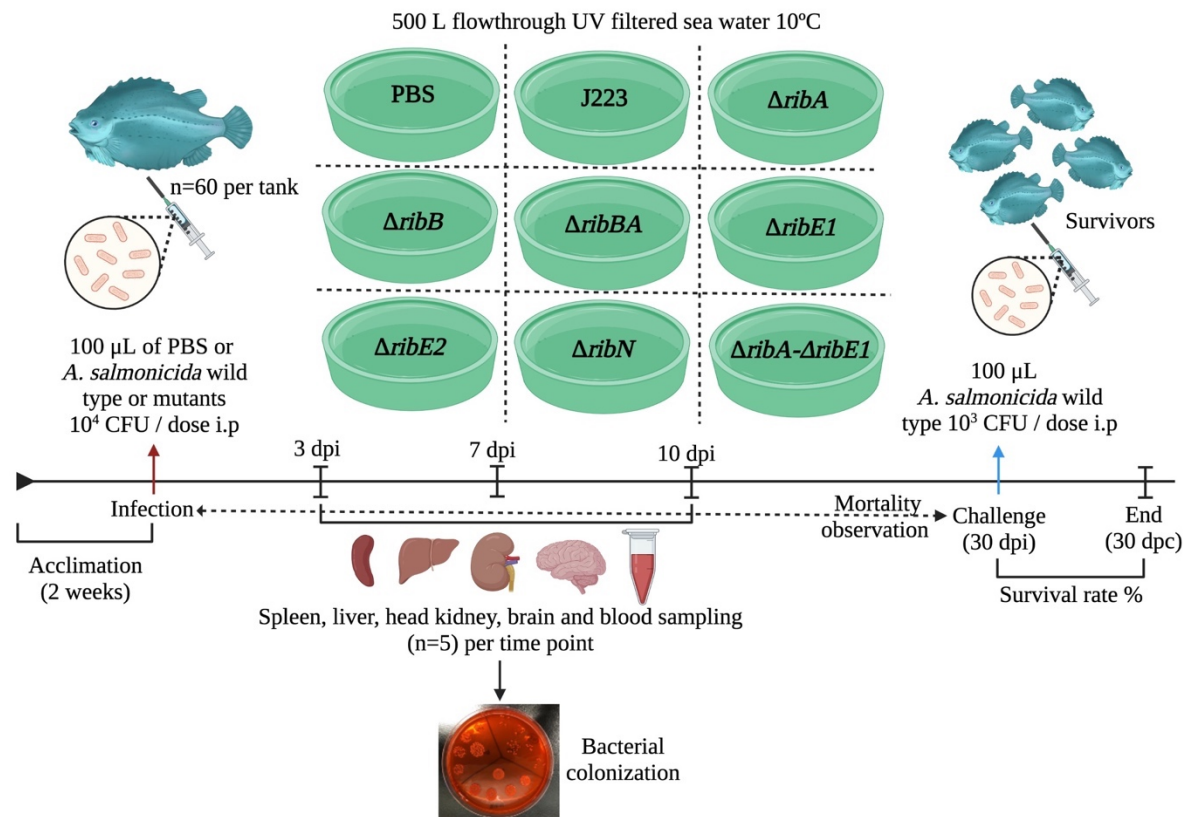


Supplementary Figure S5.1. Experimental designs for *A. salmonicida* transcriptomics and qPCR analyses

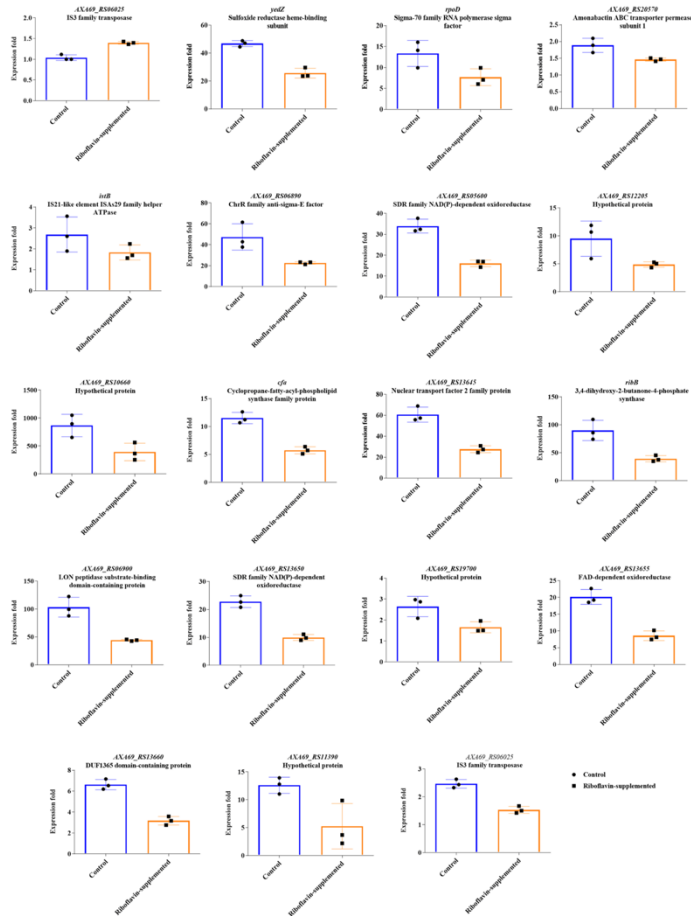
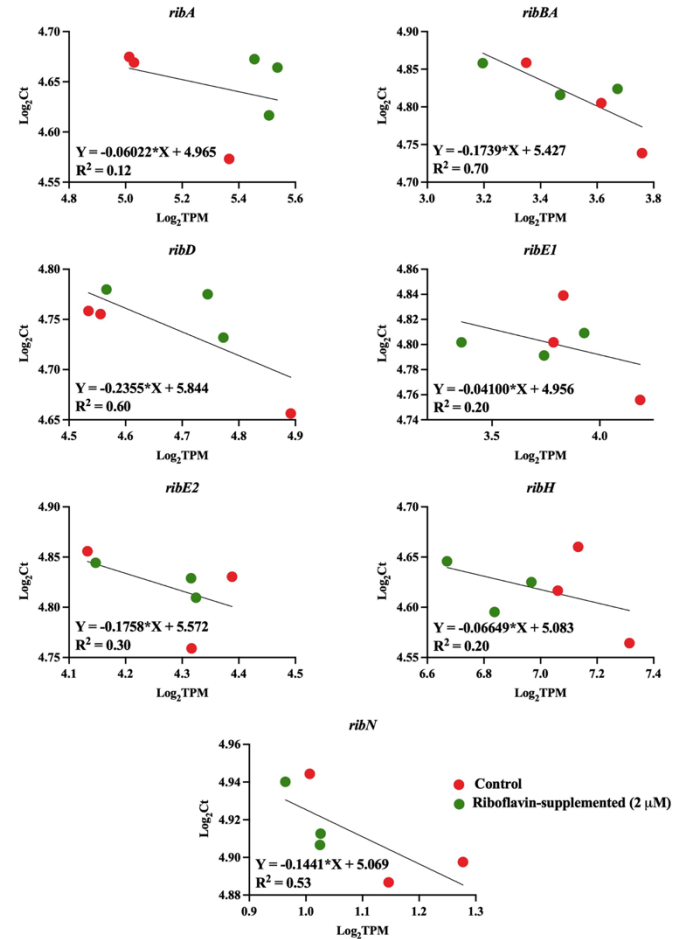


Supplementary Figure S5.2. Gradient PCR, Primer efficiency and Endogenous control genes selection for qPCR analysis. **A.** Optimum annealing temperatures were determined and melting curves were constructed for each primer set designed to amplify riboflavin supply pathway genes *ribA*, *ribBA*, *ribB*, *ribE1*, *ribD*, *ribE2*, *ribH*, and *ribN*. Gradient PCR with temperatures from 55-60 °C was used to determine optimum annealing temperatures of each set of primer used. M means 100 kb molecular weight marker. **B.** qPCR melting curves for each primer pair evaluated. The single peaks observed for each gene's melting curves representing single amplicon and verify the absence of primer dimers. **C.** Raw C_T values for five candidate reference genes across

all experimental treatments (control and riboflavin-supplemented groups); *A. salmonicida* grown with (2 μ M) and without riboflavin. A line across the box represents the median value. Upper and lower boxes indicate the 25th and 75th percentile, respectively, and the whisker caps represent the maximum and minimum C_T values.

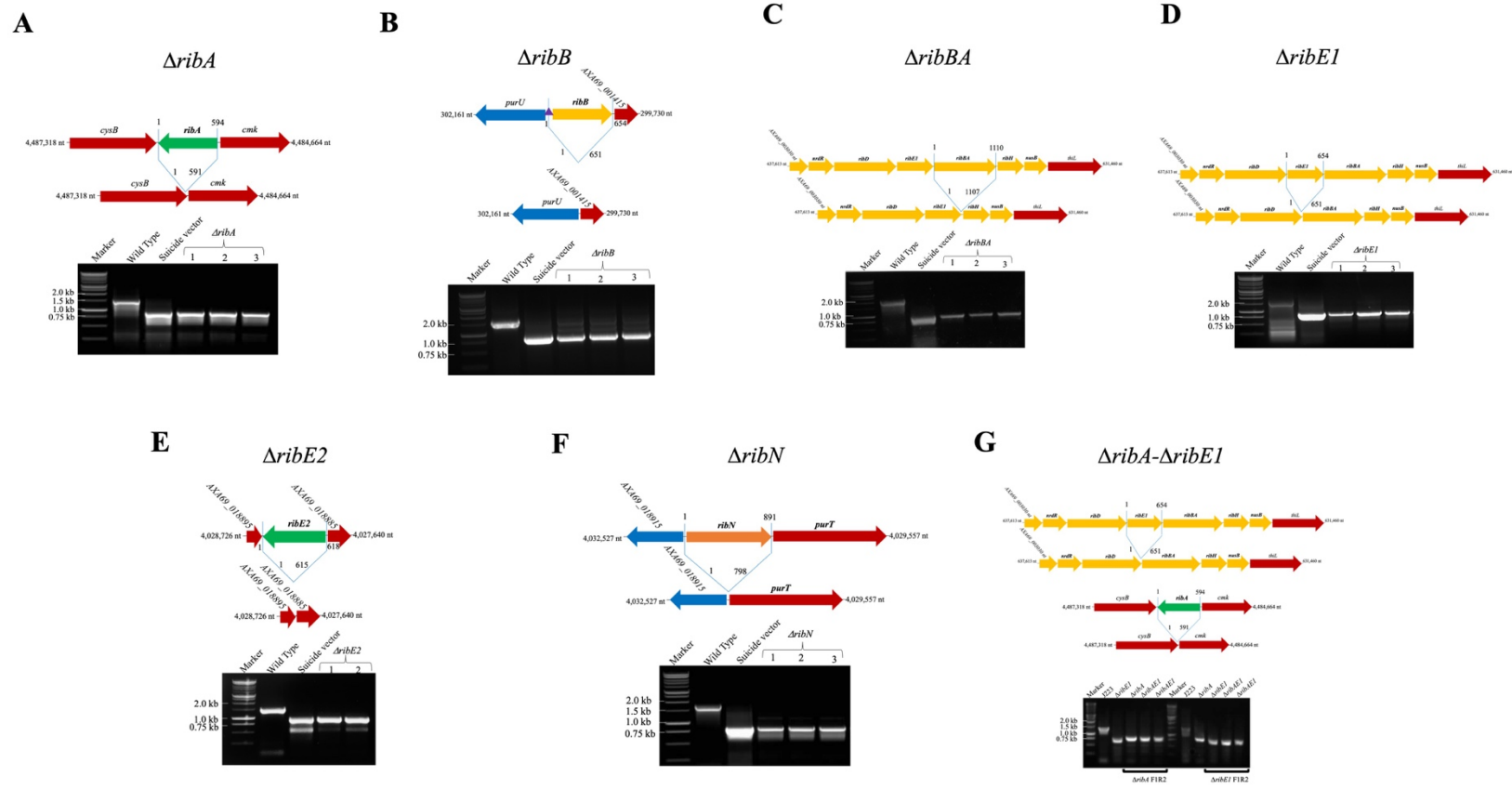


Supplementary Figure S5.3. Evaluation of *A. salmonicida* J223 wild type and mutant strains virulence in lumpfish (*C. lumpus*)

A**B**

Supplementary Figure S5.4. *A. salmonicida* RNA-seq and gene expression correlation. **A.** Differentially Expressed Genes (DEG) in *A. salmonicida* J223 grown in presence (2 μ M) and absence of riboflavin. The expression folds (in terms of TPM values) of

significant 19 DEGs from control and riboflavin-supplemented groups were compared and visualized in bar plots. **B.** Gene expression correlation between RT-qPCR and RNA-Seq data of *ribA*, *ribBA*, *ribD*, *ribE1*, *ribE2*, *ribH*, and *ribN*. RNA-Seq data are presented as Log_2TPM (X-axis). RT-qPCR data are represented as Log_2Ct (Y-axis).



Supplementary Figure S5.5. Deletion maps and PCR verifications of Single (A-F) and double (G) deletion mutants of *A. salmonicida* constructed and used in this study.

Chapter 6: General Conclusions

6.1. Summary of results

Aquaculture has been predicted to serve as the primary source for meeting future global demand for fish consumption [1]. However, marine finfish aquaculture faces several health challenges, including bacterial diseases [2]. Disease development is a complex process that occurs when a virulent pathogen and a susceptible fish host meet in an environment that supports such an occurrence. Investigating host-pathogen interactions is crucial for understanding disease and its prophylaxis [3]. Fundamental research to better understand the intricate insights of pathogenicity and/or virulence of economically important Gram-positive and Gram-negative fish pathogens would be valuable. In Atlantic salmon farming, lumpfish is a popular cleaner fish for delousing (i.e., removal of sea lice). Lumpfish are susceptible to several Gram-positive and Gram-negative bacterial pathogens [4]. There are still knowledge gaps in lumpfish health, such as its immune functions, host-pathogen interactions, susceptibility to bacterial diseases, and vaccines [5]. As salmonid aquaculture's need for lumpfish rises, knowledge of how lumpfish and its immune system interact with well-known Gram-positive and Gram-negative fish pathogens is certainly needed. Therefore, in this thesis, I studied interactions between Gram-positive *R. salmoninarum* and Gram-negative *A. salmonicida* and the lumpfish host with an emphasis on the fundamental aspects of bacterial pathogenicity, virulence, and physiology. Together, this thesis research developed the first *R. salmoninarum* experimental disease challenge model in non-salmonid lumpfish, investigated the transcriptome response of lumpfish head kidney in early and chronic stages of *R. salmoninarum* infection, described the riboflavin

supply pathways in *A. salmonicida*, and constructed deletion mutants of riboflavin biosynthesis and transport genes of *A. salmonicida* to study their role in virulence and potential as live-attenuated vaccine candidates. Overall, the knowledge gained from this thesis will be valuable for developing immunoprophylactic measures for lumpfish against bacterial kidney disease and furunculosis.

Chapter 2 presented a comprehensive analysis of known host-pathogen interactions of marine Gram-positive bacteria, published in *Biology* [6]. In this chapter, I provided a holistic view of the host-pathogen interactions between marine finfish and economically important Gram-positive pathogens, such as *R. salmoninarum*, *M. marinum*, *N. seriolae*, *L. garvieae*, and *Streptococcus* spp. From the pathogen-centric point of view, I summarized the intricate details of marine Gram-positive bacteria's adhesion, invasion, evasion, and proliferation in the respective fish-host systems, with examples of the unique set of virulence factors or mechanisms employed at different phases of host-pathogen interactions. I examined the fish host immune responses from a host-centric point of view, focusing on pathogen recognition, nutritional immunity, innate immunity, and humoral and cell-mediated adaptive immunity. Marine Gram-positive pathogens have established a unique set of machinery or strategies to interact with their exclusive fish host cells and manipulate the sophisticated molecular and cellular networks of these cells to facilitate bacterial proliferation in the host system. Further, the pathogenicity of a marine Gram-positive bacteria depends on the host it is trying to infect. Overall, this comprehensive review provided an overview of what is known about the host-centric and pathogen-centric points of view at the host-pathogen interface and identified the knowledge gaps or areas that require future research.

Chapter 3, published in *Frontiers in Immunology* [7], developed the first experimental disease challenge model of *R. salmoninarum* chronic infection in the non-salmonid lumpfish. In this chapter, I evaluated the lumpfish susceptibility (via infection kinetics-based assays such as survival, tissue colonization, and histopathology) and immune response (via qPCR in the head kidney) to *R. salmoninarum* infection. Typical clinical signs and histopathological damages of bacterial kidney disease were present in infected lumpfish and were comparable to salmonids. Infected lumpfish with a high dose of *R. salmoninarum* (1×10^9 cells/dose) showed 35% mortality. Examination of tissue (i.e., spleen, liver, and head kidney) colonization revealed the highest bacterial loads at 28 days post-infection (dpi) and chronic persistence of *R. salmoninarum* in tissues until 98 dpi. To provide fundamental knowledge on lumpfish immune response to *R. salmoninarum* at early (28 dpi) and chronic (98 dpi) infection stages, I then analyzed the expression of 33 genes associated with innate and adaptive immunity in the head kidney of high-dose *R. salmoninarum* infected fish. At 28 dpi, cytokines (e.g., *il1b*, *il8*), pattern recognition receptor (e.g., *tlr5*), iron regulator (e.g., *hamp*), acute phase reactant (e.g., *saa5*), and interferon effectors/regulators (e.g., *rsad2*, *mx*) exhibited upregulation, whereas genes related to humoral (e.g., *igha*, *ighd*, *ighma*, *ighmb*) and cell-mediated (e.g., *cd4a*, *ly6g6f*, *cd8a*, *cd74*) adaptive immunity showed significant downregulation. In contrast, at 98 dpi, cytokines associated with chronic infection and intracellular pathogens (e.g., *tnfa*, *ifng*) [8,9] and cell-mediated immunity (e.g., *cd74*) were induced. This work is the first to elucidate the lumpfish susceptibility to *R. salmoninarum* type strain ATCC 33209 i.p. infection. According to the gene expression results, *R. salmoninarum* causes immune suppression in lumpfish during early infection stages, and a cell-mediated immune response

is elicited by lumpfish at chronic infection stages. Overall, the findings from Chapter 3 presented baseline insights on how lumpfish, a non-salmonid host, and *R. salmoninarum*, a Gram-positive fish pathogen, interact.

Chapter 4, submitted to *Scientific Reports*, profiled the transcriptome response of lumpfish head kidney to *R. salmoninarum* at early (28 dpi) and chronic (98 dpi) infection stages using the RNA-seq approach. The head kidneys from control and high-dose *R. salmoninarum*-infected lumpfish at 28 and 98 dpi were used. Using a reference genome-guided transcriptomic assembly, and pathway enrichment analyses, I provided a general overview of the lumpfish molecular pathways regulated by *R. salmoninarum* infection. Compared to 98 dpi, *R. salmoninarum* affected many pathways and genes in lumpfish at 28 dpi. However, only a small percentage of them (7%) were related to immune responses, suggesting that this pathogen may have suppressed the lumpfish immune system during early infection [10–12]. Upregulated (i.e., *R. salmoninarum*-induced) genes at 28 dpi were mainly involved in innate and adaptive immune responses. In contrast, downregulated (i.e., *R. salmoninarum*-suppressed) genes in lumpfish at 28 dpi were associated with processes beyond the canonical lumpfish host-immune related responses, such as amino acid metabolism, cellular and developmental processes. However, lumpfish's head kidney transcriptome response to this pathogen was minimal at 98 dpi, with *R. salmoninarum*-dependent dysregulation of genes mostly linked to cell-mediated adaptive immunity. Taken together, the immune-signaling pathways that were dysregulated in response to *R. salmoninarum* in lumpfish at early and chronic infection phases included NFκB signalling, apoptosis, complement alternative cascading, JAK-STAT signaling, and MHC-I dependent pathways. I then used prior qPCR results from Chapter 3 [7] to validate the RNA-seq data

from Chapter 4 and found significant correlations between 83% of the qPCR-studied genes and the RNA-seq results. Additionally, to understand some innate (i.e., lysozyme activity) and adaptive (i.e., antibody titers) immune functions of lumpfish in response to *R. salmoninarum* infection, I conducted fluorescence-based lysozyme activity assay and indirect ELISA in fish serum from control and infected fish at 1, 14, 28, 42, 56, and 98 dpi. Lysozyme activity in *R. salmoninarum*-infected lumpfish serum was higher at an earlier time point and followed by reduction at later time points. Examination of antibody titers suggested that *R. salmoninarum* infection did not significantly affect the antibody titers in lumpfish. Overall, Chapter 4 is the first report profiling the transcriptome response of lumpfish head kidney to *R. salmoninarum* at early and chronic infection stages and provides a comprehensive picture of biological processes and molecular mechanisms underlying the lumpfish response to *R. salmoninarum* infection.

Chapter 5, published in *Virulence* [13], explored the riboflavin supply pathways of *A. salmonicida* and examined the role of riboflavin biosynthesis gene duplication and transporter in this pathogen's virulence in a lumpfish infection model. The riboflavin provision pathways of *A. salmonicida* had not been investigated prior to the current study. Therefore, first, I characterized the riboflavin biosynthesis and transport pathways using in-silico tools and reverse transcription PCR. The findings showed that the riboflavin biosynthetic operon of *A. salmonicida* contains putative *ribD*, *ribE1*, *ribBA*, and *ribH* genes. Intriguingly, *A. salmonicida* was found to have putative redundant riboflavin biosynthesis genes (*ribA*, *ribB*, and *ribE*) and a gene encoding a riboflavin importer (*ribN*). Monocistronic *ribA*, *ribB*, and *ribE2* were shown to encode for the respective functional riboflavin biosynthesis enzymes based on sequence comparison and heterologous

complementations. The product of *ribBA* conserved RibB function but had no RibA function, similar to what was reported in other bacteria with a functional RibB and a domain with an unknown function and named *ribBX* [14,15]. When complementing *E. coli* Δ *ribB* with the *A. salmonicida* *ribN* in M9 minimal media with low riboflavin, *ribN* conserved the riboflavin transport function. To study the effect of extracellular riboflavin in *A. salmonicida* transcriptome response, I compared the gene expression profiles of bacteria grown in M9 minimal media with (2 μ M) and without riboflavin. Subsequently, I found that external riboflavin affected only a small number of *A. salmonicida* genes (i.e., 19 differentially expressed genes), including genes with putative roles in iron metabolism and riboflavin biosynthesis. Gene duplications or multiplications in the riboflavin biosynthetic pathways (RBP) of bacteria may serve particular purposes and benefit adaptation [16]. For instance, intracellular bacterial survival and host colonization of *Brucella abortus* were linked to the second *ribH* gene copy, which is outside of the main RBP operon [17]. Based on the literature and my results from homology search and transcriptional orchestration analysis, I hypothesized that the extra RBP gene copies (*ribA*, *ribB*, and *ribE1*) and transporter *ribN* might have an impact on *A. salmonicida* virulence and physiology. Mutants of RBP genes (Δ *ribBA*, Δ *ribE1*), their duplicated gene copies (Δ *ribA*, Δ *ribB*, Δ *ribE2*), and riboflavin transporter (Δ *ribN*) were constructed. A mutant (Δ *ribA*- Δ *ribE1*) combined deletions in a unique duplicated biosynthesis gene copy (*ribA*; GTP cyclohydrolase II) and in a duplicating main-operon biosynthesis gene (*ribE1*). The in-vitro growth assays revealed that the Δ *ribA* and Δ *ribA*- Δ *ribE1* mutants were riboflavin auxotrophs, indicating that the *ribBA* lacked *ribA* function and that the independent *ribA* was the only gene in *A. salmonicida* encoding GTP cyclohydrolase II activity. Finally, I

evaluated the virulence of *A. salmonicida* wild type and mutants in a lumpfish infection model, where $\Delta ribA$, $\Delta ribB$, $\Delta ribE1$, and $\Delta ribA-\Delta ribE1$ mutants were completely attenuated, and the fish infected with them showed 100% survival. When analyzing the potential of the attenuated mutants as the live-attenuated vaccine for lumpfish, I observed low levels of immune protection (i.e., relative percent survival ranging from 10-15%) to lumpfish against virulent *A. salmonicida*. Thus, mutations in *ribA*, *ribB*, and *ribE1* affect bacterial virulence, host colonization, and immune protection. Overall, this chapter is the first to identify the riboflavin supply pathways of *A. salmonicida* and suggests that riboflavin biosynthesis is crucial for *A. salmonicida* virulence and physiology.

6.2. Future directions

R. salmoninarum and *A. salmonicida* are well-known bacterial pathogens in marine finfish aquaculture due to their prevalence and the economic losses they caused to the industry. These pathogens have been studied in terms of their pathogenicity, virulence or virulence factors, host-specificity, genomics, proteomics, transcriptomics, and fish response [11,12,18,19]. The fish host-centric research among these studies mostly focused on salmonids. Since lumpfish is an emerging non-salmonid finfish aquaculture candidate, there are still knowledge gaps regarding host-pathogen interactions between this fish and *R. salmoninarum* or *A. salmonicida*; the areas that deserve attention are lumpfish susceptibility, immune functions, response to Gram-positive and Gram-negative fish pathogens, and immune prophylaxis development. The studies presented in this thesis set a solid groundwork of fundamental insights into *R. salmoninarum* and *A. salmonicida* pathogenicity and virulence using lumpfish-based infection models. However, several

aspects of host-pathogen interactions between lumpfish and *R. salmoninarum* or *A. salmonicida* still need to be investigated at functional molecular levels from BKD or furunculosis management standpoints. The work from this thesis opens exciting avenues that hold promise for future research. Some potential areas for future studies that can be derived from this work are outlined below.

Chapter 3 demonstrated that lumpfish is susceptible to *R. salmoninarum* type strain ATCC 33209 systemic infection and exhibited only 35% mortality when infected with high-dose (1×10^9 cells/dose). *R. salmoninarum* virulence is linked to the functional *msa* (*major soluble antigen*) gene copy number (i.e., ranged from 2-5) [20–23]. To be precise, mortality at lower infection doses is positively correlated with *msa* copy number [23]. The type strain I used in this work has two copies of the *msa* gene and is described as having less virulence than other *R. salmoninarum* strains [22]. Thus, lumpfish susceptibility to more virulent strains with multiple *msa* gene copies could be studied. The risk of disease transmission from lumpfish to Atlantic salmon is moderate [24]. The ability of lumpfish to serve as a disease vector and spread parasite amoebae (*Paramoeba perurans*), the causative agent of amoebic gill disease, to Atlantic salmon has also been demonstrated [25]. *R. salmoninarum* chronically persisted in lumpfish tissues until 98 dpi. Since the study ended before the bacterial clearance, it is unknown if *R. salmoninarum* will be eliminated from the host or if lumpfish with persisted *R. salmoninarum* would act as a carrier and pose a disease threat (i.e., horizontal transmission) to cohabiting salmon. Therefore, designing a long-term cohabitation bioassay in natural sea-cage conditions to explore the interactions between *R. salmoninarum*, lumpfish, and Atlantic salmon and to validate the disease

transfer potential of lumpfish would be valuable from the fish health management perspective.

Chapter 4 provided a global understanding of biological processes and molecular pathways underpinning lumpfish responses to *R. salmoninarum* at early and chronic infection stages using the RNA-seq approach. It also analyzed lysozyme activity and antibody titers in the serum of infected fish. The results presented in this study gave an overview of significantly up- and down-regulated genes in response to *R. salmoninarum* infection and validated some of the genes' expression using qPCR but did not reveal their precise functional role in immune modulation. Few previous studies used functional analyses to explore lumpfish immunity (e.g., phagocytosis, respiratory burst, antigen-specific antibodies upon immunization), key immune molecules (e.g., characterization of IL-1 family ligands and IgM⁺ B cells), and signaling pathways (e.g., IL-1 signaling) [26–29]. However, lumpfish immune mechanisms of defense against bacterial pathogens still need to be investigated. Although my results suggested putative roles of the genes identified herein (Table 4.1), functional characterization of these genes and their encoded proteins would be valuable in expanding the current knowledge of lumpfish molecular processes and conserved structures/functions of these genes across various teleost species. JAK-STAT and NFκB signaling are crucial pathways engaged in the host-pathogen interactions between lumpfish and *R. salmoninarum*. Functional analysis of the proteins (i.e., CARD, CISH, SOCS) implicated in these signaling pathways will be necessary to determine the roles of specific proteins and protein-protein interactions among them. Luciferase reporter gene assays are employed in teleost (e.g., Miiuy croaker (*Miichthys miiuy*)) primary cells or cell lines to verify signaling pathways [30,31]. To enable such future experiments using

lumpfish primary cells, efficient transfection and luciferase activity protocols should be developed. Interestingly, *R. salmoninarum*-specific antibody response was poor in lumpfish serum at all sampling points. The research question of whether or not there were non-*R. salmoninarum*-specific antibody responses (i.e., autoreactive antibodies, which could be related to the accompanying pathology) in lumpfish would be intriguing. Chapter 4 reported only the host-centric genes or pathways dysregulated in lumpfish upon *R. salmoninarum* infection. Future research involving the simultaneous investigation of the transcriptomes of lumpfish and *R. salmoninarum* (Dual RNA-seq) might be helpful in differentiating between the complex host- and pathogen-centric viewpoints. In addition, comparing transcriptomes of Atlantic salmon and lumpfish infected with *R. salmoninarum* would also be intriguing to compare and contrast the salmonid and non-salmonid host responses and to identify comparative molecular biomarkers for BKD detection and control in sea cages.

Chapter 5 is a complete study that explored *A. salmonicida* riboflavin supply pathways, general regulatory effects of external riboflavin, the role of different riboflavin provision components (i.e., biosynthesis genes, their extra copies, transporter) in virulence, and the potential use of flavin-impaired mutants as live-attenuated lumpfish vaccines. Unfortunately, completely attenuated *A. salmonicida* mutants (i.e., $\Delta ribA$, $\Delta ribB$, $\Delta ribE1$, and $\Delta ribA-\Delta ribE1$) only provided modest immune protection to lumpfish with low RPS (10-15%) when challenged with virulent *A. salmonicida*. Lumpfish may not establish a protective immunity because of the severe immune suppression imposed by *A. salmonicida* [32]. On the other hand, the lack of rounds of mutant replication within the fish host may be the cause of these mutants' inability to offer protective immunity. Simply put, mutants

may be too attenuated to properly colonize at the ideal time or in enough quantities to elicit a proper and protective memory immune response in lumpfish. Maintaining a balance between the vectors' immunogenicity and attenuation is one of the potential drawbacks of live bacterial vectors. For instance, poor immunogenicity may result from the bacterial vector's excessive attenuation [33]. Thus, further research needs to improve the immunogenicity of the attenuated *A. salmonicida* mutants. Regulated delayed attenuated strategies (RDAS) allow live *Salmonella* vaccine to effectively colonize the lymphoid tissues during the invasion employing a wild-type invasion mechanism and then fully attenuated by silencing the virulence factor while triggering strong protective immunity in mice [34,35]. Similarly, developing RDAS or overexpressing the protective immunogenic antigens by the attenuated *A. salmonicida* mutant strains would be a promising vaccine design for lumpfish aquaculture against this pathogen's infection. Only a few studies, including Chapter 5, used high-throughput methods like RNA-seq to examine the bacterial response to riboflavin despite its vital role in bacterial physiology [13,36]. It would be interesting to compare the effects of eliminating endogenous biosynthesis or uptake as well as to detail the specific effects of synthesized or internalized riboflavin in future studies examining the transcriptomic responses of *A. salmonicida* to deletions of riboflavin biosynthesis and transporter genes. The mutants constructed in Chapter 5 that are riboflavin-biosynthesis-deficient (e.g., $\Delta ribBA$, $\Delta ribA$, $\Delta ribB$, $\Delta ribE1$, $\Delta ribE2$, $\Delta ribA-\Delta ribE1$) or riboflavin-transporter-deficient ($\Delta ribN$) would be ideal candidates for the aforementioned investigation. From the genetics and evolutionary perspective of bacterial genomes, genomics-based studies to gain deeper insights into the origin of gene duplication events (i.e., intra-genome duplication or horizontal/vertical gene transfer) and the

evolutionary fate of duplicated genes (i.e., hypofunctionalization, subfunctionalization, neofunctionalization) in *A. salmonicida* genome would be valuable.

6.3. Overall thesis conclusion

Overall, the work in the thesis explored some fundamental insights into *R. salmoninarum* and *A. salmonicida* virulence and pathogenicity using lumpfish infection models and provided solid knowledge of host-pathogen interactions between them. Interestingly, this thesis was the first to study several pathogen-centric and host-centric perspectives of *R. salmoninarum*, *A. salmonicida*, and lumpfish. For instance, from the pathogen point of view, *R. salmoninarum* infection in lumpfish (Chapter 3) and *A. salmonicida* riboflavin pathways (Chapter 5) were first reported herein. From the host point of view, susceptibility and transcriptome response of lumpfish to Gram-positive *R. salmoninarum* (Chapters 3 and 4) and potential of *A. salmonicida* mutants (carrying deletions in riboflavin biosynthesis and transport genes) as live-attenuated vaccines to lumpfish against *A. salmonicida* infection (Chapter 5) have been first elucidated. Beyond these, the findings also contribute significantly to the current efforts in understanding lumpfish response to Gram-positive and Gram-negative bacterial fish pathogens and provide a valuable base for developing immune prophylaxis measures against BKD and furunculosis.

6.4. References

1. FAO. *The State of World Fisheries and Aquaculture 2022. Towards Blue Transformation.*; Rome, 2022, doi:10.4060/cc0461en.
2. Lafferty, K. D.; Harvell, C. D.; Conrad, J. M.; Friedman, C. S.; Kent, M. L.; Kuris, A. M.; Powell, E. N.; Rondeau, D.; Saksida, S. M. Infectious Diseases Affect Marine Fisheries and Aquaculture Economics. **2015**.
3. Southwood, D.; Ranganathan, S. *Host-Pathogen Interactions*; Elsevier Ltd., 2018; Vol. 1–3, doi:10.1016/B978-0-12-809633-8.20088-5.
4. Powell, A.; Treasurer, J. W.; Pooley, C. L.; Keay, A. J.; Lloyd, R.; Imsland, A. K.; Garcia de Leaniz, C. Use of Lumpfish for Sea-lice Control in Salmon Farming: Challenges and Opportunities. *Rev. Aquac.* **2018**, *10* (3), 683–702.
5. Brooker, A. J.; Papadopoulou, A.; Gutierrez, C.; Rey, S.; Davie, A.; Migaud, H. Sustainable Production and Use of Cleaner Fish for the Biological Control of Sea Lice: Recent Advances and Current Challenges. *Vet. Rec.* **2018**, *183* (12), 383.
6. Gnanagobal, H.; Santander, J. Host-Pathogen Interactions of Marine Gram-Positive Bacteria. *Biology (Basel)*. **2022**, *11* (9), doi:10.3390/biology11091316.
7. Gnanagobal, H.; Cao, T.; Hossain, A.; Dang, M.; Hall, J. R.; Kumar, S.; Van Cuong, D.; Boyce, D.; Santander, J. Lumpfish (*Cyclopterus lumpus*) Is Susceptible to *Renibacterium salmoninarum* Infection and Induces Cell-Mediated Immunity in the Chronic Stage . *Frontiers in Immunology* . 2021, p 4647.
8. Zou, J.; Secombes, C. J. The Function of Fish Cytokines. *Biology (Basel)*. **2016**, *5* (2), doi:10.3390/biology5020023.
9. Kaufman, S. H. E. Immunity to Intracellular Bacteria. In *Fundamental immunology*; Paul, W. E., Ed.; Philadelphia, 1999; pp 1335–1371.
10. Fredriksen, Å.; Endresen, C.; Wergeland, H. I. Immunosuppressive Effect of a Low Molecular Weight Surface Protein from *Renibacterium salmoninarum* on Lymphocytes from Atlantic Salmon (*Salmo salar* L.). *Fish Shellfish Immunol.* **1997**, *7* (4), 273–282, doi:10.1006/fsim.1997.0082.
11. Wiens, G. D. Bacterial Kidney Disease (*Renibacterium salmoninarum*). In *Fish Diseases and Disorders*; Woo, P. T. K., Bruno, D. W., Eds.; CABI: Wallingford, UK, 2011; pp 338–374.
12. Elliott, D. G. *Renibacterium salmoninarum*. In *Fish Viruses and Bacteria: Pathobiology and Protection*; Woo, P.T.K and Ciaprino, R. ., Ed.; CABI, U.K, 2017; pp 286–297.
13. Gnanagobal, H.; Cao, T.; Hossain, A.; Vasquez, I.; Chakraborty, S.; Chukwu-Osazuwa, J.; Boyce, D.; Espinoza, M. J.; García-Angulo, V. A.; Santander, J. Role of Riboflavin Biosynthesis Gene Duplication and Transporter in *Aeromonas salmonicida* Virulence in Marine Teleost Fish. *Virulence* **2023**, *14* (1), 2187025, doi:10.1080/21505594.2023.2187025.
14. Brutinel, E. D.; Dean, A. M.; Gralnick, J. A. Description of a Riboflavin Biosynthetic Gene Variant Prevalent in the Phylum Proteobacteria. *J. Bacteriol.* **2013**, *195* (24), 5479–5486, doi:10.1128/JB.00651-13.
15. Nouwen, N.; Arrighi, J. F.; Gully, D.; Giraud, E. RibBX of *Bradyrhizobium* ORS285

- Plays an Important Role in Intracellular Persistence in Various *Aeschynomene* Host Plants. *Mol. Plant-Microbe Interact.* **2021**, *34* (1), 88–99, doi:10.1094/MPMI-07-20-0209-R.
16. García-Angulo, V. A. Overlapping Riboflavin Supply Pathways in Bacteria. *Crit. Rev. Microbiol.* **2017**, *43* (2), 196–209, doi:10.1080/1040841X.2016.1192578.
 17. Bonomi, H. R.; Marchesini, M. I.; Klinke, S.; Ugalde, J. E.; Zylberman, V.; Ugalde, R. A.; Comerci, D. J.; Goldbaum, F. A. An Atypical Riboflavin Pathway Is Essential for *Brucella abortus* Virulence. *PLoS One* **2010**, *5* (2), e9435, doi:10.1371/journal.pone.0009435.
 18. Beaz-Hidalgo, R.; Figueras, M. J. *Aeromonas* spp. Whole Genomes and Virulence Factors Implicated in Fish Disease. *J. Fish Dis.* **2013**, *36* (4), 371–388, doi:10.1111/jfd.12025.
 19. Dallaire-Dufresne, S.; Tanaka, K. H.; Trudel, M. V.; Lafaille, A.; Charette, S. J. Virulence, Genomic Features, and Plasticity of *Aeromonas salmonicida* subsp. *salmonicida*, the Causative Agent of Fish Furunculosis. *Vet. Microbiol.* **2014**, *169* (1–2), 1–7, doi:10.1016/j.vetmic.2013.06.025.
 20. O’Farrell, C. L.; Strom, M. S. Differential Expression of the Virulence-Associated Protein P57 and Characterization of Its Duplicated Gene *msa* in Virulent and Attenuated Strains of *Renibacterium salmoninarum*. *Dis. Aquat. Organ.* **1999**, *38* (2), 115–123, doi:10.3354/dao038115.
 21. Coady, A. M.; Murray, A. L.; Elliott, D. G.; Rhodes, L. D. Both *msa* Genes in *Renibacterium salmoninarum* Are Needed for Full Virulence in Bacterial Kidney Disease. *Appl. Environ. Microbiol.* **2006**, *72* (4), 2672–2678, doi:10.1128/AEM.72.4.2672-2678.2006.
 22. Rhodes, L. D.; Coady, A. M.; Deinhard, R. K. Identification of a Third *msa* Gene in *Renibacterium salmoninarum* and the Associated Virulence Phenotype. *Appl. Environ. Microbiol.* **2004**, *70* (11), 6488–6494, doi:10.1128/AEM.70.11.6488-6494.2004.
 23. Brynildsrud, O.; Gulla, S.; Feil, E. J.; Nørstebø, S. F.; Rhodes, L. D. Identifying Copy Number Variation of the Dominant Virulence Factors MSA and p22 within Genomes of the Fish Pathogen *Renibacterium salmoninarum*. *Microb. genomics* **2016**, *2* (4), e000055, doi:10.1099/mgen.0.000055.
 24. Rimstad, E.; Basic, D.; Gulla, S.; Hjeltne, B.; Mortensen, S. Risk Assessment of Fish Health Associated with the Use of Cleaner Fish in Aquaculture. *Opin. panel Anim. Heal. Welf. Nor. Sci. Comm. Food Environ. VKM Rep.* **2017**, *32*.
 25. Haugland, G. T.; Olsen, A.-B.; Rønneseth, A.; Andersen, L. Lumpfish (*Cyclopterus lumpus* L.) Develop Amoebic Gill Disease (AGD) after Experimental Challenge with *Paramoeba perurans* and Can Transfer Amoebae to Atlantic Salmon (*Salmo salar* L.). *Aquaculture* **2017**, *478*, 48–55.
 26. Haugland, G. T.; Jakobsen, R. A.; Vestvik, N.; Ulven, K.; Stokka, L.; Wergeland, H. I. Phagocytosis and Respiratory Burst Activity in Lumpfish (*Cyclopterus lumpus* L.) Leucocytes Analysed by Flow Cytometry. *PLoS One* **2012**, *7* (10), e47909–e47909, doi:10.1371/journal.pone.0047909.
 27. Rønneseth, A.; Ghebretnsae, D. B.; Wergeland, H. I.; Haugland, G. T. Functional Characterization of IgM+ B Cells and Adaptive Immunity in Lumpfish (*Cyclopterus*

- lumpus* L.). *Dev. Comp. Immunol.* **2015**, *52* (2), 132–143, doi:10.1016/j.dci.2015.05.010.
28. Eggestøl, H. Ø.; Lunde, H. S.; Rønneseth, A.; Fredman, D.; Petersen, K.; Mishra, C. K.; Furmanek, T.; Colquhoun, D. J.; Wergeland, H. I.; Haugland, G. T. Transcriptome-Wide Mapping of Signaling Pathways and Early Immune Responses in Lumpfish Leukocytes upon in vitro Bacterial Exposure. *Sci. Rep.* **2018**, *8* (1), 5261, doi:10.1038/s41598-018-23667-x.
 29. Wang, T.; Santander, J.; Boudinot, P.; Eggestøl, H. Ø.; Lunde, H. S.; Knutsen, T. M.; Haugland, G. T. Interleukin-1 Ligands and Receptors in Lumpfish (*Cyclopterus lumpus* L.): Molecular Characterization, Phylogeny, Gene Expression, and Transcriptome Analyses. *Front. Immunol.* | www.frontiersin.org **2020**, *1*, 502, doi:10.3389/fimmu.2020.00502.
 30. Bi, D.; Wang, Y.; Gao, Y.; Li, X.; Chu, Q.; Cui, J.; Xu, T. Recognition of Lipopolysaccharide and Activation of NF- κ B by Cytosolic Sensor NOD1 in Teleost Fish. *Front. Immunol.* **2018**, *9* (JUN), 1–15, doi:10.3389/fimmu.2018.01413.
 31. Chen, Y.; Wang, P.; Li, Q.; Yan, X.; Xu, T. The Protease Calpain2a Limits Innate Immunity by Targeting TRAF6 in Teleost Fish. *Commun. Biol.* **2023**, *6* (1), 355, doi:10.1038/s42003-023-04711-7.
 32. Chakraborty, S.; Hossain, A.; Cao, T.; Gnanagobal, H.; Segovia, C.; Hill, S.; Monk, J.; Porter, J.; Boyce, D.; Hall, J. R.; Bindea, G.; Kumar, S.; Santander, J. Multi-Organ Transcriptome Response of Lumpfish (*Cyclopterus lumpus*) to *Aeromonas salmonicida* subspecies *salmonicida* Systemic Infection. *Microorganisms.* 2022, doi:10.3390/microorganisms10112113.
 33. Shi, H.; Wang, S.; Curtiss, R. Evaluation of Regulated Delayed Attenuation Strategies for *Salmonella enterica* Serovar Typhi Vaccine Vectors in Neonatal and Infant Mice. *Clin. Vaccine Immunol.* **2013**, *20* (6), 867–876, doi:10.1128/CVI.00003-13.
 34. Curtiss, R.; Soo-Young, W.; M., G. B.; Xin, Z.; A., T. S.; Vidya, A.; Hua, M.; Shifeng, W.; Wei, K. *Salmonella enterica* Serovar Typhimurium Strains with Regulated Delayed Attenuation in vivo. *Infect. Immun.* **2009**, *77* (3), 1071–1082, doi:10.1128/IAI.00693-08.
 35. Swain, B.; Powell, C. T.; Curtiss, R. Pathogenicity and Immunogenicity of *Edwardsiella piscicida* Ferric Uptake Regulator (*Fur*) Mutations in Zebrafish. *Fish Shellfish Immunol.* **2020**, *107*, 497–510, doi:https://doi.org/10.1016/j.fsi.2020.10.029.
 36. Sepúlveda-Cisternas, I.; Lozano Aguirre, L.; Fuentes Flores, A.; Vásquez Solís de Ovando, I.; García-Angulo, V. A. Transcriptomics Reveals a Cross-Modulatory Effect between Riboflavin and Iron and Outlines Responses to Riboflavin Biosynthesis and Uptake in *Vibrio cholerae*. *Sci. Rep.* **2018**, *8* (1), 3149, doi:10.1038/s41598-018-21302-3.